Final Report (RG/2012/BS/05)

Investigation of Sorption of Industrial Pollutants on Selected Natural Substances and Development of a Prototype Treatment Facility for Industrial Effluents

Prof. Namal Priyantha
Department of Chemistry
University of Peradeniya

TABLE OF CONTENTS

1. A.N. Navaratne, N. Priyantha and T.P.K. Kulasooriya, Removal of heavy metals using rice husk and brick clay as adsorbents - dynamic conditions.
2. T.P.K. Kulasooriya, N. Priyantha and A.N. Navaratne, "Adsorption of heavy metal ions on rice husk: Isotherm modeling and error analysis".
3. A.N. Navaratne, N. Priyantha and T.P.K. Kulasooriya, Removal of heavy metal ions using rice husk: Investigation on adsorption kinetics of heavy metals (submitted).
4. N. Priyantha, A.N. Navaratne and T.P.K. Kulasooriya, Removal of phosphate ions using brick clay: static and dynamic conditions (submitted).
5. N. Priyantha, A.N. Navaratne and T.P.K. Kulasooriya, Treatment of textile industry dye effluent by using naturally available substances (in preparation).
6. N. Priyantha, A.N. Navaratne, T.P.K. Kulasooriya and W. S. A. Weththasinghe, Comparison of the removal of Cu(II) and Zn(II) by using coir dust and brick clay (in preparation).
7. N. Priyantha, A.N. Navaratne and T.P.K. Kulasooriya, Prototype treatment facility for Zn(II) removal from synthetic effluents (Patent in preparation).
8. T.P.K. Kulasooriya, N. Priyantha and A.N. Navaratne, Treatment of industrial effluents using fired brick clay based filter (Patent in preparation).
9. A.N. Navaratne, N. Priyantha and T. P. K. Kulasooriya, Removal of heavy metals using rice husk and brick clay as adsorbents: a study of dynamic conditions.
10. N. Priyantha, A.N. Navaratne and T.P.K. Kulasooriya, Adsorption isotherm studies of heavy metal ions on rice husk.
11. T.P.K. Kulasooriya, A.N. Navaratne and N. Priyantha, Optimization of efficiency of phosphate removal by brick clay.
12. N. Priyantha, A.N. Navaratne and T.P.K. Kulasooriya, Sorption studies of textile dyes using naturally available substances.

SECTION 1

Information Regarding Project/Project Personnel

i) **Grant Number**: RG/2012/BS/05

ii) **Title of the Project**: Investigation of Sorption of Industrial Pollutants on Selected Natural Substances and Development of a Prototype Treatment Facility for Industrial Effluents

iii) **Principal Investigator:** Prof. Namal Priyantha

iv) **Co-Investigators:** None

v) **Institution(s) where the research was carried out**: University of Peradeniya

vi) **Date of award:** 01/10/ 2012-

vii) **Date of completion of Project:** 30/09/2015

viii) **Total allocation of funds (Rs.):** 2,933,489.50

ix) **Total spent (Rs.):** 2,933,461.24

x) **Number of Research Students employed:** One

xi) **Postgraduate degree completed with dates:** M.Phil. (to be completed in Jan 2016)

xii) **Number of Technical Assistants /laborers employed:** None

xiii) **Publications/Communications arising from the project**

1. A.N. Navaratne, N. Priyantha and T.P.K. Kulasooriya, Removal of heavy metals using rice husk and brick clay as adsorbents - dynamic conditions, *International Journal of Earth Science and Engineering*, **6**, 807-811 (2013).
2. T.P.K. Kulasooriya, N. Priyantha and A.N. Navaratne, "Adsorption of heavy metal ions on rice husk: Isotherm modeling and error analysis", *International Journal of Earth Science and Engineering*, **8**, 346-352 (2015).
3. A.N. Navaratne, N. Priyantha and T.P.K. Kulasooriya, Removal of heavy metal ions using rice husk: Investigation on adsorption kinetics of heavy metals (submitted).
4. N. Priyantha, A.N. Navaratne and T.P.K. Kulasooriya, Removal of phosphate ions using brick clay: static and dynamic conditions (submitted).
5. N. Priyantha, A.N. Navaratne and T.P.K. Kulasooriya, Treatment of textile industry dye effluent by using naturally available substances (in preparation).

6. N. Priyantha, A.N. Navaratne, T.P.K. Kulasooriya and W. S. A. Weththasinghe, Comparison of the removal of Cu(II) and Zn(II) by using coir dust and brick clay (in preparation)
7. N. Priyantha, A.N. Navaratne and T.P.K. Kulasooriya, Prototype treatment facility for Zn(II) removal from synthetic effluents (Patent in preparation).
8. T.P.K. Kulasooriya, N. Priyantha and A.N. Navaratne, Treatment of industrial effluents using fired brick clay based filter (Patent in preparation).
9. A.N. Navaratne, N. Priyantha and T. P. K. Kulasooriya, Removal of heavy metals using rice husk and brick clay as adsorbents: a study of dynamic conditions, *2nd Int. Symposium on Water Quality and Human Health: Challenges Ahead*, PGIS, University of Peradeniya (2013).
10. N. Priyantha, A.N. Navaratne and T.P.K. Kulasooriya, Adsorption isotherm studies of heavy metal ions on rice husk, *Proc. Pera Univ. Res. Ses.*, University of Peradeniya (2014).
11. T.P.K. Kulasooriya, A.N. Navaratne and N. Priyantha, Optimization of efficiency of phosphate removal by brick clay, *PGIS Research Congress* (2014).
12. N. Priyantha, A.N. Navaratne and T.P.K. Kulasooriya, Sorption studies of textile dyes using naturally available substances, *4th Int. Symposium of Water Quality and Human Health: Challenges Ahead,* PGIS, University of Peradeniya (2015).

SECTION 2

EXECUTIVE SUMMARY OF THE PROJECT

Effluents released from industries contain many hazardous materials which are harmful to the environment as well as to the human being, and consequently, the removal of such materials from the environment has become a priority. In this context, the study is based on the removal of heavy metal ions, anions and textile dyes from industrial effluents using naturally available materials, such as rice husk, brick clay, coir dust, saw dust, dolomite and feldspar, which can be used to develop cost-effective and eco-friendly effluent treatment procedures. Metal ions commonly present in effluents of metal finishing industries, such as Cd(II), Cr(III), Cu(II), Ni(II), Pb(II) and Zn(II); commonly present anions, such as Cl^-, NO_3^- and PO_4^{3-}; and a mixture of textile dyes were specially considered for their removal.

This project was mainly based on the investigation of sorption of industrial pollutants on selected natural substances through parameter optimization, adsorption isotherm studies, kinetics under static conditions, and extending toward dynamic experiments. Further optimization of bed height of and flow rate was performed as an initial step of the prototype treatment system. As the final step, prototype (medium scale) treatment system was constructed for the removal of Zn(II) from synthetic effluents. Among two different flow rates of the prototype treatment systems, a flow rate of 100 cm^3 min^{-1} was selected at which the treatment system achieved 100 % removal efficiency at the beginning, more importantly, the sample concentrations at the discharging point of the system remain below the CEA guidelines for a long time period of more than 3 days.

It is evident that the higher efficiency in pollutant removal is resulted in by natural substances which have higher absorbents sites on their surface. The implemented prototype treatment system could be further modified for the removal of many other pollutants. Modification of the surfaces of absorbents fallowed by further adjustment by parameters could be possible as a future expansion for treatment of industrial effluents on large-scale.

SECTION 3

3.1 INTRODUCTION

3.1.1 Water Pollution

3.1.1.1 Properties of water

Water, a transparent fluid which forms streams, lakes, oceans and rain, is the primary need of all living organisms. Water covers 71% of the earth surface and among that, only 2.5% of earth's water is fresh water. Water dipoles are attracted to each other resulting in hydrogen bonding, a strong inter-molecular attractive force. Different isotope molecules of water (H_2O, D_2O) show different physical and chemical characteristics [1]. In ground water, the D_2O content increases with increasing depth. An increased amount of heavy water has been found in some lakes, the Dead Sea and in great depths of oceans.

In nature, water exists in liquid, solid and gaseous states. At standard temperature and pressure, water is in dynamic equilibrium between liquid and gaseous states. All three states of water can be studied at the same time at the triple point. By further increase in temperature and pressure, it becomes the critical state. At critical temperature and critical pressure, the densities of both states, vapour and liquid, are equal. Any differences in both phases disappear at this state and it is known as the fluid zone. The density of liquid water increases from 0 °C, reaching its maximum at 3.98 °C and decreases up to the boiling point [1,2]. The viscosity of water decreases with increasing temperature. These characters give much impact on life in water as well as on the users of water. Water has the highest surface tension of all common liquids except mercury. Surface tension decreases with decreasing temperature. Water shows many other properties as well as shown below [2]:

- It has a high dielectric constant compared to other pure liquids.
- It shows higher heat of evaporation than that of any other material.
- It shows higher latent heat of fusion than that of any other liquid except ammonia.
- It shows higher heat capacity than that of any other liquid except ammonia

Another important property of water is its ability to dissolve substances. Only few compounds do not dissolve at least to some extent in water. Main reasons for this ability are ionization capacity, dipole character and high dielectric constant. Hydraulic reactions are important in chemical degradation of some water pollutants, such as phosphates, sulfur esters and organometallic compounds. These compounds undergo hydrolysis and may release dangerous pollutants to the environment.

3.1.1.2 Pollution of water

Pollution of water is the contamination of water bodies by chemical species to have their concentrations greater than the natural value. Water pollution is mainly due to discharge of pollutants into water bodies without adequate treatment to remove harmful compounds, and natural factors, such as volcanic eruptions and flood. Pollution of water resources has become a global problem.

Surface water and ground water are interrelated because surface water seeps through the soil and becomes ground water. Pollutants enter the water environment through two types of sources, point sources and non-point sources. A point source is a single identifiable source of pollution, such as a pipe or a drain. For example, industrial effluents are usually released to rivers and sea from point sources. On the other hand, non-

point sources lead to diffuse pollution, and its impact occurs over a wide area, which is not easily attributed to a single source. Therefore, it is difficult to control pollution due to non-point sources as compared to that due to point sources. Rainfall runoff as storm water is a common example of pollution due to non-point sources, through which the water is contaminated with oil, dust and soil sediments. In farming areas; pesticides, fertilizers, animal manure and soil are washed into streams by rainfall runoff. As a non-point source, forestry operations would also result in pollution through soil erosion and sediment runoff [3].

The effect of pollutants on river communities depends on the type of pollutant, concentration of pollutants in the water and the duration of exposure to the community. According to their physico-chemical nature, there can be some effects due to following activities: the addition of toxic substances, suspended solids, non-toxic salts, and human, animal and plant pathogens; deoxidization; heating of water, and the effects of the buffering system [4].

3.1.2 Industrial Water Pollutants

3.1.2.1 Types of pollutants

Industrial revolution results in many achievements, such as more efficient and productive manufacturing processes, and advancement of science. Nevertheless, industrial development led to many problems including water, soil, and atmospheric pollution. There are basically five primary sources of water pollution: domestic sewage, agricultural runoff, industrial effluents, waste water from septic tanks and storm water runoff.

Main reasons for industrial water pollutants are lack of strict pollution control policies, uses of old and out dated technologies that produce large amount of pollutants as compared to modern technologies, lack of capital to invest on pollution control equipment, lack of proper waste disposal sites, lapses of implementation of pollution control, and mining and dwelling operations. Among many industries, metal finishing industry, textile industry, dye industry, leather tanning industry, paint industry, fertilizer and pesticides are some industries that release heavy metal contaminated effluents [5].

3.1.2.2 Heavy metals

Heavy metal is a general term applying to the group of metals and metalloids with an atomic density greater than 6 g cm^{-3} [6]. This term is usually applied to the elements, such as Cd, Cr, Cu, Zn, Ni, Pb and Hg, which are commonly associated with pollution and toxicity problems. Most of the heavy metals are trace metals, which occur naturally in rock forming as rare minerals, and hence there is a range of natural background concentrations of these elements in soils, sediments, waters and living organisms, concentrations higher than natural level would cause pollution [7]. The availability and annual usage of metals vary with the type of each metal. Some metals are abundant and widely used in structural applications, while some others are precious and their use is confined to applications, such as catalysts, filaments or electrodes, for which only small quantities are required. Some metals are considered to be crucial because of their applications for which no substitutes are available and shortages or uneven distribution in supply occur [2]. For instance, chromium is used to manufacture stainless steel which is corrosion–resistant at high temperatures in the presence of corrosive gases. The platinum group metal is used as catalyst in chemical industry, in petroleum refining and automobile exhaust antipollution devices. Metals show wide variety of properties and uses and they form different compounds [8,9]. Table 3.1.1 shows properties and uses of heavy metals and their impact on health and the environment.

Table 3.1.1: Properties, uses and impacts of heavy metals [10-15].

Metal	Properties	Uses	Health/Environment impacts
Cd	Soft, ductile, silvery white	Corrosion resistant plating on steel and iron, alloys, pigments, rechargeable batteries.	Affects kidney and liver, adverse effects on pigmentation and protein concentration.
Cr	MP 1903 °C; BP 2642 °C SG 7.14; hard, silver color	Metal painting, stainless steel, wear resistant, and cutting tool alloys, chemicals.	Fumes may cause bronchial cancers.
Cu	MP 1083 °C BP 2582 °C SG 8.96; ductile, malleable	Electrical conductors, alloys, chemicals.	
Pb	MP 327 °C BP 1750 °C SG 11.35; silver color	Storage batteries, chemicals, used in gasoline, pigments.	Affects bone marrow; formation of blood hemoglobin; replace Ca in bone.
Ni	MP 1455 °C BP 2835 °C SG 8.90; silver color	Alloys, coins, storage batteries, catalysts.	
Zn	MP 420 °C BP 907 °C SG 7.14; bluish white	Brass, galvanized steel, paint pigments, chemicals.	Vomiting, diarrhea

Note: MP-melting point, BP-boiling point and SG-specific gravity

This section briefly discusses sources, effects, health impacts of individual heavy metal ions, such as cadmium, copper, chromium, lead, zinc and nickel.

Cadmium

Cadmium is non-essential metal and it is the 64th most abundant element in earth crust. Unlike other heavy metals, cadmium does not spread globally in different ecosystems. Cadmium reaches the atmosphere and water through natural or man-made sources. Volcanic eruptions, ocean sprays, forest fires and weathering of rocks are main natural sources. Among them volcanoes release large quantities of aerosols containing chromium. Some man-made sources of cadmium are non-metal smelters and refineries, coal combustion, incineration of solid waste, iron and steel industries and Zn ores.

Cadmium is mostly used in cadmium nickel batteries, alloys, steel painting, pigments, polymer stabilization and electronics. Cadmium uptake by plants depends on its concentration and pH. Increase in soil pH by adding lime, drastically decreases cadmium intake by plants. Addition of fertilizer contaminated with Cd results in its uptake by vegetables and corps. Further, cadmium can enter water bodies during manufacturing use or in discharging steps.

Cadmium is highly toxic heavy metal, which is accumulated in certain parts in the human body, such as kidney and skeleton. Highly populated areas contaminated with cadmium, such as certain areas in Japan, have been reported to have many renal diseases,

particularly "itai-itai" disease, nephritits and nephosis due to consumption of rice fields effected [1,9].

Copper

Copper is an essential element for plants and animals, which is available in water in different forms. It is the 26th most abundant element in earth crust and the requirement of an adult human is 2 mg [8]. Copper is an essential component of ascorbic acid oxidase, tyrosinase, uricase, cytochrome oxidase and galactose oxidase. Its higher concentration in water may be due to several sources, such as copper mining and smelting, brass manufacture, electroplating, paints, chemicals, pesticides.

Copper is a corrosion resistant metal, widely used due to ductile ability, malleability, electrical conductivity and ability to conduct heat. In addition to its use as electrical wires, copper is used in tubing shims, gaskets and other applications. Copper salts are used in water supply systems to control the growth of algae and fungi.

Copper salts may favorably influence feed conversion efficiency, growth rates. Higher concentration of copper leads to acute toxicity in humans, possibly due to redox cycling and generation of reactive oxygen species that damage DNA. Humic acid presents in natural waters is known to form complexes with copper in the pH range between 6 and 8. These complexes are less toxic to water, plants and animal [8,9].

Chromium

Chromium is the 22nd most abundant element in earth crust with an average concentration of 100 mg L^{-1}. Chromium compounds are found in the environment due to corrosion of chromium containing rocks and can be distributed by volcanic eruptions. Chromium normally occurs in the form of inorganic ions in trivalent and hexavalent forms. The trivalent form, Cr(III), is more toxic than Cr(VI) to living organisms, including human. Chromium is the second most abundant inorganic pollutant when industrial emission is considered.

A large number of chromium salts are used in industries, such as wood dying, tanneries, electroplating, ceramic, explosives and corrosion control units [9]. Therefore, pollution of soil and water occurs as a result of dumping of chromium containing waste.

Chromium ion, CrO_4^{2-} enters biological cells due to its structural similarity to the sulfate ion, SO_4^{2-}, and oxidizes DNA and RNA bases, leading to a health risk [1]. When chromium enters plants, it causes yellowing of leaves of crops. It causes cancer in respiratory organs, especially in workers chronically exposed to chromium containing dusts.

Lead

Lead is the 37th most abundant element in earth crust which is regarded as a heavy metal as well as a poor metal. Some characteristic properties of lead are high density, softness, ductility and malleability, poor electrical conductivity. It is highly resistant to corrosion and shows ability to react with organic chemicals. Metallic lead occurs in nature although it is a rare element. It is found in ores with other most abundant elements and is extracted together with these metals.

Lead was used as a structural metal in ancient times and for weather proofing buildings, in water ducks and cooking vessels [1]. Lead acid batteries, bullets and shots, fusible alloys, as a radiation shield are some of other uses of lead. The main source of lead pollution is petrol combustion, fossil fuel combustion in soils, paint flakes from paint containing Pb and Pb containing in pipes and pesticides [9]. Owing to its toxicity, lead-containing petrol is banned in many countries.

Lead, above a certain concentration, is poisonous to animals, including humans. It damages the nerve systems, cardiovascular system, kidneys, and immune system and may cause brain disorders [16]. Excessive lead also causes blood disorder to mammal. If affects almost every organ and system in the body. Long term exposure to lead or its salts can cause nephropathy and abnormal pains, increase blood pressure. Exposure to high levels can severely damage the brain and kidney and ultimately cause death.

Zinc

Zinc is an essential trace element for plant and animals including humans, and it plays a vital role in metabolic processes. In natural water, zinc is found in traces less than 1 mg L^{-1} which is in safe limits. Zinc makes up about 75 mg L^{-1} of the earth's crust, making it the 25^{th} most abundant element. Soil contains Zn in a large range of 5 - 770 mg $L^{-1}$with an average of 64 mg L^{-1}; sea water has 30 mg L^{-1}; the atmosphere contains $(0.1 - 4.0)\times10^{-6}$ mg L^{-1}. Zinc sulfide is the most heavily mined zinc containing ore because its concentrate contains 60 – 62% zinc.

The metal is widely used in iron galvanizing process. Industrial manufacturing of zinc containing fungicides, viscose process in rayon fibers, zinc smelters, galvanizing units, dezincification of brass are some zinc releasing industries.

Concentration above 5 mg L^{-1} causes a bad taste. The free zinc ion in solution is highly toxic to plants, invertebrates and even to vertebrate fish. Excessive zinc may give a white scum or greasy layer on water surface. In rivers passing by zinc smelters, the zinc load of water has been reported up to 25 mg L^{-1} [8]. This effects nature via absorption of water and its accumulation in the body of fish may cause severe hemolytic anemia, liver and kidney damage, vomiting diarrhea.

Nickel

Nickel (24^{th} most abundant element in earth crust) belongs to transition metal and is hard and ductile. On earth, nickel occurs most often in combination with other metallic and non-metallic compounds. The bulk of the nickel mine comes from different types of ore deposits.

Nickel is considered as a corrosion resistant metal because of its slow rate of corrosion, and about 6% of world nickel production is used for corrosion resistant nickel plating. Nickel was a common component of coins in the past. It is used in many industrial and consumer products, including stainless steel magnets, rechargeable batteries, electric guitar strings, microphone capsules and alloys. Nickel is used as a binder in the cemented tungsten carbide in hard metal industry.

Nickel is largely been replaced by cheaper iron because of its skin allergic reactions to some people. Nickel sulfide fume and dust are believed carcinogenic, and nickel carbonyl is an extremely toxic gas [17].

3.1.2.3 Anions

Ions in their gaseous states are highly reactive, although gas phase ions do not occur in large amounts on earth, except in flames, lighting, electrical sparks and other plasmas. Anions rapidly interact with opposite charges and give neutral molecules or ionic salts. The most common stabilizer species is sea water and are most commonly found in the environment at low temperature. Table 3.1.2 shows properties and uses of anions and their impact on health and the environment.

Table 3.1.2: Properties, uses and impacts of anions [8,9].

Anion	Uses	Health/Environment impacts
Sulfate	Production of batteries; use as a fertilizer, ingredient in rubber vulcanization and a food preservative.	Dehydration
Phosphate	Use in the production of water based paints and coatings, and detergents; use in processing in ceramics and treatment of drinking water.	Eutrophication; may cause damage to liver, heart and kidney.
Nitrate	Use as a fertilizer and an oxidizing agent.	Blue baby syndrome; causes problems in thyroid gland; results in algae in water preventing photosynthesis.
Chloride	Use as a disinfectant and an oxidizing agent; use to make PVC.	Can cause liver damage; free chlorine strongly oxidize biological materials

This section briefly discusses sources, effects, health impacts of individual heavy anions, such as cadmium, copper, chromium, lead, zinc and nickel.

Phosphate

Many phosphates are not soluble in water under normal temperature and pressure. Phosphate species exist as PO_4^{3-}, HPO_4^{2-} and $H_2PO_4^-$ in aqueous medium, and the relative concentrations of these species depend on the solution pH according to the following equilibria with pK values of 2.12, 7.24 and 12.67.

$$H_3PO_4(aq) + H_2O(l) \rightleftharpoons H_3O^+(aq) + H_2PO_4^-(aq)$$

$$H_2PO_4^-(aq) + H_2O(l) \rightleftharpoons H_3O^+(aq) + HPO_4^{2-}(aq)$$

$$HPO_4^{2-}(aq) + H_2O(l) \rightleftharpoons H_3O^+(aq) + PO_4^{3-}(aq)$$

Since these pKa values differ by more than 4, different forms of acids behaves as separate weak acids. The region of acid in equilibrium with its conjugate base is defined by pH $\approx$ pK $\pm$ 2, and hence, the pH ranges for the predominant existence of $H_2PO_4^-$, HPO_4^{2-} and PO_4^{3-} are 0-4, 5-9 and 10-14, respectively. Neutral aqueous systems thus contain pH contains $H_2PO_4^-$ and HPO_4^{2-} ions in significant amounts.

Phosphates are naturally occurring from elemental phosphorous found in many phosphate minerals. Phosphate mines are primarily found in North America, Africa and the Middle East. Phosphate minerals in phosphate rock are in hydroxyapatite and fluoroapatite forms. Phosphorous is mainly used in agriculture and industry. Industrial wastewater released from industries, such as ceramics, aluminum alloy production, textile and plastics, is contaminated with phosphate. As there are so many sources of phosphorous, this is an easy way to pollute water.

Slight increase in nutrient concentration entering the water body can increase the rate of eutrophication. Eutrophication would happen when the concentration of phosphorous in water body becomes higher than 0.02 mg L^{-1} [18,19]. In order to remove

the excess phosphorous from wastewater, many treatment techniques are available, such as chemical precipitation, biological treatment and adsorption technique [20,21].

Chloride

Chloride, naturally present as sodium, potassium and calcium chlorides, is an essential nutrient for plants and animals including humans, although higher concentration of chloride contamination can be harmful. Most inorganic compounds containing chlorine readily dissolve in water. Hydrochloric acid, an irritant gas, is a main source of chloride [9,22].

Major uses of sodium chloride in industries are, the production of chlorine gas and caustic soda, production of plastic PVC, use in de-icing roads, and use as a water softener. Inorganic chloride is mainly released from industries as a waste product of many processes [23]. Weathering of chloride containing minerals and coal combustion are some naturally polluting paths. Although many plants and animals show high tolerance to chloride, some animals and plants are sensitive to chloride and excessive exposure can cause serious effects.

Sulfate

Sulfate is the second most available anion in hard water reservoirs, which is second to bicarbonate. In natural occurrence, water passes through rock or soil containing gypsum and other common minerals release sulfur. Further, sulfate is released to the environment as a result of municipal and industrial discharges. Industries that release sulfate include tanneries, pulp mill sand textile mills [24].

Sulfate is an essential plant nutrient which utilizes sulfur and it affects algal growth. When the sulfate concentration is less than 0.5 mg L^{-1}, algal growth does not occur. Sulfate present in water is however important in certain industrial processes, such as sugar production and concrete manufacturing.

Sulfates are not considered toxic to plants or animals at normal concentrations. In humans, concentrations of 500-750 mg L^{-1} cause a temporary laxative effect. However, doses of even several thousand mg L^{-1} would not cause any long-term ill effects. Sulfates are toxic to cattle at very high concentrations. Problems caused by sulfates are usually related to their ability to form strong acids which changes the pH of the environment. Sulfate ions also are involved in complexing and precipitation reactions which affect solubility of metals and other substances.

3.1.2.4 Textile Dyes

Dye pigments are substances which when applied to a substrate lead to selective reflection or transmission of incident light. Pigments usually show extremely low solubility in water. Dyes are mainly use in industries, such as textile, pulping, pharmaceutical, tanneries and bleaching [25]. In dying process, 10-25% of dyes lost during the drying operation. Discharge of dye effluents into the water environment is undesirable; not only because of their colour but also because of many of dyes released and their breakdown products are toxic and carcinogenic. Another problem associated with dyes in textiles industry is the excessive use water, which would ultimately get contaminated with dyes. Polluting effects of dyes against aquatic environment can result in toxic effects due to the long-term stability of dyes or their degraded products. These substances could be accumulated in sediments, fish or other aquatic life forms.

Most dyes are non-biodegradable, having carcinogenic action or cause allergies, dermatitis, skin irritation. Various azo dyes, mainly aromatic compounds, show both acute and chronic toxicity. High potential health risk is caused by adsorption of azo dyes and

their breakdown products through the gastro-intestinal tract, skin, lungs and also formation of hemoglobin adducts and disturbance of blood formation. LD_{50} values reported for aromatic azo dyes range between 100 and 2000 mg kg^{-1} body weight. Several azo dyes cause damage on DNA that can lead to the genesis of malignant tumors [25,26].

3.1.3 Treatment of Polluted Water

Surface water is often contaminated by harmful chemicals from human activities or from natural sources. Although many techniques can be employed for the treatment of inorganic effluents, the ideal treatment should not be only suitable, appropriate and applicable for local conditions, but also should meet the maximum contaminant level (MCL) standards established. Due to the presence of above mentioned pollutants in water, many treatment techniques have been adopted by industries. Some conventional methods available for this purpose are chemical precipitation, flotation, Ion exchange and electrochemical deposition.

3.1.3.1 Chemical precipitation

Chemical precipitation is the most common method used to remove dissolved pollutants, mainly inorganic pollutants, from wastewater. As heavy metal ions are present in ionic form in solutions, they can be precipitated as hydroxides or sulfides. In hydroxide precipitation, hydroxide ions react with heavy metal ions to produce their precipitates. Adjustment of the medium pH is the most important parameter that significantly improves the metal ion removal process through chemical precipitation. In hydroxide precipitation, NaOH, $Ca(OH)_2$, CaO, and $Mg(OH)_2$ are used as chemical reagents, while Na_2S, Fe_2S and CaS are used as reagents in sulfide precipitation [27,28]. Among these reagents, owing to availability and low cost nature, lime and limestone are used in most industries. These substances can be successfully used to treat inorganic effluents with a pollutant concentration even higher than 1000 mg L^{-1}. Sulfide precipitation is much popular due to its ability of very low solubility and it precipitates as sulfides over a broad range of pH. Other than all these reagents, carbonates (e.g.: Na_2CO_3 and $CaCO_3$) can also be used in chemical precipitation [29].

3.1.3.2 Ion exchange

Ion exchange is another method used successfully in the treatment of industrial effluents for the removal of pollutants. An ion exchanger is a solid capable of exchanging either cations or anions from the surrounding materials. Ion exchangers can be synthetic (e.g.: organic ion exchange resins) or natural (e.g.: clay), which are usually nonselective and highly sensitive to the pH of the solution [28]. In every ion exchange process, stationary phase is the exchanger while the mobile phase is wastewater or industrial effluents. Compounds containing sulfonic acid ($-SO_3H$) and carboxylic acid (-COOH) groups can function as cation exchangers, where hydrogen ions in the sulfonic/carboxylic group serve as exchangeable ions with metal cations. Therefore, metal ions present in wastewater can be easily removed by a cation exchange process.

3.1.3.3 Membrane filtration

The membrane acts as a very specific filter that allows water to flow through, while suspended solids and other substances are remained. It is a porous continuous film with pores ranging from 10 μm to 10 Å which is made from natural or synthetic polymers. The pore size of the membrane depends on the specific application. These membranes provide physical barriers that effectively remove solids, heavy metals, viruses, bacteria and other unwanted molecules by applying a high pressure, concentration gradient or an

electric potential across the membrane to separate substances. Ultrafiltration and reverse osmosis are the two types of membrane filtration methods, and the former utilizes permeable membrane to separate heavy metals, macromolecules and suspended solids from solution on the basis of the pore size (5–20 nm) and molecular weight of the separating compounds (1,000 –100,000 Da). These unique specialties enable ultrafiltration to allow the passage of water and low-molecular weight solutes, while retaining the macromolecules, which have a size larger than the pore size of the membrane [30].

3.1.3.4 Electrodialysis

Electrodialysis (ED) is a membrane separation in which ionized species in the solution are passed through an ion exchange membrane by applying an electric potential. The membranes are usually thin sheets of plastic materials with either anionic or cationic characteristics. When a solution containing ionic species passes through the cell compartments, the anions migrate toward the anode and the cations toward the cathode, crossing the anion exchange and cation-exchange membranes [31].

3.1.3.5 Coagulation

Coagulation is the destabilization of colloids, which are either positively or negatively charged, by neutralizing the forces that keep them apart. Size of the colloidal particles range between 10^{-6} m to 10^{-9} m. Due to repulsive forces, particles do not contact with each other, and hence, coagulation is achieved with the help of a coagulant, such as $Al_2(SO_4)_3$, $AlCl_3$, $Fe_2(SO_4)_3$ or $FeCl_3$. These salts neutralize the charges on the particle, resulting in lower repulsive forces between them. Further, coagulation process can be increased by proper mixing [27].

3.1.3.6 Flocculation

Flocculation is the action of polymers to form bridges between the flocs and bind the particles into large agglomerates or clumps. This can be achieved by adding high molecular weight, water soluble organic polymers which increase the size of the floc, leading to settle down particles [27].

3.1.3.7 Adsorption

Adsorption is a process that occurs when a gas or liquid solute accumulates on the surface of a solid or a liquid forming a molecular or atomic film. The process of adsorption arises due to the presence of unbalanced or residual forces at the surface of a liquid or solid phase. These forces have a tendency to attract and retain the molecular species with which it comes in contact with the surface. Adsorption mainly divides into two as physisorption (The adsorbate molecules adhere to the surface of the adsorbent through the weak interaction such as Van der waals) and chemisorption (The adsorbate molecules attached to the surface of the adsorbent by forming chemical bonds). High adsorption capacity, porosity, high specific surface area and high thermal stability are some of the qualities of a good adsorbent. Some commonly use adsorbents reported are activated carbon, zeolites, clay, rice husk, coir dust, saw dust and tea waste [12,14,15].

Table 3.1.3 summarizes the advantages and disadvantages of each wastewater treatment technique.

3.1.4 Use of Natural Adsorbent Materials for Treatment of Wastewater

Among all other treatment techniques described in Table 3.1.3, adsorption is becoming an attractive treatment technique to remove pollutants from waste water.

Table 3.1.3: Advantages and disadvantages of wastewater treatment techniques [27,32].

	Advantages	**Disadvantages**
Chemical precipitation	• Simplicity of the process • Inexpensive equipment requirement • Convenient and safe operations	• Requirement of a large amount of chemicals. • Long-term environmental impacts of sludge disposal • Requirement of excessive sludge production for further treatment. • Slow metal precipitation • Poor settling • Aggregation of metal precipitates
Ion exchange	• High treatment capacity • High removal efficiency (99.9%) • High selectivity • Fast process • Produced sludge volume is less	• High initial cost • High operational cost • Difficulty in handling concentrated metal solution as the matrix
Membrane filtration	• Increase heavy metal removal efficiency • Reduce operational and chemical cost • Can be used for large scale application • Small space is enough • Membranes are highly selective	• Membranes cannot be used at high temperatures. • High concentration of chemical substances can reduce the lifetime of membranes.
Electrodialysis (ED)	• Relatively low energy consumption • Only limited pretreatment needed • Suitable for separating non–ionized from ionized compounds	• Organic matter, colloids and SiO_2 are not removed. • Feed water pre-treatment is necessary.
Coagulation and Flocculation	• Simple method • Rapid process	• High operational cost • High sludge production and formation of large particles • Requirement for considerable quantities of coagulants and flocculants
Adsorption	• Low cost • High efficiency • Minimization of chemical or biological sludge • Regeneration of biosorbent • Possibility of metal recovery	• Relatively high capital cost • Difficulty in separation of biosorbents after adsorption.

Adsorption is a simple process, which is environmentally friendly and low cost, as compared to others. It is a mass transfer process by which a substance is transferred from the liquid phase to the surface of a solid. Various adsorbents, derived from agricultural waste, industrial byproducts, natural materials or modified biopolymers have been recently developed and applied to remove pollutants from wastewater.

There is an enormous number of literature on the removal of various pollutants by naturally available substances and industrial byproducts. Equilibrium studies, mainly adsorption isotherms and the determination of the capacity of a particular pollutant on a selected adsorbent (q_{max}) have been reported in many instances. Both the Langmuir and the Freundlich adsorption models have been fulfilled by many sorption systems although it can be argued to be contradictory from the point of view in chemical principles because it is unlikely to have a metallic pollutant layer deposited on top of another such layer. Such molecular level issues have not been considered in many literature reports although the removal of pollutants have been considered as a bulk process.

Table 3.1.4 summarizes recent literature reports on the use of natural adsorbents to remove heavy metal ions, anions and dyes, together with desirable pH and the capacity of removal.

Kinetics of removal of pollutants by natural sorbents have also been reported in the literature although much less attention has been paid on this issue, probably due to the complexity of performing kinetics experiments because rate processes should be investigated before the system reaches equilibrium, which is fast in many natural adsorption systems due to the presence of the pore structure of natural sorbents.

3.1.5 Basic Characteristics of Natural Adsorbents

Natural adsorbents are heterogeneous systems containing many reactive moieties to capture pollutants, demonstrating their effectiveness in effluent treatment.

Brick clay consists of an inorganic colloidal fraction, comprising of clay minerals, oxides and hydrous oxides of minerals, is the most responsible fraction for sorption by its mineral particles. Most typical types of clays are kaolinite, montmorillonite and illite, and the composition of each depends on the geographic location [50]. Due to cation exchange ability, these clay minerals show a much greater ability for immobilizing chemicals, such as metal ions. Having negatively charge on clay particles is an important factor influencing sorption properties toward metal ions [51].

Rice husk, a byproduct of rice processing industry, is a fibrous material containing a huge amount of silica of approximately 95% [52], together with organic compounds, such as cellulose, hemicellulose, and lignin. This composition of rice husk makes it possible to be regarded as an adsorbent. Although it is used as a raw material for production of xylitol, furfural, ethanol, acetic acid and used as a cleaning or polishing agent in metal and machine industry in manufacturing of building materials [53], it is a waste in the local context. It has been revealed that rice husk can be used for removing ionic dyes from aqueous solutions [54] and pre-treated rice husk has been used for the sorption of cadmium from effluents [55].

Coir dust is a light brown to dark brown colour fluffy material which falls off from coconut husk when it is shredded during coir processing [56,57]. Coir dust is about 70% of the weight of the coconut husk. This fall off material is available as a waste product since it has no industrial value [58]. Coir dust has been used as a sorbent to remove heavy metals ions [59]. Since it consists of high cellulose (ca. 36%) and lignin (ca. 54%) with low ash content [57], coir dust is characterized as lignocellulosic material which is

hygroscopic having the affinity for water. More importantly, carboxylate and phenolic groups of lignin, pectin and hemicellulose are known as the main sites for metal binding where the bonds are predominantly of covalent character.

Table 3.1.4: Use of natural adsorbents to remove pollutants in industrial effluents using adsorption technique.

Type	Pollutant	Adsorbent	pH	% removal	q_{max}/ mg g^{-1}	Ref
Heavy metals	Zn(II)	Rice husk	7.0	70	19.6	[33]
	Pb(II)	Rice husk	9.0	97	0.62	[33]
		Tea waste	5.0-6.0	-	65	[34]
	Cu(II)	Tea waste	5.0-6.0	-	48	[34]
		Irish peat	6.0-9.0	91	7.4	[35]
	Ni(II)	Irish peat	6.0-9.0	87	6.4	[35]
	Cr(III)	Banana peel	5.0	40	3	[35]
		Orange peel	5.0	65	9	[35]
	Cd(II)	Duriyan peel	5.0	72	18.6	[36]
		Irish peat	6.0-9.0	78	5.2	[35]
		Corn peel	5.0	51	-	[36]
		Banana peel	5.0	73	20.9	[36]
	Cr(VI)	Muthurajawela peat	3.8-4.2	-	0.12	[37]
Anions	F^-	Brick powder	8.0	54	-	[38]
	SO_4^{2-}	Modified coir pith	2.0	70	8.8	[39]
		Activated carbon	7.0	43	-	[40]
		Feldspar	5.0	52	-	[41]
	PO_4^{3-}-P	Processed brick clay	-	-	3.8	[42]
		Feldspar	5.0	42	-	[41]
		autoclaved aerated concrete (AAC)	-	98	14.3	[43]
	NH_4^+-N	Processed brick clay	-	-	0.73	[42]
Dyes	Crystal Violet	NaOH–modified rice husk	8.0-10.0	98	45	[44]
		Grapefruit peel	6.0-10.0	98	254	[45]
		Wood apple shell	10.0	95	19	[46]
		Palm kernel fiber	7.0-11.0	88	79	[47]
		Acacia nilotica leaves	-	-	33	[48]
	Methylene blue	Wood apple shell	10.0	90	95	[46]
		Palm kernel fiber	7.0-11.0	96	95	[47]
		Coffee husks	6.0-11.0	87	90	[49]
	Rhodamine B	*Acacia nilotica* leaves	-	-	37	[48]

Saw dust is a complex substance and it can have different extractives such as, trepenes, trepenoide, phenol, lignans and tannins. Saw dust is mainly composed of cellulose (45-50%) and lignin (23-30%), both with a capacity for binding metal cations due to hydroxyl, carboxylic and phenolic groups present in their structures. Thermal stability of saw dust is determined by cellulose, hemicellulose and lignin contents [60].

Feldspar and dolomite are considered as ion exchange properties. Ion exchange reactions that would take place on the surface make them used as adsorbents for pollutant removal [61,62].

3.2 SCIENTIFIC SCOPE OF THE PROJECT (OVERALL AND SPECIFIC OBJECTIVES)

Environmental contamination with metal ions, anions and dyes has been a potential threat to the ecosystem because most of such substances do not undergo biodegradation, accumulating in the environment [63]. Treatment of waste water is therefore a necessity. Available conventional methods, which require chemicals, need pre-treatment steps, and they are neither economical nor environmentally friendly. Consequently, effluent and treatment methods based on sorption on naturally available substances have become attractive. Many naturally available materials and industrial waste have already been tested at research level leading to successful results for the removal of various pollutants.

Use of natural and industrial byproducts in solving real environmental problems (e.g.: treatment of real industrial effluents) is still at early stages and use of them has not been sufficiently expanded. An early finding of this nature is the use of burnt brick pieces to remove fluoride to produce clean water for drinking [64]. Similar work has been continued attempting other types of industrial byproducts [65,66]. Heat treatment of adsorbents would significantly change their chemical and physical properties, leading to changes in both surface and bulk properties. Optimization of parameters, including the firing temperature, medium pH and time of exposure would thus be necessary before treatment of industrial effluents at large scale is conducted. Initialization of such experiments has lead to successful results [67,68]. However, most of the reported methods are yet at research stage, limited to small-scale, laboratory experiments conducted under static conditions (batch experiments). In order to fill the void between laboratory findings and industrial applications, it is important that a series of basic laboratory experiments under dynamic conditions be first conducted and subsequently expanded to pilot scale, before the application in industries for large-scale industrial effluent treatment. Optimization of parameters under dynamic experimental conditions, kinetics and equilibrium studies of sorption of various pollutants and selection of suitable adsorbents for different types of industrial effluents for efficient removal of pollutants at pilot scale will be of novelty.

The general objective is to investigate interaction between industrial pollutants and selected natural sorbents and industrial byproducts under static and dynamic conditions with extension towards the development of a prototype industrial effluent treatment unit. The specific objectives of the project are listed below:

1. Analysis of different types of industrial effluents.
   E.g.: Textile effluents, metal finishing industry
2. Optimization of parameters for efficient removal of individual pollutants using each substance (static conditions).
3. Optimization of parameters for efficient removal of individual pollutants using each substance (dynamic conditions).
4. Processing of selected sorbents and characterization after processing.
5. Equilibrium and kinetics studies of sorption.
6. Investigation of removal of pollutants from synthetic and real effluents under dynamic conditions.
7. Extension for experiments for larger volumes using filters consisting of different types of selected sorbents.
8. Construction of a prototype treatment unit and investigation of pollutant removal efficiencies of different industrial effluents in the prototype unit.

3.3 MATERIALS AND METHODS

3.3.1 Materials

Standard aqueous solutions of Cd(II), Cr(III), Cu(II), Ni(II), Pb(II) and Zn(II) were prepared using analytical grade reagents of their nitrates or sulfates. Standard solutions of phosphate, sulfate and chloride were prepared using analytical grade $KH_2(PO_4)$, Na_2SO_4 and NaCl, respectively. Solutions pH was controlled using HNO_3 and NaOH. Solutions of $NaNO_3$ of concentrations of 0.1 mol dm^{-3}, 0.01 mol dm^{-3}, and 0.001 mol dm^{-3} were used for the investigation of the surface charge of the adsorbents while methylene blue was used for the determination of the surface area of the adsorbent.

Adsorbents were collected from different locations of Sri Lanka as shown in Table 3.3.1. All adsorbents were thoroughly mixed, sieved using 1.0 mm sieve. For all static and dynamic conditions, rice husk was used in its natural form, and coir dust and saw dust were used with particles of diameter (d) < 1.0 mm. Brick clay particles were crushed, and particles of d < 1.0 mm were used for all static experiments, while particles of 0.5 cm < d < 1.0 cm were used for column studies. Dolomite and feldspar were crushed using a ball mill and particles of d < 1.0 mm were used for adsorption studies.

Table 3.3.1: Location of each sorbent collected.

Adsorbent	Place collected
Rice husk	Sangarajapura, Kandy
Brick clay	Gelioya, Peradeniya
Dolomite	Matale
Feldspar	Raththota
Coir dust	Rambukkana
Saw dust	Akurana

3.3.2 Instrumentation

Adsorbent samples were heated up to pre-determined temperatures using Carbolite CTF 12/100/900 tube furnace; Spectro-electronic M series atomic absorption spectrophotometer (AAS) was used to measure the total concentration of each metal in solutions. Metals present in adsorbents were determined using X-ray fluorescence (XRF) spectrophotometer (Fischerscope Model-DF500FG-456) and X-ray diffractometer (XRD) (Siemens Model D50000) using Cu-K X-ray beam (1.54056 Å). Surface titration experiments were conducted with digital pH meter (Orion Model 960, USA). Fourier transform infrared (FTIR) spectra were recorded on Thermo Nicolet Model-Avater 320 FTIR spectrophotometer, while scanning electron microscopic (SEM) images were taken using Oxford Instruments – EVO LS 15 (Zeiss) instrument. Mass changes of adsorbent and heat flow with different firing temperatures were studied by Thermal Gravimetric Analyzer (TGA) (Model STA-N-650). UV/Vis Spectrophotometer (Shimadzu UV 1800 series) was used in order to determine the concentrations of coloured species.

3.3.3 Research Design

3.3.3.1 Meta analysis of industry data

Questionnaires were prepared by considering different aspects of the treatment of pollutants present in selected industries: Metal finishing, textile and dye. Information was gathered from Katunayake, Biyagama and Seethawaka export processing zones (Annexure 1).

3.3.3.2 Analytical methods

Standard analytical methods were used for the determination of various chemical species: Cl^- by ion-selective electrode technology; PO_4^{3-} by Vanadomolybdophosphate method; and SO_4^{2-} by turbidimetry. Total concentration of all metal ions was determined using AAS. All determinations were done with the aid of a calibration curve. The extent of removal of each species by an adsorbent was determined as a percentage removal using Equation (3.3.1),

$$\text{Percentage removal} = \frac{C_i - C_f}{C_i} \times 100\% \qquad (3.3.1)$$

where C_i is the initial concentration of the species and C_f is the concentration of the species in the supernatant solution after treatment.

3.3.3.3 Analysis of industrial effluents

Effluent samples were collected from the above selected industries, and analyzed for basic physico-chemical parameters, heavy metal ions and anions in order to identify pollutants present in each effluent sample. UV-Visible spectra were obtained for all effluent samples in order to select an industry for further dye removal experiments.

3.3.3.4 Characterization of adsorbents

Sample preparation

As none of the natural adsorbents used (brick clay, rice husk, feldspar, dolomite, coir dust and saw dust) was homogeneous, bulk samples were crushed, mixed well, representative samples were taken and separated into desired sizes using a set of sieves. Heat treatment at the pre-determined temperatures was applied for certain adsorbents. The temperature programme applied for firing consisted of three steps, as listed below:

1. Linear temperature scan from room temperature to the firing temperature,
2. Maintaining the temperature at constant for a period of 4.0 h,
3. Allowing natural cooling down to room temperature.

Surface titration

Experiments of surface titrations were carried out to investigate the surface charge of adsorbent particles. For surface titrations, 1.25 g of adsorbent, stirred with 250 cm^3 of 0.10 mol dm^{-3} $NaNO_3$ solution, was used. This is equivalent to 5.00 g dm^{-3} adsorbent suspension in 0.10 mol dm^{-3} $NaNO_3$. The pH of the suspension was adjusted to 4.0 by adding 0.10 mol dm^{-3} HNO_3 acid (standardized with a primary standard Na_2CO_3 solution of 0.100 mol dm^{-3}). Then, it was titrated up to the pH of 9.5 with a 0.10 mol dm^{-3} NaOH solution (standardized with the secondary standard HNO_3 acid solution above). This experiment was repeated for 0.010 mol dm^{-3} $NaNO_3$ and 0.0010 mol dm^{-3} $NaNO_3$ solutions. Changes in pH of suspensions were recorded when the NaOH solution was added dropwise. Surface charge – pH curves were then constructed in the same plot for

different ionic strengths of $NaNO_3$ solutions in order to determine the point of zero charge (pH_{pzc}), the common point of intersection of surface charge - pH curves.

Thermogravimetric analysis

Adsorbents were analyzed for mass changes and heat flow by varying the treatment temperature. This experiment was conducted using Thermogravimetric apparatus by changing the operational temperature of the powdered sample from room temperature up to 1000 °C.

XRF and XRD analysis

Samples were powdered and particles of $d < 0.063$ mm were used in XRD analysis. Each adsorbent sample was separately treated with 1000 mg L^{-1} metal ion solution with stirring at 150 rpm for 60 min. Each suspension was filtered and dried. Dry samples of metal-sorbed adsorbents and respective untreated adsorbents were used for XRF analysis.

FTIR and SEM analysis

Powdered adsorbent ($d < 0.063$ mm) samples before and after treatment with metal ion solutions were analyzed on the FTIR spectrophotometer using the KBr pellet method. Microscopic adsorption sites of adsorbents were investigated through SEM images.

Analysis of leachates

In order to understand the extent of leaching of metal ions from different adsorbents, leachate solutions were tested for different metal ions. All six adsorbents were shaken with distilled water for 60 min and allowed to stand for 60 min in order to reach equilibrium. Then, solutions were analyzed for heavy metal ions (Cd, Cr, Pb, Zn, Ni and Cu) and common metal ions (Ca, Mg, K and Na).

Determination of specific surface area

A sample of 0.100 g of adsorbent was shaken with 10.00 cm^3 of deionized water (Solution A). A sample of 0.0120 g of methylene blue dye was dissolved in 100.00 cm^3 of deionized water (Solution B). Solutions A and B were allowed to mix for 2.0 h, and the mixture was allowed to stand overnight. A 5.00 cm^3 aliquot of the supernatant was removed and centrifuged. The concentration of methylene blue in the supernatant was determined at 662 nm. The same procedure was followed using different concentrations of methylene blue solutions.

3.3.3.5 Metal ion removal by rice husk and burnt brick particles under static conditions

General aspects

Standard solutions of Cd(II), Cr(III), Cu(II), Zn(II), Ni(II) and Pb(II) were separately treated with rice husk (air-dried and heated at different temperatures) under static conditions. According to the analysis of industrial effluents, the most prominent metals present in industrial effluents are Cu(II) and Zn(II). Therefore, removal of these two metals using brick clay was primarily focused on using static conditions. All static experiments were conducted in triplicate at a rotation speed of 150 rpm, and the average values were reported.

Parameter optimization of heavy metal removal using rice husk and fired brick clay

Optimization of firing temperature: Representative rice husk samples were heated at predetermined temperatures in the range from 60 °C to 200 °C. All experiments were

performed using rice husk in its natural size without any particle size modification, under static conditions using metal ion solutions of 10.0 mg L^{-1}. In each experiment, 50.0 cm^3 of each metal ion solution was shaken with 2.50 g of rice husk, and the system was allowed to reach equilibrium. The extent of removal at different treatment temperatures was calculated to determine the optimum temperature of treatment for rice husk.

Based on literature reports, brick clay fired at 400 °C was selected to conduct the experiments for both heavy metal ions, Cu(II) and Zn(II) [69].

Optimization of contact time: The effect of contact time on adsorption was observed by varying shaking time and settling time. For optimization of stirring time, 50.0 cm^3 aliquot of 10.0 mg L^{-1} metal ion solution was thoroughly shaken with 2.50 g of rice husk, which had been heated at 100 °C, for different shaking times from 0 min to 60 min followed by a constant settling time of 1.0 h. The extent of removal at different treatment shaking times was calculated to determine the optimum shaking time. After optimization of shaking time, similar experiments were carried out to optimize settling time (waiting time) by employing the pre-determined optimum shaking time for different settling times from 0 min to 60 min.

Similar experiments were conducted with brick clay fired at 400 °C using 5.0 g brick clay for different shaking times from 0 min to 90 min followed by a constant settling time of 1.0 h to determine the optimum shaking time, and repeating the experiment at the optimum shaking time for different settling times from 0 min to 90 min to optimize settling time (waiting time).

Optimization of pH: Heavy metal ion solutions of 10.0 mg L^{-1} having pH ranging from 2-10 were prepared using HNO_3 and NaOH solutions. Solutions of higher pH were not prepared as precipitation problems were encountered for certain metal ions. Each solution was then treated with rice husk or brick clay fired at 400 °C for the respective optimum shaking and settling time periods, and the extent of removal was calculated at different pHs to determine the optimum pH.

Adsorption isotherms and kinetics modeling: The amount of heavy metal ions adsorbed on rice husk fired at the optimum firing temperature of 100 °C or brick clay fired at 400 °C for previously optimized contact time was studied using solutions of concentration varying from 2-2000 mg L^{-1}. After each solution was filtered, atomic absorption measurements were recorded. The extent of adsorption was calculated as mass of metal ion adsorbed (in mg) on 1.0 kg of rice husk. The graph was plotted between the extent of adsorption (q) and equilibrium concentration (C) of metal ion solutions. Further, these data were fitted to different adsorption isotherm models, namely Langmuir, Freundlich, Temkin, Dubinin-Raduskevich, Redlich-Peterson and Sips [70].

To investigate the validity of kinetics models, 500 cm^3 of 10.0 mg L^{-1} solutions of each metal ion were stirred with 1:20 (w/v) of rice husk heated at 100 °C, or 1000 cm^3 of 10.0 mg L^{-1} solutions of each metal ion were stirred with 1:10 (w/v) of brick clay fired at 400 °C. Then, in every 1.0 min interval, samples were withdrawn, for a period of 20 min, immediately filtered and the remaining concentration of each metal ion was determined using AAS. The data obtained in these experiments were used for the investigation of the order of reaction by applying kinetics models, such as first order, second order and pseudo second order.

3.3.3.6 Metal ion removal by rice husk and burnt brick particles under dynamic conditions

Columns were packed with rice husk for the height of 30.0 cm and adsorbate was prepared by mixing all cation solutions such that the concentration of each cation after mixing was 10.0 mg L^{-1}. Solution mixture was passed through the column and allowed 5 min residence time within the column. Eluent samples were then collected at every 5 min interval. In order to combine the use of adsorbents, rice husk alone and brick clay alone and layered type packings were prepared using rice husk on bottom and brick clay on top and vice versa. The length of packing in each column was 30.0 cm, and layered columns had 15.0 cm of each type of packings. The same adsorbate was used with same experimental procedure for the study and performances were checked to get an overall idea on the efficiency of removal of heavy metals in dynamic conditions. The extent removal of a metal ion by packed columns in each experiment was determined as the percentage removal.

3.3.3.7 Anion removal by natural adsorbents under static conditions

Removal of chloride using natural adsorbents

A 50.0 cm^3 of 50.0 mg L^{-1} Cl^- solution was shaken with appropriate masses of an adsorbent (0.5 g of each rice husk, saw dust or coir dust, or 1.0 g of brick clay, dolomite and feldspar) for 1.0 h and allowed to stand for 2.0 h to reach equilibrium. The concentration of Cl^- in each of the supernatant solution was then determined.

Removal of sulfate using natural adsorbents

A 50.0 cm^3 aliquots of 10.0 mg L^{-1} SO_4^{2-} solution was shaken with appropriate masses of adsorbents for 1.0 h and allowed to stand for 1.0 h to reach equilibrium. The concentration of SO_4^{2-} in each of the supernatant solution was then determined.

Removal of phosphate using natural adsorbents

Selection of an adsorbent: In order to remove phosphate from synthetic effluent solutions, experiments were conducted to find the most efficient adsorbent among dolomite, feldspar and brick clay without any heat treatment. A 50.0 cm^3 aliquot of 10.0 mg L^{-1} PO_4^{3-} solution was shaken with 5.0 g of each adsorbent for 10 min and solutions were allowed to stand for 1.0 h to reach equilibrium. Samples were filtered using 0.045 μm filter paper and charcoal was added to remove colour of the solutions before the colour development for the analysis of phosphate. Then, samples were tested using UV/Vis Spectrophotometer at the wavelength of 420 nm for the remaining phosphate concentrations. With the results obtained, further experiments were conducted using the most efficient adsorbent selected.

Optimization of firing temperature: With the results obtained for different adsorbents, burnt brick clay particles showed the highest percentage removal for the removal of phosphate from synthetic effluent samples. All experiments were performed under static conditions using the same experimental parameters as in previous experiments and percentage removal was calculated for brick clay fired at different temperatures to determine the optimum firing temperature.

Optimization of contact time: The effect of contact time on adsorption was investigated for brick clay samples, fired at the optimum firing temperature of 200 °C. For the optimization of shaking time, a 50.0 cm^3 aliquot of 10.0 mg L^{-1} phosphate solution was shaken with 5.0 g of fired brick clay particles (d < 1.0 mm), for different shaking times from 0 min to 90 min followed by a constant settling time of 1.0 h. After optimization of shaking time, similar experiments were carried out to optimize settling time (waiting time)

by employing the pre-determined optimum shaking time for different settling times from 0 min to 90 min.

Adsorption isotherms: The amount of phosphate adsorbed, on brick clay fired at 200 °C, for previously optimized contact time, was studied using solutions of concentration varying from 2-1000 mg L^{-1}. After each solution was filtered, colour was removed and samples were prepared for the vanadomolybdophosphate method. The data were fitted to linearized forms of different adsorption isotherm models, namely Langmuir, Freundlich and Temkin [70].

Kinetics modeling: To investigate the validity of kinetics models, experiments were conducted for brick clay fired at 200 °C by withdrawing 35.0 cm^3 volumes of samples from different sample containers prepared under identical conditions under previous optimized conditions. Samples were withdrawn at every 1.0 min interval for 20 min before the system reached equilibrium. Samples collected were immediately filtered, and the remaining concentration of phosphate in samples was determined. The data obtained in these experiments were used for the investigation of the order of reaction by applying kinetics models, such as pseudo first order and pseudo second order.

3.3.3.8 Phosphate removal by natural adsorbents under dynamic conditions

The extent of removal of phosphate under dynamic conditions was conducted for fired brick clay as the prior step of real applications.

Optimization of experimental parameters

Phosphate solution of concentration 10.0 mg L^{-1} was passed through columns (d = 2.0 cm) packed with brick clay fired at 200 °C up to different heights (15.0 cm, 22.5 cm, 30.0 cm, 37.5 cm) at a constant flow rate of 8 cm^3 min^{-1}. The concentration of phosphate in the elute, and hence the extent of removal for each packing height, was calculated to determine the optimum height of the packing.

Optimization of the flow rate was done using the optimized column height of 30.0 cm under the same conditions for different flow rates of 8 cm^3 min^{-1}, 12 cm^3 min^{-1} and 20 cm^3 min^{-1}.

Adsorption isotherms

In order to understand adsorption characteristics of phosphate under dynamic conditions, column studies were conducted for different initial concentrations (3.08, 8.83, 21.46, 110.83, 425.95, 748.65 and 1027.03 in mg L^{-1}) at the optimum column height of 30.0 cm and the optimum flow rate of 8.0 cm^3 min^{-1}. For each concentration, 20 eluent samples were collected at 5.0 min intervals to determine the concentration of phosphate. The breakthrough curves at different concentrations were plotted and the validity of dynamic adsorption models was investigated.

3.3.3.9 Removal of dyes using fired brick clay

Characterization of dyes

Synthetic dye samples were obtained from a selected dye releasing industry, and the extent of removal of individual dyes was determined, followed by treatment of mixtures of synthetic dyes and real dye effluent samples.

Raw dye samples and dye effluent samples were obtained from a textile dyeing industry. The λ_{max} values of individual dyes, namely, Sumifix Blue Exf (Dye 1), Sumifix Rubine Exf (Dye 2) and Sumifix Yellow Exf (Dye 3), were determined as 605 nm, 545 nm and 415 nm, for Dye 1, Dye 2 and Dye 3, respectively. Standard series of each dye was

used to determine the linear dynamic range. For each dye, the linear dynamic range was 2.0–50.0 mg L^{-1}.

Selection of an adsorbent for dye removal

In order to remove dyes from synthetic effluent solutions, experiments were conducted to determine the removal ability of natural substances listed in Table 3.3.1. The most efficient adsorbent was obtained among different adsorbents without any heat treatment for all three individual dyes in order to get an overall idea about real effluent sample. For this purpose, 2.5 g each of rice husk, coir dust, saw dust and 5.0 g each of brick clay, feldspar and dolomite was shaken with 50.0 cm^3 of 50.0 mg L^{-1} Dye 1 solution for 1.0 h and solutions were allowed to stand for 1.0 h to reach equilibrium. Then, samples were filtered and concentrations were determined with respect to the calibration curve at the predetermined wavelength. The same procedure was followed for all three individual dyes and the most efficient adsorbent was selected for further experiments.

Optimization of experimental parameters for dye removal

Optimization of firing temperature: With the results obtained for different adsorbents, brick clay showed the highest removal ability for the dyes under investigation. Representative samples of unfired brick clay and that fired at different temperatures (100 °C, 200 °C and 400 °C) were treated with dye solution of 50 mg L^{-1} concentration under static conditions. The extent of removal for each sample was determined to identify the optimum firing temperature.

Optimization of adsorbent dosage: The effect of adsorbent dosage on adsorption was investigated for the brick clay samples, fired at the optimum firing temperature. The experiment was conducted by varying the mass of brick clay from 1.0 g to 5.0 g by keeping the other parameters unchanged. The extent of removal was calculated, and the optimum dosage was obtained for all three individual dyes, and used for further experiments.

Optimization of contact time: The effect of contact time on adsorption was investigated for brick clay samples, fired at the optimum temperature, by varying shaking time and settling time. For the optimization of shaking time, a 50.0 cm^3 aliquot of 50.0 mg L^{-1} Dye 1 solution was shaken with the optimized mass (4.0 g) of brick clay particles ($d < 1.00$ mm), which had been fired at 200 °C for different shaking times from 0 min to 75 min followed by a constant settling time of 1.0 h. After optimization of shaking time, similar experiments were carried out for different settling times from 0 min to 60 min to optimize settling time (waiting time) at the pre-determined optimum shaking time. These optimized contact time was applied for all further experiments for all three individual dyes.

Optimization of pH: Dye solutions of 100.0 mg L^{-1} pH ranging from 1-12 were prepared using HNO_3 and NaOH solutions. A 50.0 cm^3 aliquot of the above solution was treated with fired brick clay for optimum shaking and settling time periods, and the extent of removal was determined in order to optimize the pH for the most efficient removal.

Adsorption isotherms

The amount of dye adsorbed on brick clay fired at the optimized firing temperature of 200 °C for previously optimized contact time was studied using solutions of concentration varying from 2 to 2000 mg L^{-1}. The remaining concentrations of the dye in the supernatant solution were determined at the corresponding wavelength for each dye. Data obtained were then fitted to linearized forms of different adsorption isotherm models, namely Langmuir, Freundlich, Dubinin Raduskevich and Temkin [70].

Kinetics modeling

To investigate the validity of kinetics models, 1000 cm^3 of 50.0 ppm solutions of each dye solution was stirred with 80.0 g of brick clay fired at 200 °C. First 12 samples were withdrawn in every 10 s interval, and thereafter in every 1.0 min interval for a period of 20 min. Samples were immediately filtered and the remaining concentration of each metal ion was determined at the relevant λ_{max}. The data obtained in these experiments were used for the investigation of the order of reaction by applying kinetics models, such as pseudo first order and pseudo second order.

Treatment of mixtures of synthetic dye solutions

Mixtures of synthetic dye solutions with known dye concentrations were treated with fired brick clay for the optimized shaking time, settling time and solution pH under static conditions. However different dosages of the adsorbent were tested to investigate whether there was any difference in the extent of removal by the mass of the adsorbent optimized for individual dyes. The results confirmed that there is no significant difference in the efficiency of removal of individual dyes as compared to dye mixtures.

Desorption of dyes from the adsorbent

After completion of adsorption (dye removal) experiments with synthetic dyes, dye-adsorbed brick clay sample was washed with deionized water, and allowed to air-dry until a constant mass was obtained. Then, 2.0 g of dye-adsorbed brick clay was shaken with 50.0 cm^3 of pH-adjusted water for 1.0 h and allowed to stand for 1.0 h. Then, the concentration of each dye leached out was determined to calculate the extent of desorption. The same desorption experiment was repeated for different initial pH values in the range of 2 – 12, adjusted with HNO_3 (0.1 mol dm^{-3}) and NaOH (0.1 mol dm^{-3}).

3.3.3.10 Construction of prototype treatment system

Under this sub-activity, two adsorbents (rice husk and fired brick clay) were initially selected to investigate the removal of Zn(II) at an initial concentration of 35 mg L^{-1}. The main reason for the selection of this metal ion is its presence in many industrial effluents according to effluent samples analyzed. The concentration of 35 mg L^{-1} was selected as it is the average concentration of Zn in real effluents. Rice husk and brick clay were selected as adsorbents, as they were found to be effective for the removal of many metal ions, anions and dyes. Therefore, after implementing this treatment system for the removal of Zn(II), the system design can be further refined for other pollutants as well. Calculations of extrapolation from small-scale laboratory experiments toward large-scale prototype treatment were carried out using "Wastewater Treatment Concepts and Design Approach" [71].

Laboratory-prepared Zn(II) solution of 35 mg L^{-1} concentration was passed through the prototype treatment facility designed at a flow rate of 400 cm^3 min^{-1}. Treated samples were continuously withdrawn hourly for a period of 3 days, and the Zn(II) concentration was determined. The treatment system was further modified in order to improve the efficiency of the Zn(II) removal process, and the experiment was repeated at a flow rate of 100 cm^3 min^{-1}, and hourly sample withdrawals were done for a period of 10 days to determine the remaining Zn(II) concentration.

3.3.3.11 Treatment of real effluents

As the final step of the project, real effluent treatment was considered in addition to the treatment of synthetic effluents prepared in the laboratory. With the results obtained from the laboratory prepared treatment system, the configuration of the prototype

treatment system was modified to treat the real industrial effluent obtained from a wire nail industry which contains about the same concentration of Zn(II) in their effluent. Among two adsorbents used for the laboratory scale prototype treatment plant, rice husk needs more modifications to be used for a long time period. Therefore, only brick clay was used to remove Zn(II) from the above industrial effluent. Calculations required for the treatment system design were carried out using "Wastewater Treatment Concepts and Design Approach".

As an additional step beyond the initially designed objectives, the prototype treatment system was fixed at the site of the wire nail industry (Pallekele Export Processing Zone) to treat its effluents. Samples were collected twice a week to observe the performance of the approach designed, and satisfactory results were observed. Based on the performance of this treatment system, the reactor will be modified to treat other pollutants using different adsorbents as well.

3.4-3.5 RESULTS/OUTPUTS AND DISCUSSION

3.4.1 Current Status of Industrial Effluents

3.4.1.1 Meta-analysis of industrial data

Results obtained from questionnaires (Annexure 1) were summarized in order to get an overall idea on the current status of the treatment systems available in industries, which was of highly importance to design the research plan. Consequently, suitable adsorbents, having strong ability to remove major metal ions and anions present in selected effluents, were investigated.

According to the information gathered from selected industries in Government approved industrial zones, most of the industries use both biological and chemical treatment methods in order to treat effluents. Further, most treatment systems are in good condition according to their knowledge, and no industry releases industrial effluents and wastewater without any treatment. Partially treated effluents were released to the common wastewater treatment system, operated by the Board of Investments (BOI), for further treatment, where the biological treatment methods are applied as the final step to complete the waste water purification process. According to the responses obtained, 90% industries are willing to adopt an environmentally friendly treatment system, provided that the method is low-cost and efficient. The summary of responses obtained from industries is given in Annexure 2.

3.4.1.2 Characterization of industrial effluents

Untreated industrial effluents collected from a metal finishing industry, a dye industry and a textile industry located in industrial zones were analyzed in the laboratory for different chemical parameters. Although the parameters measured do not have to conform to the CEA guidelines (Annexure 3), it would be important to compare which parameters need more attention during treatment.

The pH values of many industrial effluents were not in the neutral region. Therefore, pH is a main parameter to be considered in designing a treatment system. Conductivity, a measure of the total ions present in the effluent, is also an important on-sight parameter. Phosphate levels were not much high when compared with the other parameters (COD and sulfate). Effluent samples collected from metal finishing industries contain only Cu and Zn, and other metals such as Cd, Cr, Pb and Ni were not present in any effluent sample. In order to get a comprehensive idea about the data, samples analyzed were separated according to the type of industries, and the Spearman correlation coefficient was used to identify variables which showed a significant correlation. It was determined that all chemical variables in textile effluents have significant correlation except for pH and phosphate. Dye effluent samples showed a significant correlation except for conductivity and sulfate. Analysis of industrial data is shown in Annexure 4.

3.4.2 Characterization of Adsorbents

3.4.2.1 General aspects

As the natural adsorbents investigated in the research project were not homogeneous, bulk samples were prepared for analysis with different preparation procedures as listed in Table 3.4.1.

Table 3.4.1: Preparation procedures of natural adsorbents.

Adsorbent	Availability	Preparation/Surface modification	Particle size (d) – static/dynamic conditions
Brick clay	Clay used for construction of bricks	Crushed using mortar and pestle; Fired at different temperatures	$d < 1$ mm (static); 0.5 cm $< d <$ 1.0 cm (dynamic)
Rice husk	Husk produced from processing of rice; Yellow coloured material	Sieved and removed particles of $d < 1$ mm; Washed thrice with tap water and twice with distilled water and air dried; Fired at different temperatures	Natural size (static and dynamic)
Saw dust	Byproduct of cutting, grinding, drilling, sanding wood with a saw or other tool; yellow to brown colour material	Sieved without crushing; Washed thrice with tap water and twice with distilled water; Fired at different temperatures	$d < 1$ mm
Coir dust	Falls out from coconut husk when shredded during coir production; brown coloured fluffy material	Sieved without crushing; Washed thrice with tap water and twice with distilled water; Fired at different temperatures	$d < 1$ mm
Feldspar	($KAlSi_3O_8$ - $NaAlSi_3O_8$ – $CaAl_2Si_2O_8$); A group of rock-forming mineral in pink, white, gray or brown colour	Crushed using ball mill; No heat treatment	$d < 1$ mm
Dolomite	$CaMg(CO_3)_2$; A sedimentary carbonate rock in white, gray or pink	Crushed using ball mill; No heat treatment.	$d < 1$ mm

These adsorbents serve as an effective sorbent for cations, anions and organic substances. Constituents of rice husk, saw dust and coir dust are mainly organic compounds, such as cellulose, hemicelluloses, lignin, pectins and tannins. Brick clay, feldspar and dolomite mainly consist of many minerals, and hence, some chemical species interact with minerals present in the adsorbent, and some species are trapped between layers of the clay or the mineral matrix. In order to understand the adsorption behaviour of these adsorbents, it is important to identify their characteristics, such as active functional groups, specific surface area and charge density. Therefore, the initial step of this research was to characterize these adsorbent particles through a variety of instrumental methods. Thereafter, attempts were taken to predict the mechanism of the interaction of adsorbates and adsorbents. Once the mechanism is known, the rate and the extent of sorption of adsorbates can be controlled, as needed, by adjusting experimental conditions.

3.4.2.2 Bulk characterization of rice husk

Since this research includes many adsorbents other than rice husk, characterization experiments were conducted for other adsorbents as well. The details of the results of characterization experiments of rice husk are given below, and the results of other adsorbents are summarized in relevant sections.

Thermogravimetric analysis

Evaporation of moisture and decomposition of organic substances would occur during firing as stated earlier. These processes are accompanied with mass reduction as observed in thermogravimetric curves shown in Figure 3.4.1. The major mass losses are observed in three temperature ranges;

- Between the room temperature and 100 °C (steep change), mainly due to the evaporation of water,
- 200 °C to 350 °C (steep change), due to combustion of organic matter, such as humic acid
- 350 °C to 500 °C (gentle change), due to the combustion of organic matter, such as calcite, which require higher temperatures for their combustion.

Both the evaporation of water and combustion processes are confirmed from heat flow measurements, where negative flow is recorded for the evaporation of water as it is an endothermic reaction, and a positive heat flow for combustion reactions, which are exothermic.

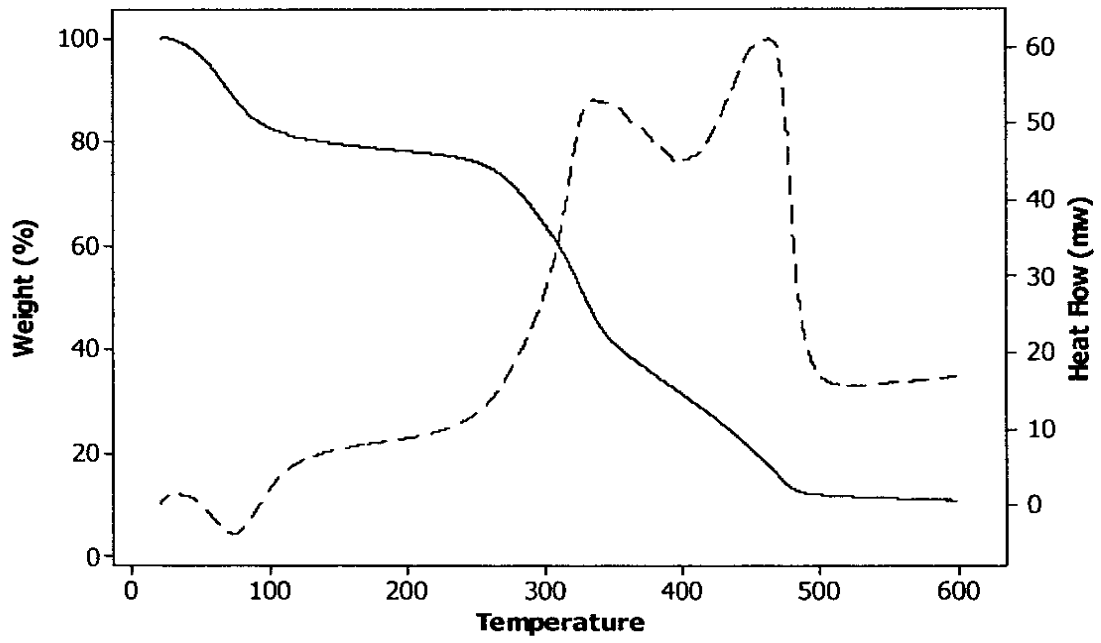

Figure 3.4.1: Variation of mass of rice husk (—) and heat flow (----) when firing at different temperatures (in °C).

X-ray diffraction analysis (XRD)

XRD is a rapid analytical technique primarily used for phase identification of a crystalline material. Figure 3.4.2 shows the XRD spectrum of a natural rice husk sample, which has a broad peak and a wide angle of 2θ, indicating the presence of amorphous silica in rice husk. These features did not change upon heat treatment up to 200 °C [72].

Fourier transform infrared (FTIR) spectroscopic analysis

FTIR spectroscopy is used to determine the quality of a sample. Figure 3.4.3 shows the FTIR spectra of rice husk samples heated at different temperatures. According to the figure, it is clearly shown that peaks do not shift upon heat treatment although the peak intensity decreases, indicating the loss of compounds due to volatilization or combustion.

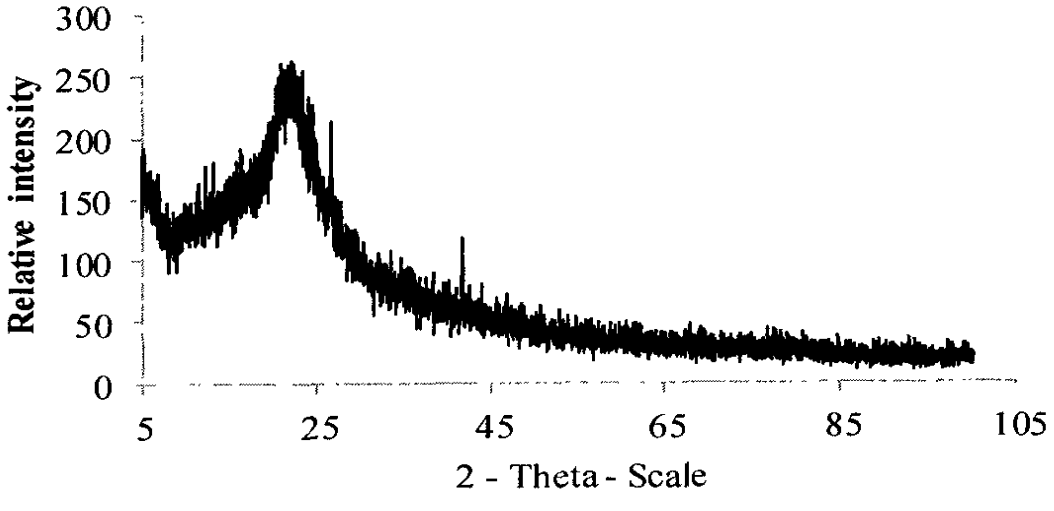

Figure 3.4.2: XRD spectrum of a powdered rice husk sample.

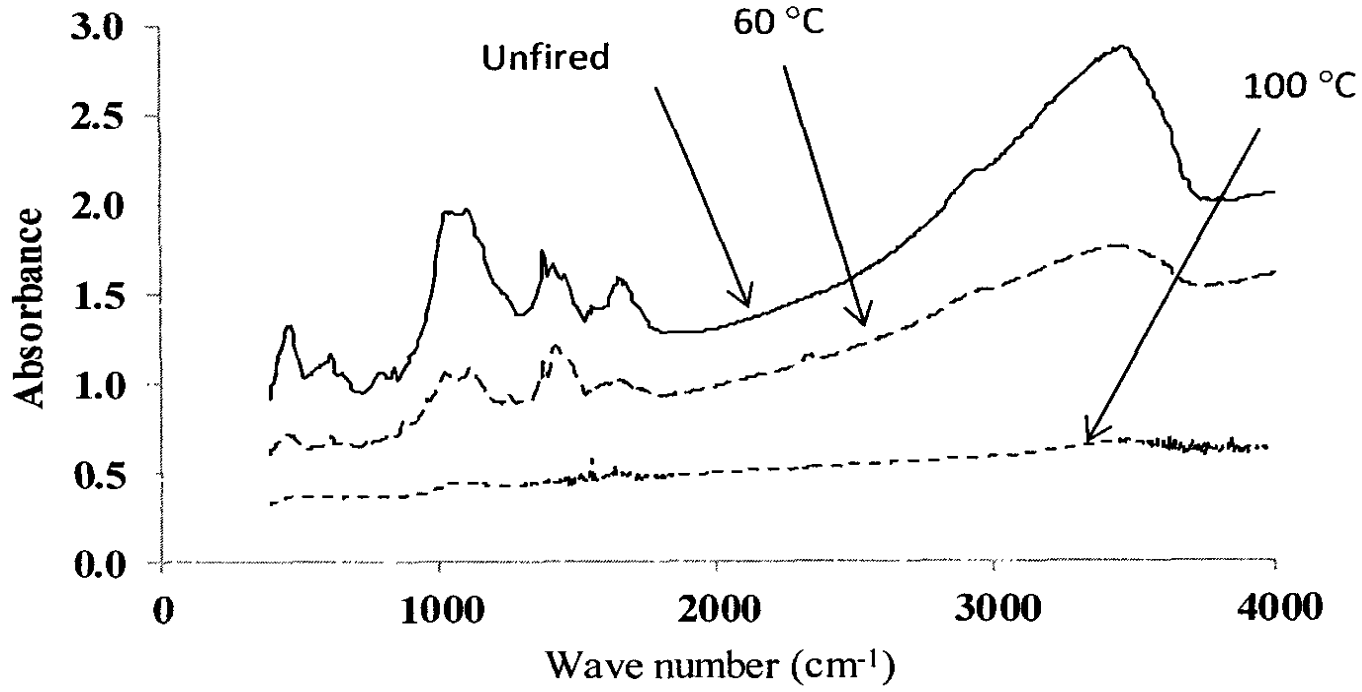

Figure 3.4.3: FTIR spectra for rice husk heated at different temperatures.

Neither XRD patterns nor FTIR spectra provide sufficient information on chemical/physical changes that would occur during heat treatment. Although XRD provides information on the crystalline nature and minerals present, the composition of individual elements (metals) cannot be obtained. On the other hand, XRF is useful in obtaining the composition of metallic elements, while FTIR spectroscopy provides information on organic functional groups.

X-ray fluorescence (XRF) analysis

Figure 3.4.4 shows the XRF spectrum of a rice husk sample, which indicates that rice husk contains mainly Si, Fe, K and Ca, which is supported by previous studies [73]. Heat treatment up to 200 °C does not show any change in the XRF peaks as expected.

3.4.2.3 Bulk characterization of other adsorbents

According to the XRF spectra recorded, dolomite contains mainly Ca and Fe (Ca is predominant) and feldspar contains many metal ions, including Si, K, Ca, Fe Br, Rb, Sr and Ag as shown in Figures 3.4.5(a) and 3.4.5(b). Figure 3.4.5(c) shows that saw dust contains mainly K, Ca, Fe and Cu, with Ca being predominant. Further, FTIR spectra recorded for feldspar and dolomite samples indicate the presence of C-Cl stretching, C=C stretching, surface-OH groups, H-bonded OH, free H_2O, Si-O stretching and C-O stretching.

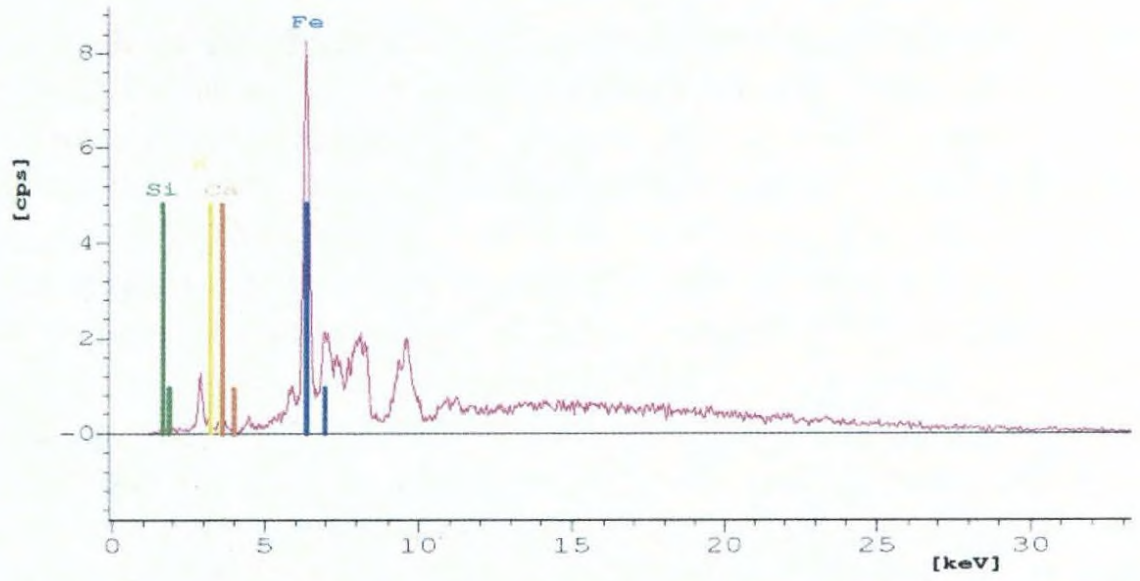

Figure 3.4.4: XRF spectrum of powdered rice husk. Lines indicate the specific peak locations of respective elements.

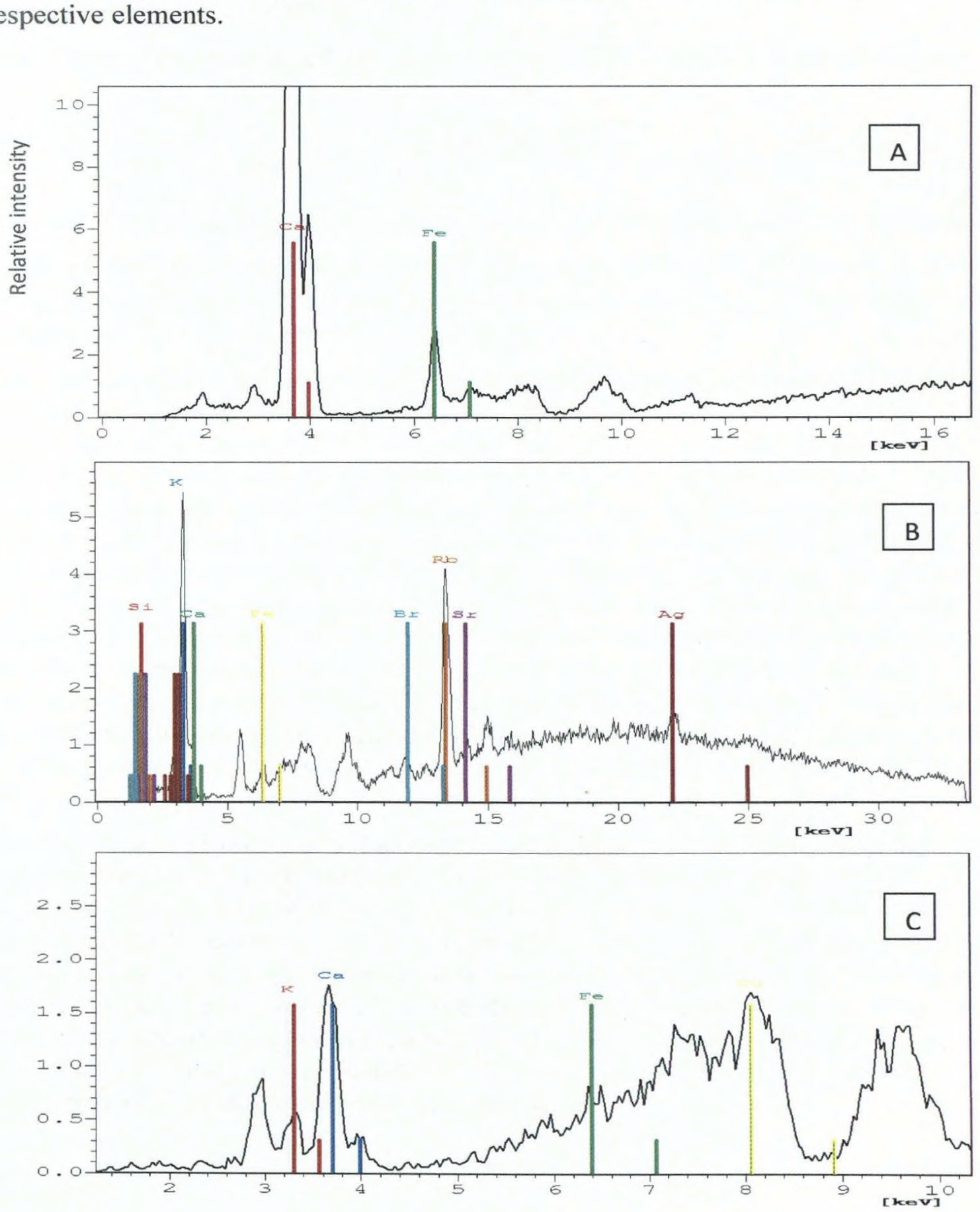

Figure 3.4.5: XRF spectra of samples (A) Dolomite (B) Feldspar (C) Saw dust. Lines indicate the specific peak locations of respective elements.

Surface titrations

The surface charge of an adsorbent is highly dependent on the pH of the medium as clearly observed from the plots of the surface charge vs. pH, constructed for media of different ionic strengths. Surface charge of a system depends on the ionic strength of the medium. Depending on the surrounding pH, the surface charge of the adsorbent can be positive, negative or zero [76]. The pH, at which the sum of all positive charges balances the sum of all surface negative charges, is called the point of zero charge (PZC). At this point, adsorption of protons is independent of ionic strength [77]. $NaNO_3$ is commonly used for surface titrations because its constituent ions do not bind specifically to the adsorbent surface. Hence, it is assumed that no other ion other than protons in the medium binds to the biosorbent during surface titrations [78]. The three curves drawn for three different concentrations of $NaNO_3$ intersect at the PZC. When the solution pH is lower than the PZC, the sites on the surface become protonated with the development of an excess positive charge on the surface. On the contrary, higher extents of removal of metal ions are expected in basic conditions.

The charge density of an adsorbent can be calculated according to Equation (3.4.2),

$$\sigma = \frac{F}{a \times s} \{(C_a - C_b) - [H^+] + [OH^-]\} \qquad (3.4.2)$$

where σ is the charge density of the surface, F is the Faraday constant, a is the specific surface area, s is the composition of adsorbent in the suspension, $[H^+]$ and $[OH^-]$ are the equilibrium concentrations of hydronium and hydroxyl ions, C_a is the initial acid concentration, and C_b is the initial base concentration.

The surface charge vs. pH curves (surface titration curves) obtained for natural rice husk and that heated at different temperatures, in $NaNO_3$ solutions of different ionic strengths are shown in Figure 3.4.7. For natural rice husk, the curves obtained for three ionic strengths do not intersect at a common point, and the curves obtained are almost parallel to each other for certain pH ranges, indicating that the pH independent surface charge of rice husk is more predominant compared to the pH dependent charge [79]. At the point of intersection, the charge density is not affected by the mobility of other ions such as Na^+ and NO_3^- present in the solution. At the PZC, two curves of $NaNO_3$ concentrations of 0.0010 mol dm^{-3} and 0.010 mol dm^{-3} intersect and the third curve is being very close to the intersection. The PZC can however be estimated as pH of 4.6, 4.5, 4.1 and 5.2 for natural rice husk and that heated at 60 °C, 100 °C and 200 °C, respectively. The PZC, obtained for rice husk heated at 100 °C, is less negative than other rice husk samples. This perspective proves the highest removal of metal ions from 100 °C heated rice husk.

Surface charge of feldspar and saw dust, determined with the same procedure, was plotted against the charge on the surface with different solution pH values (Figure 3.4.8). The PZC can be estimated by considering two curves obtained for lower concentrations at pH of 8.9 and 4.0 for feldspar and saw dust, respectively. Since the PZC of saw dust is less negative, it is in favour to remove heavy metal ions from aqueous solution. Although the PZC of feldspar is 8.9, the removal of heavy metal ions may be due to the cation exchange mechanism which occurs at higher pH values. This method cannot be applied for dolomite as it dissolves in the acidic medium due to the presence of $CaMg(CO_3)_2$. Table 3.4.3 gives PZC values of different adsorbents.

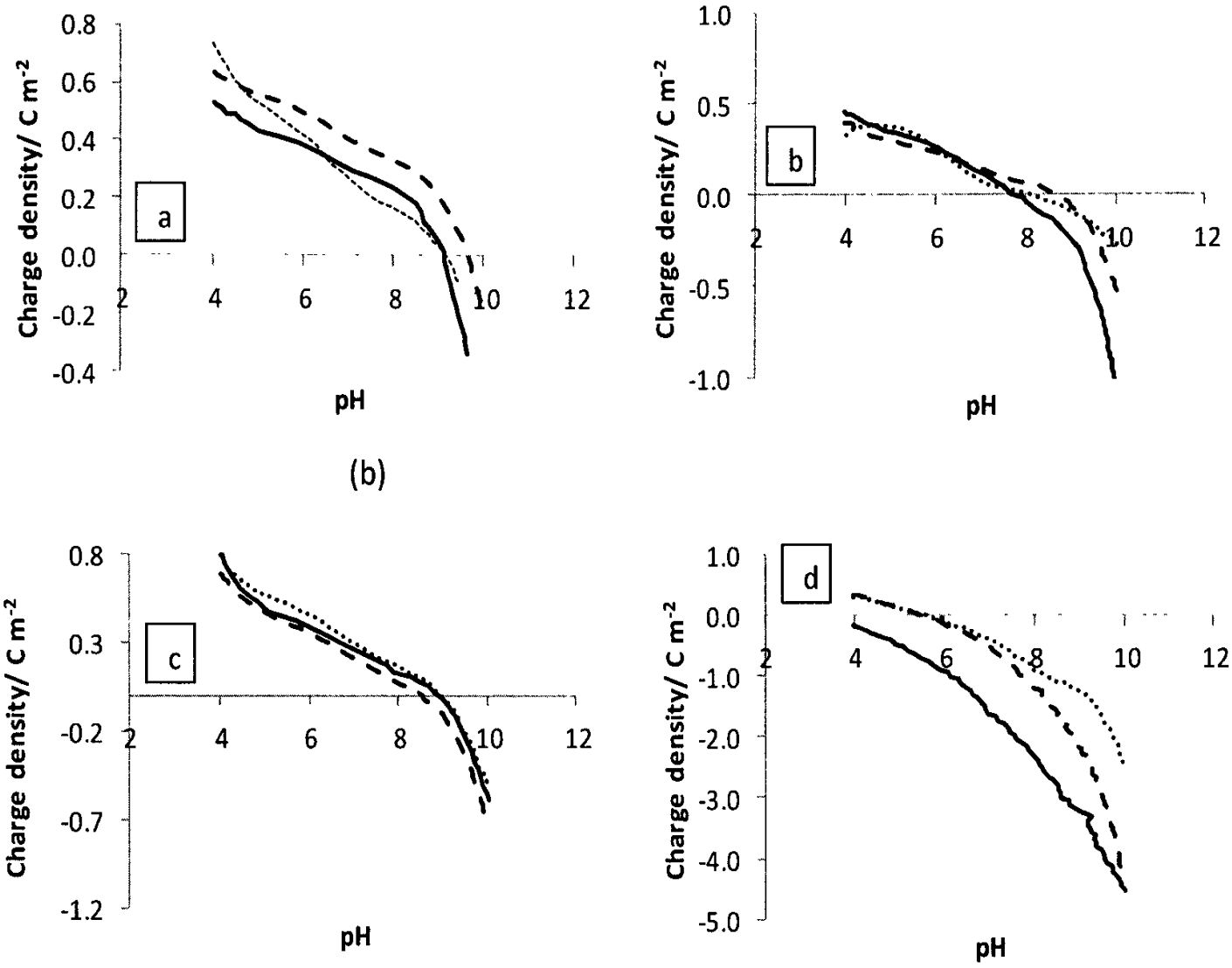

(b)

Figure 3.4.7: Surface titration curves of rice husk suspensions, plotted as variation of surface charge with pH controlled by different additions of NaOH for rice husk heated at different temperatures. (a) unfired, (b) heated in to 60 °C (c) heated in to 100 °C (d) heated in to 200 °C. Ionic strengths are 0.1 M (——), 0.01 M (— —) and 0.001 M (·····).

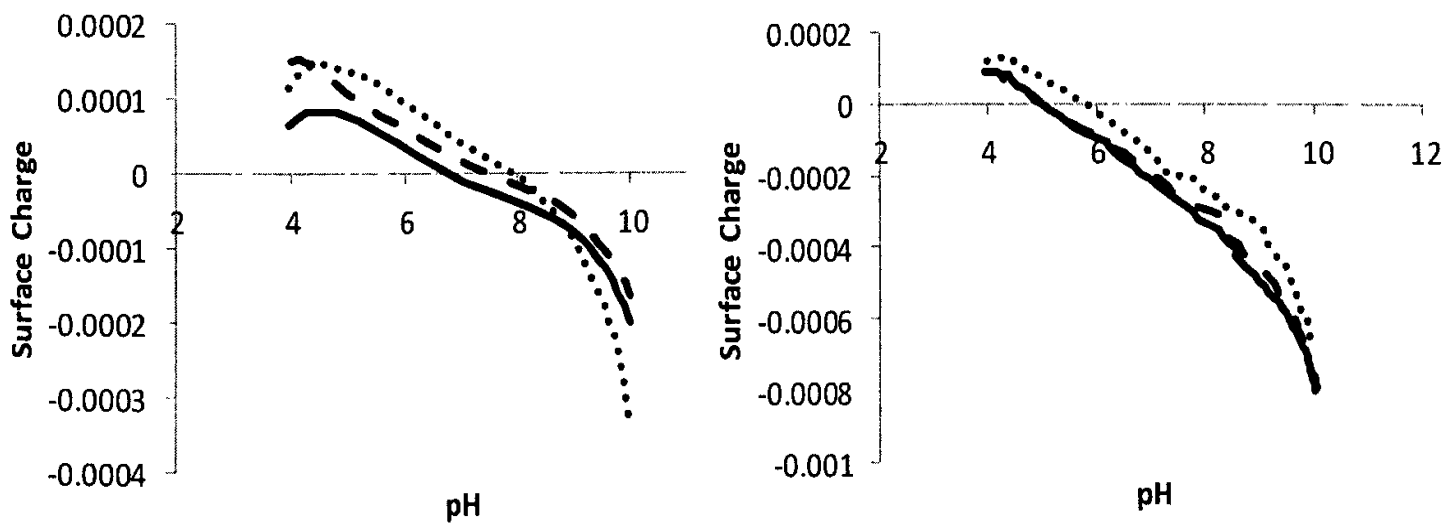

Figure 3.4.8: Surface titration curves of adsorbent suspensions, plotted as the variation of surface charge with pH for feldspar (left) and saw-dust (right) heated at 100 °C. Ionic strengths are 0.1 mol dm^{-3} (- - - -), 0.01 mol dm^{-3} (——) and 0.001 mol dm^{-3} (.....).

Table 3.4.3: PZC values for adsorbents obtained from surface charge density – pH curves.

Adsorbent	Processing condition	PZC	Ref
Brick clay	200 °C	6.5	[74]
Coir dust	natural	5.0	[75]
k Ricehus	100 °C	4.1	This study
Feldspar	natural	8.9	This study
Saw dust	100 °C	4.0	This study

Scanning electron microscopic (SEM) analysis

SEM images for rice husk samples that have been heated at different temperatures clous nature of the surface with pores of different sizes (Figure 3.4.9). It is further evident that the surface becomes more porous when the adsorbent is heated at 100 °C. These observations indicate the possibility for metal ions to be trapped and adsorbed on the rice husk surface.

3.4.2.5 Leaching of metal ions from adsorbent matrices

Extent of leaching of metal ions from natural adsorbents is an important aspect that should be investigated in order to consider them as environmentally friendly adsorbents. Leachate solutions of adsorbents investigated are found to contain only Ca, Mg, K and Na at different levels, and heavy metals, such as Cd, Cr, Pb, Zn, Ni and Cu were not detected in the leachates of any of the adsorbent (Table 3.4.4). Therefore, it can be concluded that the adsorbents, be used to investigate the heavy metal ion removal potential.

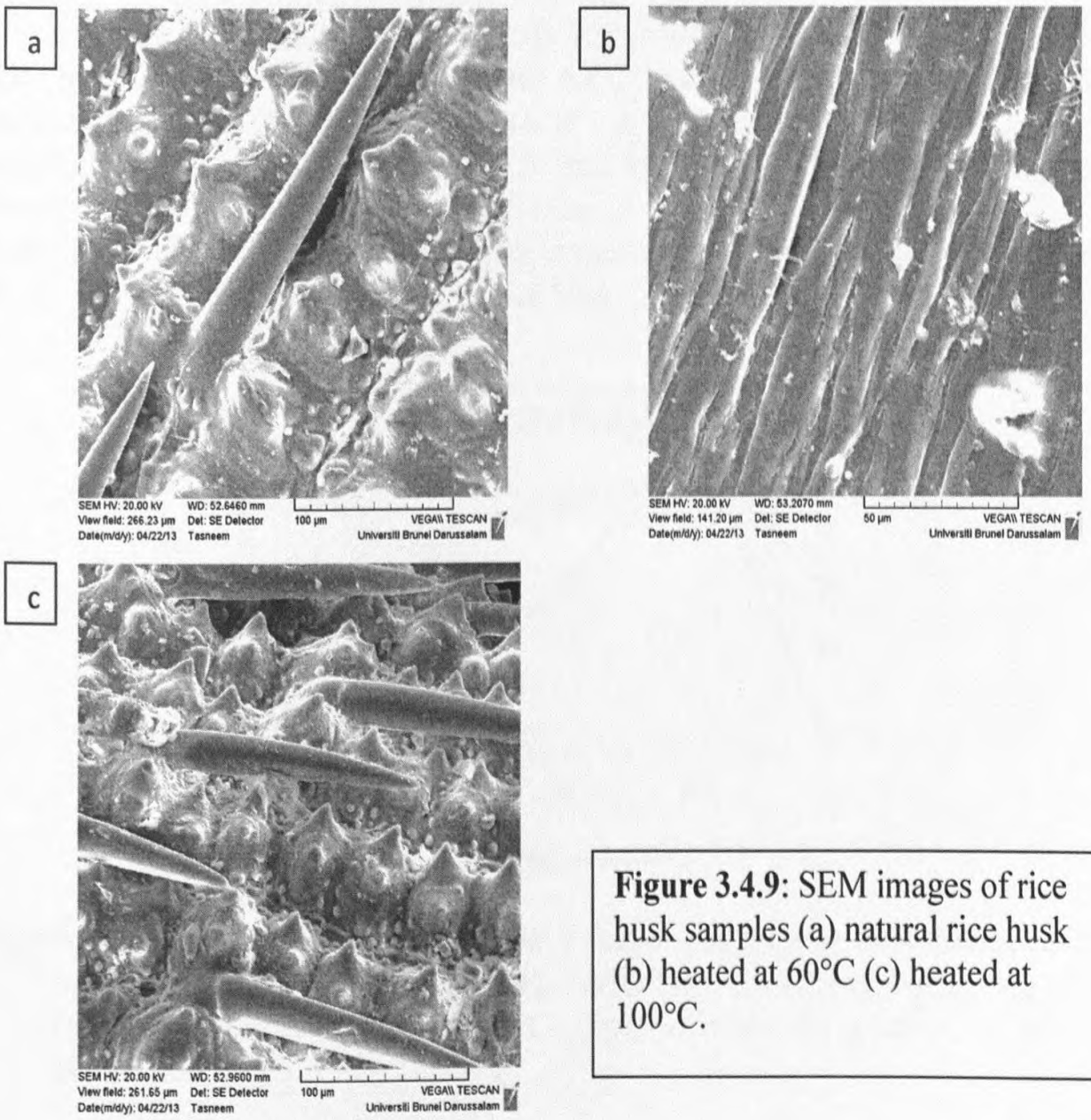

Figure 3.4.9: SEM images of rice husk samples (a) natural rice husk (b) heated at 60°C (c) heated at 100°C.

Table 3.4.4: Metal ion concentrations of leachate samples of different adsorbents.

Adsorbent	Concentration/ppm			
	Ca	Mg	K	Na
Brick clay	4.01	0.72	0.75	8.33
Coir dust	0.62	0.32	0.61	6.29
Dolomite	6.36	1.74	0.76	2.37
Feldspar	0.59	0.39	2.93	1.05
Rice husk	0.60	0.12	0.98	4.94
Saw dust	8.71	5.01	6.13	9.14

3.4.3 Removal of heavy metal ions using rice husk under static conditions

The extent of removal of an adsorbent depends on experimental parameters, including contact time (shaking time and settling time), initial solution pH and pre-treatment conditions (*e.g.*: heating temperature of adsorbent). In order to determine the optimum value of experimental parameters for the most efficient removal, effect of one parameter on the percentage removal should be studied by changing the parameter selected, while keeping other parameters constant. In this study, percentage removal of heavy metal ions by adsorbents for different experimental parameters is determined using Equation 3.3.1 (Page 19).

3.4.3.1 Optimization of firing temperature of rice husk

Figure 3.4.10 shows the percentage removal of heavy metal ions determined with rice husk heated at different temperatures for different metal ion solutions. According to the results obtained, the extent of removal of Cd(II), Zn(II), Cu(II) and Pb(II) is increased with temperature of treatment up to 100 °C and then decreased up to 200 °C. However, the extent of removal of Cr(III) and Ni(II) remains constant up to 100 °C, followed by a decreased with rice husk heated at higher temperatures. Therefore, 100 °C can be taken as the optimum treatment temperature of rice husk for the metal ion removal experiments.

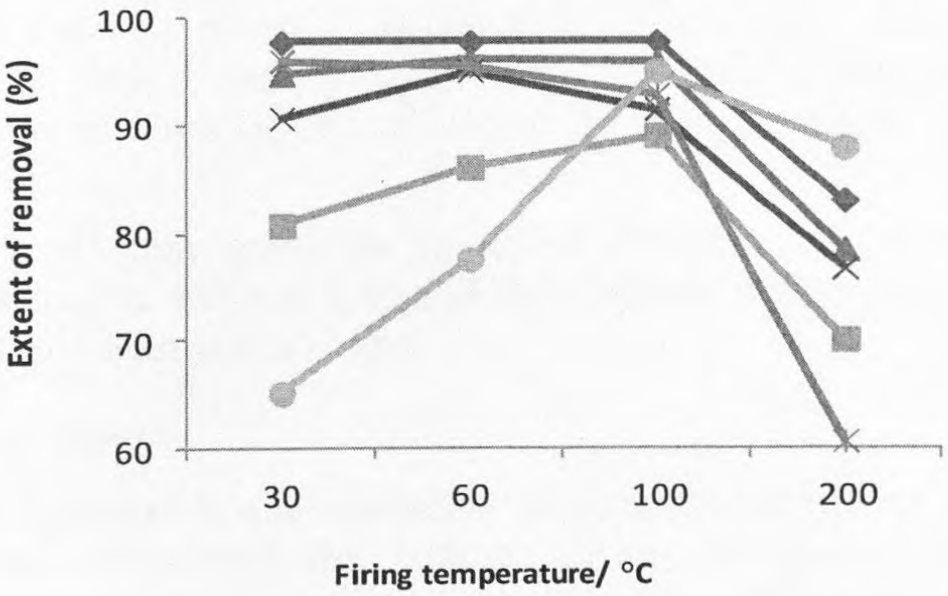

Figure 3.4.10: Extent of removal of heavy metal ions by rice husk heated at different temperatures: Cd(II) (◆), Cu(II) (■), Zn(II) (▲), Cr(III) (×), Ni(II) (∗) and Pb(II) (●) [2.50 g rice husk, 50.0 cm^3 of 1 0.0 mg L^{-1} metal ion solution, 60 min shaking, 60 min settling].

3.4.3.2 Optimization of contact time

First, shaking time was optimized by using the rice husk heated at optimized temperature of 100 °C within a broad range of shaking times at a fixed settling time is shown in Figure 3.4.11. It is clear that the rice husk-metal ion solution system attains equilibrium quickly. The percentage removal is leveled off both Cd(II) and Ni(II) after 10 min shaking time. Therefore, it is reasonable to consider that the optimum shaking time for all metal ions used in this study to be taken as 10 min.

Settling time was optimized for the same heavy metal ions at the optimum shaking time of 10 min. It was determined that the extent of removal of Cd(II) and Ni(II) at the optimum shaking time did not change over a wide range of settling times up to 60 min. Therefore, a time period of 10 min was selected as the optimum settling time to assure that the establishment of equilibrium is complete.

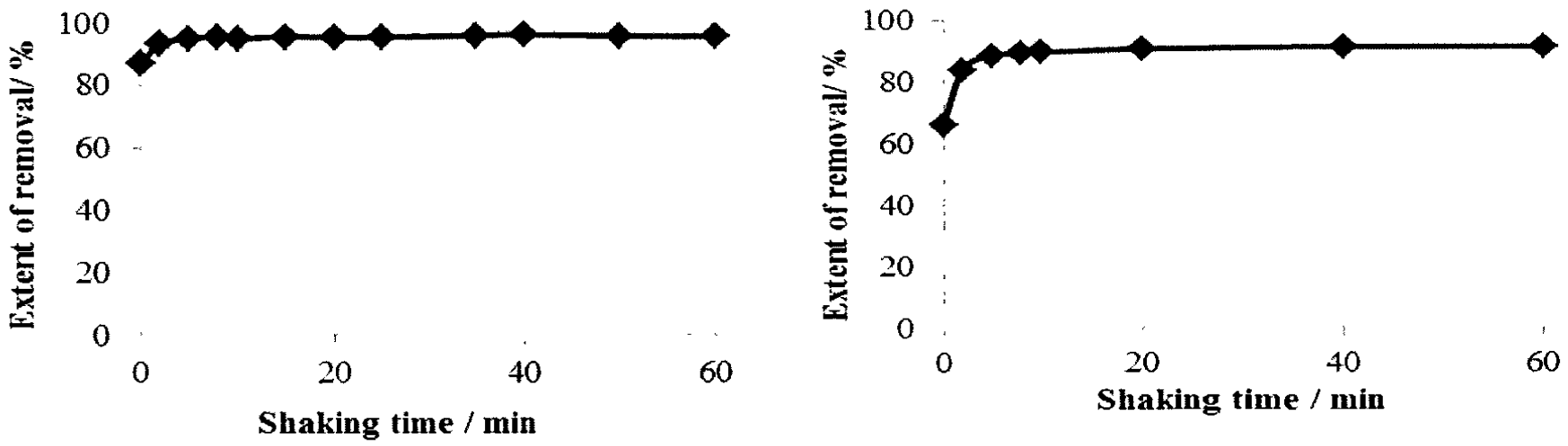

Figure 3.4.11: Percentage removal – shaking time curves for heavy metal ions: Cd(II) (left) and Ni(II) (right) [50.0 cm^3 of 10.0 mg L^{-1} concentration of metal ion solutions treated with 2.50 g of 100 °C rice husk, 50.0 cm^3 10.0 mg L^{-1} metal ion solution, 60 min settling].

3.4.3.3 Optimization of initial solution pH

The percentage removal vs. pH investigated from an initial pH from 1.0 up to a value at which corresponding hydroxide precipitation occurs is shown in Figure 3.4.12. It is clear that the extent of removal is lower at low pH values, due to the competition of metal ions with H_3O^+ ions present in solution for a limited number of binding sites in the adsorbent. The extent of removal of each metal ion then increases with the increase in pH up to a certain value.

The lowest pH that leads to the most effective removal of metal ions was determined to be between 4.0 and 5.0, and thus, all the experiments were carried out by adjusting the initial pH within this range.

3.4.3.4 Isotherm studies

Adsorption isotherm is a relationship between the amount of adsorbate adsorbed by a unit mass of adsorbent and the activity of the adsorbate after establishment of equilibrium, which is expressed as the pressure or the concentration of the adsorbate, at constant temperature. Adsorption isotherms provide information about adsorption mechanism, surface properties and degree of affinity of adsorbents [80]. First classification on adsorption isotherms was introduced by Stephen Brunauer, which later led to the modern classification of isotherms by IUPAC. As illustrated in Figure 3.4.13,

IUPAC classification describes six types of isotherms, named Type I, Type II, Type III, Type IV, Type V and Type VI. Each type has unique properties about the adsorbate - adsorbent interaction, and the classification depends on the shapes of the curves. Type I isotherms characterize microporous adsorbents, while Type II and Type III describe adsorption on macroporous adsorbents with strong and weak adsorbate-adsorbent interactions. Types IV and V represent adsorption isotherms with hysteresis and Type VI isotherm has steps [80].

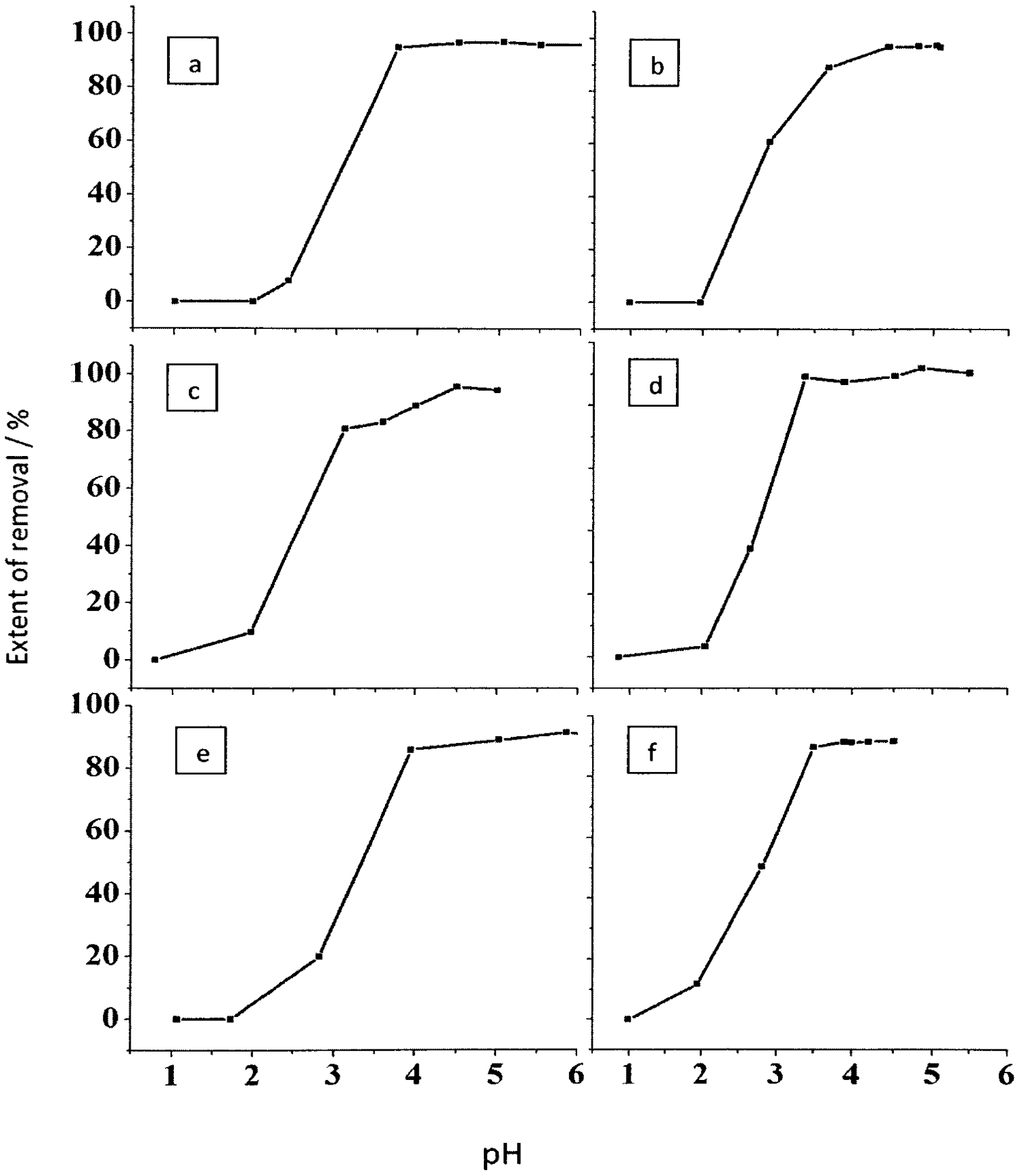

Figure 3.4.12: Variation of the extent of removal with initial pH for (a) Cd(II), (b) Zn(II), (c) Pb(II), (d) Cu(II), (e) Ni(II), (f) Cr(III) (50.0 cm^3 of 10.0 mg L^{-1} concentration of metal ion solutions treated with 2.50 g of rice husk heated at 100 °C (10 min shaking time, 10 min settling time).

The amount adsorbed plotted against the initial concentration of each metal ion provides clear indication that the adsorption of all metal ions investigated on rice husk

qualify Type I isotherm according to the IUPAC isotherm classification (Figure 3.4.14). This overall behavior suggests that rice husk shows microporous characteristics for adsorption of these metals. However, the extent of removal depends on the type of the metal ion [80].

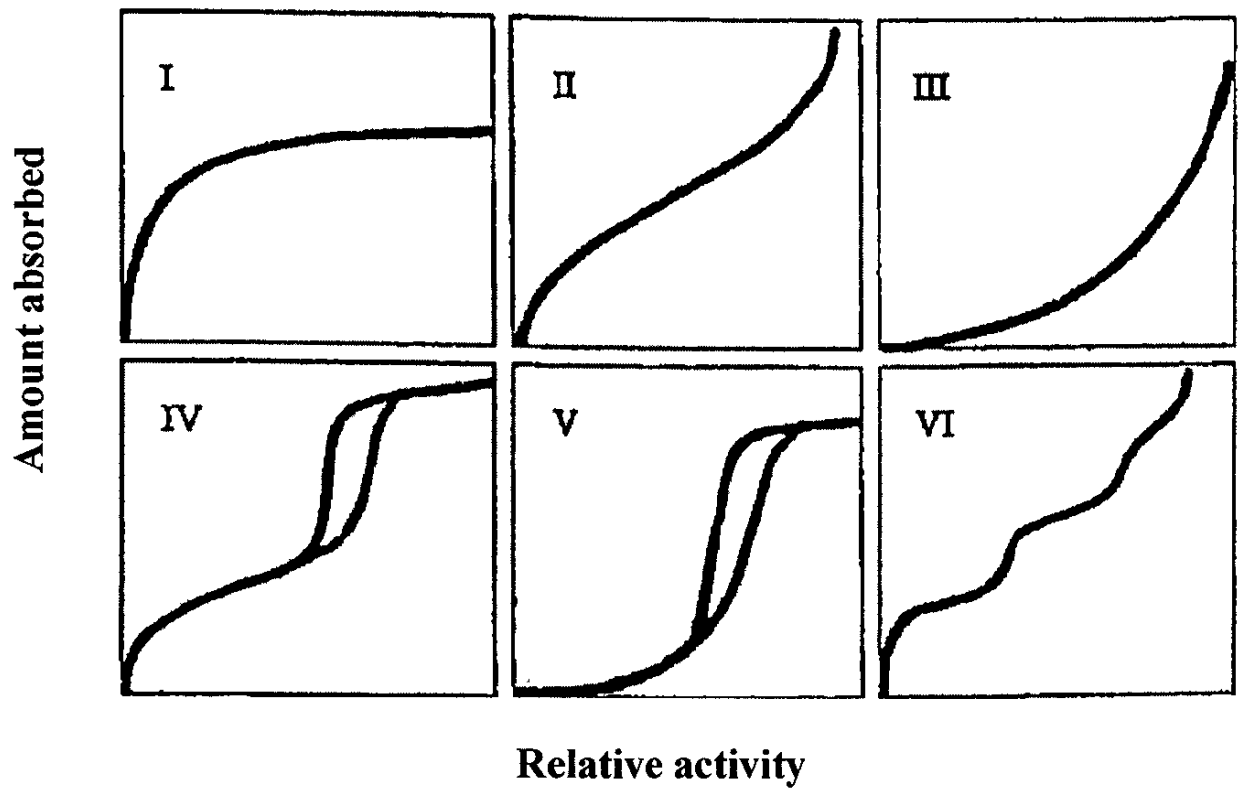

. **Figure 3.4.13**: The IUPAC classification of adsorption isotherms.

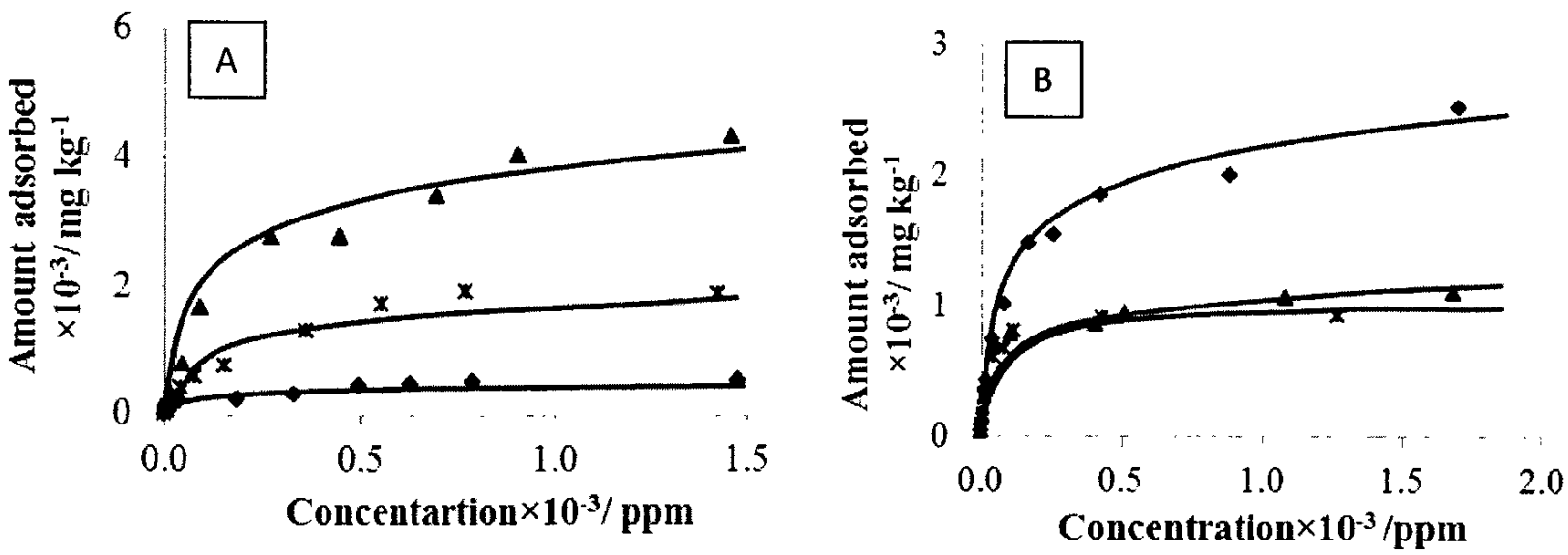

Figure 3.4.14: Amount of heavy metal ions adsorbed on rice husk. (A) Cr(III) (◆), Ni(II) (∗), Pb(II) (▲); (B) Cd(II) (◆), Cu(II) (▲), Zn(II) (∗) (2.50 g rice husk 50.0 cm^3 of metal ion solutions, 100 °C treatment temperature, 10 min shaking, 10 min settling).

Using the equilibrium concentration of the same experimental data, validity of different adsorption isotherm models, namely Langmuir, Freundlich, Temkin, Dubinin–Radushkevich, Redlich-Peterson and Sips, were checked to characterize the adsorption behavior. The Langmuir adsorption isotherm is mainly applied for the chemisorption process leading to a monolayer, and it is based on some assumptions [85]. A linear form of this isotherm can be given as,

$$\frac{C_e}{q_e} = \frac{C_e}{q_{max}} + \frac{1}{K_L q_{max}} \qquad (3.4.3)$$

where q_e is the amount of metal sorbed at equilibrium (mg g^{-1}), q_{max} is the monolayer sorption capacity (mg g^{-1}), K_L is Langmuir constant (dm^3 mg^{-1}), C_e is concentration of metal ion in solution at equilibrium (mg L^{-1}). The Langmuir model can be used to

calculate the specific surface area of monolayer coverage of a certain metal ion on a specific adsorbent [82].

Freundlich isotherm, which is presented by Freundlich in 1906 [82], is written as,

$$q_e = K_f C_e^{1/n} \tag{3.4.4}$$

where K_f is the Freundlich adsorption constant (mg g^{-1}), n is a dimensionless constant, q_e is the amount of metal adsorbed at equilibrium (mg g^{-1}) and C_e is the equilibrium concentration (mg L^{-1}). The linear form of this equation is given as,

$$\ln q_e = \ln K_F + \frac{1}{n} \ln C_e \tag{3.4.5}$$

This model is applied to nonideal sorption on heterogeneous surfaces which explains multilayer sorption [81,83]. The assumption made in this isotherm is that adsorption sites are distributed exponentially with respect to the heat of adsorption [84].

The Temkin isotherm assumes that the heat of adsorption decreases linearly with the coverage. This isotherm takes into account of adsorbate adsorbent interactions [80,85]. The first three-parameter isotherm formulated incorporates features of both the Langmuir and Freundlich equations. At low concentrations, the Redlich-Peterson (R-P) isotherm approximates to Henry's law, and at high concentrations its behavior approaches that of the Freundlich isotherm. The Sips isotherm *(Langmuir-Freundlich Isotherm)* is a combination form of Langmuir and Freundlich expressions deduced for predicting the heterogeneous adsorption systems. Langmuir also considered the case of a molecule occupying two sites. At low adsorbate concentrations, it reduces to Freundlich isotherm and at high concentrations it predicts a monolayer adsorption capacity characteristic of the Langmuir isotherm [86]. The standard equations of the six isotherm models are given in Table 3.4.5.

Table 3.4.5: Standard equations of the six isotherm models.

Isotherm Model	Standard equations
Langmuir	$\frac{C_e}{q_e} = \frac{C_e}{q_{max}} + \frac{1}{K_L q_{max}}$
Freundlich	$\ln q_e = \frac{1}{n} \ln C_e + \ln K_F$
Temkin	$q_e = B \ln K_T + B \ln C_e$
Dubinin-Radushkevich	$\ln q_e = \ln q_s - B\epsilon^2$ $\epsilon = RT \ln [1 + \frac{1}{C_e}]$
Redlich-Peterson	$q_e = \frac{K_R C_e}{1 + a_R C_e^{b_R}}$
Sips (Langmuir - Freundlich Isotherm)	$q_e = \frac{K_s C_e^{1/b_s}}{1 + a_s C_e^{1/b_s}}$

In order to obtain the best fitted adsorption isotherm model, the amount adsorbed was plotted against the equilibrium concentration as per the linearized equation of each model. Among the six isotherms, constants for Langmuir and Freundlich isotherms, the

most widely used models, are given in Table 3.4.6 and Table 3.4.7, respectively. It is clear from the values in Tables that the Langmuir adsorption isotherm model, having regression coefficients (R^2) close to unity for all six metal ion systems, is better suited to explain adsorption characteristics of metal ions on rice husk heated at 100 °C.

Table 3.4.6: Isotherm constants and regression coefficients (R^2) for Langmuir adsorption isotherm model.

Metal ion	$k_L \times 10^2$/ L mg^{-1}	q_{max}/ mg kg^{-1}	R^2
Cd(II)	22.2	2500	0.988
Cu(II)	13.9	1000	0.990
Ni(II)	15.3	909	0.985
Pb(II)	3.30	5000	0.986
Zn(II)	37.5	833	0.964
Cr(III)	3.00	769	0.983

According to Table 3.4.6, the adsorption capacity varies in the order of Pb(II) > Cd(II) > Cu(II) > Ni(II) > Zn(II) > Cr(III). The highest adsorption capacity towards Pb(II) can be attributed to the lowest hydrated radius of Pb(II), which changes in the order of Cu(II) > Cd(II) > Pb(II), being able to be trapped easily in the pores of the adsorbent [87].

Table 3.4.7: Isotherm constants and regression coefficients (R^2) for Freundlich adsorption isotherm model.

Metal ion	n	K	R^2
Cd(II)	2.73	239	0.895
Cu(II)	2.77	111	0.812
Ni(II)	2.19	97	0.958
Pb(II)	2.12	214	0.915
Zn(II)	2.86	147	0.879
Cr(III)	5.32	130	0.904

Isotherm constants calculated for the adsorption models are given in Table 3.4.8, and corresponding regression coefficients are listed in Table 3.4.9. It is clear that the removal of all six heavy metal ions by rice husk is best described by the Langmuir adsorption isotherm. Redlich-Peterson isotherm and Sips isotherm also were obeyed to a certain extent with high R^2 values; but the other isotherms do not explain the adsorption behavior. Many agricultural waste containing cellulose and lignin, and natural substances such as clay, peat and zeolites obey the Langmuir adsorption isotherm supporting the findings of this research [82,88].

As the D-R model did not show any trend with respect to heavy metal ions investigated, it was not considered for error analysis. The results of error analysis, namely, average relative error (ARE), Sum square error (SSE), Hybrid fractional error function

(HYBRID), Nonlinear chi-square test and Sum of absolute error (EABS) are shown in Table 3.4.10 [89].

Table 3.4.8: Isotherm constants and respective regression coefficient (R^2) for Temkin, D-R, Sips and R-P isotherm model for considered heavy metal ions.

Temkin Isotherm			
Metal ion	B	K_T	R^2
Cd(II)	231	7.74	0.963
Cu(II)	130	3.57	0.968
Ni(II)	228	1.38	0.874
Pb(II)	516	2.03	0.962
Zn(II)	114	9.17	0.990
Cr(III)	58.9	3.21	0.885

Dubinin-Reduskevich (D-R) Isotherm (for higher concentrations)			
Metal ion	$B\times10^3$	q_s	R^2
Cd(II)	0.10	1894	0.698
Cu(II)	5.6	1106	0.998
Ni(II)	1.9	1798	0.927
Pb(II)	7.1	4298	0.934
Zn(II)	0.20	968.9	0.925
Cr(III)	4.1	518.3	0.940

Sips Isotherm				
Metal ion	K_s	$a_s\times10^2$	b_s	R^2
Cd(II)	394	9.60	1.69	0.987
Cu(II)	167	16.5	1.20	0.970
Ni(II)	68.9	2.40	1.57	0.975
Pb(II)	451	7.60	2.08	0.967
Zn(II)	264	26.6	1.69	0.987
Cr(III)	76.0	-43.3	2.97	0.947

Redlich-Peterson (R-P) Isotherm				
Metal ion	$K\times10^{-2}$	a	β	R^2
Cd(II)	12.5	2.3	0.79	0.994
Cu(II)	1.92	0.30	0.93	0.984
Ni(II)	0.195	0.020	0.89	0.966
Pb(II)	4.67	0.40	0.82	0.978
Zn(II)	4.46	0.95	0.88	0.993
Cr(III)	-2.51	-2.9	0.74	0.936

Table 3.4.9: Regression coefficients of adsorption isotherm models for all heavy metal ions under investigation.

Metal ion	Langmuir isotherm	Freundlich isotherm	Temkin isotherm	D-R isotherm Higher concentrations (>100 ppm)	R-P isotherm	Sips isotherm
Cd(II)	0.988	0.895	0.963	0.698	0.994	0.987
Cu(II)	0.990	0.812	0.968	0.998	0.984	0.970
Ni(II)	0.985	0.958	0.874	0.927	0.966	0.975
Pb(II)	0.986	0.915	0.962	0.934	0.978	0.967
Zn(II)	0.964	0.879	0.990	0.925	0.993	0.987
Cr(III)	0.983	0.904	0.885	0.940	0.936	0.947

The error values obtained for different isotherms vary significantly. However, the Langmuir isotherm shows the smallest error values in general, and hence, the selection of the Langmuir isotherm as the best fitted model is further convinced. The validity of other isotherm models by considering all types of error analyses can be given in the order of Langmuir > R-P > Sips > Temkin > Freundlich for heavy metal ions Cd(II), Cu(II) and Pb(II). However, this order is slightly different for Ni(II), Zn(II) and Cr(III).

The above results have already been disclosed in

- *T.P.K. Kulasooriya, N. Priyantha and A.N. Navaratne, Adsorption of heavy metal ions on rice husk: Isotherm modeling and error analysis, International Journal of Earth Science and Engineering, **8**, 346-352 (2015).*
- *N. Priyantha, A.N. Navaratne and T.P.K. Kulasooriya, Adsorption isotherm studies of heavy metal ions on rice husk, Proc. Pera. Univ. Res. Ses., University of Peradeniya (2014).*

Please see Annexure 5.

Table 3.4.10: Values of different error analyses for isotherm models.

	Metal ion	ARE	SSE	HYBRID	Non-linear chi-square test	EABS
Langmuir isotherm	Cd(II)	25.82	0.000	0.024	0.002	0.007
	Cu(II)	6.590	0.000	0.001	0.000	0.001
	Ni(II)	50.47	0.000	0.034	0.003	0.005
	Pb(II)	19.20	0.000	0.004	0.000	0.002
	Zn(II)	9.457	0.000	0.004	0.000	0.002
	Cr(III)	2.127	0.000	0.000	0.000	0.000
Freundlich isotherm	Cd(II)	6.217	2.220	4.410	0.485	4.210
	Cu(II)	8.294	2.736	7.431	0.594	4.201
	Ni(II)	3.971	0.852	2.196	0.198	2.116
	Pb(II)	5.818	2.154	3.680	0.331	4.025
	Zn(II)	6.002	1.457	3.819	0.306	3.064
	Cr(III)	1.578	0.196	0.387	0.035	0.995
Temkin isotherm	Cd(II)	High	High	High	High	High
	Cu(II)	198.1	High	High	High	High
	Ni(II)	184.2	High	High	High	High
	Pb(II)	High	High	High	High	High
	Zn(II)	High	High	High	High	High
	Cr(III)	41.76	High	High	High	High
R-P isotherm	Cd(II)	16.17	High	High	94.50	High
	Cu(II)	25.63	High	High	114.1	High
	Ni(II)	38.02	High	High	High	High
	Pb(II)	32.63	High	High	High	High
	Zn(II)	10.91	High	High	43.77	High
	Cr(III)	28.31	High	High	153.3	High
Sips isotherm	Cd(II)	41.33	High	High	High	High
	Cu(II)	28.85	High	High	146.5	High
	Ni(II)	18.14	High	High	196.4	High
	Pb(II)	66.66	High	High	High	High
	Zn(II)	19.06	High	High	69.94	298.7
	Cr(III)	26.87	High	High	143.9	High

3.4.3.5 Kinetics modeling

Basic kinetics models

Kinetics modeling was done for better understanding of the rate process. The generalized equation for kinetics, assuming that the activity of the adsorbent is constant, can be written as [69],

$$\frac{d(q_t)}{dt} = k'(q_e - q_t)^n \tag{3.4.6}$$

where k' is the apparent rate constant, t is the contact time, q_e and q_t are the masses of metal ions adsorbed by unit mass of the sorbent at equilibrium and at time t, respectively. A linearized integrated form of the above equation leads to the following kinetics models [90,91].

Pseudo first order:

$$\log (q_e - q_t) = -\frac{k'}{2.303} t + \log q_e \tag{3.4.7}$$

Pseudo second order:

$$\frac{t}{q_t} = \frac{1}{q_e} t + \frac{1}{k' q_e^2} \tag{3.4.8}$$

If the initial adsorption rate is h_o,

$$h_0 = k' q_e^2 \tag{3.4.9}$$

In order to identify the boundary layer diffusion, the intra-particle diffusion models, as given below were considered [92].

McKay and Poots intra-particle diffusion model, which assumes that a fraction of solute adsorbed can be expressed in terms of the square root of time, is given by,

$$q_t = X_i + k' t^{0.5} \tag{3.4.10}$$

Webber and Morris intra-particle diffusion model can be expressed as,

$$\log R = \log k_{id} + n \log(t) \tag{3.4.11}$$

where R is the percentage adsorption of a heavy metal, n is the gradient of linear plots and k_{id} is the intra-particle diffusion rate constant.

Figure 3.4.15 illustrates the variation of the extent of adsorption with contact time for different metal ions when an aqueous solution of each metal ion was individually treated with rice husk, heated at the optimum temperature. The extent of removal of heavy metal ions by rice husk, determined after the system reaches equilibrium, according to the figure follows the order, Ni(II) < Cr(III) < Cd(II) ≈ Zn(II) < Cu(II) < Pb(II). On the other hand, the rate at which rice husk-metal ion solution reaches equilibrium is different for each ion according to the figure. Adsorption of Pb(II) has reached equilibrium almost instantly, followed by Cd(II), Zn(II) and Ni(II). Adsorption of Cr(III) and Cu(II) takes the longest time to reach equilibrium. Owing to fast adsorption reaction rates, kinetics modeling cannot be applied for the investigation of adsorption of Pb(II) and Cd(II). Further, kinetics modeling for the adsorption of other metal ions should be applied within the time period up to 8 min, beyond which many systems would have reached equilibrium according to the observations of the figure.

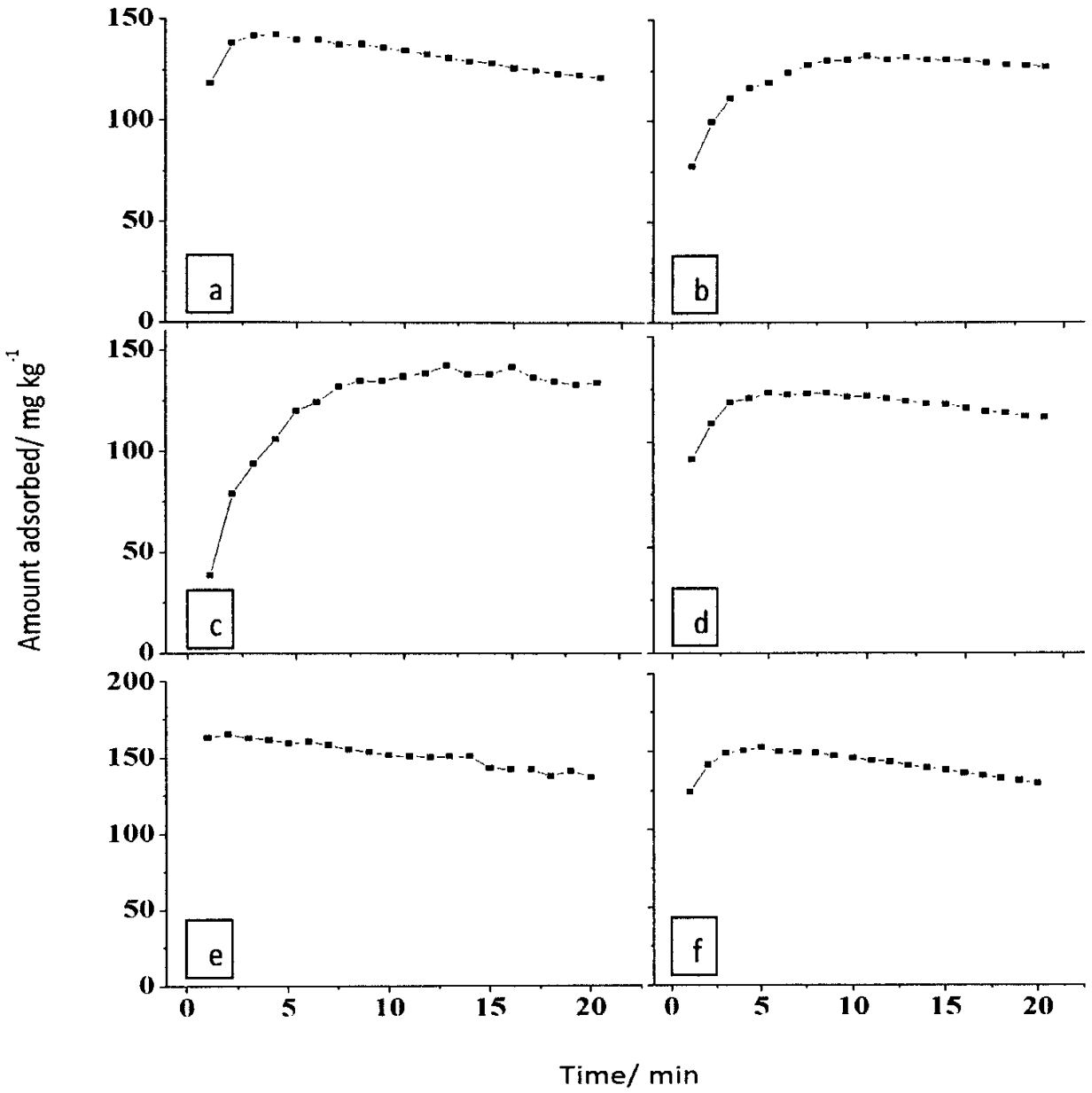

Figure 3.4.15: Variation of the amount of metal ions adsorbed with contact time (a) Cd(II) (b) Cr(III) (c) Cu(II) (d) Pb(II) (e) Ni(II) (f) Zn(II) (500 cm^3 of 10.0 mg L^{-1} metal ion solution (25.0 g rice husk; treatment temperature100 °C).

Application of adsorption data of metal ions for the linearized pseudo first order model [Equation (3.4.7)] does not lead to satisfactory regression coefficients. It is therefore concluded that the pseudo first order kinetics is not much in agreement with adsorption of heavy metal ions on rice husk. Therefore, the determination of kinetics parameters based on the pseudo first order model was not attempted. More importantly, application of the pseudo second order kinetics model [Equation (3.4.8)] shows a much better agreement of experimental data for the heavy metal ions selected, as shown in Figure 3.4.16.

All adsorption processes can be best described by the pseudo second order rate equation, according to the R^2 values obtained (Table 3.4.11). The data reported in the table indicates that the initial rate of adsorption (h_o) of metal ions follows the order, Zn(II) > Ni(II) > Cr(III) > Cu(II), which is a measure of how fast the reaction proceeds. Since ionic radius follows the order Pb(II) > Cd (II) > Zn (II) > Ni(II) ≈ Cr(II) ≈ Cu (II), it may be the reason for the highest rate of adsorption obtained for Zn(II) among other metals. The order determined based on kinetics, which depends on the path to reach equilibrium, is not in agreement with the order of the extent of removal of metal ions determined when the system has reached equilibrium, due to the fact that kinetics and equilibrium aspects are not inter-dependent.

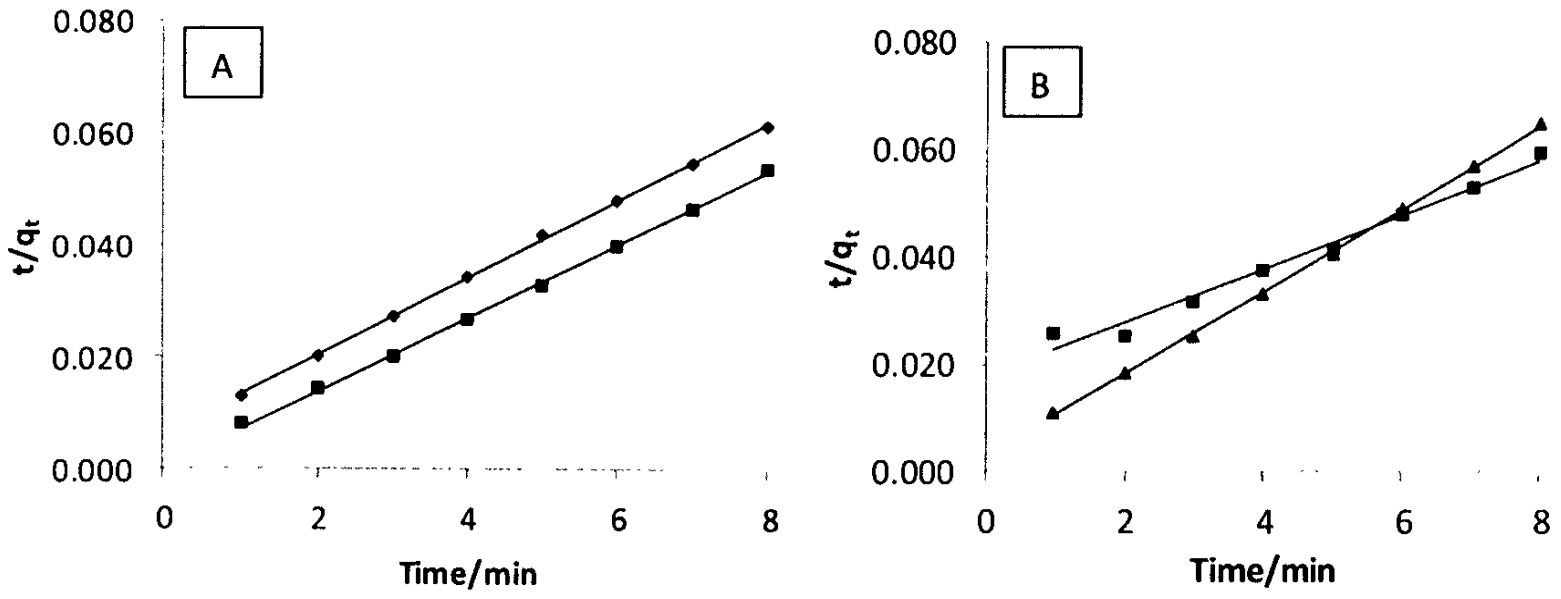

Figure 3.4.16: Plots of linearized pseudo second order kinetics model for adsorption of metal ions on heated rice husk; Plot (A): Zn(II) (■) and Cr(III) (◆); Plot (B): Cu(II) (■) and Ni(II) (▲) (500 cm^3 of 10.0 mg L^{-1} metal ion solution, 25.0 g heated rice husk).

Table 3.4.11: Kinetic parameters from the pseudo second order model for adsorption of heavy metal ions on rice husk.

Metal ions	R^2	q_e/mg kg^{-1}	k'/kg mg^{-1} min^{-1}	h_0/mg kg^{-1} min^{-1}
Cu(II)	0.981	200	0.001	56
Ni(II)	0.999	130	0.023	385
Zn(II)	0.999	154	0.047	1111
Cr(III)	0.999	143	0.008	159

Among many models available for mechanistic investigation on metal ion - adsorbent interactions, intraparticle diffusion and external mass transfer diffusion models are common [93].

External mass transfer diffusion model

This is also called the boundary model which assumes that the surface concentration of a metal ion is negligible at $t = 0$, and consequently, intraparticle diffusion is negligible. The change in the metal concentration with respect to time is related to the liquid-solid mass transfer coefficient (β_L) [93]. The simplified equation of the above model is,

$$\frac{C_t}{C_0} = -\beta_L S t \qquad (3.4.12)$$

where C_t and C_0 are metal ion concentrations in solution at time t and at $t = 0$, β_L is the liquid-solid mass transfer coefficient and S is the specific surface area for mass transfer.

The regression coefficient (R^2) values of graphs of C_t/C_0 vs. t according to Equation (3.4.12) for Cu(II), Ni(II), Zn(II) and Cr(III) are 0.788, 0.766, 0.415 and 0.872, respectively. As R^2 values were not satisfactory, intraparticle diffusion models were tested for the same data set.

Intra-particle diffusion models

The adsorption of metal ions on rice husk would be controlled by either film-diffusion or particle-diffusion [91]. The adsorbate may diffuse from the bulk of the solution to the film surrounding the adsorbent and then into the micropores/macropores of the adsorbent in the film diffusion model [10,90]. In the particle diffusion model, the bulk of the solution diffuses through the pores present in the sorbent and the adsorbate goes along the pore walls to the sorbent [10].

Variation of the amount of metal ions adsorbed with $t^{1/2}$ plotted to check the validity of the McKay and Poots intra-particle diffusion model shown in Figure 3.4.17 does not lead to desirable regression coefficients [R^2 values for Cu(II), Ni(II), Zn(II) and Cr(III) are 0.949, 0.764, 0.603 and 0.929, respectively], suggesting that the rate limiting step has another contribution in addition to the mode of diffusion proposed by this model. On the other hand, the plots of the Weber and Morris intra-particle diffusion for the four heavy metals investigated are shown in Figure 3.4.18 results in satisfactory regression coefficients as shown in Table 3.4.12. The gradient of plots (n) and the intra-particle diffusion rate constant (k_{id}) determined are given in Table 3.4.12.

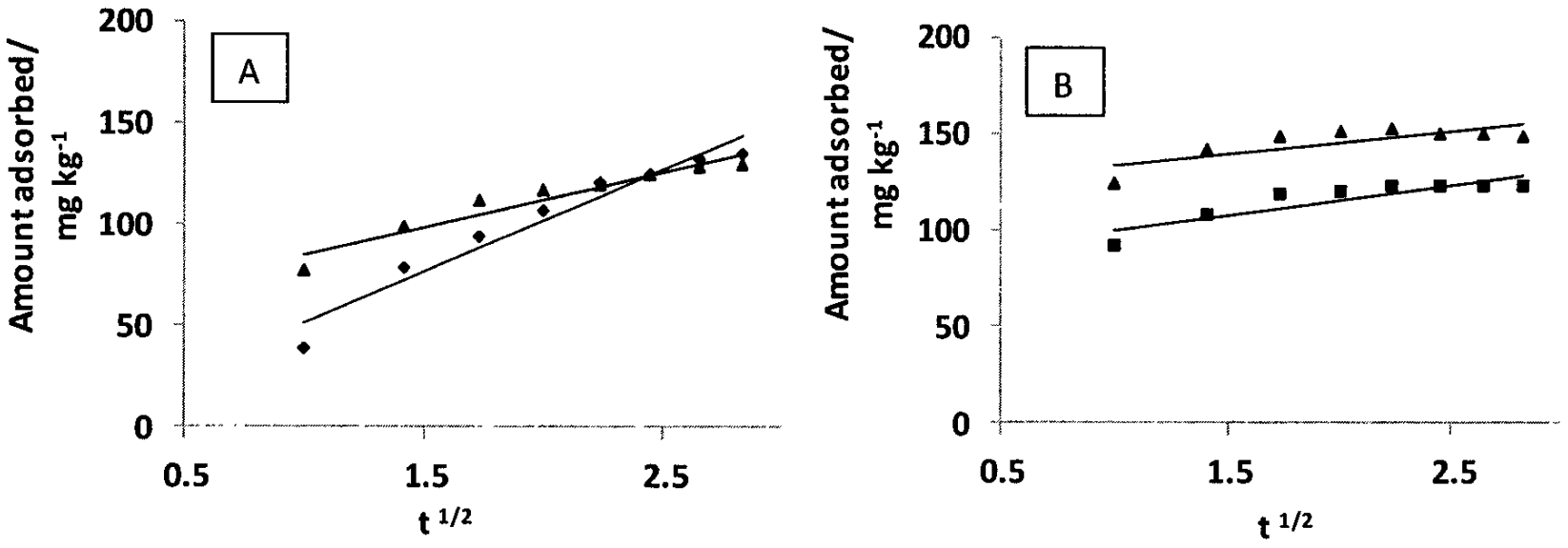

Figure 3.4.17: McKay and Poots intra-particle diffusion model for adsorption of metal ions on rice husk; Plot (A): Cu(II) (◆) and Cr(III) (▲); Plot (B): Ni(II) (■) and Zn(II) (▲).

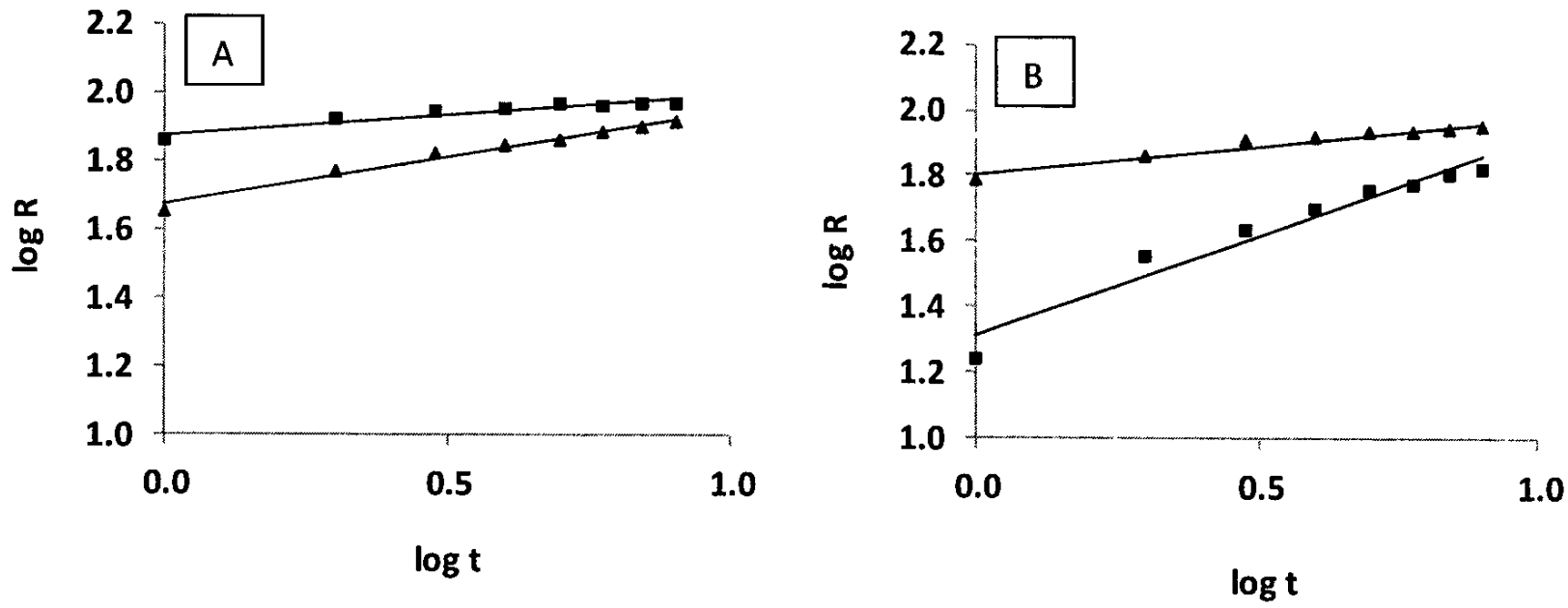

Figure 3.4.18: Weber and Morris intra-particle diffusion model for sorption of heavy metals on heated rice husk plotted according to Equation (7). Plot (A): Zn(II) (■) and Cr(III) (▲); Plot (B): Cu(II) (■) and Ni(II) (▲).

Table 3.4.12: Weber and Morris intra-particle diffusion model parameters for heavy metal ions.

Metal ion	R^2	n	k_{id}
Cu(II)	0.948	0.61	20.40
Ni(II)	0.936	0.17	63.59
Zn(II)	0.901	0.12	74.87
Cr(III)	0.980	0.27	47.08

The value k_{id} is taken as a rate factor, which increases in the order of Zn(II) > Ni(II) > Cr(III) > Cu(II), where higher values of k_{id} show an improvement in the rate of adsorption. The increasing order of the intra-particle diffusion rate constant (k_{id}), determined from the Weber and Morris model, and that of the pseudo second order rate constant (k') follow the same trend, demonstrating the validity of the two models for adsorption of heavy metal ions investigated on rice husk. Further, larger n values show strong adsorption indicating strong bonding between the metal ion and the adsorbent [90].

These results have been submitted for possible publication [A.N. Navaratne, N. Priyantha and T.P.K. Kulasooriya, Removal of heavy metal ions using rice husk: Investigation on adsorption kinetics of heavy metals] – Annexure 5.

3.4.4 Removal of Heavy Metal Ions Using Brick Clay under Static Conditions

In addition to rice husk, brick clay can also be employed to remove heavy meal ions from aqueous solution. Mixtures of these two, or combinations in the form of sandwich packings would also be possible in this regard. Owing to the fact that the presence of Zn(II) and Cu(II) in industrial effluents, these two metals were initially considered as adsorbates for the removal experiments, under static conditions. The results obtained would be very much important for further experiments involving for large scale operations.

3.4.4.1 Removal of Zn(II)

Removal studies of Zn(II) were performed with brick clay fired at 400 °C at which the maximum extent of removal and the minimum turbidity for many pollutants have been reported [74].

According to Figure 3.4.19, shaking time and settling time were optimized for the selected brick clay samples. The optimum shaking time and optimum settling time for Zn(II) removal were selected as 30 min and 15 min, respectively, for further experiments. Variation of the extent of removal at different pH values from 1.0 to 6.0 at the optimized contact time results in an optimum pH range of 3.0–6.0 for the removal of Zn(II) with brick clay treated at 400 °C [Figure 3.4.19(C)].

Variation of the extent of Zn removal with the initial concentration of Zn(II) indicates that the brick clay surface treated at 400 °C does not reach saturation even at concentrations as high as 800 mg L^{-1} (Figure 3.4.20). The entire concentration range when used for the investigation of the validity of many isotherms results in regression coefficients close to 1.0 for the Langmuir and Freundlich adsorption isotherms (Figure 3.4.21, Table 3.4.13). More importantly, the adsorption capacity of brick clay for Zn(II) is 1429 mg kg^{-1}, which is higher as compared to rice husk under similar conditions.

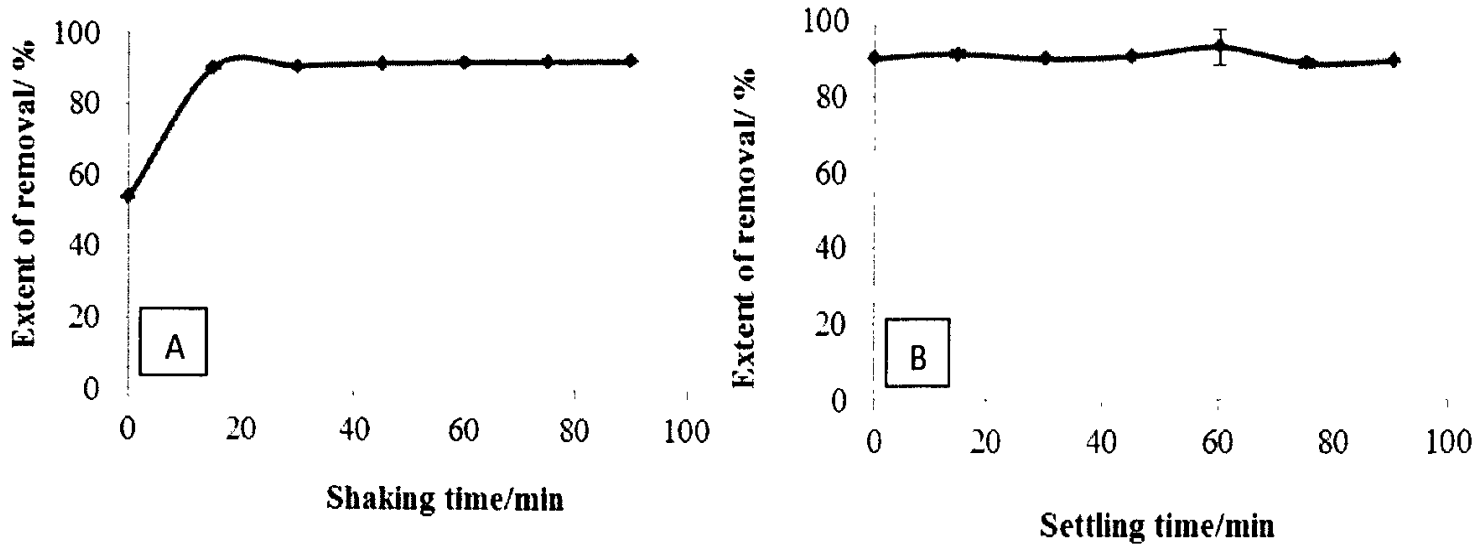

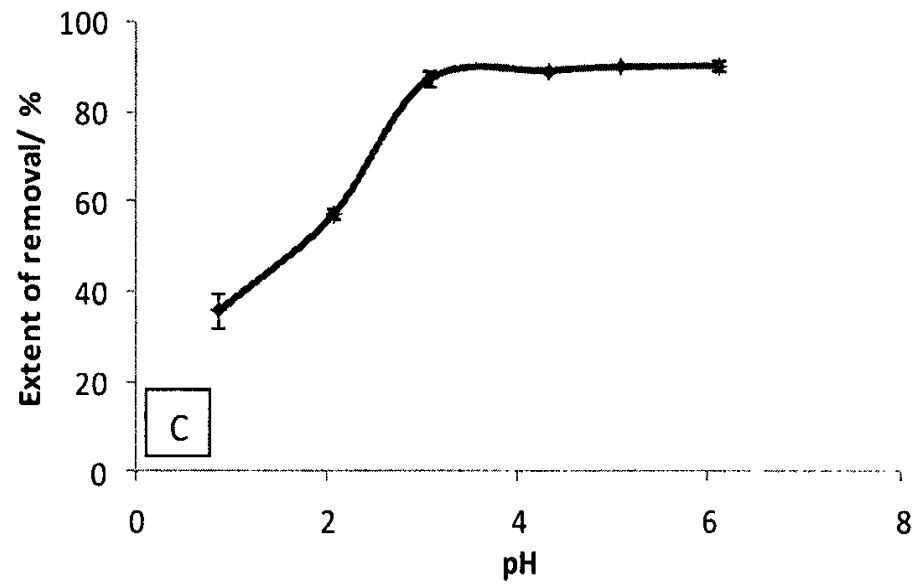

Figure 3.4.19: Parameter optimization the removal of Zn(II) ions: (A) Shaking time (B) Settling time (C) initial solution pH (50.0 cm^3 of 10.0 mg L^{-1} Zn(II) solution treated with 5.0 g of brick clay fired at 400 °C).

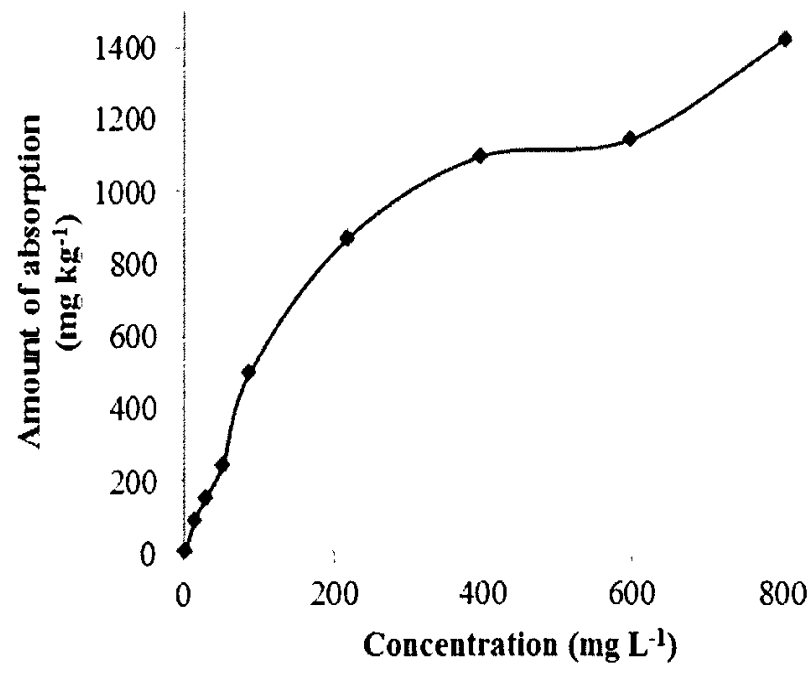

Figure 3.4.20: Amount of Zn(II) adsorbed on brick clay (50.0 cm^3 of Zn(II) solution, 5.0 g of brick clay treated at 400 °C).

Table 3.4.13: Regression coefficient values for different adsorption isotherm models for the removal of Zn(II) using brick clay.

Isotherm model	Regression coefficient	Isotherm constants
Langmuir	0.9565	q_e = 1429 mg kg^{-1}; K_L = 0.011 L mg^{-1}
Freundlich	0.9689	n = 1.5121; K_F = 26.17
Temkin	0.8257	
Dubinin-Raduskevich	0.3044	

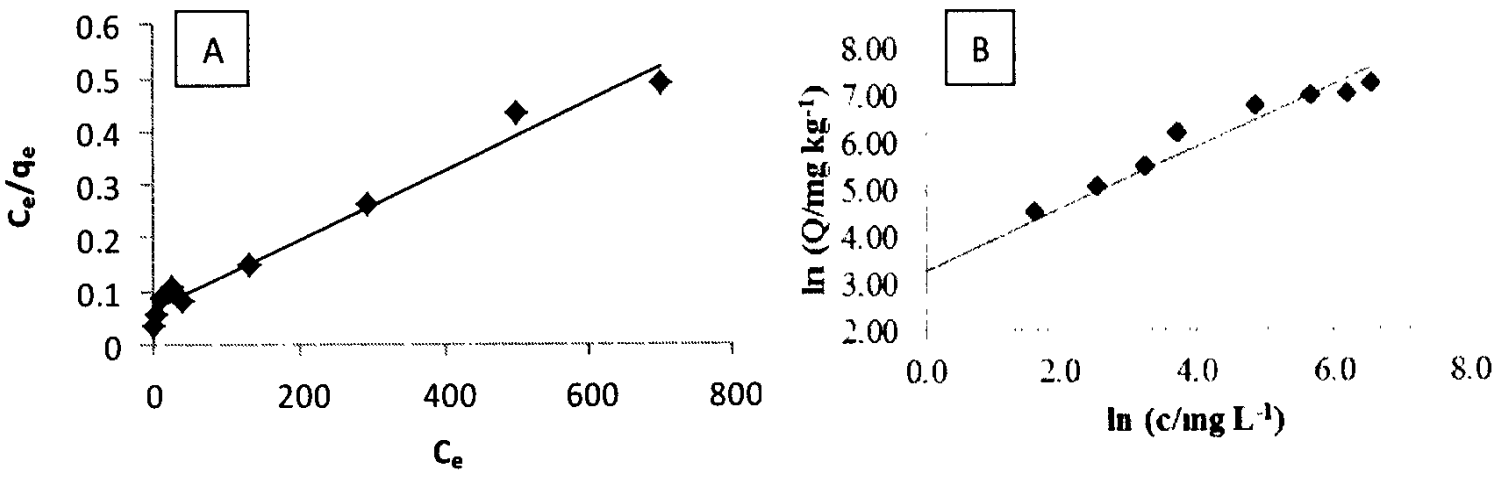

Figure 3.4.21: Isotherm models for removal of Zn(II) from brick clay: (A) Langmuir isotherm (B) Freundlich isotherm.

Kinetics studies, conducted with brick clay treated at 400 °C by withdrawing 5.0 cm^3 volumes of samples at every 1.0 min interval for a period of 20 min before the equilibrium was established, lead to the agreement of the pseudo second order model to describe the brick clay-Zn(II) interaction with a high regression coefficient of 1.000 (Figure 3.4.22).

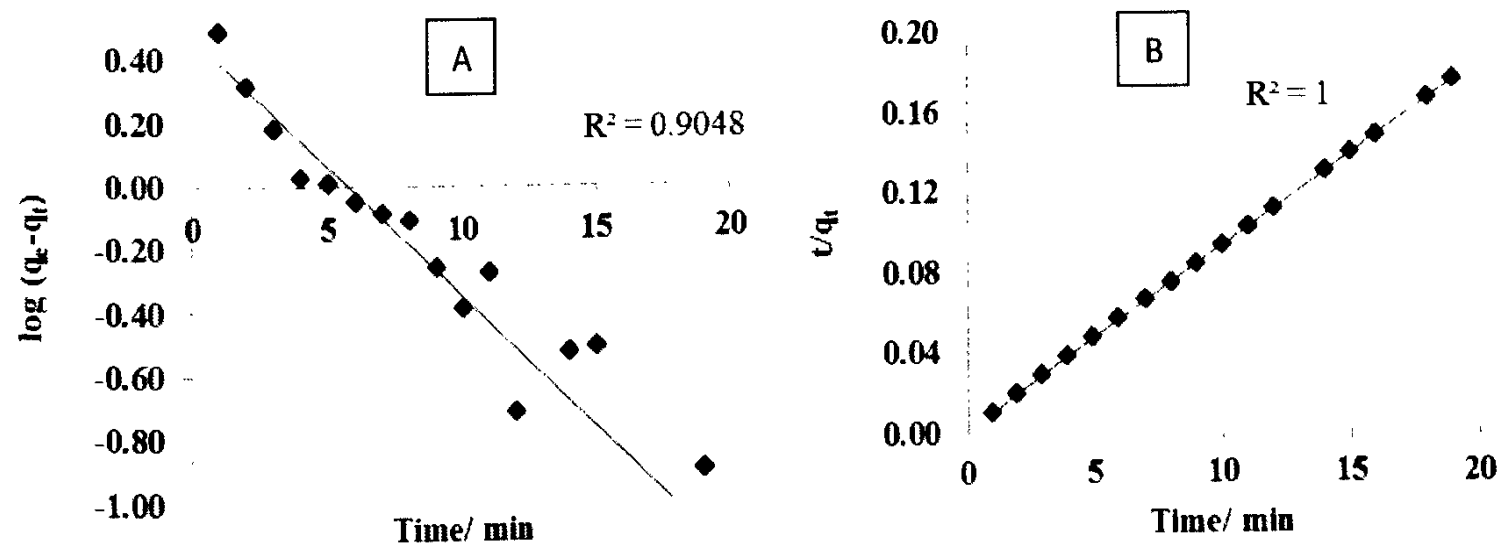

Figure 3.4.22: Adsorption kinetics studies for removal of Zn(II) from brick clay: (A) Pseudo first order kinetics (B) Pseudo second order kinetics (1000 cm^3 of 10.0 ppm metal ion solution, 100.0 g brick clay).

Application of the same kinetics data to check the validity of the external mass transfer diffusion model did not produce satisfactory R^2 (= 0.721) value when C_t/C_0 was plotted against time (t) (Figure 3.4.23). Hence, McKay and Poots, and Weber and Morris intraparticle diffusion models were investigated (Figure 3.4.24). Among two models, R^2 values describes the validity of Weber and Morris intraparticle diffusion model with a higher R^2 value of 0.945 as compared to the latter model which results in a R^2 value of 0.849. The gradient of plots (n) and intra-particle diffusion rate constant (k_{id}) determined from the slope and the intercept of the plots are 0.0087 and 95.34 min respectively. The value k_{id} is much higher when compared to the values obtained for adsorption of Cu(II), Ni(II), Zn(II) and Cr(III) on rice husk, demonstrating the higher rate of adsorption of Zn(II) on brick clay.

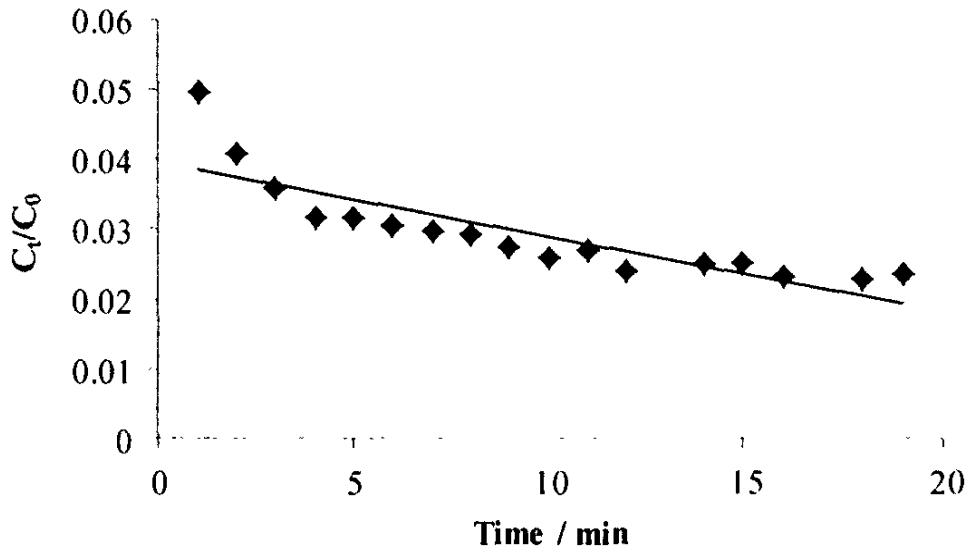

Figure 3.4.23: External mass transfer diffusion model for adsorption of Zn(II) on brick clay.

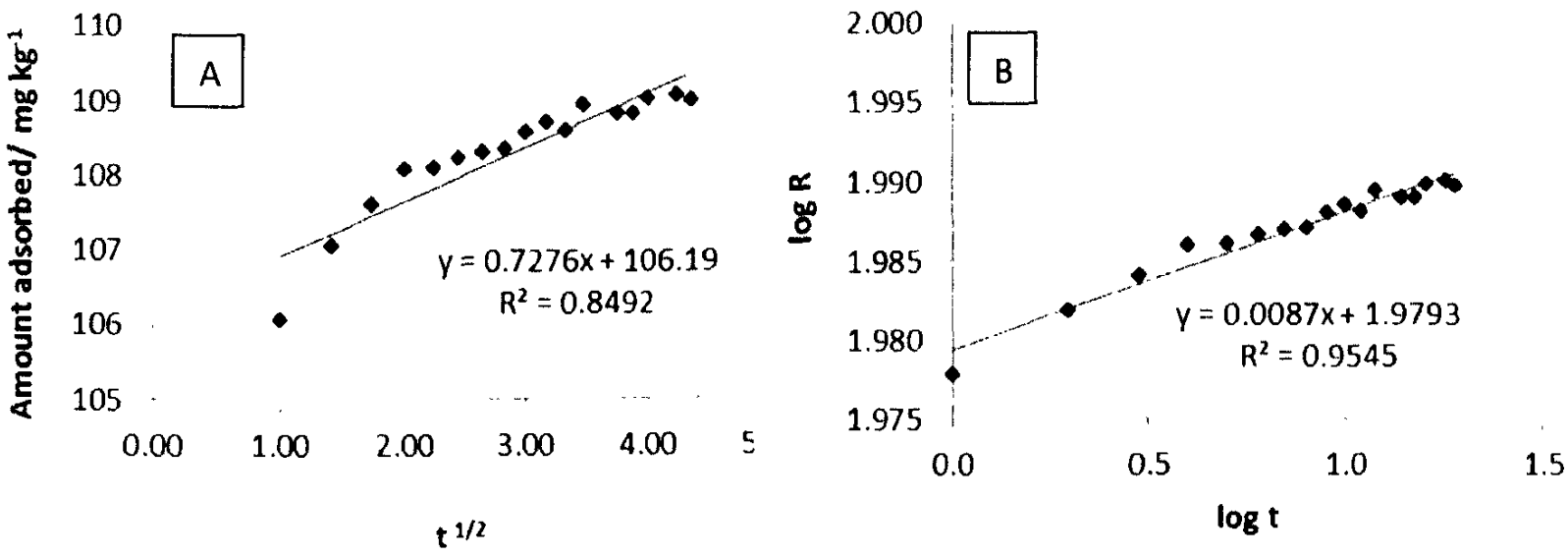

Figure 3.4.24: Intra-particle diffusion models for adsorption of Zn(II) on brick clay; Plot (A): McKay and Poots intra-particle diffusion model and Plot (B): Weber and Morris intraparticle diffusion model.

3.4.4.2 Removal of Cu(II)

Removal studies of Cu(II) was performed with brick clay fired at 400 °C at which the maximum extent of removal and the minimum turbidity have been observed for many pollutants. Results of the experiments conducted to investigate the effect of experimental parameters on the extent of removal of Cu(II), shown in Figure 3.4.25, it is reasonable to consider that the optimum shaking time, optimum settling time and initial solution pH for Cu(II) removal are 45 min, 15 min and neutral initial pH, respectively.

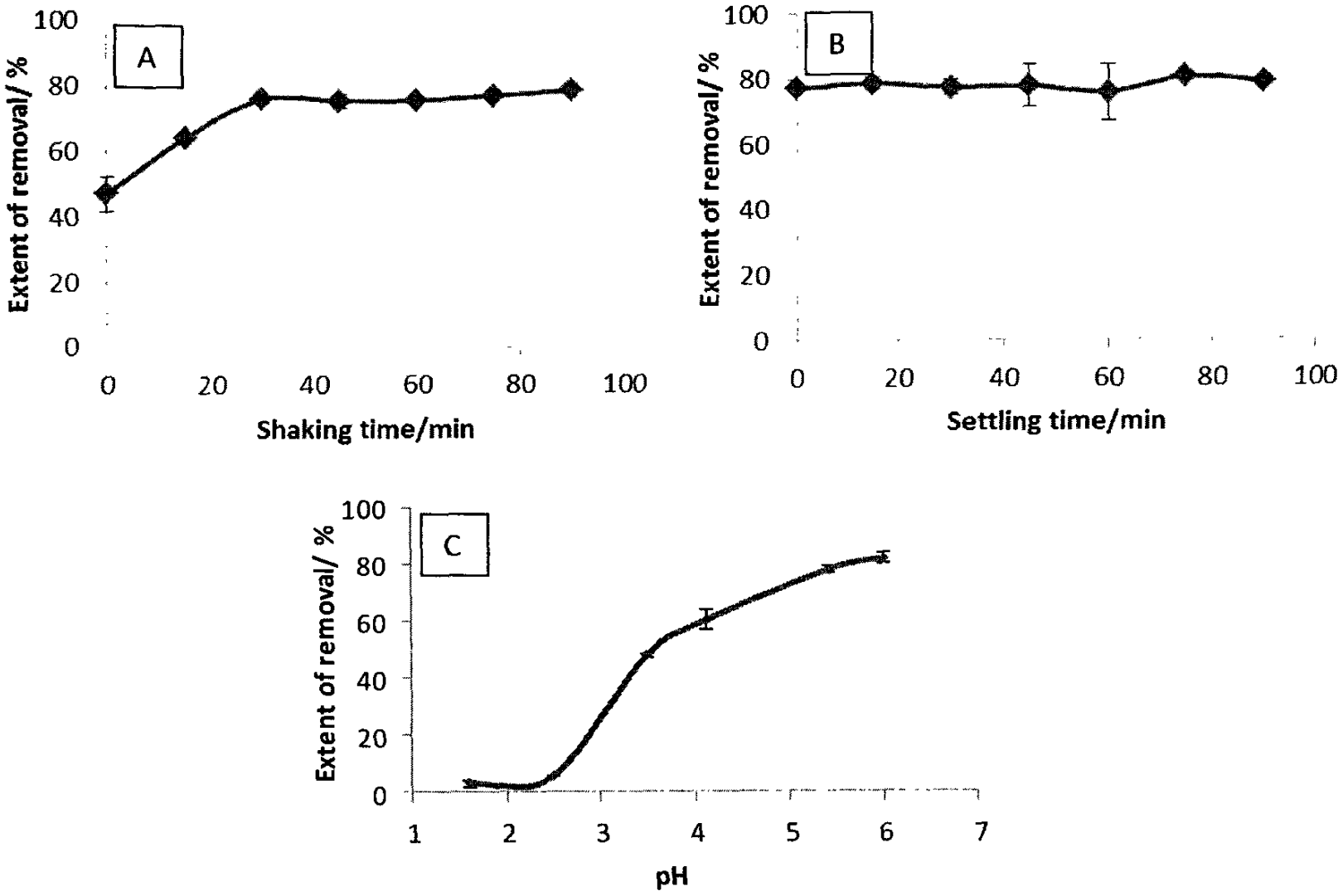

Figure 3.4.25: Parameter optimization for the removal of Cu(II) ions using brick clay: (A) Shaking time (B) Settling time (C) Initial solution pH (50.0 cm^3 of 10.0 mg L^{-1} Cu(II) solution treated with 5.00 g of brick clay fired at 400 °C).

Similar variation has been observed for other metal ions as well. Adsorption isotherm analysis, performed within a broad concentration range in order to understand adsorption characteristics of the Cu(II) – fired brick clay system, indicate the validity of the Langmuir and Freundlich adsorption isotherms having regression coefficients close to 1.0. Table 3.4.14 shows the results calculated from the data obtained. According to the table, the adsorption capacity of brick clay toward Cu(II) is 238 mg kg^{-1}, which is smaller compared to many other adsorbents.

Table 3.4.14: Regression coefficient (R^2) values for different adsorption isotherm models for the removal of Cu(II) using brick clay.

Isotherm model	R^2	Isotherm constants
Langmuir	0.9924	$q_e = 238$ mg kg^{-1}; $K_L = 0.088$ L mg^{-1}
Freundlich	0.9125	$n = 6.998$; $K_F = 94.13$
Temkin	0.8506	
Dubinin-Raduskevich	0.6213	

Kinetics studies, conducted with brick clay treated at 400 °C by withdrawing 5.0 cm^3 volumes of samples at every 1.0 min interval for a period of 20 min before the establishment of equilibrium, lead to the validity of the pseudo second order model to describe the brick clay-Cu(II) equilibrium (Figure 3.4.26).

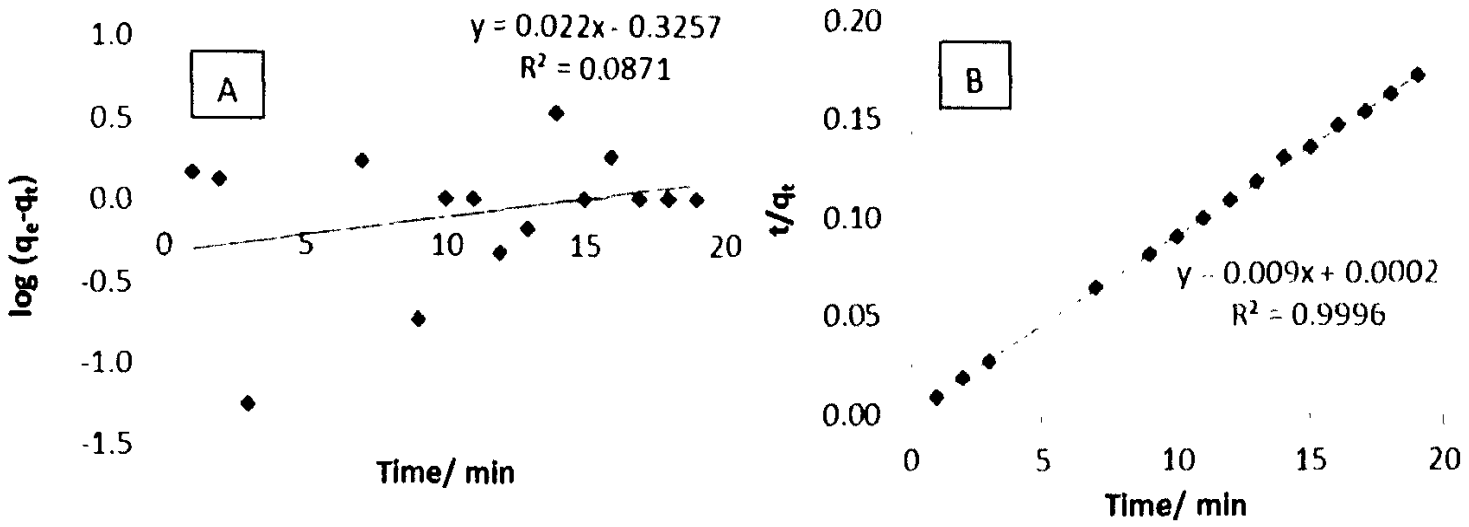

Figure 3.4.26: Adsorption kinetics studies for removal of Cu(II) from brick clay: (A) Pseudo first order kinetics (B) Pseudo second order kinetics (1000 cm^3 of 10.0 mg L^{-1} metal ion solution, 100.0 g brick clay).

The same data fitted to the external mass transfer diffusion model according to Equation (3.4.12) by plotting C_t/C_0 vs. t gives a poor regression coefficient (R^2) of 0.416 (Figure 3.4.27). Figure 3.4.28 shows the linearized fitting of the intra-particle diffusion models for the same kinetics data: McKay & Poots model and Weber & Morris model.

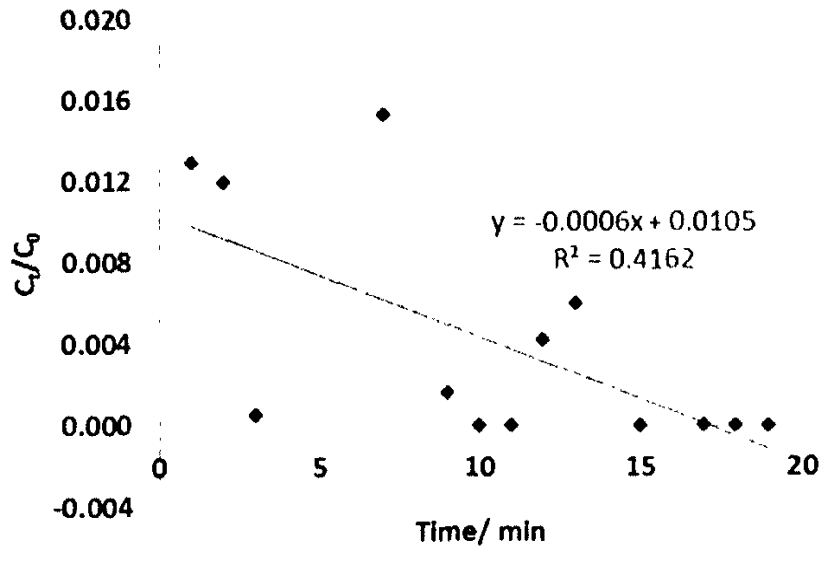

Figure 3.4.27: External mass transfer diffusion model for adsorption of Cu(II) on brick clay.

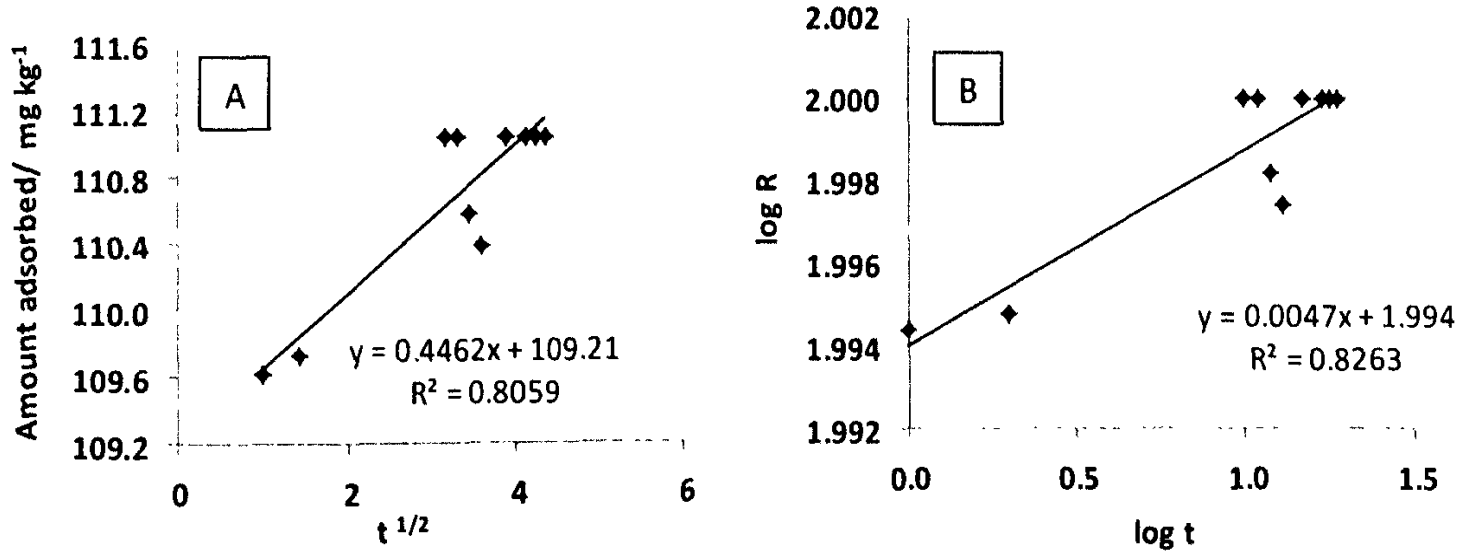

Figure 3.4.28: Intra-particle diffusion models for adsorption of Cu(II) on brick clay; Plot (A): McKay and Poots intra-particle diffusion model and Plot (B): Weber and Morris intraparticle diffusion model.

Between two models, R^2 values describes the validity of Weber and Morris intraparticle diffusion model ($R^2 = 0.826$) than McKay and Poots model ($R^2 = 0.806$, does not go through the origin). The gradient of the plot (n) and intra-particle diffusion rate constant (k_{id}) determined from the McKay and Poots plot are 0.0047 and 98.63 min, respectively. The value k_{id}, a rate factor, is much higher for adsorption of Cu(II) on brick clay when compared to the values obtained for adsorption of Cu(II), Ni(II), Zn(II) and Cr(III) on rice husk, and Zn(II) on brick clay.

These results have been included in a manuscript under preparation for submission [N. Priyantha, A.N. Navaratne, T.P.K. Kulasooriya and W. S. A. Weththasinghe, Comparison of the removal of Cu(II) and Zn(II) by using coir dust and brick clay] – Annexure 5.

3.4.5 Removal of heavy metal ions under dynamic conditions

3.4.5.1 Removal of metal ions present in a mixture of solution using brick clay and rice husk

Experiments conducted by passing solutions of heavy metal ions through columns packed with rice husk, brick clay, and layered type combined adsorbents show that the maximum removal is obtained with columns packed with brick clay alone. In dynamic experiments, 13 representative samples were taken within 5 min apart when metal ion solutions were eluted from the column at a constant flow rate of 50 cm^3 min^{-1}. Subsequently, the concentration of each metal ion was determined, and the variation between the concentration and the time of sampling was investigated. Figure 3.4.29 illustrates the variation of the extent of removal, determined as the percentage removal, for brick clay packed columns. Although this does not decrease within 60 min indicating the long-term efficiency of the column, it was clogged due to the wetting of brick clay particles heated at 200 °C. To overcome this problem, a column packed with rice husk was attempted.

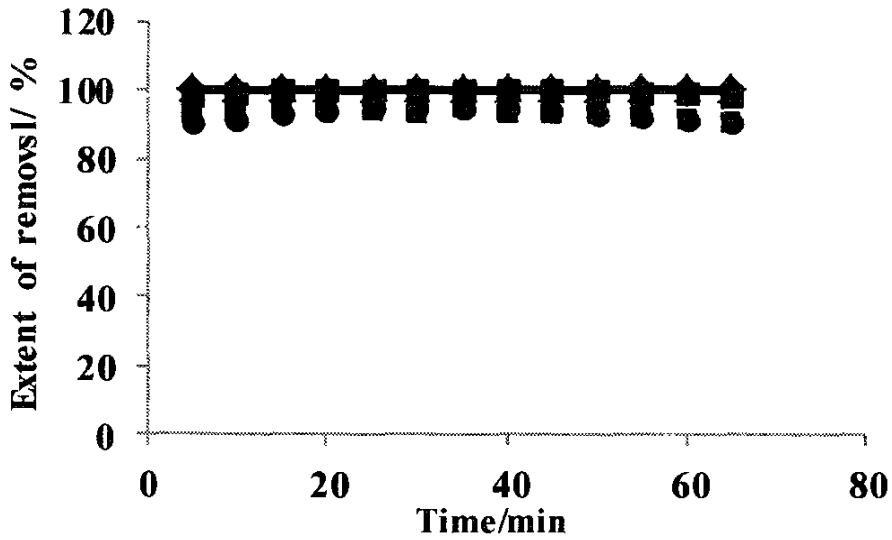

Figure 3.4.29: Extent of removal of heavy metal ions by columns packed with brick clay fired at 200 °C: Cu(II) (◆), Cd(II) (■), Cr(III) (▲), Pb(II) (×), Zn(II) (∗) and Ni(II) (●).

Figure 3.4.30 shows that the extent of removal of all heavy metal ions investigated by rice husk packed columns is decreased with time in contrast to the constant efficiency of brick clay packed columns. However, Pb(II) and Cu(II) show much higher removal ability as compared to Cd(II), Cr(III), Zn(II) and Ni(II). Although the removal ability of rice husk packed columns is much lower, the column does not get clogged as with brick clay. The efficiency of brick clay and the non-clogging behavior of rice husk can thus be used complimentary to each other using both adsorbents simultaneously.

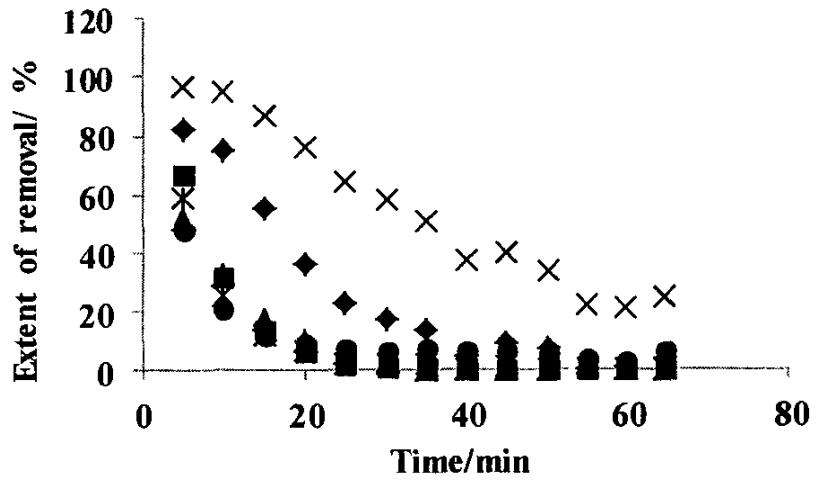

Figure 3.4.30: Extent of removal of heavy metal ions by columns packed with rice husk heated at 100 °C: Cu(II) (◆), Cd(II) (■), Cr(III) (▲), Pb(II) (×), Zn(II) (∗) and Ni(II) (●).

Figure 3.4.31 shows the effect of layered type packed columns of brick clay fired at 200 °C and rice husk fired at 100 °C, both of which are better than the columns packed with rice husk alone.

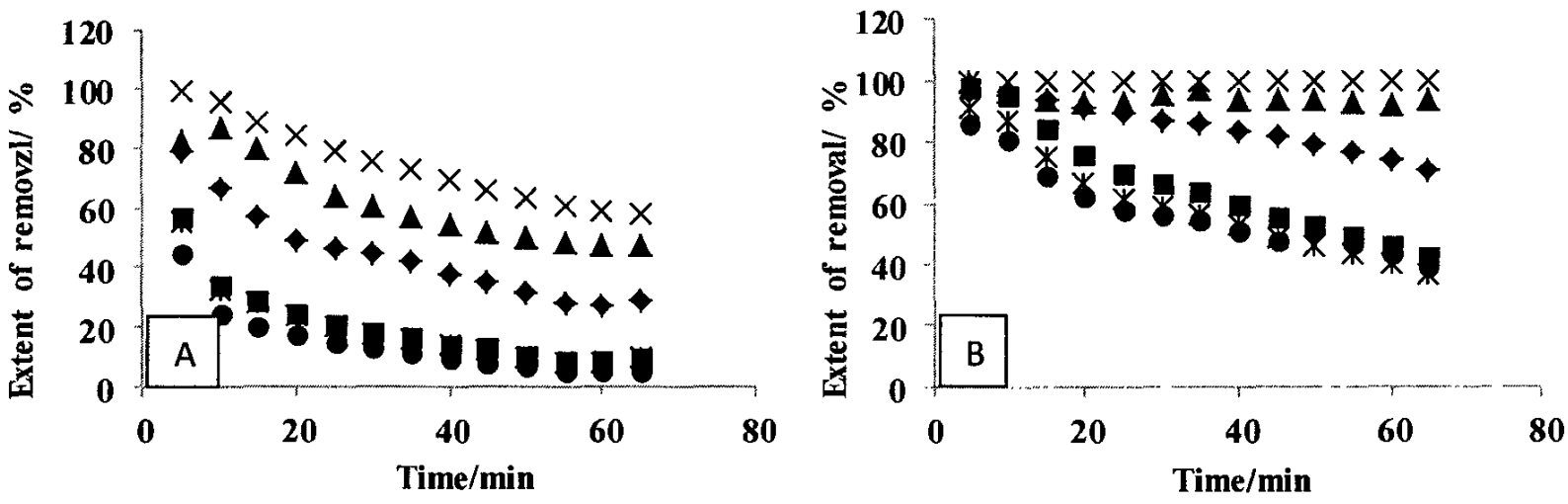

Figure 3.4.31: Removal percentage of heavy metal ions by columns packed with different adsorbents: (A) Brick clay (bottom)-rice husk (top) (B) Rice husk (bottom)-Brick clay (top). Heavy metals are Cu(II) (◆), Cd(II) (■), Cr(III) (▲), Pb(II) (×), Zn(II) (∗) and Ni(II) (●).

The rice husk-brick clay layered column, whose results are shown in Figure 3.4.31(B), is superior to the brick clay-rice husk column in terms of both efficiency and stability, for all the metal ions investigated. The extent of removal of Pb(II) and Cr(III) by this column is steady at almost 100% even after one hour elution. Further, the clogging behavior encountered for brick clay only packed columns was not observed in any of the layered type columns. It is clearly shown from these results that the efficiency of the column strongly depends on the order of packings. It is suggested that the adsorbent of higher efficiency of removal be packed on top so that the extent of interaction is better.

3.4.5.2 Order of the removal ability of heavy metals

Percentage removal values of first 10 samples collected from the eluent were averaged to investigate the order of the removal ability of the cations under investigation. Table 3.4.15 shows the results for all cations in every arrangement of adsorbents in columns.

Table 3.4.15: Average percentage removal values for each column packing.

Adsorbent	Cu(II)	Cd(II)	Cr(III)	Pb(II)	Zn(II)	Ni(II)
Rice husk	32	13	12	64	11	13
Brick clay	≈100	≈100	≈100	≈100	94	94
Rice husk-brick clay	88	72	95	≈100	64	62
Brick clay-rice husk	49	24	66	79	23	17

According to the results shown in the above table, Pb(II) is the most easily removable metal ion from all types of arrangements. Brick clay shows almost 100% removal ability for Cu(II), Cd(II), Cr(III) and Pb(II), while rice husk-brick clay column shows almost 100% removal ability for Pb(II) only. The order of the removal ability by rice husk is determined to be Pb(II) > Cu(II) > Ni(II) ≈ Cd(II) > Cr(III) > Zn(II). Brick clay alone and both types of layered columns show similar order of removal, Pb(II) ≥ Cr(III) ≥ Cu(II) ≥ Cd(II) ≥ Zn(II) ≥ Ni(II). On the other hand, the efficiency of removal of metal ions is in the order of brick clay > rice husk-brick clay > brick clay-rice husk > rice husk. The highest removal ability of Pb(II) for all arrangements can be explained using the relative mobility, charge and hydrated radius of the metal ions. Relative mobility is decreased in the order of Pb(II) > Cu(II) > Cd(II) > Zn(II) > Ni(II) and the hydrated radius varies in the order of Cu(II) > Cd(II) > Pb(II) [10]. Since Pb(II) has lowest hydrated radius among these cations, it easily diffuses into the adsorbent media and its highest relative mobility promotes the fast diffusion in solution.

3.4.5.3 Comparison of static and dynamic conditions

Rice husk was used to compare the removal ability of cations present in mixtures of solutions in both static and dynamic conditions, as shown in Table 3.4.16, which indicates that static conditions are more successful in removing metal ions as compared to dynamic conditions. This is due to the longer time period of interaction receiving the treatment under static conditions. Nevertheless, there are many advantages of using dynamic conditions for the removal of metal ions, such as cost effectiveness and possibility of expansion towards the treatment of real industrial effluents. Small processing time for the whole process, less space required and small amount of adsorbent required are additional advantages. Many of these advantages lead to save energy.

Table 3.4.16: Average percentage removal values of rice husk for dynamic and static conditions.

Metal ion	Average percentage removal (%)	
	Dynamic	Static
Cd(II)	13	71
Cu(II)	32	80
Zn(II)	11	66
Cr(III)	12	82
Ni(II)	13	53
Pb(II)	64	≈100

The above results have been disclosed as follows:

- *A.N. Navaratne, N. Priyantha and T.P.K. Kulasooriya, Removal of heavy metals using rice husk and brick clay as adsorbents - dynamic conditions, International Journal of Earth Science and Engineering, **6**, 807-811 (2013) - Annexure 5.*
- *A.N. Navaratne, N. Priyantha and T. P. K. Kulasooriya, Removal of heavy metals using rice husk and brick clay as adsorbents: a study of dynamic conditions, 2nd Int. Symposium on Water Quality and Human Health: Challenges Ahead, PGIS, University of Peradeniya (2013) – Annexure 5.*

3.4.6 Removal of anions using Adsorbents

According to the real effluent analysis data, other than heavy metal ions, many anions were present in the effluent samples in considerable amount. Therefore, in order to apply this method on anions, all selected adsorbents were checked for some anions such as SO_4^{2-}, PO_4^{3-} and Cl^- ions.

3.4.6.1 Removal of chloride using naturally available substances

The extent of removal of chloride from synthetic effluent samples were tested for brick clay, rice husk, coir dust, saw dust, feldspar and dolomite using a chloride ion selective electrode. According to the results obtained, none of the selected adsorbent can be used to remove chloride. These ions are not removed by rice husk even after heat treatment.

3.4.6.2 Removal of sulfate using naturally available substances

The extent of removal of sulfate from synthetic effluent samples was tested for the same adsorbents using a turbidimetric method. Among them, saw dust shows the highest removal ability (40%) from synthetic effluent solution, while coir dust and rice husk do not show any removal ability (Figure 3.4.32)

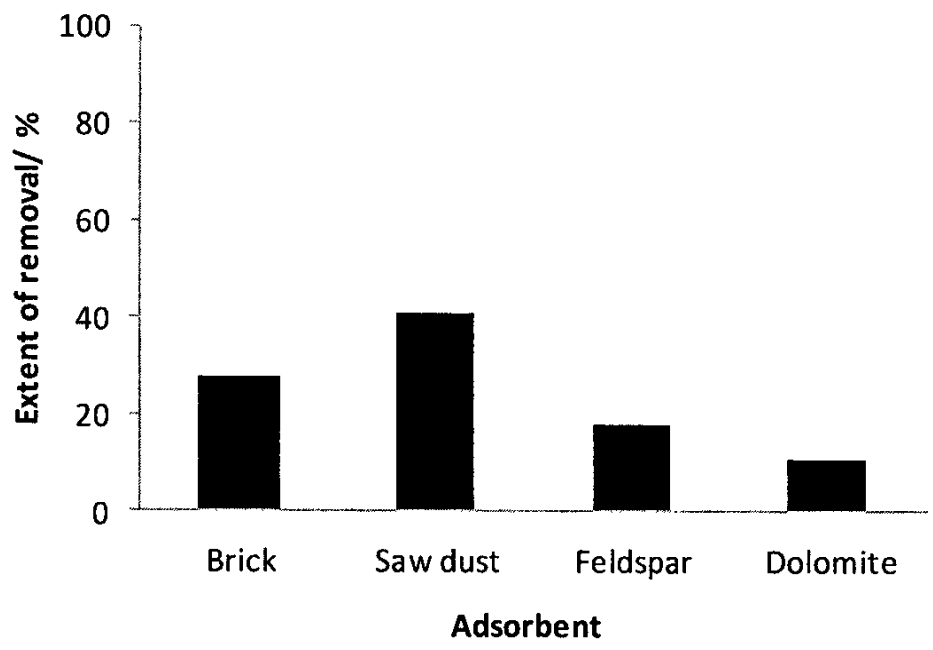

Figure 3.4.32: Percentage removal of sulfate using various adsorbents (50.0 cm^3 of 10.0 mg L^{-1}sulfate, 1.0 g of unfired adsorbents).

After the selection of saw dust as the sulfate removal adsorbent, experimental parameters were optimized. Under experimental conditions, shaking time and settling time were obtained as 30 min time and 1.0 h, respectively (Figure 3.4.33).

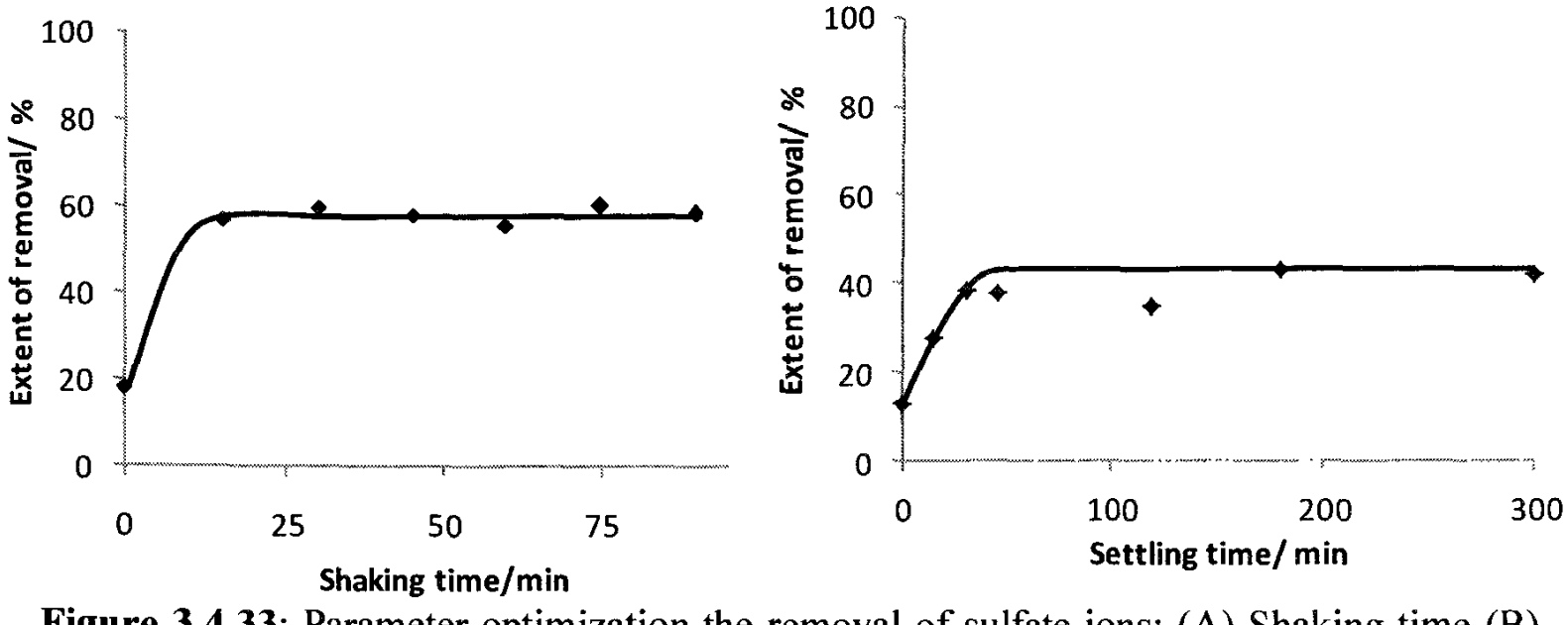

Figure 3.4.33: Parameter optimization the removal of sulfate ions: (A) Shaking time (B) Settling time (50.0 cm^3 of 10.0 mg L^{-1} sulfate, 1.0 g of saw dust).

3.4.6.3 Removal of phosphate using naturally available substances

Batch adsorption study

The extent of removal of phosphate from synthetic solutions prepared in the laboratory by three natural adsorbents is shown in Figure 3.4.34. Among them, unfired brick clay is found to be the most efficient adsorbent with more than 80% removal under experimental conditions. As feldspar and dolomite shows much less removal ability for phosphate, further experiments were conducted using brick clay.

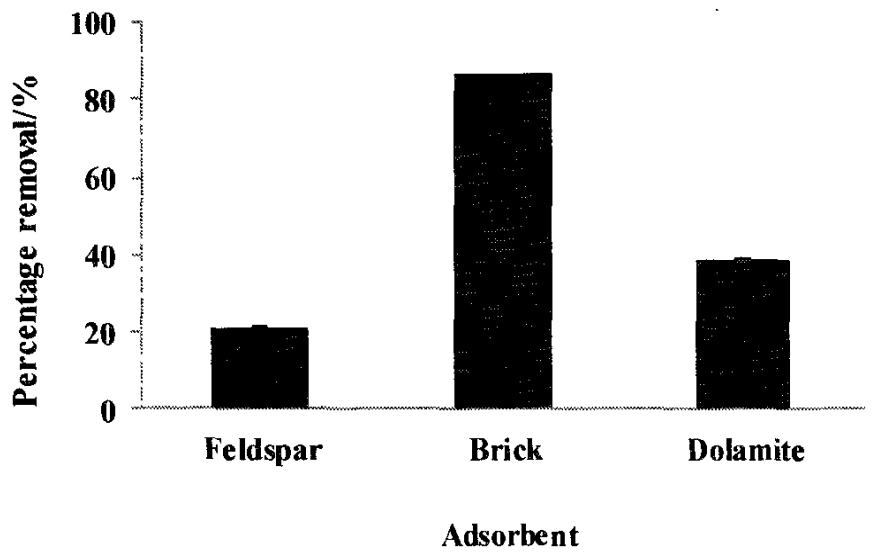

Figure 3.4.34: Extent of removal of phosphate using various adsorbents (50.0 cm^3 of 10.0 mg L^{-1} PO_4^{3-} solution, 5.0 g of each adsorbent).

Optimization of firing temperature of adsorbent

The extent of removal of phosphate by brick clay treated at three temperatures, as compared to untreated adsorbent is shown in Figure 3.4.35. As shown in the figure, the percentage removal is not significantly changed at the temperatures employed for treatment.

However, brick clay treated at low temperatures results in turbid solutions, and hence, it is not possible to control particles. Further, brick clay treated at 200 °C or higher temperatures has been shown to have strong ability for the removal of heavy metal ions and dyes [74]. Therefore, brick clay fired at 200 °C was selected for phosphate removal experiments as well so that a common temperature of treatment would be used for the removal of many pollutants including phosphate.

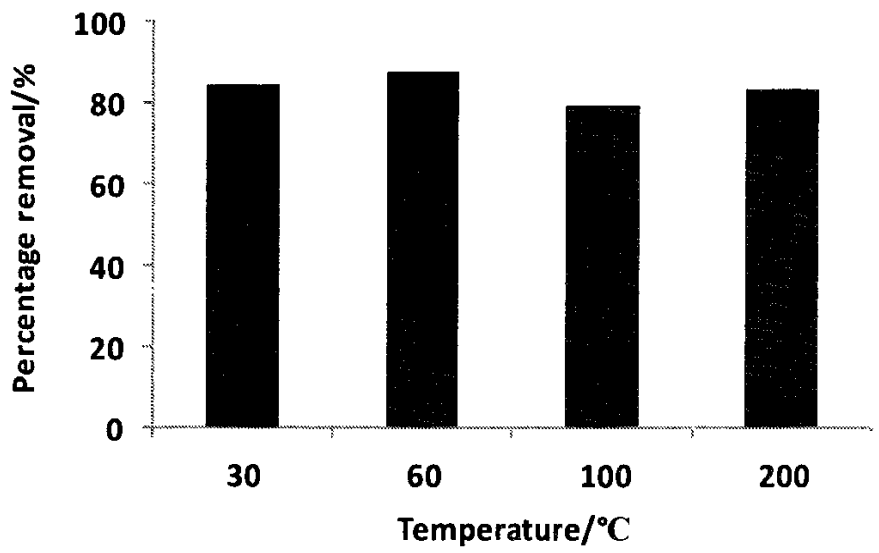

Figure 3.4.35: Extent of removal of phosphate for different adsorbent firing temperatures: (50.0 cm^3 of 10.0 mg L^{-1} PO_4^{3-} solution, 5.0 g of brick clay fired at 200 °C).

Optimization of contact time

The variation of the extent of removal of phosphate determined within a range of shaking times and settling time is shown in Figure 3.4.36. The extent of removal becomes levelled off after certain period shaking and settling. Therefore, the optimum time periods for both shaking and settling were selected as 30 min each for future adsorption experiments.

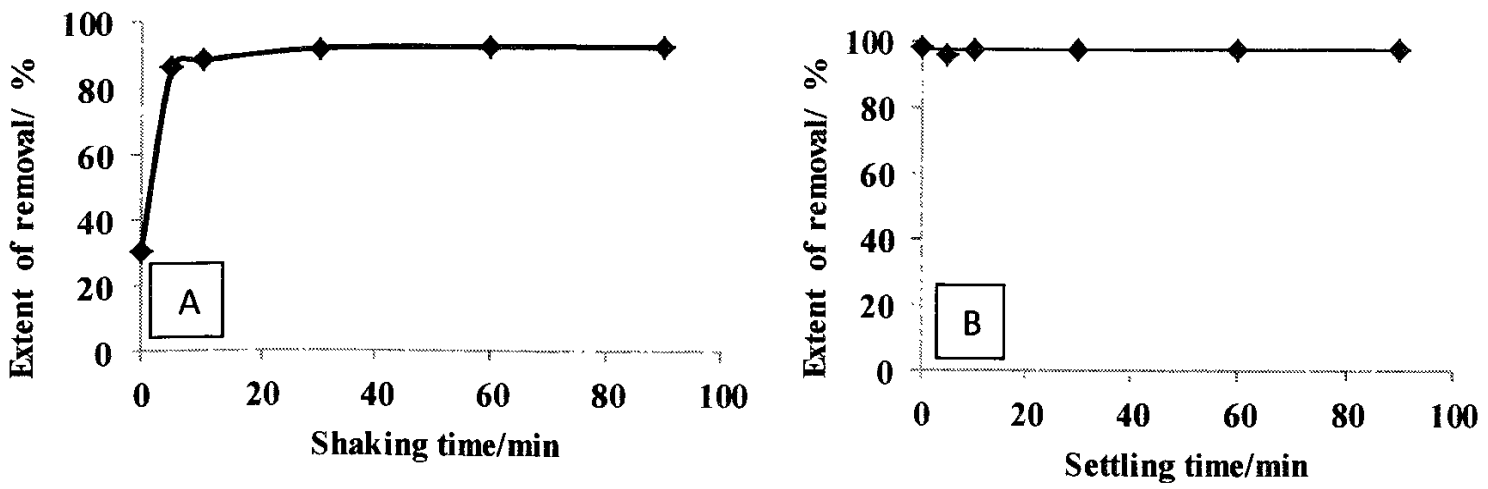

Figure 3.4.36: Optimization of (A) shaking time with 1.0 h settling time (B) settling time at optimized shaking time for the removal of phosphate ions (50.0 cm^3, 10.0 mg L^{-1} PO_4^{3-}, 5.0 g brick clay fired at 200 °C).

Adsorption Isotherms

Variation of the amount of phosphate removal with the initial concentration of phosphate indicates that the brick clay surface heated at 200 °C does not reach saturation even at concentrations as high as 1000 mg L^{-1} (Figure 3.4.37). The extent of removal is continuously on the increase, indicating that the adsorption of phosphate on burnt brick clay particles is not limited to monolayer coverage.

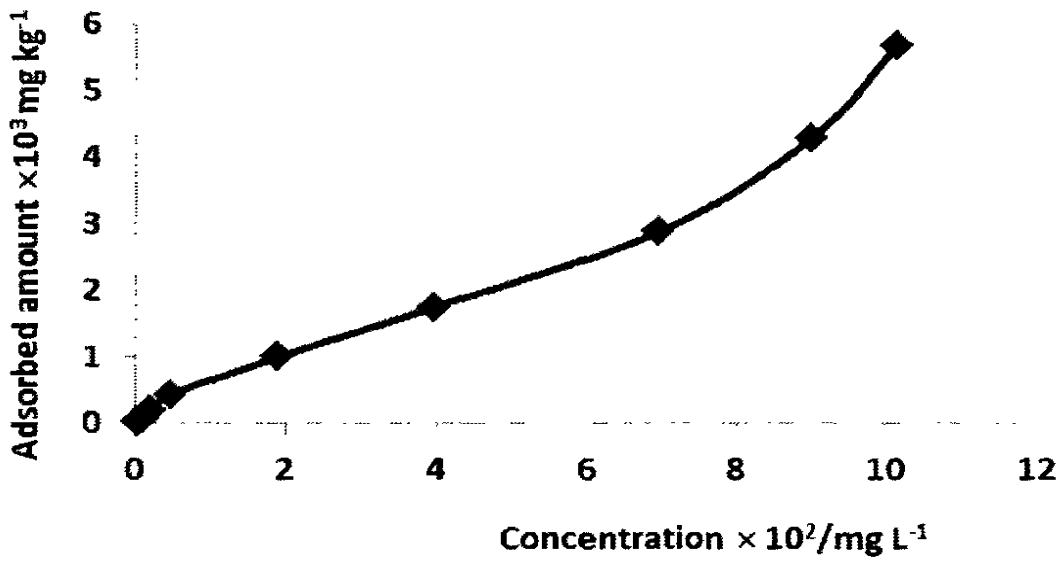

Figure 3.4.37: Amount of phosphate adsorbed on burnt brick clay (50.0 cm^3 solutions of different concentrations of phosphate shaken with 5.0 g of brick clay fired at 200 °C).

Among Langmuir, Freundlich and Temkin adsorption isotherms tested for adsorption data of phosphate, the Freundlich model fits the best. Figure 3.4.38 illustrates the Langmuir and Freundlich adsorption isotherm models which show regression coefficients of 0.8104 and 0.9929, respectively. Further, the Langmuir isotherm provides the maximum adsorption capacity (q_m) of 3333 mg kg^{-1}, while the Freundlich model provides an n value of 1.16, indicating favorable physisorption [94].

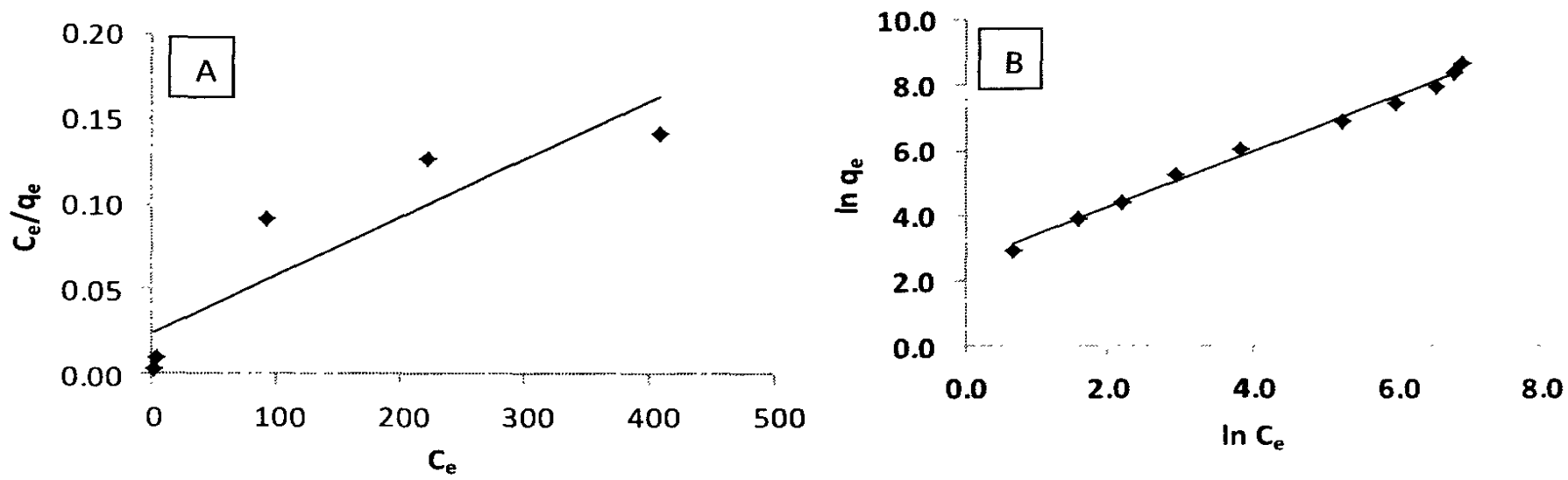

Figure 3.4.38: Isotherm models for removal of phosphate from brick clay: (A) Langmuir isotherm (B) Freundlich isotherm (50.0 cm^3 PO_4^{3-}, 5.0 g brick clay fired at 200 °C).

Kinetics of phosphate adsorption

Kinetics studies, conducted with brick clay fired at 200 °C by withdrawing 5.0 cm^3 volumes of samples at every 1.0 min interval for a period of 20 min before the equilibrium was established. Graphical analysis of kinetics data based on Equations (3.4.7) and (3.4.8) clearly show that pseudo second order kinetics is valid for adsorption of phosphate on brick clay (Figure 3.4.39). This is further supported by having a higher regression coefficient, R^2 of 0.996 for pseudo second order kinetics as compared to a much smaller R^2 value of 0.429 for the pseudo first order model. Calculations proceeded for the pseudo second order model result in a rate constant (k') of 22.5 g mg^{-1} min^{-1} and adsorption capacity of 83.33 mg kg^{-1}.

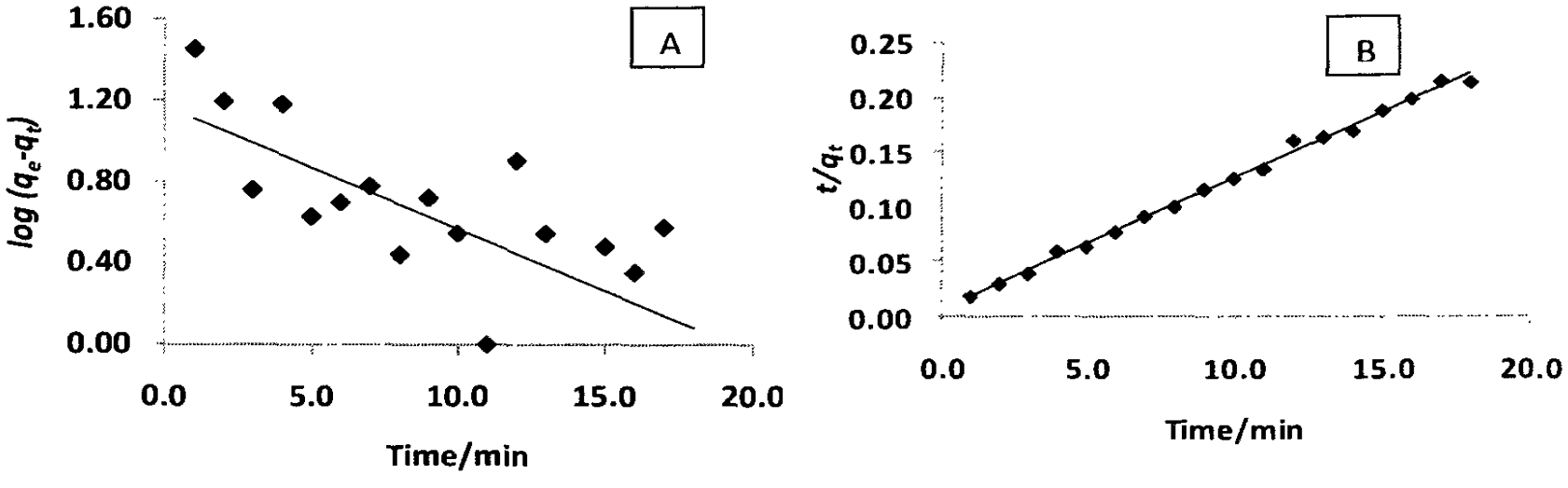

Figure 3.4.39: Adsorption kinetics studies for removal of phosphate from brick clay: (A) Pseudo first order kinetics (B) Pseudo second order kinetics (1000 cm^3 of 10 mg L^{-1} PO_4^{3-}, 100.0 g brick clay fired at 200 °C).

Application of the same kinetics data to check the validity of the external mass transfer diffusion model (Equation 3.4.12) did not produce satisfactory R^2 (= 0.498) value when C_t/C_0 was plotted against t (Figure 3.4.40). Hence, McKay and Poots, and Weber and Morris intraparticle diffusion models were investigated according to Equations (3.4.10) and (3.4.11) (Figure 3.4.41). The regression coefficient of none of the models is in agreement with the linearity of the models. However, it is reasonable to assume that the Webber and Morris model, having a higher regression coefficient, R^2 of 0.725 contributes more to the phosphate removal process.

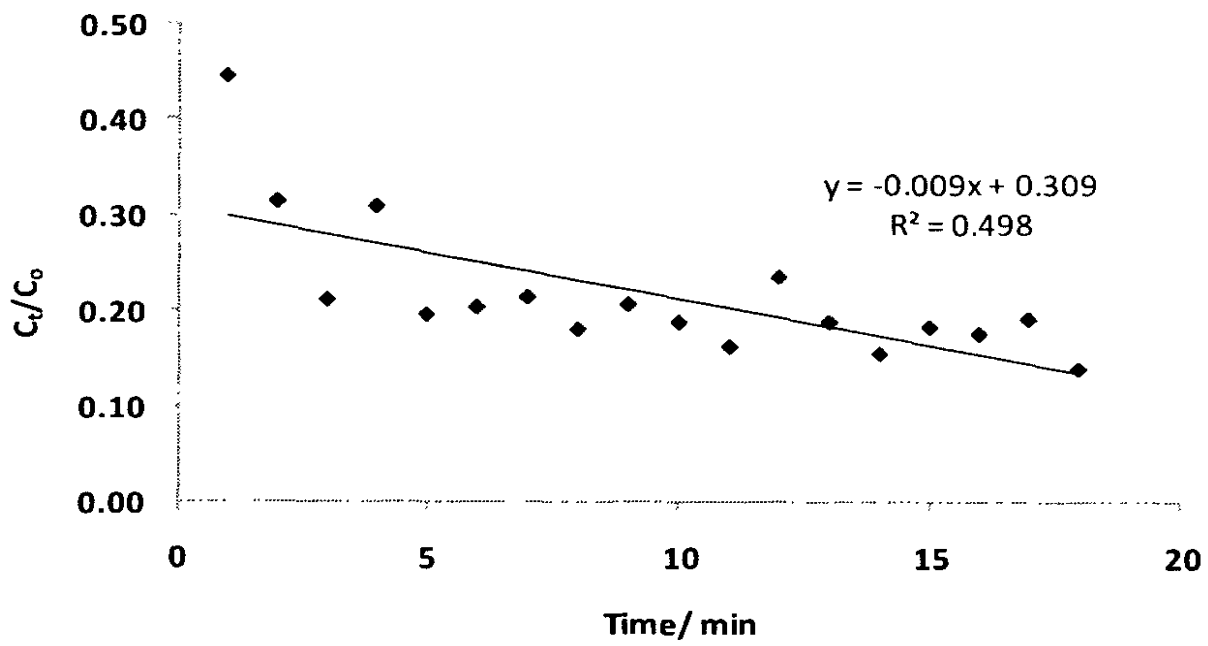

Figure 3.4.40: External mass transfer diffusion model for adsorption of phosphate on brick clay.

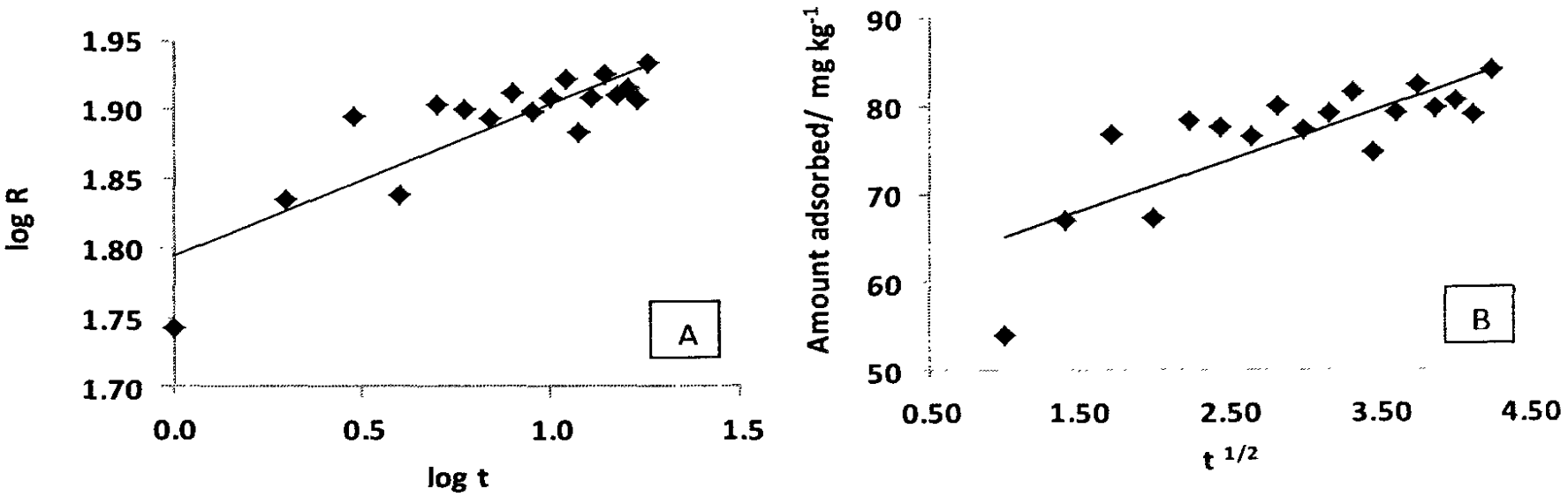

Figure 3.4.41: Adsorption kinetics studies for removal of phosphate from brick clay: (A) Weber and Morris intra-particle diffusion model (B) Mckay and Poots intra-particle diffusion model.

Phosphate removal under dynamic conditions

Effect of flow rate: Breakthrough characteristics for the removal of phosphate is monitored by investigating the relative concentration of phosphate in the eluent as a function of time with continuous supply of phosphate solution through the adsorbent packing at a constant flow rate are shown in Figure 3.4.42.

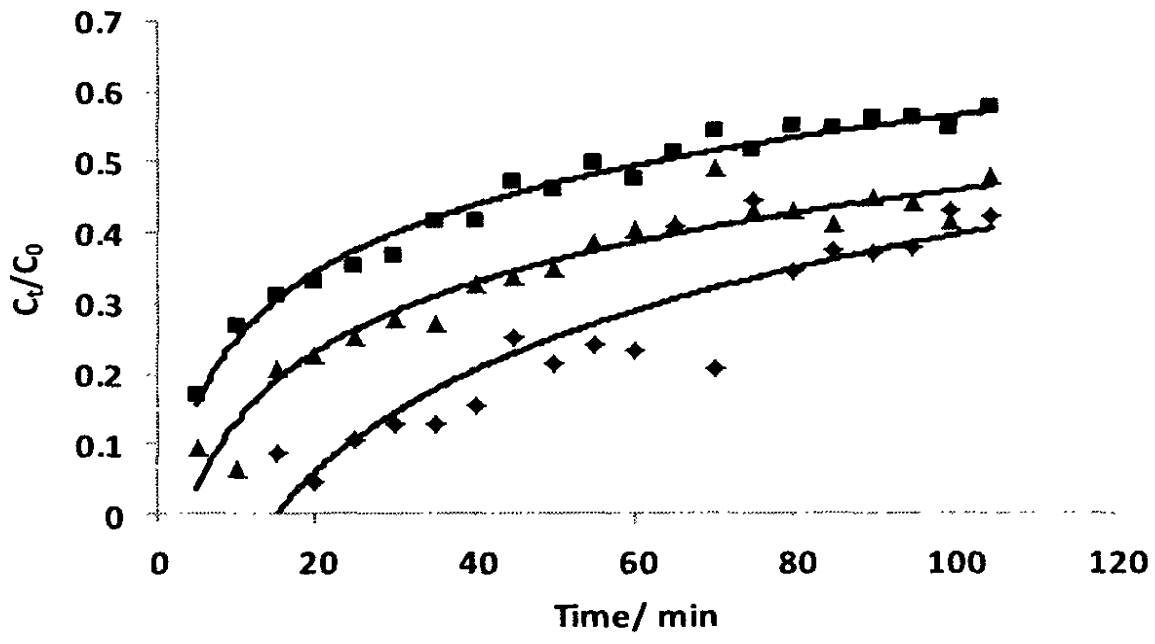

Figure 3.4.42: Flow rate optimization for the removal of phosphate by using brick clay, at rate of 8.0 $cm^3 min^{-1}$ (◆), 12.0 $cm^3 min^{-1}$ (▲) and 20.0 $cm^3 min^{-1}$ (■). (Bed height of 30 cm and initial concentration of 10 mg L^{-1}).

The adsorption process increased rapidly at the initial stage. As expected, the column performed better at lower feed flow rates, resulted in a longer breakthrough and exhaustive time. With the increase in feed flow rate from 8 to 20 cm^3 min^{-1}, an earlier breakthrough and exhaustion time were observed. Increasing hydraulic loading rate illustrates a steady increase in adsorption zone speed resulting in decrease in breakthrough time, saturation time and column capacity. According to mass transfer fundamentals, this behavior is mainly due to the diffusion limitation and insufficient residence time for the solution within the bed at higher feed flow rate [95]. By considering the above facts, the flow rate of 8 cm^3 min^{-1} was taken as the optimized flow rate for further experiments.

Effect of bed height: Figure 3.4.43 illustrates the breakthrough curves obtained at different bed heights with a constant influent concentration of 10.0 mg L^{-1} and a feed flow rate of 8 cm^3 min^{-1}. As the bed height increases, both breakthrough and exhaustive time increases for the removal of phosphate from brick clay. The increase in adsorbent mass availability at higher bed heights provide a greater service area and more binding sites for the adsorbate species to be interacted. The slope of the breakthrough curve decreases with increase in the bed height, which resulted in a broadened mass transfer zone. At lower bed heights, the solute molecules have insufficient time to diffuse into the pores of brick clay resulting in shorter breakthrough time.

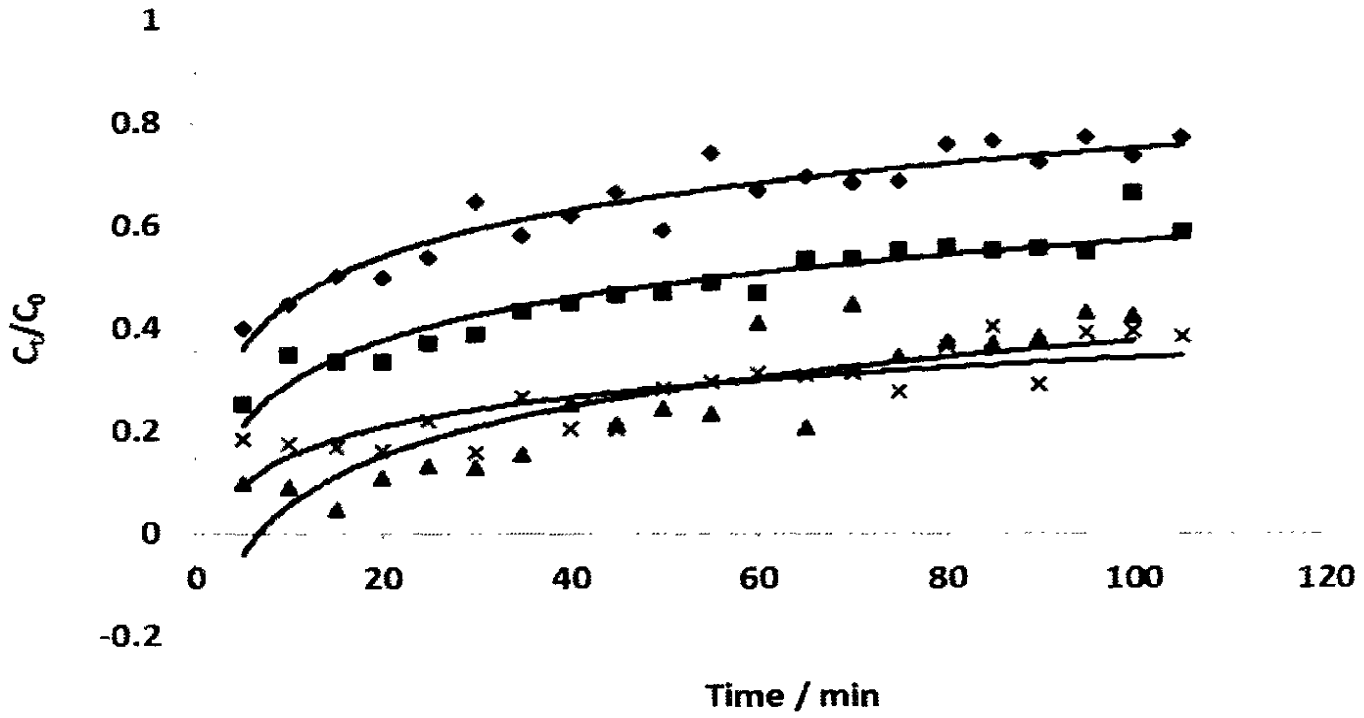

Figure 3.4.43: Optimization of column height for removal of phosphate using brick clay fired at 200 °C. Column height: 15.0 cm (◆), 22.5 cm (■), 30.0 cm (▲), 37.5 cm (×) (Flow rate of 8 cm^3 min^{-1} and initial concentration of 10 mg L^{-1}).

Since there is no much difference in exhaustion time for column heights of 30.0 cm and 37.5 cm, and by considering the amount of the adsorbent, a bed height of 30.0 cm was taken as the optimized column height for the removal of phosphate using brick clay heated at 200 °C.

Effect of initial influent concentration: The effect of initial influent concentration on the extent of phosphate removal by brick clay packed column determined for previously optimized conditions is shown in Figure 3.4.44. Increase in influent concentration results in a sharper breakthrough curve as well as a shorter bed service time indicating that brick clay fixed bed system is saturated more quickly at high concentrations, and hence the time to reach both the breakthrough and exhaustion time is much less [96]. Increase in the influent concentration affects to the volume of effluent treated and finally the removal of total phosphate may decrease. Low influent concentration causes the slow transport of phosphate ions from the film layer to the surface of brick clay adsorbent, which implies a decreased diffusion coefficient and decreased mass transfer driving force.

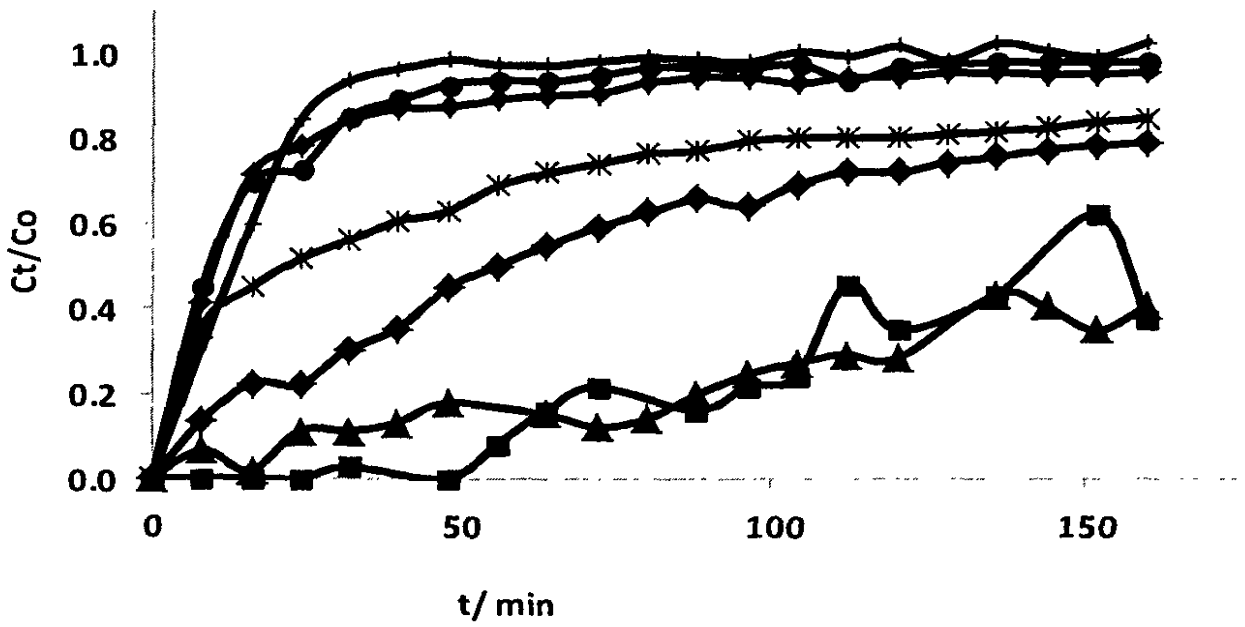

Figure 3.4.44: Optimization of column height for removal of phosphate using brick clay fired at 200°C. Column height: 3.08 mg L^{-1} (▬), 8.83 mg L^{-1} (▲), 21.46 mg L^{-1} (◆), 110.83 mg L^{-1} (✳), 425.95 mg L^{-1} (●), 748.65 mg L^{-1} (●), 1027.03 mg L^{-1} (+) (bed height of 30.0 cm and flow rate of 8 cm^3 min^{-1}).

Dynamic adsorption models

Among dynamic adsorption models, Adam–Bohart model, Bed Depth Service Time model, Thomas model and Yoon–Nelson model are more common, whose significance aspects are given below.

Adams-Bohart model [97]

Adam-Bohart sorption model was applied in order to describe the initial part of the breakthrough curve.

$$\ln\left(\frac{C_t}{C_0}\right) = k_{AB} C_0 t - k_{AB} N_0 \left(\frac{z}{U_0}\right) \qquad (3.4.12)$$

where z is bed height (cm), k_{AB} is mass transfer coefficient (L/mg min), N_0 – saturation concentration (mg/L), U_0 is superficial velocity (cm/min) [U_0= flow rate / cross sectional area of column], and C_0, and C_t are inlet and outlet concentrations.

From the plot of $ln\frac{C_t}{C_0}$ against t at a given bed height and flow rate, the maximum adsorption capacity (N_0) and mass transfer coefficient (k_{AB}) can be estimated. Values of these parameters calculated for kinetics of phosphate adsorption under dynamic conditions from linear plots of the Adam-Bohart model for different bed heights, flow rates and initial concentrations are given in Table 3.4.17. According to the results, both mass transfer coefficient (k_{AB}) and the sorption capacity (N_0) are decreased with increase in flow rate and concentration, but increased with increase in column bed height.

Bed Depth Service Time (BDST) model [96]

The BDST model is one of the simplified fixed bed model initially described by Bohart-Adams, and later modified by Hutchins [98]. It is assumed that the rate of adsorption is governed by the surface reaction between the adsorbate and the unused sites of the adsorbent. The linear relationship of this model is given by,

$$\ln\left(\frac{C_t}{C_0} - 1\right) = \left(\frac{N_0 z k}{U_0}\right) - C_0 k\, t \qquad (3.4.13)$$

where k is rate constant (L mg^{-1} min^{-1}), which describes the mass transfer from the liquid phase to the solid phase. According to the results shown in Table 3.4.17, k and N_0 are increased with increase in flow rate, column height and initial solution concentration.

Thomas model [96,97]

Thomas model is one of the most widely used in describing the column performance and prediction of breakthrough curves. The model follows the Langmuir kinetics of adsorption–desorption. The linearized form of the Thomas model is given by, follows.

$$ln\left[\left(\frac{C_0}{C_t}\right)-1\right]=\left(\frac{k_{Th}q_0m}{Q}\right)-\left(\frac{k_{Th}C_0V_{Eff}}{Q}\right) \qquad (3.4.14)$$

where Q is the flow rate, q_0 is Sorption capacity of the adsorbent per unit mass of the adsorbent, m is Mass of adsorbent, k_{TH} is Thomas rate constant, V_{eff} is volume of effluent treated and t is service time. The correlation coefficient values obtained for phosphate indicates a good agreement to Thomas model (Table 3.4.17). According to the constants obtained from the Thomas model, the values of q_0 are increased while k_{TH} is decreased with increase in initial concentration. The opposite trend is observed for the column data obtained in varying flow rate. The similar trend has been observed for sorption of Mn(II) ions on *Mangostana garcinia* peel based granular activated carbon [97].

Yoon-Nelson model [97]

The Yoon–Nelson model is derived based on the assumption that the rate of decrease in the probability of adsorption for each adsorbate molecule is proportional to the probability of adsorption of adsorbate and the probability of adsorbate breakthrough on the adsorbent. It is given as,

$$ln\left[\frac{C_t}{C_0-C_t}\right]=k_{YN}t-\tau k_{YN} \qquad (3.4.15)$$

where k_{YN} is Yoon-Nelson rate constant and τ is time required for 50% adsorbate breakthrough. The values of Yoon–Nelson rate constant (k_{YN}) and the time required for 50% adsorbate breakthrough were estimated for phosphate adsorption at different flow rates, bed heights and initial concentrations are given in Table 3.4.17. The k_{YN} values decrease with increase in flow rate and column height. However, τ values show a similar trend for flow rate, but increase in its value with increase in column height.

Table 3.4.17: Kinetics model parameters for four kinetic model- Dynamic conditions.

Adams-Bohart model	**$k_{AB}\times10^{-3}$ (L min^{-1} mg^{-1})**	**N_0 (mg L^{-1})**	**R^2**
Flow rate (cm^3 min^{-1})			
8.0	1.711	122.02	0.657
12.0	1.357	181.61	0.657
20.0	0.743	377.30	0.774
Column height (cm)			
15.0	0.564	230.22	0.807
22.5	0.729	183.14	0.878
30.0	1.708	122.02	0.657
37.5	0.951	132.84	0.818

Concentration (mg L^{-1})			
3.1	10.130	29.04	0.790
8.8	2.492	98.01	0.746
21.5	0.718	174.99	0.790
110.8	0.063	984.17	0.753
425.9	0.010	3134.58	0.420
748.6	0.006	4975.38	0.455
1027.0	0.003	5880.58	0.304
BDST model	**$k \times 10^{-3}$ (L min^{-1} mg^{-1})**	**N_0 (mg L^{-1})**	**R^2**
Flow rate (cm^3 min^{-1})			
8.0	2.198	93.24	0.684
12.0	1.858	122.48	0.720
20.0	1.249	176.04	0.846
Column height (cm)			
15.0	1.475	21.88	0.852
22.5	1.348	72.20	0.910
30.0	2.198	93.24	0.684
37.5	1.298	90.07	0.825
Concentration (mg L^{-1})			
3.1	13.149	23.76	0.818
8.8	3.069	79.76	0.796
21.5	1.449	80.11	0.911
110.8	0.192	66.31	0.886
425.9	0.062	1269.83	0.772
748.6	0.048	1694.44	0.793
1027.0	0.043	3619.61	0.598
Yoon – Nelson model	**$k_{YN} \times 10^{-2}$ (min^{-1})**	**τ (min)**	**R^2**
Flow rate (cm^3 min^{-1})			
8.0	2.15	112.36	0.684
12.0	1.89	94.63	0.720
20.0	1.48	70.03	0.846
Column height (cm)			
15.0	1.44	13.21	0.852

22.5	1.33	64.67	0.910
30.0	2.15	112.36	0.684
37.5	1.27	135.68	0.825
Concentration (mg L^{-1})			
3.1	4.05	90.91	0.818
8.8	2.71	106.46	0.796
21.5	3.11	44.00	0.912
110.8	2.13	7.05	0.886
425.9	2.66	35.14	0.772
748.6	3.60	26.68	0.793
1027.0	4.47	41.54	0.598
Thomas model	**$K_{TH} \times 10^{-3}$ (L min^{-1} mg^{-1})**	**q_0 (mg g^{-1})**	**R^2**
Flow rate (cm^3 min^{-1})			
8.0	2.21	145.84	0.684
12.0	2.83	126.31	0.720
20.0	3.04	113.73	0.846
Column height (cm)			
15.0	1.48	34.38	0.852
22.5	1.38	110.96	0.910
30.0	2.21	145.84	0.684
37.5	1.31	140.43	0.825
Concentration (mg L^{-1})			
3.1	13.25	37.06	0.818
8.8	3.08	124.88	0.796
21.5	1.45	125.48	0.912
110.8	0.19	102.76	0.886
425.9	0.06	2010.57	0.772
748.6	0.05	2662.70	0.793
1027.0	0.04	5675.26	0.598

These findings have been disclosed as follows:

- *N. Priyantha, A.N. Navaratne and T.P.K. Kulasooriya, Removal of phosphate ions using brick clay: static and dynamic conditions (submitted for publication).*
- *T.P.K. Kulasooriya, A.N. Navaratne and N. Priyantha, Optimization of efficiency of phosphate removal by brick clay, PGIS Research Congress (2014).*

3.4.7 Removal of Textile Dyes Using Naturally Available Substances

Removal of textile dyes from industrial effluent samples was carried out using mixtures of dyes. First, real dye effluent samples taken from different dyeing industries was screened to select a suitable industry for further studies. The industrial effluent selected contains three dyes, namely Sumifix blue exf (Dye 1), Sumifix rubine exf (Dye 2) and Sumifix yellow exf (Dye 3).

UV-Visible spectra of individual dyes recorded indicate that λ_{max} values of Dye 1, Dye 2 and Dye 3 are 605 nm, 545 nm and 415 nm, respectively (Figure 3.4.45).

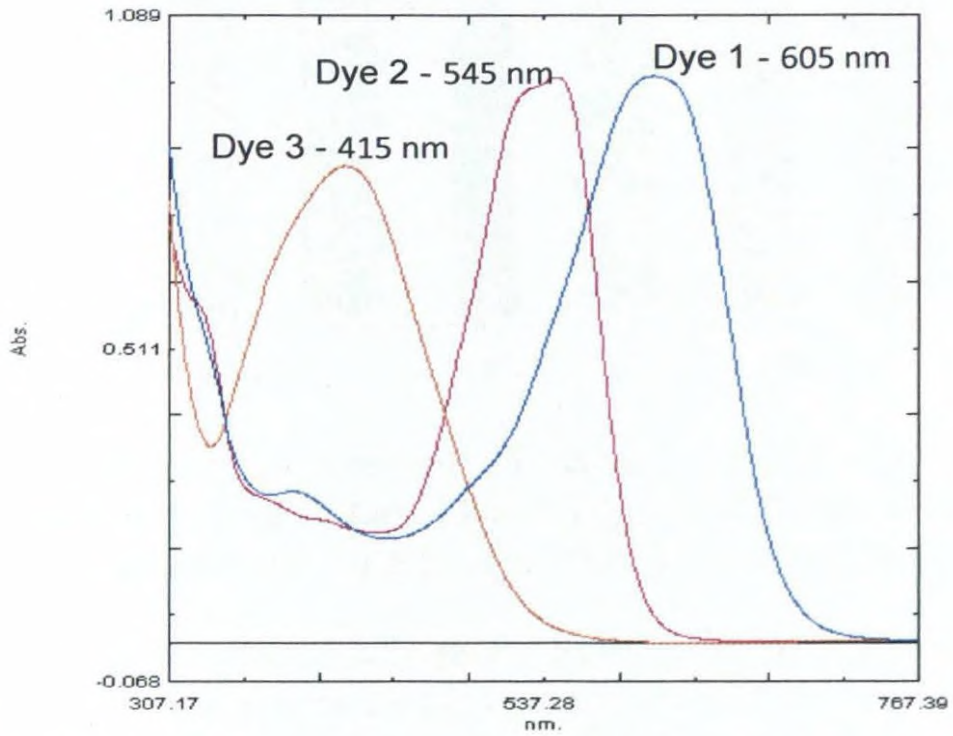

Figure 3.4.45: UV-Visible spectra of individual dyes.

The removal ability of dyes from aqueous solution was subsequently tested at the relevant λ_{max} with all six adsorbents. According to the results obtained, brick clay is found to be the best adsorbent which removes each of the three dyes by about 60% (Figure 3.4.46). Therefore, further experiments were conducted with brick clay.

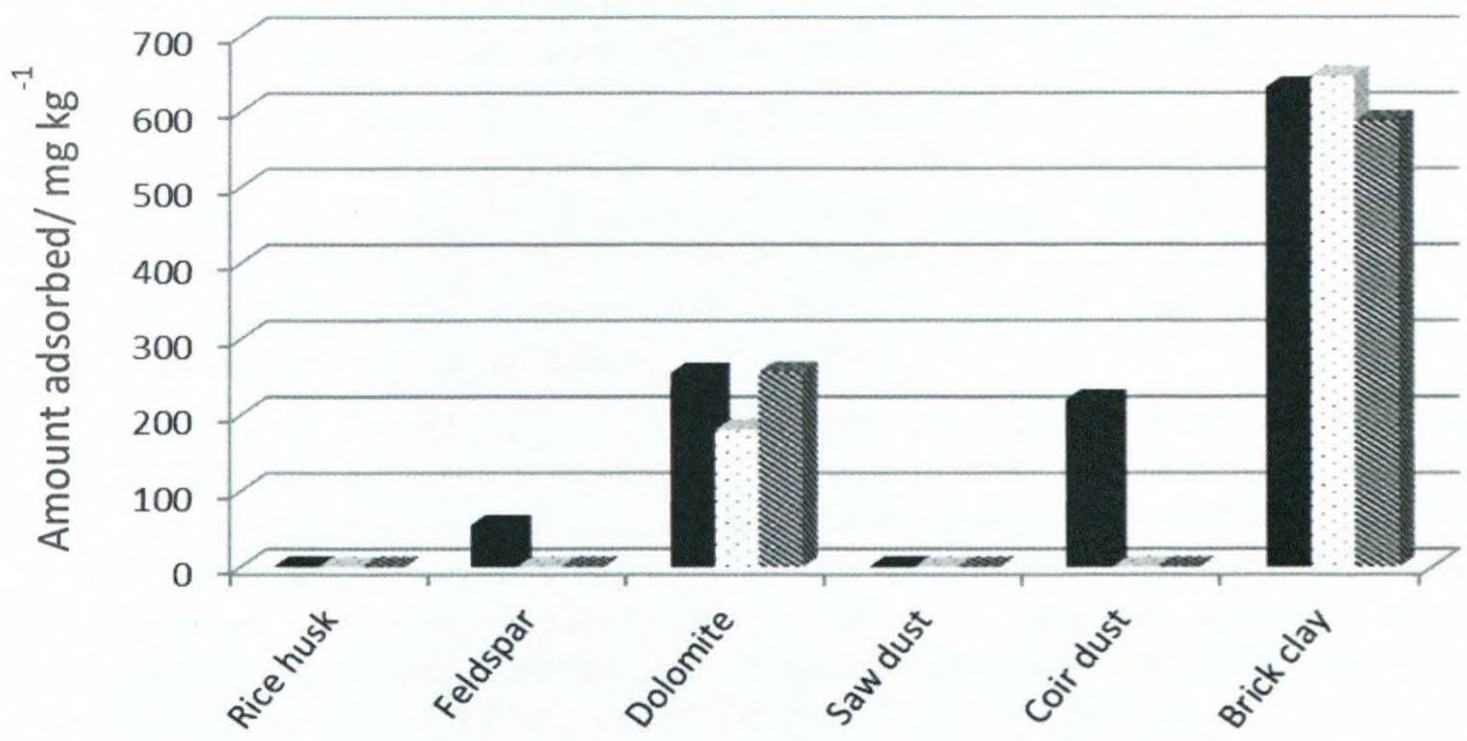

Figure 3.4.46: Adsorbed amount of three dyes with different adsorbents: Dye 1 (■), Dye 2 (□) Dye 3 (▨) (50.0 cm^3 of 50.0 mg L^{-1} dye solution treated with 5.0 g of adsorbent, 1.0 h shaking time, 1.0 h settling time).

The extent of removal of each dye determined using brick clay treated at three different temperatures by keeping all other parameters constant is shown in Figure 3.4.47. Brick clay treated at 200 °C, being the most efficient, was thus selected for further experiments.

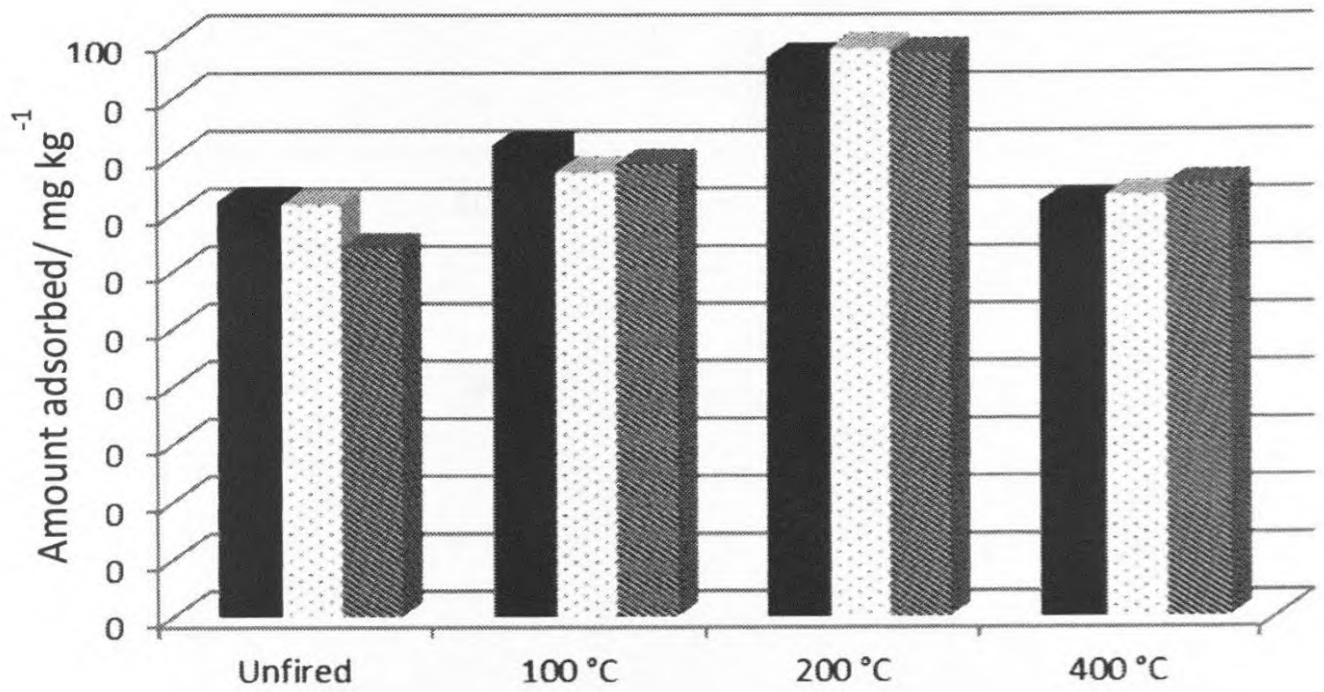

Figure 3.4.47: Extent of removal of dyes by brick clay treated at different firing temperatures: Dye 1 (■), Dye 2 (⊡), Dye 3 (▧) (50.0 cm^3 of 50.0 mg L^{-1} dye solution treated with 5.0 g brick clay,1.0 h shaking time, 1.0 h settling time).

The extent of removal was found to increase with the adsorbent dosage in a similar manner. Therefore, 4.0 g of brick clay treated at 200 °C was used to treat 50.0 cm^3 of dye solution in subsequent experiments.

Since the three dyes under consideration behave similarly, optimization of parameters, such as shaking time, settling time and solution pH was carried out under static conditions only for Dye 1, to be used for the other two dyes. Variation of the percentage removal of Dye 1 with different variables is shown in Figure 3.4.48, and both shaking and settling times were selected as 15 min each for future experiments. The optimum initial pH of the solution is less than pH 10 which gives the maximum percentage removal as shown in Figure 3.4.48(C). The same optimized parameters were used for adsorption isotherm and kinetics studies as well for all three dyes.

Variation of the amount of dye adsorbed with the initial concentration of all three dyes indicates that the brick clay surface treated at 200 °C reaches saturation limit at concentrations beyond 700 mg L^{-1} (Figure 3.4.49), qualifying Type I isotherm according to the IUPAC isotherm classification given in Figure 3.4.13. Although ther are some differences depending on the type of the dye, it is evident that brick clay shows microporous characteristics for the adsorption process.

Figures 3.4.50, 3.4.51 and 3.4.52 illustrate the linearized plots of Langmuir, Freundlich and Temkin adsorption isotherms. It apprears from the plots that the Langmuir isotherm is the best fitted, which is confirmed from regression coefficients calculated (Table 3.4.18). Further, adsorption capacity of the dyes determined from the Langmuir model demonstrates the stronger ability of brick clay for sorption of these dyes when compared to some adsorbents reported [99]. The differences among adsorption capacities can be attributed to structural differences of the three dyes.

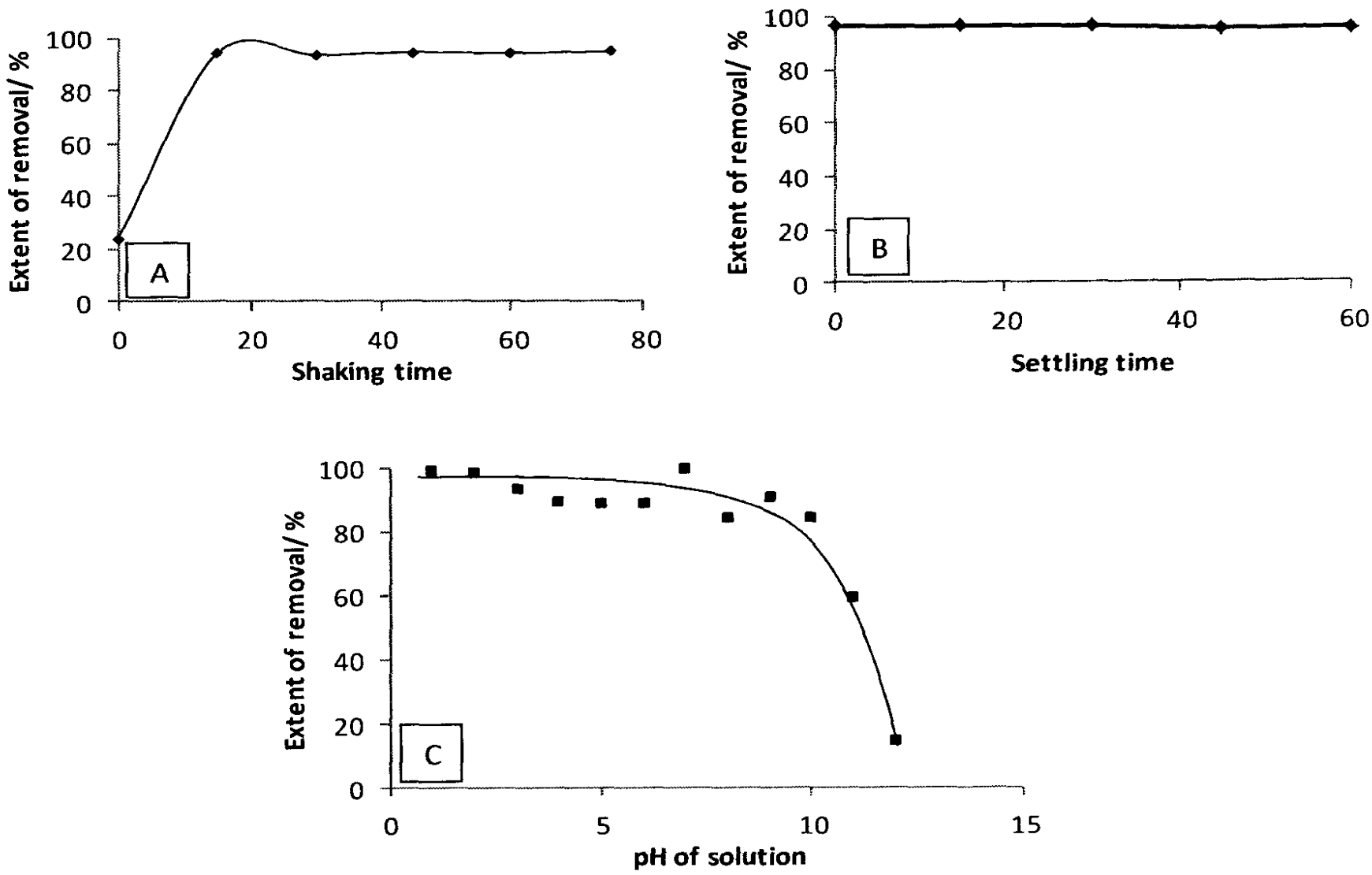

Figure 3.4.48: Parameter optimization for the removal of textile dye (Dye 1): (A) Shaking time (B) Settling time (C) Initial solution pH (50.0 cm^3 of 50.0 mg L^{-1} dye solution treated with brick clay treated at 200 °C).

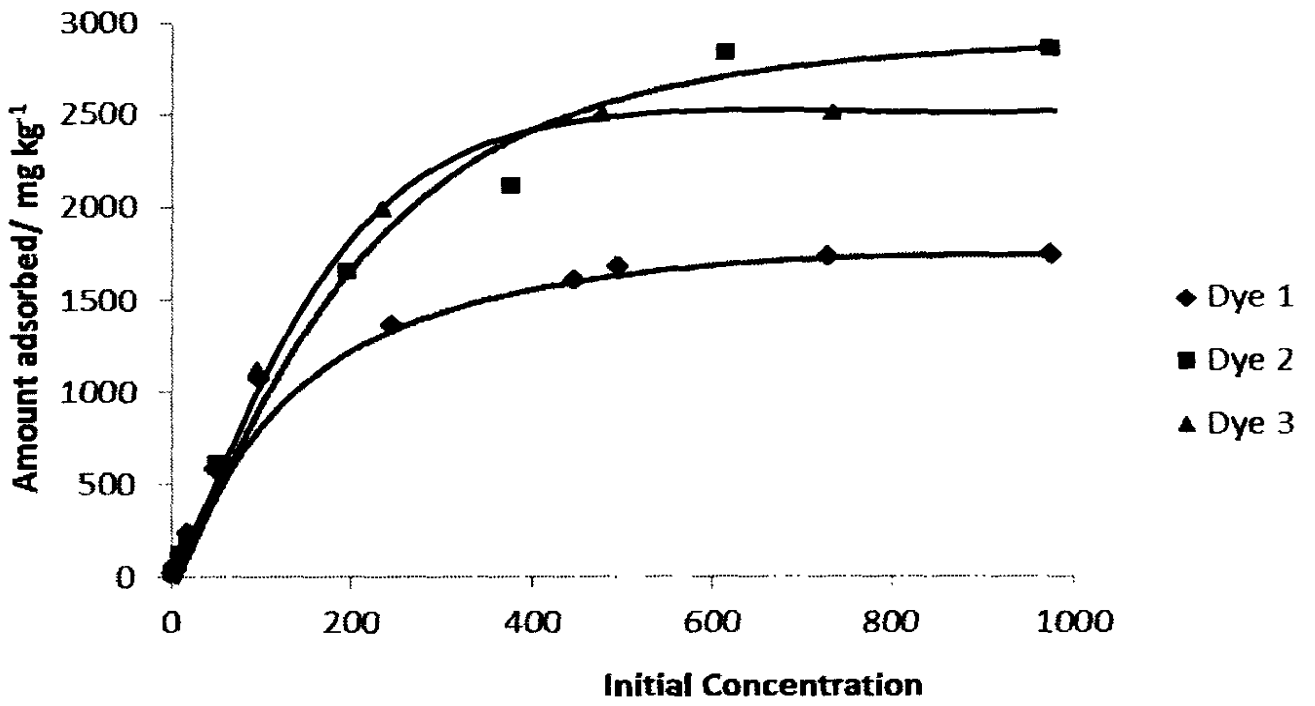

Figure 3.4.49: Amount of Dye 1 adsorbed on brick clay (50.0 cm^3 solutions of different concentrations of dye solution shaken with 4.00 g of brick clay treated at 200 °C).

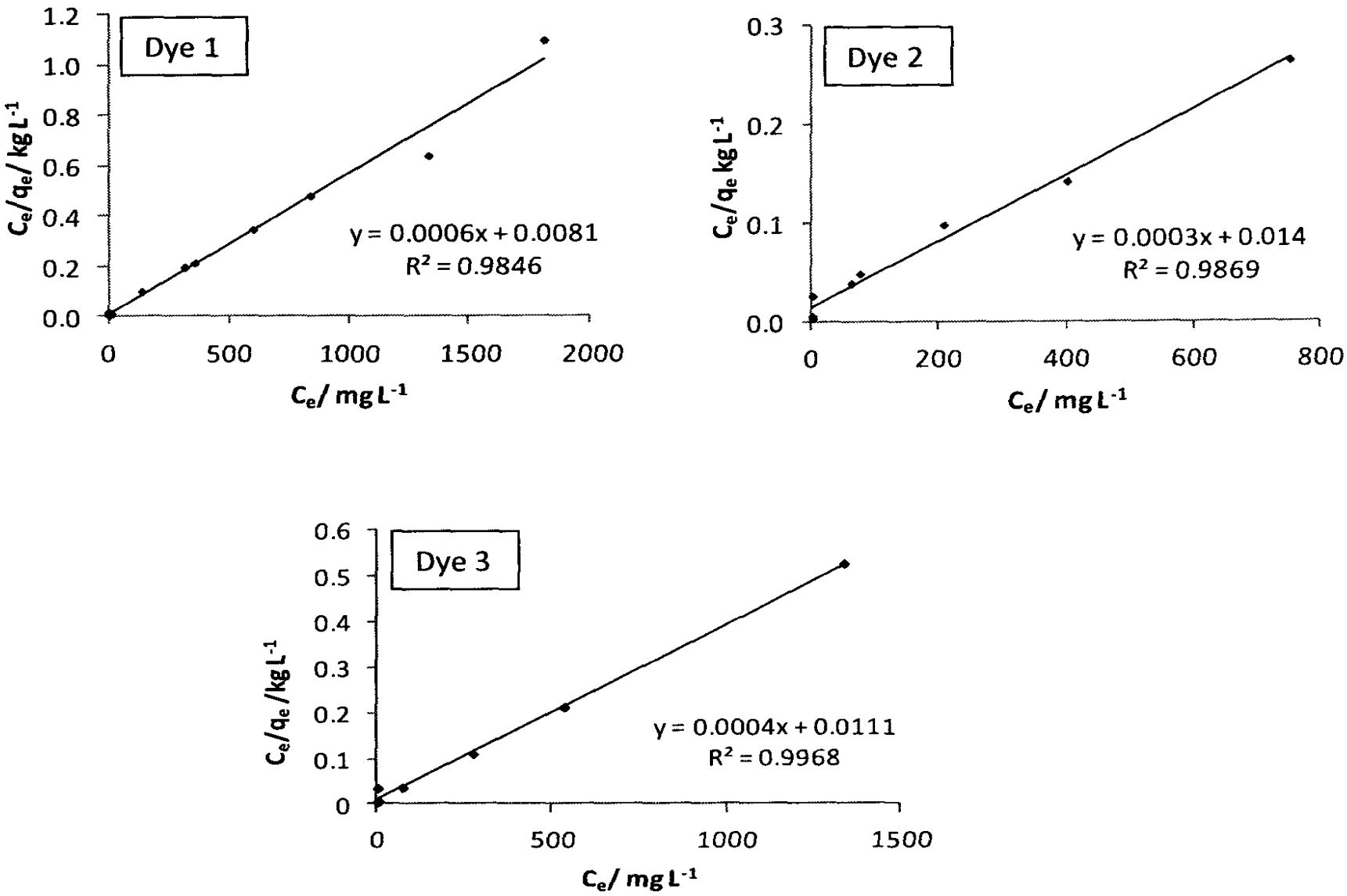

Figure 3.4.50: Langmuir adsorption isotherm model for removal of dyes using brick clay.

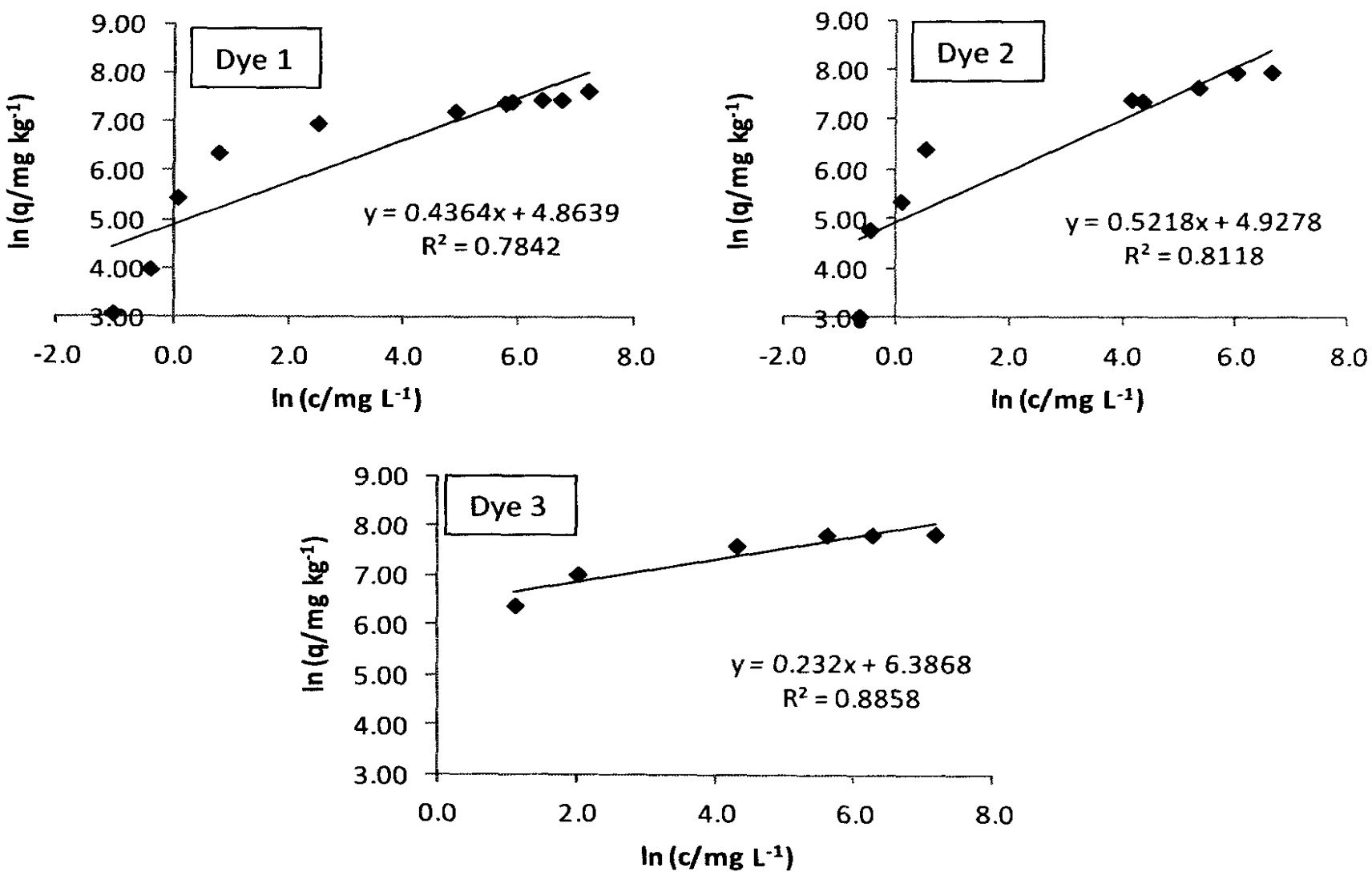

Figure 3.4.51: Freundlich adsorption isotherm model for removal of dyes using brick clay.

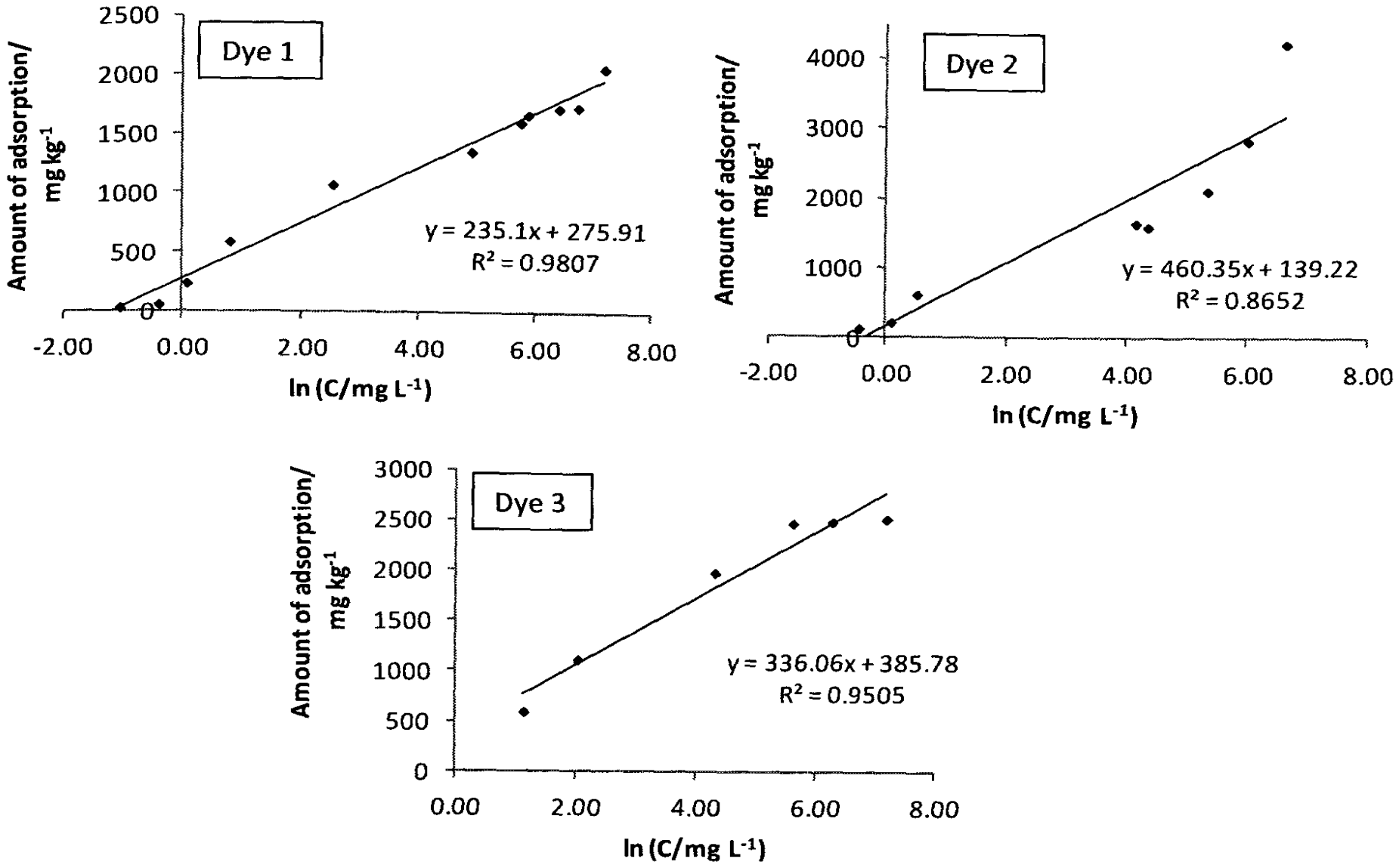

Figure 3.4.52: Temkin adsorption isotherm model for removal of dyes using brick clay.

Table 3.4.18: Adsorption isotherm constant values for different adsorption isotherms.

	Langmuir isotherm			**Freundlich isotherm**			**Temkin isotherm**		
	q_{max}	K_L	R^2	n	K_F	R^2	B	K_T	R^2
Dye 1	1667	0.074	0.985	2.29	129.53	0.784	235.1	3.23	0.981
Dye 2	5000	0.014	0.987	1.92	138.06	0.812	460.3	1.35	0.865
Dye 3	2500	0.036	0.997	4.31	593.60	0.886	336.1	1.15	0.951

Kinetics studies were then conducted for brick clay heated at 200 °C by withdrawing 5.0 cm^3 volumes of samples from a bulk solution of 1000 cm^3 at every 10 s interval for 2 min followed by 1 min interval for 20 min before the system reached equilibrium. Figure 3.4.53 illustrates the variation of the extent of adsorption with contact time for different dye solutions when an aqueous solution of each dye sample was individually treated with brick clay which had been heated at the optimum temperature.

The amount of dyes adsorbed by brick clay heated at 200 °C, determined after establishment of equilibrium according to Figure 3.4.53, follows the order, Dye 1 < Dye 2 < Dye 3. Further, the rate at which brick clay-dye solution reaches equilibrium is different for each dye according to the figure. Since none of the dye solution reaches equilibrium instantly, investigation of kinetics is possible to determine relevant parameters. Graphs obtained for kinetics modeling are shown in Figures 3.5.54 and 3.5.55.

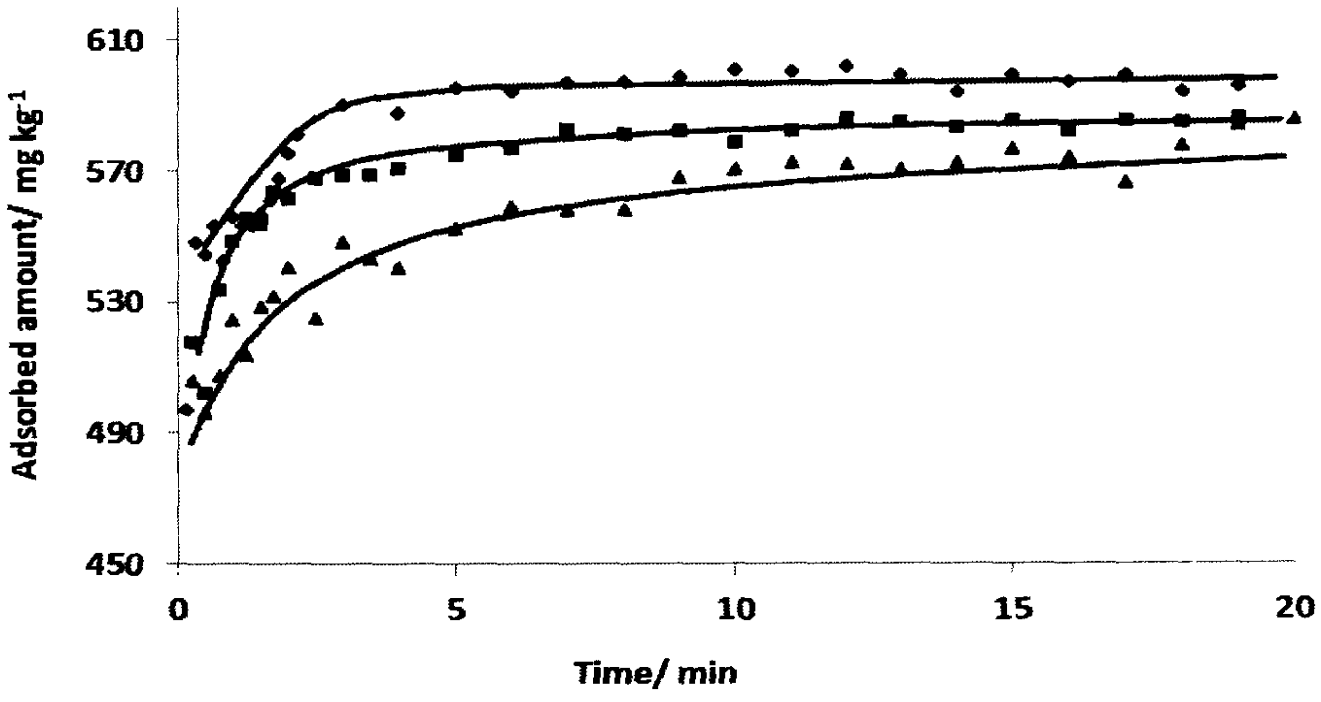

Figure 3.4.53: Variation of the amount of dye adsorbed with contact time: Dye 1(♦), Dye 2 (■), Dye 3 (▲) (1000 cm^3 of 50.0 mg L^{-1} dye solution, 80.0 g brick clay heated at 200 °C).

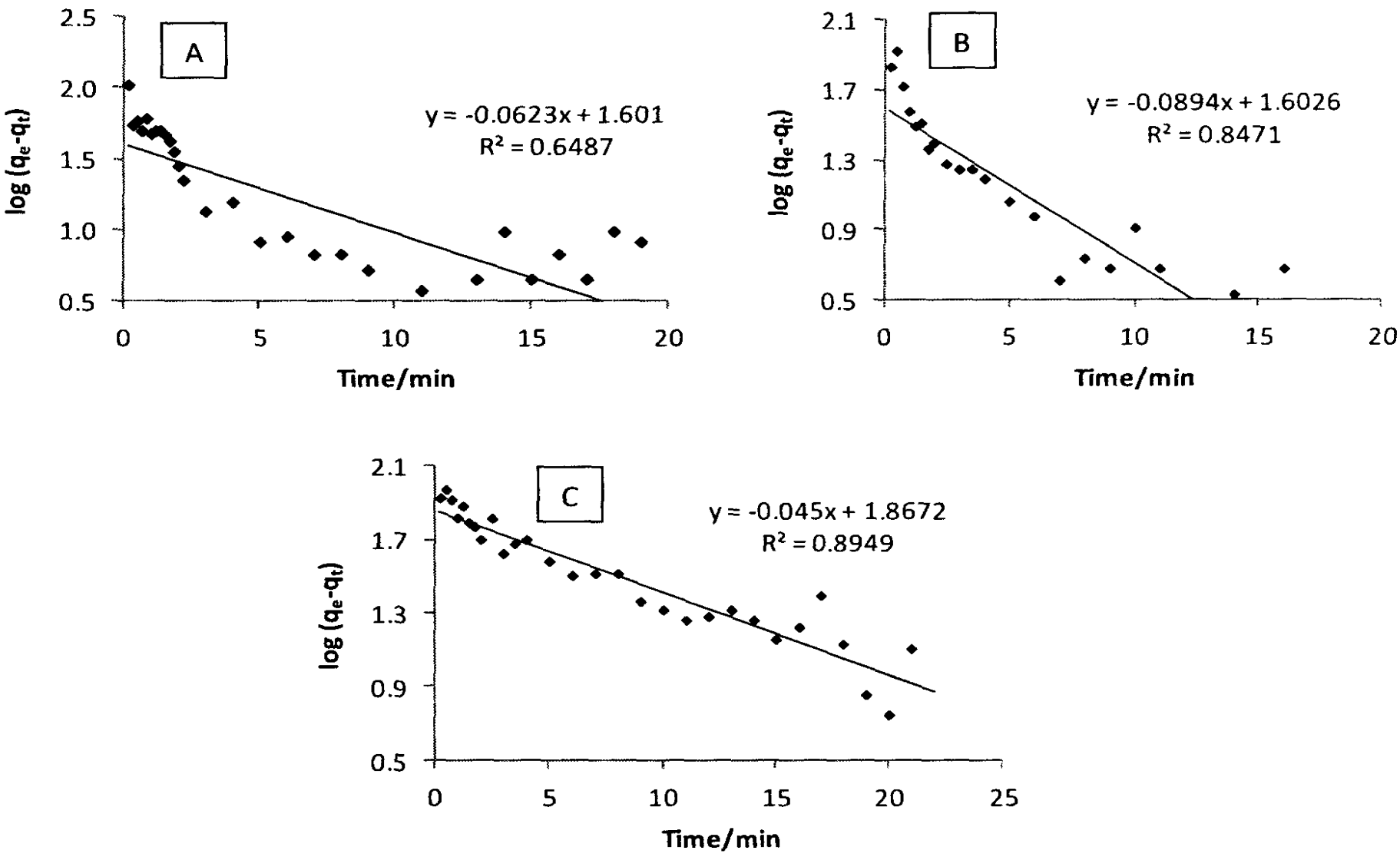

Figure 3.4.54: Pseudo first order kinetics plots for adsorption of dyes on brick clay heated at 200 °C: (A) Dye 1, (B) Dye 2 (C), Dye 3.

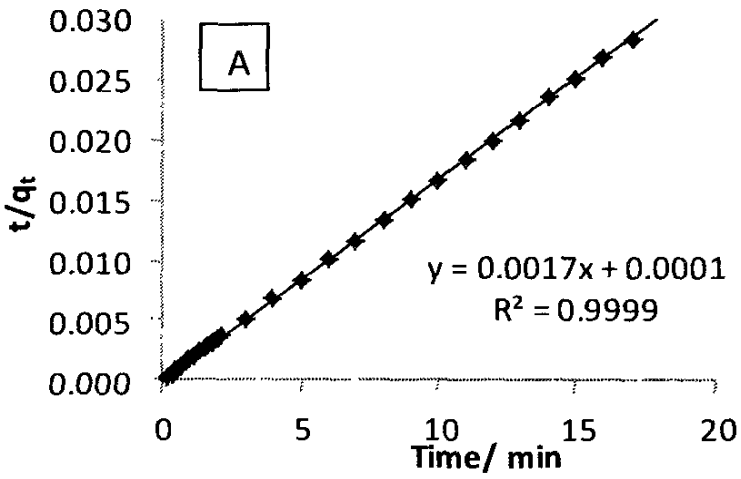

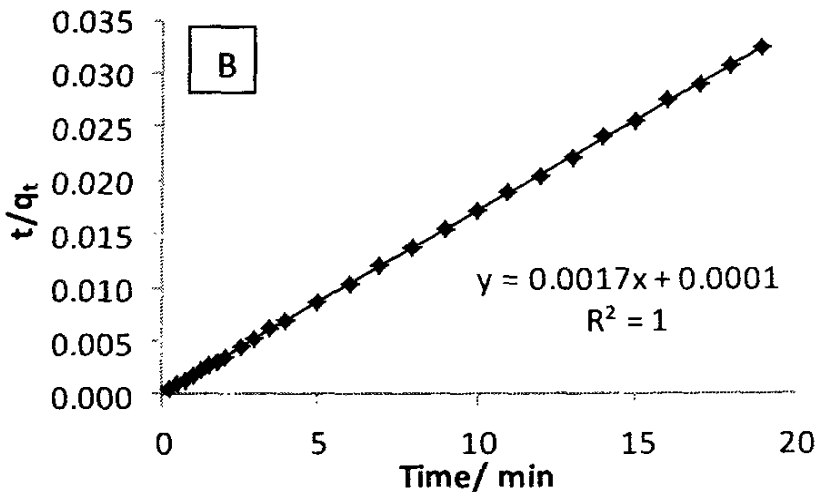

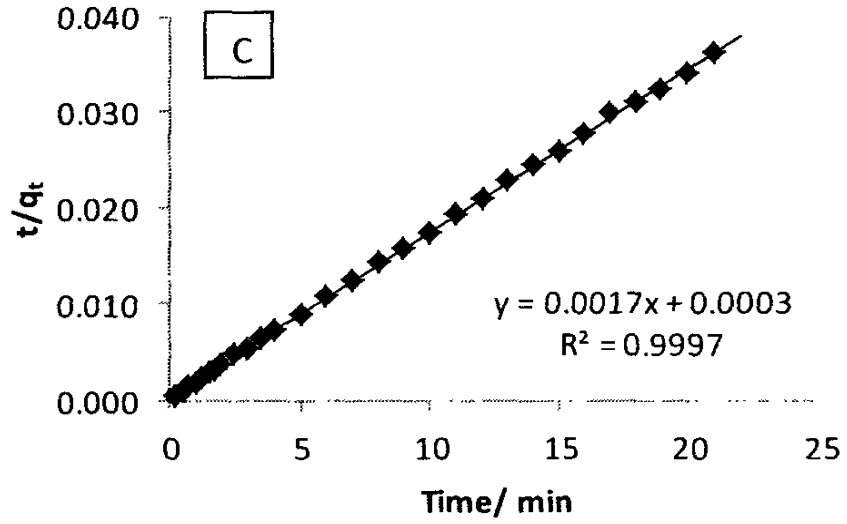

Figure 3.4.55: Pseudo second order kinetics plots for adsorption of dyes on brick clay heated at 200 °C: (A) Dye 1, (B) Dye 2, (C) Dye 3.

Regression coefficients obtained for pesudo second order kinetics plots are very close to 1 although those of pesudo first order plots are deviated, demonstrating the validity of the former. Adsorption capacity at equilibrium (q_e), pseudo second order rate constant (k'), initial adsorption rate (h_0) and correlation coefficient (R^2) obtained from the pseudo second order kinetics model are shown in Table 3.4.19. The data reported in the table indicates that the initial rate of adsorption follows the order, Dye 1 ≈ Dye 2 > Dye 3. which is a measure of how fast the reaction proceeds.

Table 3.4.19: Kinetic parameters from the pseudo second order model for adsorption of dyes on brick clay.

Dye	R^2	q_e /mg kg^{-1}	k' /kg mg^{-1} min^{-1}	h_0 /mg kg^{-1}min^{-1}
Dye 1	0.999	588	0.029	10000
Dye 2	1.000	588	0.029	10000
Dye 3	0.999	588	0.010	3333

In order to gets an idea on the mechanism of binding of dyes on brick clay, intra-particle diffusion models, external mass transfer diffusion model and chemical binding methods were employed to find the rate determining step. The regression coefficients obtained for the external mass transfer diffusion model were 0.539, 0.534 and 0.795 for Dye 1, Dye 2 and Dye 3, respectively, and hence, this model was not considered. The chemical bonding method was also not proceeded due to fast kinetics of dye adsorption.

Variation of the amount of metal ions adsorbed with $t^{1/2}$ plotted to check the validity of the McKay and Poots intra-particle diffusion model also resulted in poor desirable regression coefficients (Dye 1: 0.702; Dye 2: 0.691; Dye 3: 0.898) (Figure 3.4.56). However, having a non-zero intercept in the plots of the figure indicates that the rate limiting step has another contribution in addition to what is proposed by the McKay and Poots model. Therefore, Weber and Morris intraparticle diffusion model was also applied.

Figure

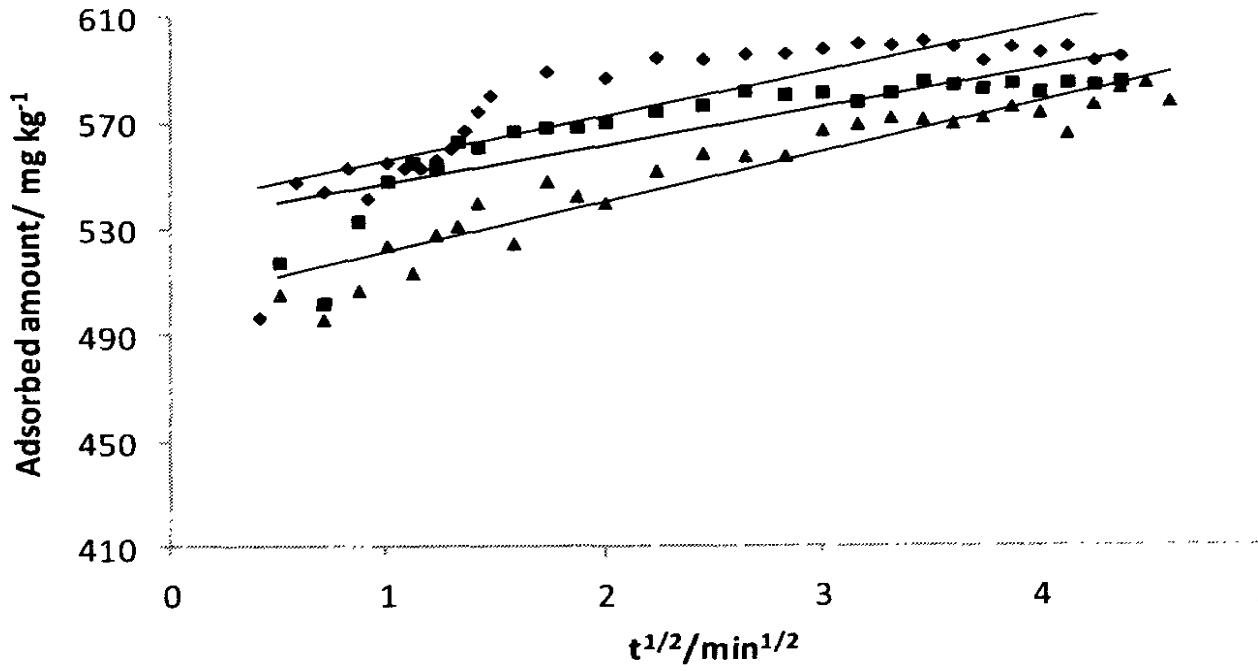

3.4.56: McKay and Poots intra-particle diffusion model for adsorption of dyes on brick clay; Dye 1 (♦), Dye 2 (■), Dye 3 (▲).

The plots of the Weber and Morris intra-particle diffusion for the three dyes tested are shown in Figure 3.4.57 results in satisfactory regression coefficients (Table 3.4.20), giving evidence that the above model is in good agreement for adsorption of dyes brick clay. The gradient of plots (n) and intra-particle diffusion rate constant (k_{id}) determined are also given in Table 3.4.20. The value k_{id} is taken as a rate factor, which is correlated to the rate of adsorption, while larger n values show strong adsorption indicating strong bonding between the dye and the adsorbent.

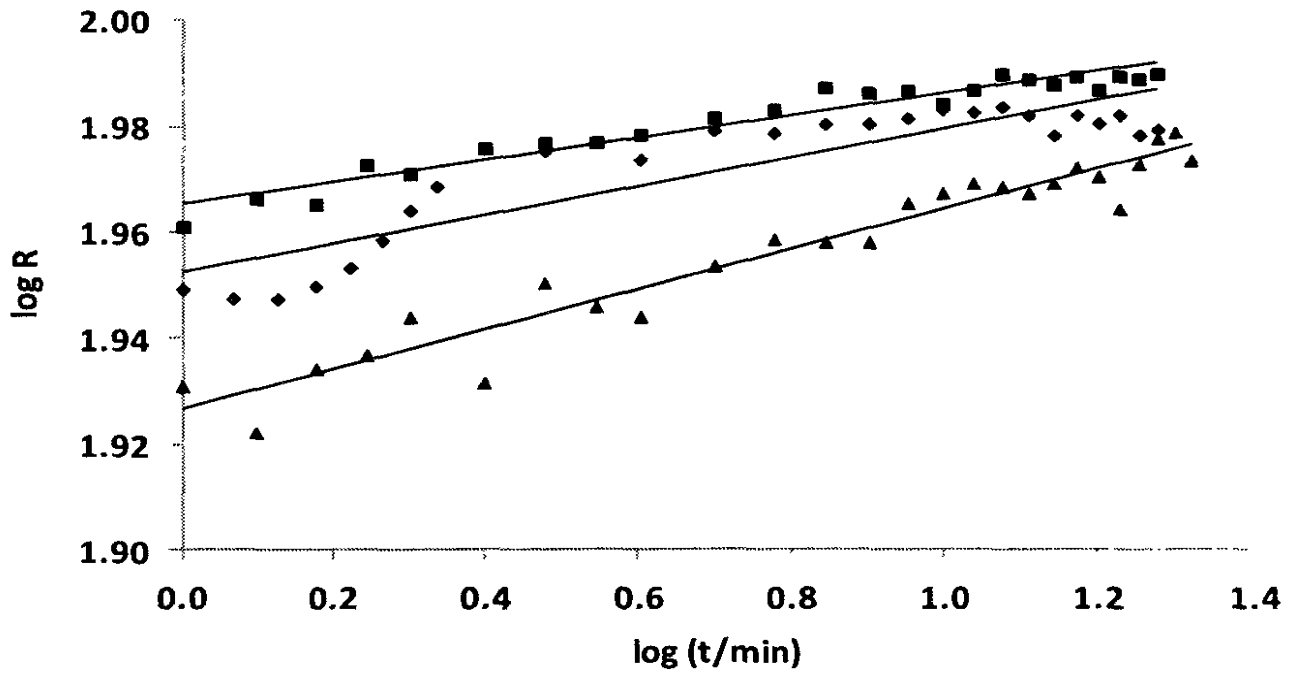

Figure 3.4.57: Weber and Morris intra-particle diffusion model for adsorption of dyes on heated brick clay; Dye 1 (♦), Dye 2 (■), Dye 3 (▲).

Table 3.4.20: Weber and Morris intra-particle diffusion model parameters for dyes.

	R^2	n	k_{id}
Dye 1	0.813	0.027	89.60
Dye 2	0.933	0.021	92.34
Dye 3	0.933	0.038	84.45

3.4.8 Adsorption Characteristics of Mixtures of dyes

According to the spectrum obtained for a real dye effluent sample, the concentrations of each individual dye present were calculated as 42 mg L^{-1} (Dye 1 - blue colour), 106 mg L^{-1} (Dye 2 - red colour) and 39 mg L^{-1} (Dye 3 - yellow colour), by comparison with the spectrum of a synthetic dye mixture prepared in the laboratory (Figure 3.4.58).

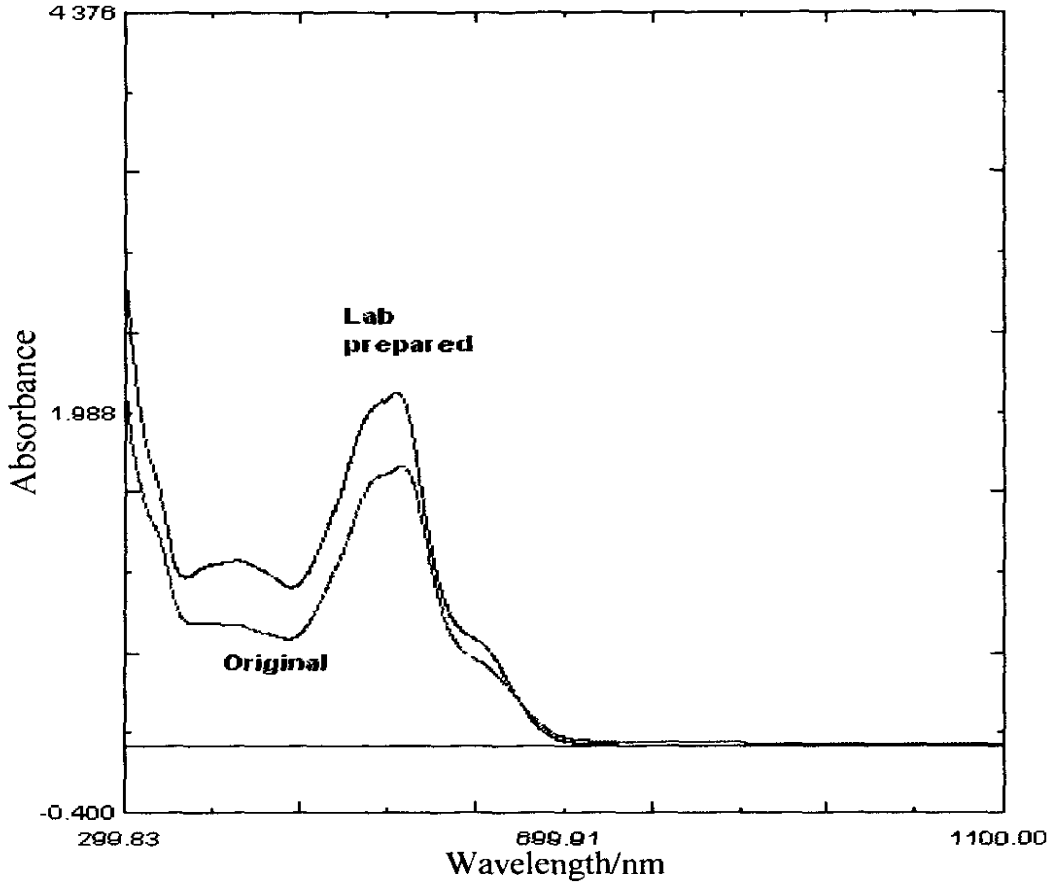

Figure 3.4.58: Spectra obtained for laboratory prepared and real dye effluent samples.

For dye removal experiments, a synthetic mixture of dyes was prepared according to the preliminary experiments carried out. By considering adsorption capacities obtained from isotherm analysis for three individual dyes, amount of brick clay needed to treat the synthetic dye mixture was calculated. Accordingly, 15.0 g of brick clay heated at 200 °C was used to treat 50.0 cm^3 of the dye mixture having concentrations of each dye given above.

The purple colour of the synthetic dye mixture, after treatment with the calculated amount of heated brick clay, almost completely disappeared, and the extent of removal of each dye calculated at the respective λ_{max} of each dye is shown in Table 3.4.21. In order to confirm the performance of the calculated mass of brick clay (15.0 g), experiments were conducted by varying the adsorbent mass from 10.0-15.0 g under the same experimental conditions. According to spectra obtained, 15.0 g of adsorbent is determined to be the optimum adsorbent dosage for treatment of synthetic effluent samples (Figure 3.4.59).

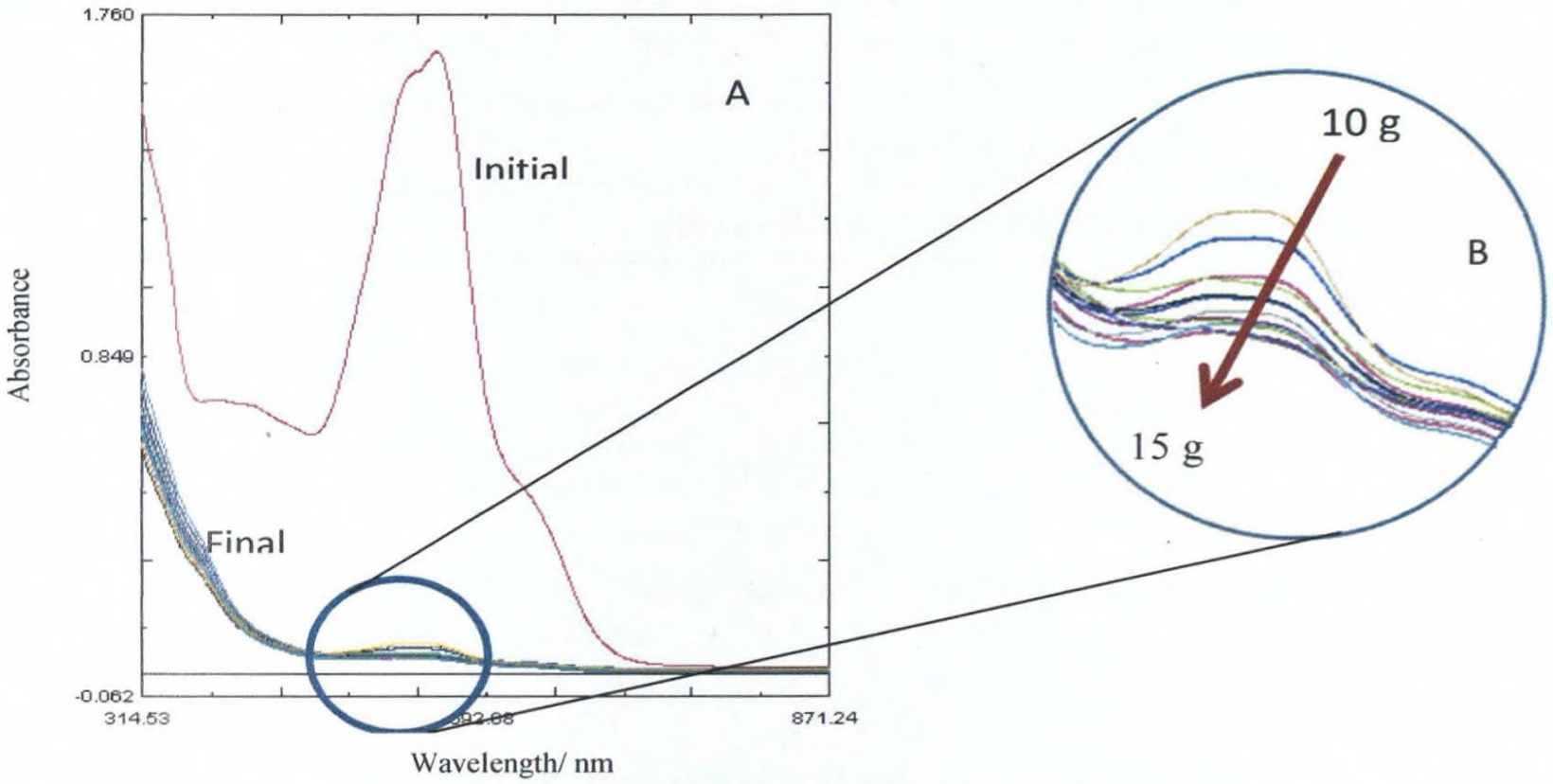

Figure 3.4.59: Spectra obtained for the treatment of synthetic dye solution with different brick clay masses. (A) Comparable initial spectrum; (B) Spectra after treatment with different masses of brick clay. Enlarged spectra obtained for treated samples are shown inside the circle.

Colour removal of real effluent sample

Similar volumes of the real dye effluent, when treated with brick clay under similar conditions, show decreased removal efficiencies, probably due to interference effects (Table 3.4.21). Nevertheless, Figure 3.4.60 shows the effectiveness of heated brick clay for the removal of dyes from the actual effluent.

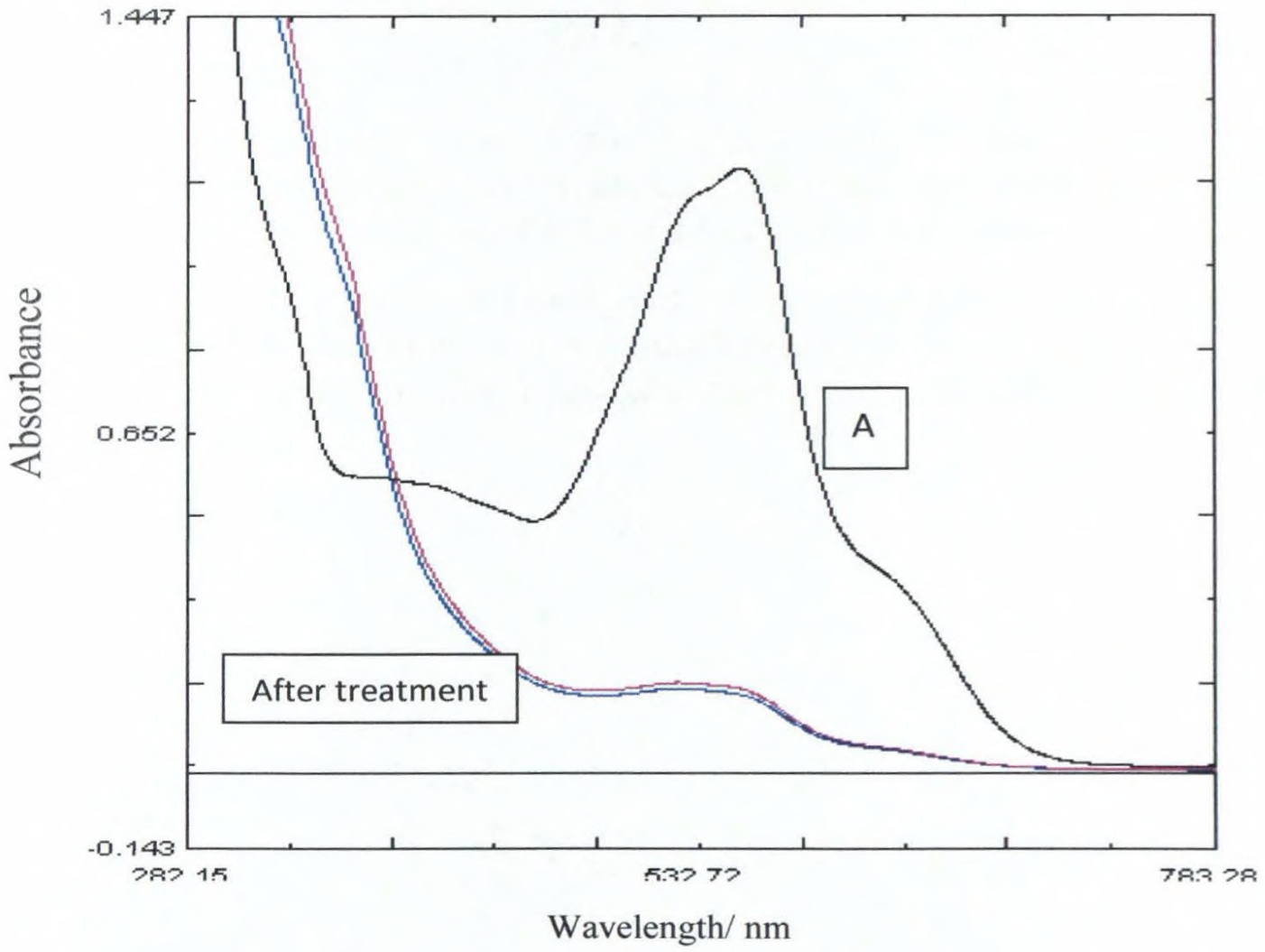

Figure 3.4.60: Spectra obtained after treatment of real dye solution with brick clay under same conditions. Spectrum A illustrates the untreated effluent as received.

Table 3.4.21: Comparison of the extent of removal at each wavelength for real dye effluent sample and synthetic dye mixture prepared at the laboratory.

Wavelength/ nm	Extent of removal/ %	
	Real effluent	Synthetic dye mixture
605	87	95
545	86	98
415	45	86

Figure 3.4.61 shows the colour difference of real effluent sample before and after treatment with brick clay.

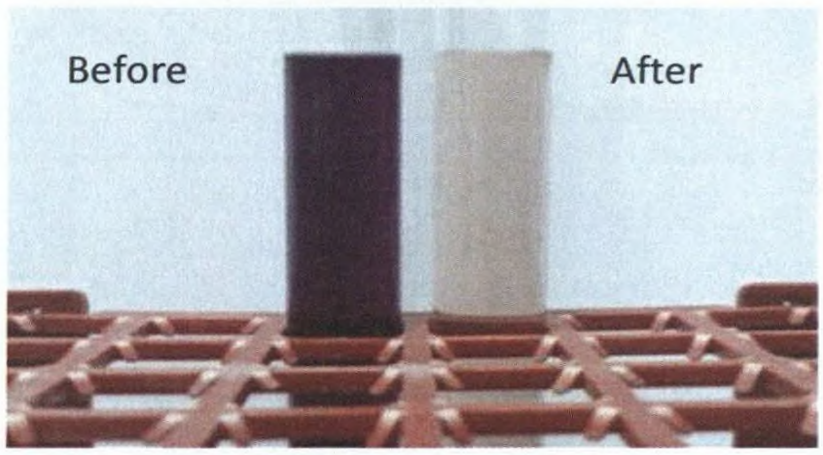

Figure 3.4.61: Colour of samples before and after treatment of real effluent sample with brick clay.

Desorption of dyes from the adsorbent

Desorption experiment also were carried out at the initial solution pH. Figure 3.4.61 shows spectra obtained for desorbed samples. It is clear from this study that desorption increases with increase in pH for the selected dye mixture.

According to the results obtained, percentage desorption significantly increases with increase in pH of the medium, and it is much higher at the pH above 10.0. Therefore, desorption experiments confirm that dyes adsorbed would not leach to the environment under normal conditions.

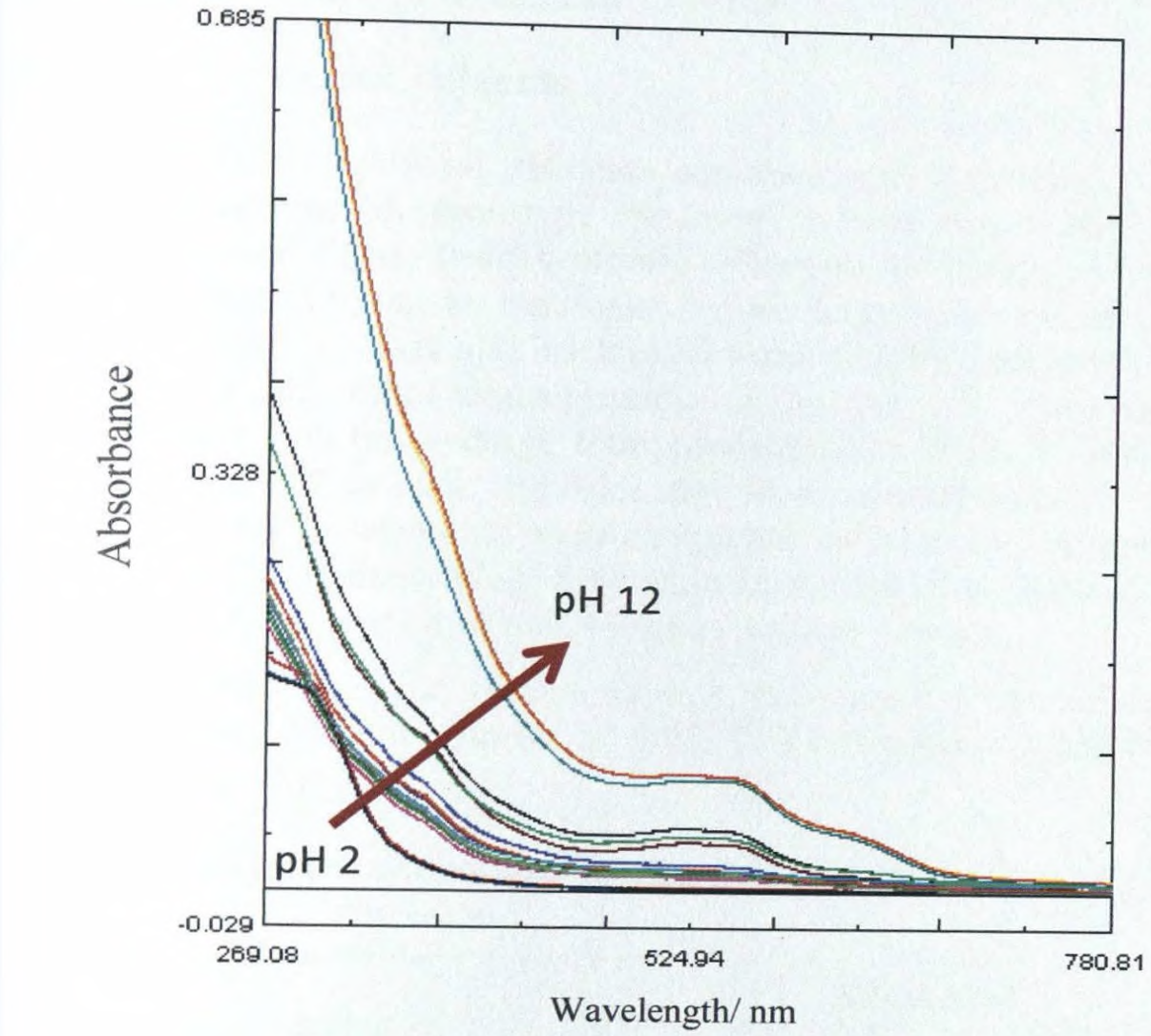

Figure 3.4.61: Spectrums obtained for desorbed sample at different initial solution pH values.

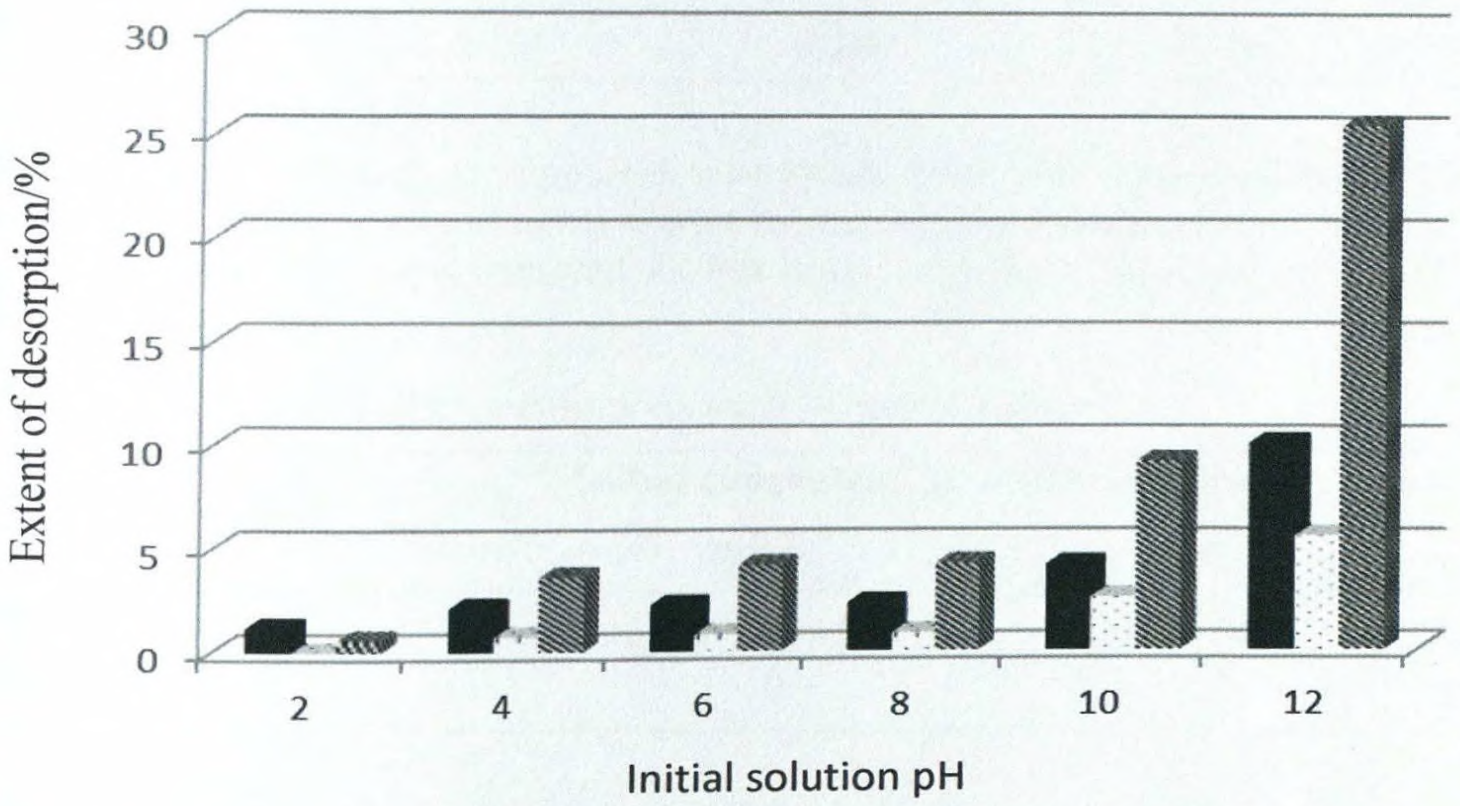

Figure 3.4.62: Extent of desorption for different initial solution pH.

3.4.9 Construction of Prototype Treatment System

3.4.9.1 Treatment of synthetic effluents

As many types of industrial effluents contain Zn(II) according to the analytical results of effluents conducted, prototype treatment system was initially designed for medium-scale removal of Zn(II) from synthetic effluents. Medium-scale treatment is the next extension of laboratory-scale treatment before large-scale treatment. Under this activity, two adsorbents (rice husk and brick clay) were initially selected to investigate the removal of Zn(II) at an initial concentration of 35 mg L^{-1}. The concentration of 35 mg L^{-1} was selected as the average total concentration of Zn in real effluents was approximately 35 mg L^{-1}. Rice husk and brick clay were selected as adsorbents as most of the heavy metal removal experiments were completed on these two adsorbents owing to their effectiveness. After implementing this treatment system, it is planned to develop the system for other adsorbents and other metal ions as a future activity.

Calculations for prototype treatment unit were carried out using "Wastewater Treatment Concepts and Design Approach" [71]. The information listed in Table 3.4.22 were used for these calculations.

Table 3.4.22: Main parameters obtained for the removal of Zn(II) using rice husk and brick clay.

Parameter	Adsorbent	
	Rice husk	**Brick clay**
Firing temperature (°C)	100	400
Surface area (m^2 g^{-1})	110	40
Adsorption capacity (mg kg^{-1})	833	1667
Porocity	0.180	0.339

As the most effective arrangement was to use brick clay first, followed by rice husk according to dynamic experiments conducted during this research, the concentrations given in Table 3.4.23 were considered as the initial and final concentrations that are expected to be observed.

Table 3.4.23: Initial and final concentrations used for calculation.

Adsorbent	Initial concentration /mg L^{-1}	Final concentration /mg L^{-1}
Rice husk	35	10
Brick clay	10	5

According to the data obtained from calculations, two treatment systems were designed for different lengths. Characteristics of each system are given in Table 3.4.24. Engineering designs were drawn for both treatment system sizes (Annexures 4.1 and Annexure 4.2).

Table 3.4.24: Characteristics of two prototype treatment systems.

Characteristics	System I	System II
Total length	167 cm (5.5 feet)	61 cm (2.0 feet)
Dimensions of the brick clay component of the reactor		
Length	45 cm	16 cm
Width	30 cm	30 cm
Depth	30 cm	30 cm
Dimensions of the rice husk component of the reactor		
Length	122 cm	45 cm
Width	30 cm	30 cm
Depth	30 cm	30 cm
Volume of brick clay tank	40,500 cm^3	14,900 cm^3
Volume of rice husk tank	110,076 cm^3	40,500 cm^3
Amount of brick clay required	27.936 kg	10.278 kg
Amount of rice husk required	11.370 kg	4.171 kg
Amount of 35 mg L^{-1} Zn(II) solution that can be treated	1862.8 dm^3	694.9 dm^3
Time taken to treat the solution at 400 cm^3 min^{-1} flow rate	78.9 h	28.9 h

Tanks were filled with rice husk heated at 100 °C and brick clay heated at 400 °C. In order to check the performance of the system, Zn(II) solution of 2000 dm^3 volume was run through the system and hourly intervals samples were taken for a period of several days continuously at the following three points of the system:

1) After the brick clay tank (middle of the system – location A)
2) After the rice husk tank (outlet of the system – location B)
3) After sand filter (final discharge point – location C)

Samples Collected were diluted as necessary, and analyzed using AAS. Figure 3.4.63 illustrates the variation of the extent of adsorption with contact time for Zn(II) removal at the flow rate of 400 cm^3 min^{-1}.

According to the graph the extent of removal plotted against time, the extent of removal of Zn(II) decreases with time at every sampling point. Further, samples collected from the outlet of the treatment system achieved 80% removal at the beginning and it decreases to about 50% after 72 h.

Figure 3.4.64 illustrates the variation in efficiency of two filter media separately.

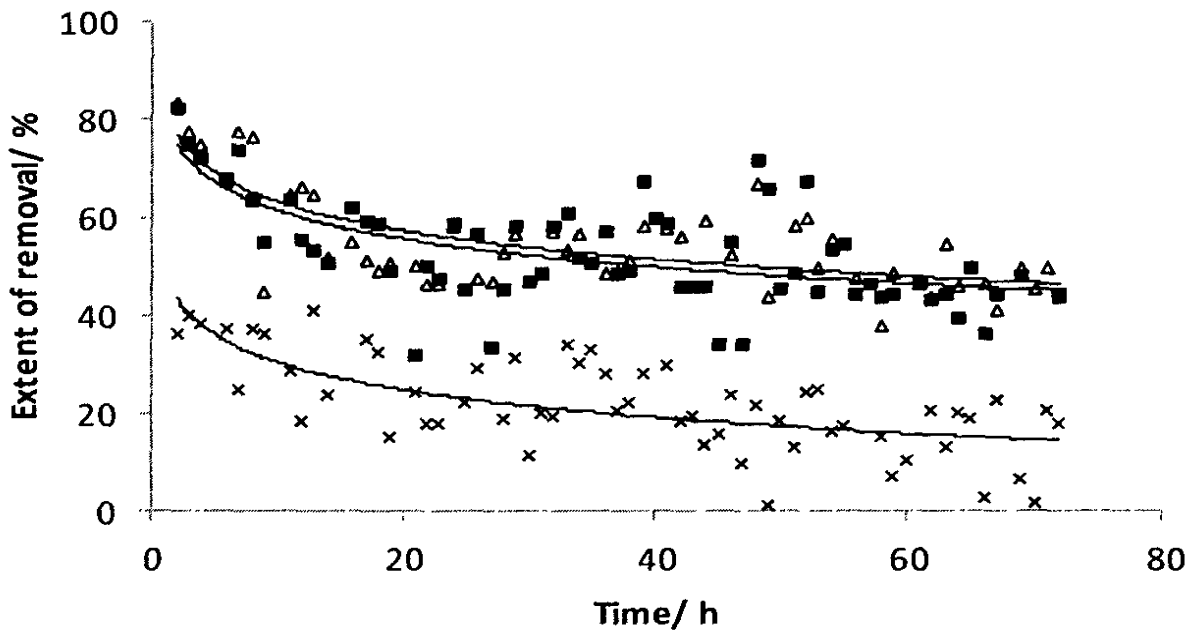

Figure 3.4.63: Graph of the extent of removal variation of three different sampling locations of the treatment system: (A) ×, (B) ■, (C) Δflow rate: 400 cm^3 min^{-1}).

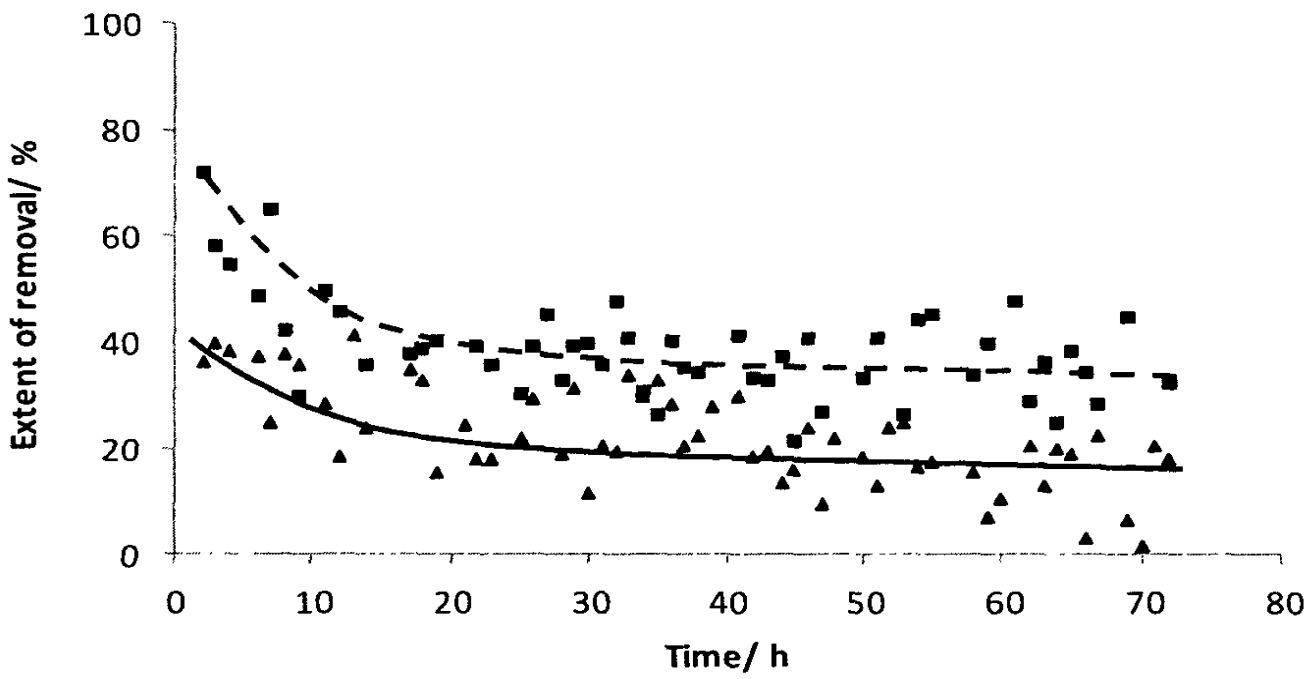

Figure 3.4.64: Variation of the extent of removal of Zn(II) in two individual tanks: Brick clay tank (▲) and rice husk tank (■) (flow rate: 400 cm^3 min^{-1}).

According to the figure, rice husk tank shows much higher removal efficiency throughout the process (initially about 70% and finally about 40%) and brick clay tank shows about 40% initial extent of removal, which decreases down to 20% at the end. Since discharge limits of CEA guidelines is at 5 mg L^{-1} level for Zn, none of the sample achieve this limit in the treatment system where influent concentration is about 35 mg L^{-1} (Figure 3.4.65).

In order to improve the performance of the treatment system, the entire experiment was repeated at a flow rate of 100 cm^3 min^{-1}, and hourly sample withdrawals were done for a period of 10 days continuously to determine the remaining Zn(II) concentration. The results are shown in Figure 3.4.66.

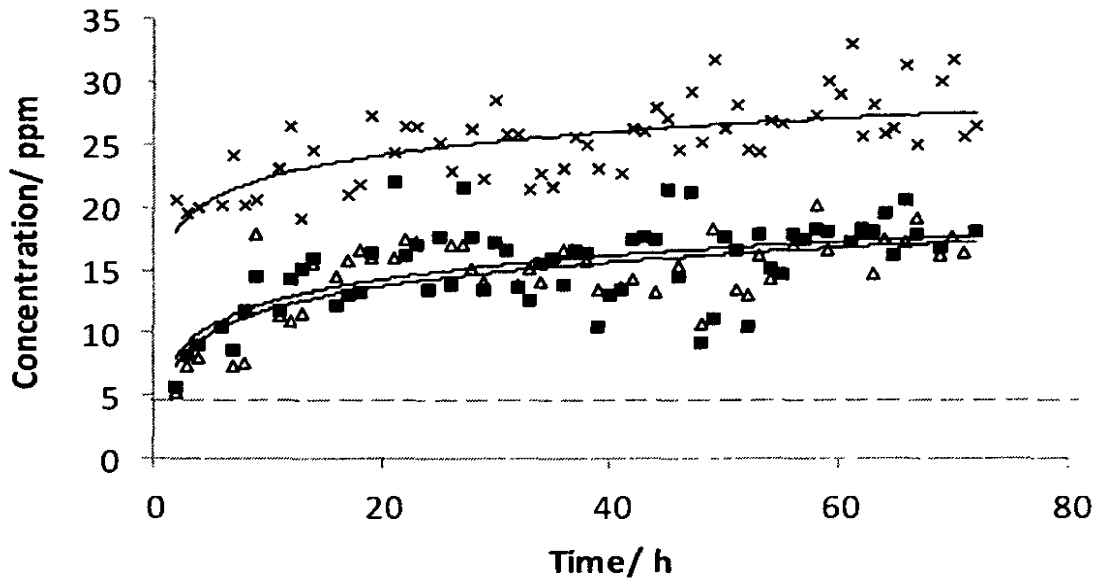

Figure 3.4.65: Variation of the concentration of Zn(II) in the treatment system at different locations: (A) ×, (B) ■, (C) Δ(flow rate: 400 cm^3 min^{-1}).

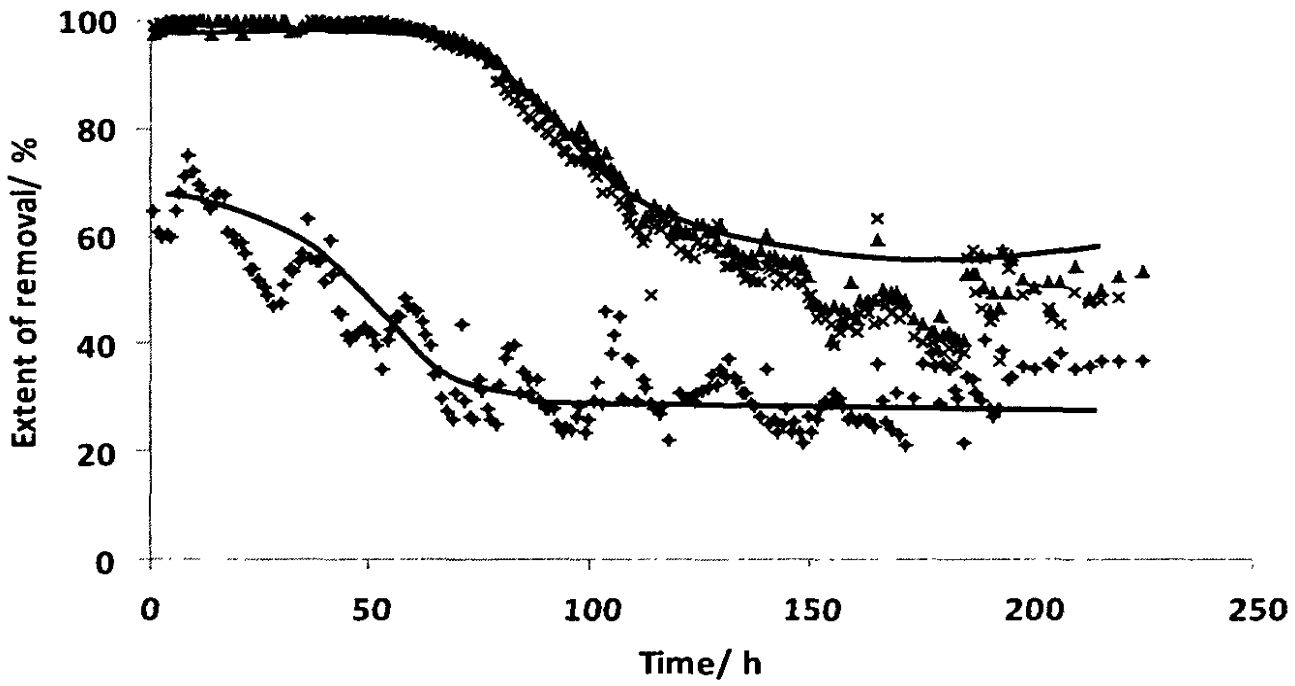

Figure 3.4.66: Variation of the extent of removal of Zn(II) at three different sampling locations of the treatment system: (A) ♦, (B) ×, (C) ▲(flow rate: 100 cm^3 min^{-1}).

According to Figure 3.4.66, samples collected from the outlet of the treatment system achieved 100% removal at the beginning and it decreases to about 50% after 225 h. The same data were resolved for two filter media separately to determine the performance of each adsorbent. The results are shown in Figure 3.4.67.

It is clear from the figure that rice husk tank shows much higher removal efficiency throughout the process (initially about 100% and finally about 20%) and brick clay tank shows about 70% initial extent of removal and it decreases down to 30% at the end. With the decreasing flow rate of the same treatment system, performance of the system increases significantly as shown in figure. According to Figure 3.4.68, the concentrations of the treated effluent at the discharging point of the system remains below the CEA guidelines for a long time period of 85 h.

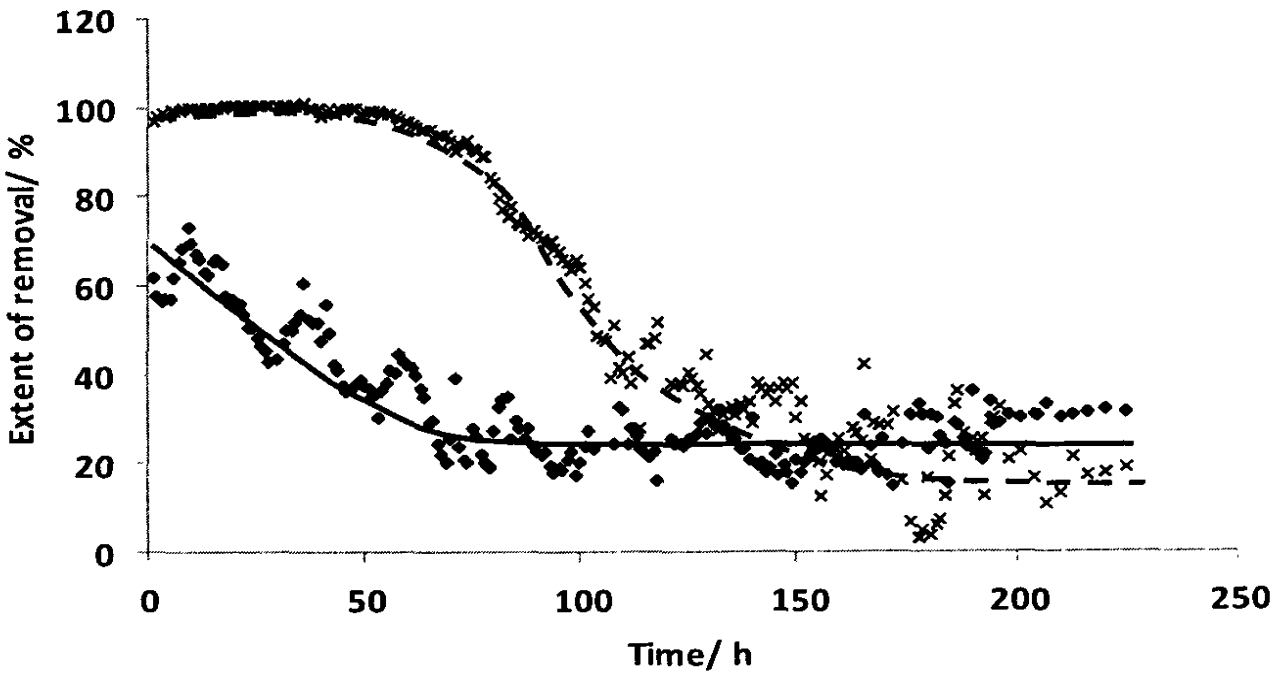

Figure 3.4.67: Variation of the extent of removal of Zn(II) two filter media of the treatment system: Brick clay tank (♦); rice husk tank (×) (flow rate: 100 cm^3 min^{-1}).

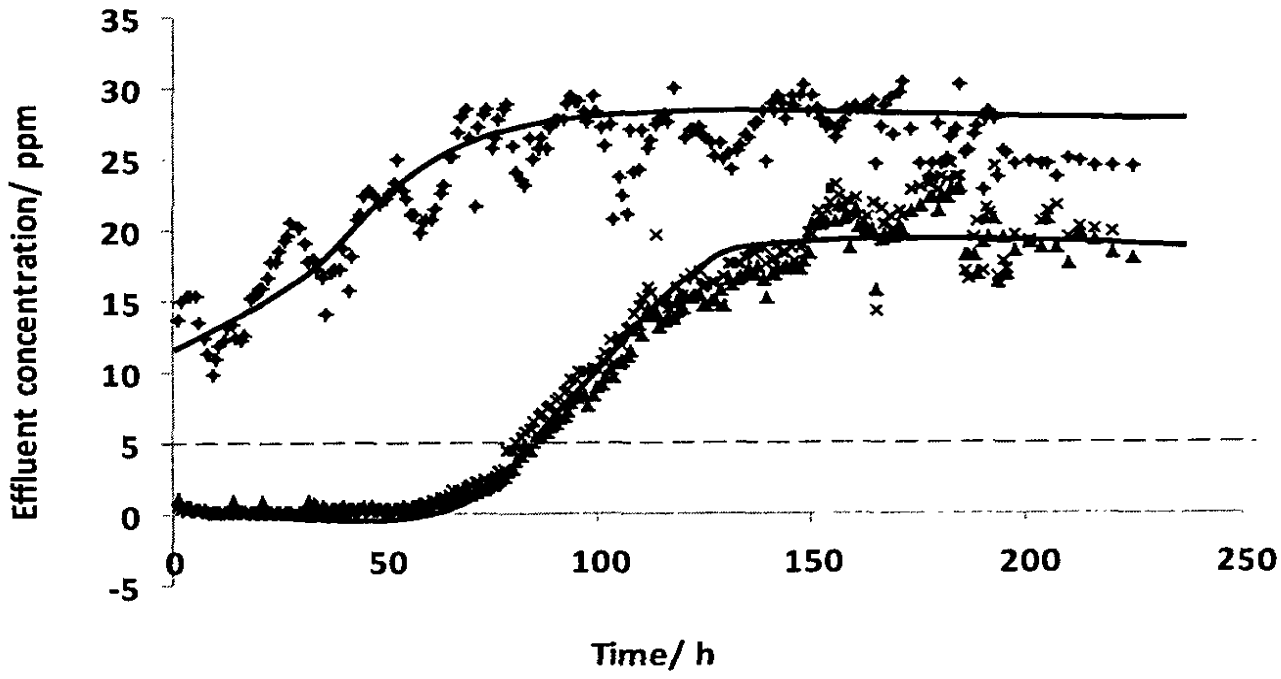

Figure 3.4.68: Variation of the concentration of Zn(II) in the treatment system at different locations: (A) ♦, (B) ×, (C) ▲(flow rate: 100 cm^3 min^{-1}).

The above results obtained demonstrates a significant achievement for the extension of basic research towards applications. This application was based on the modification of optimized parameters of the static conditions extended to dynamic conditions for construction of the prototype treatment system for Zn(II), a common heavy metal present in many industrial effluents. However, all the results were not disclosed as filing a patent on the above results is in progress.

3.4.9.2 Treatment of real effluents

The pH of the real effluent releasing from the industry selected is about 1.0. In order to increase the pH up to neutral values, dolomite was selected as a natural pH controller. In order to select the optimum dose required for this purpose, the final pH values of a synthetic effluent solution having 35 mg L^{-1} were recorded after addition of different doses of dolomite to 50.0 cm^3 of solution (Table 3.4.25). According to the results

obtained, solution pH was increased up to significant values with the addition of small amounts of dolomite.

Table 3.4.25: Optimization of mass of dolomite required to neutralizing a synthetic effluent solution [35 mg L^{-1} Zn(II) solution, initial pH adjusted to 1.0].

Mass of dolomite/g	Final pH of the solution
0.10	4.67
0.20	5.76
0.30	5.73
0.40	6.17
0.50	6.54
2.00	7.53

In order to treat the real effluent of an industry having an average Zn(II) concentration of 40 mg L^{-1}, the initial solution pH was adjusted to be within the range of 4.0–5.0. The pH-adjusted effluent was sent through a sand filter before it reached the brick clay bed. The effluent was then allowed to pass through several tanks filled with brick clay, and then the partially treated effluent was passed through another sand filter to reduce the turbidity of effluent. Treated effluent samples were collected from the outlet of the treatment system to monitor the performance of the prototype system in order to make adjustments as necessary (Annexure 4.3).

Results of this study will be disclosed later as another patent is in progress.

3.6 CONCLUSION

3.6.1 General Aspects

Industrial effluents are released to the environment/water resources, with different types of pollutants. In order to get a general idea of the status of treatment of effluents in Sri Lankan industries, a questionnaire was distributed among selected industries. According to the information gathered, most of the industries use both biological and chemical treatment methods in order to treat effluents, and almost all industries use chemicals for their treatment process. Therefore, treated effluents would eventually lead to environmental problems.

From the data obtained, 90% industries are willing to adopt for a treatment system which consists of environmentally friendly substances. They would use this method if it is low-cost and highly efficient. It is necessary to introduce environmentally-friendly adsorbents to safegueard the quality of surface water surrounding industrial areas of the country. Consequently, many natural adsorbents were tested to remove major metal ions, anions and dyes present in such effluents.

Untreated industrial effluents collected from metal finishing industry, dye industry and textile industry were analyzed. It was determined that most of the parameters were within the discharge limits of CEA guidelines. However, as the pH values of many industrial effluents were not in the neutral pH region, it was considered as a main parameter to be considered in designing a treatment system. Further, effluent samples collected from metal finishing industries contain mainly Cu and Zn; and other heavy metals such as Cd, Cr, Pb and Ni were not present in any of the effluents collected.

3.6.2 Characterization of Natural Adsorbents

Among different natural adsorbents, brick clay, rice husk, feldspar, dolomite, coir dust and saw dust, were selected for the study because of their ability to serve as effective sorbents for cations, anions and organic substances. The samples of these adsorbents were first homogenized to prepare representative bulk samples for the analysis with different preparation procedures. Constituents of rice husk, saw dust and coir dust are mainly organic compounds, such as cellulose, hemicelluloses, lignin, pectins and tannins. On the other hand, brick clay, feldspar and dolomite mainly consist of many minerals. In order to understand the adsorption behaviour of these adsorbents, characterisation of adsorbents, such as active functional groups, specific surface area and charge density were determined. X-ray fluorescence spectroscopic measurements indicate that rice husk contains mainly Si, Fe, K and Ca; dolomite contains Ca and Fe; feldspar contains Si, K, Ca, Fe, Br, Rb, Sr and Ag; and saw dust contain mainly K, Ca, Fe and Cu. Information from surface titrations lead to the pH at the point of zero charge (pH_{PZC}) values of 4.6, 4.5, 4.1 and 5.2 for natural rice husk, and that heated at 60 °C, 100 °C and 200 °C, respectively. The pH_{PZC} values for feldspar and saw dust are 8.9 and 4.0, respectively. Aqueous leachates of adsorbents are found to contain Ca, Mg, K and Na at different levels; and heavy metals, such as Cd, Cr, Pb, Zn, Ni and Cu were not detected in the leachates of any of the adsorbent.

3.6.3 Evaluation of Performance of Adsorbents

Removal of Cd(II), Cr(III), Cu(II), Pb(II), Ni(II) and Zn(II) by rice husk shows the maximum removal at the optimized shaking and settling times at 150 rpm speed at 10 min for all metal ions investigated. The initial solution pH and the firing temperature was obtained as 4.0-5.0 and 100 °C, respectively. Under their optimized conditions, adsorption isotherm experiments conducted with metal ion solutions of initial concentrations varying

from 2-1000 mg L^{-1} shows the validity of the Langmuir isotherm, followed by Redlich-Peterson, Sips, Temkin and Freundlich isotherms, based on regression analysis. The error analysis performed based on average relative error (ARE), Sum square error (SSE), Hybrid fractional error function (HYBRID), nonlinear chi-square test and Sum of absolute error (EABS) further supports the validity of the Langmuir isotherm as compared to others. Further, the adsorption capacity of the six metal ions follows order of Pb(II) > Cd(II) > Cu(II) > Ni(II) > Zn(II) > Cr(III), according to the Langmuir isotherm having 5000 mg kg^{-1} for Pb(II) under the optimized conditions employed.

Kinetics modeling was not applied for Pb(II) and Cd(II) due to their fast adsorption reaction rates. Kinetics modeling applied for the adsorption of Cu(II), Ni(II), Zn(II) and Cr(III) on rice husk within the time period up to 8 min, at which adsorption systems reach equilibrium. According to the pseudo second order kinetics (R^2 > 0.900 for all four metals), the initial adsorption rate (h_o) of the heavy metals are 56, 385, 1111 and 159 mg kg^{-1} min^{-1} for Cu(II), Ni(II), Zn(II) and Cr(III), respectively. Further, the intra-particle diffusion model, is in better agreement for the removal process according to the regression coefficient values, as compared to the external mass transfer diffusion model. Application of the Weber and Morris intra-particle diffusion model for adsorption of the metal ions investigated yields high regression coefficients (> 0.900), the rate constants of particle diffusion are 20.40 min, 63.59 min, 74.87 min, 47.08 min for Cu(II), Ni(II), Zn(II) and Cr(III), respectively.

Owing to the fact that the presence of Zn(II) and Cu(II) in industrial effluents, these two metals were considered as adsorbates for removal experiments. Removal of Cu(II) and Zn(II) using brick clay shows adsorption capacities of 238 and 1429 mg kg^{-1} for respective metal ions at the optimized conditions [Cu(II): 45 min shaking, 15 min settling, neutral initial pH; Zn(II): 30 min shaking, 15 min settling, neutral initial pH].

3.6.4 Metal ion Removal from Synthetic Effluents by Rice Husk and Heated Brick Clay under Dynamic Conditions

Although the maximum removal of metal ions from a mixture of solution is shown by columns packed with brick clay fired at 200 °C, layered columns packed with brick clay and rice husk are recommended to avoid clogging in columns. Columns packed with brick clay on top of rice husk show higher percentage removal ability than the other arrangement, and further, layered columns do not get clogged for a long period of time. The removal of heavy metal ions follows the order, Pb(II) > Cu(II) > Ni(II) ≈ Cd(II) > Cr(III) > Zn(II) for columns packed with rice husk alone and Pb(II) ≥ Cr(III) ≥ Cu(II) ≥ Cd(II) ≥ Zn(II) ≥ Ni(II) for columns packed with brick clay alone and layered type columns. The efficiency of removal of metal ions is in the order, brick clay > rice husk-brick clay > brick clay-rice husk > rice husk. Comparison of static and dynamic conditions shows that static conditions are more successful in removing metal ions as compared to dynamic conditions.

3.6.5 Anion Removal from Synthetic Effluents

Among different types of anions tested, none of the selected adsorbent can be used for the removal of chloride from synthetic effluent samples, while saw dust shows the highest removal ability (40%) for the removal of sulfate from synthetic effluent solution. Removal of phosphate using brick clay provides the maximum adsorption capacity of 3333 mg g^{-1} according to the Langmuir isotherm, while the Freundlich model provides an n value of 1.16, indicating favorable physisorption. Removal of phosphate using brick clay under dynamic conditions leads to optimum column height and flow rate as 30.0 cm and 8 cm^3 min^{-1}. Increase in influent concentration results in a sharper breakthrough curve as

well as a shorter bed service time, indicating that brick clay fixed bed system is saturated more quickly at high concentrations.

3.6.6 Dye Removal from Synthetic Effluents

Three industrial dyes, namely Sumifix blue exf (Dye 1), Sumifix rubine exf (Dye 2) and Sumifix yellow exf (Dye 3) shows the highest removal ability with 200 °C fired brick clay at optimized shaking and settling time (15 min each) at optimized pH (< 10). According to the Langmuir isotherm, the maximum adsorption capacities were determined to be 1667 mg kg^{-1}, 5000 mg kg^{-1} and 2500 mg kg^{-1} for Dye 1, Dye 2 and Dye 3, respectively, and the initial rate of adsorption (h_o) of dyes follows the order, Dye 1 ≈ Dye 2 > Dye 3, according to the pseudo second order kinetics. The extents of removal at wavelengths of 605 nm, 545 nm and 415 nm for the synthetic dye mixture were 95%, 98% and 86%, while the corresponding values for the real dye effluent samples were 87%, 86% and 45%. Such slight decreased values, which would have occurred due to interferents, are acceptable. Further, desorption of dyes from the adsorbent indicates that the extent of desorption increases with increase in pH for the selected dye mixture.

3.6.7 Design of the Prototype System for Treatment of Synthetic Effluents

Among many flow rates attempted, 100 cm^3 min^{-1} was selected as a better flow rate for the prototype treatment system. According the performance evaluation of both reactors, tank with the rice husk bed shows much higher removal efficiency throughout the process (initially about 100% and finally about 20%) and brick clay tank shows about 70% initial extent of removal which decreases down to 30% at the end).

According to the results obtained in this research, higher efficiency in pollutant removal is resulted in by natural substances, which have higher adsorbent sites on their surface. The performance of the prototype treatment system implemented for the removal of Zn(II) using rice husk and brick clay is remarkable. This system can be modified for the removal of other pollutants as a future activity after optimizination of parameters for each system. Modification of the surface of adsorbents would be another novel area to look into for further enhancement of the performance to treat real effluents at large-scale.

3.7 REFERENCES

[1] Baird, C., Cann, M., *Environmental Chemistry*, Third edition, W.H. Freeman and company, **2005.**

[2] Manahan, S.E., *Environmental Chemistry*, Seventh edition, CRC Press, **2000.**

[3] Borah, D.K., Bera, M., *Watershed-scale hydrologic and nonpoint-source pollution models: Review of mathematical bases*, **2003,** 46(6), 1553-1566.

[4] Agarwal, S.K., *Water Pollution,* APH Publishing Corporation, **2009**.

[5] Lawrence, K.W., Jiaping, P.C., Hung, Y.T., Shammas, N.K., *Heavy Metals in the Environment*, CRC Press, **2009.**

[6] Torresdey, J.L.G., Videa, J.R.P., Rosa, G., Parsons, J.G., *Coordin. Chem. Rev.*, **2005**, 249(17–18), 1797–1810.

[7] Spellman, F.R., *The Science of Environmental Pollution*, Second Edition, CRC Press **2009**.

[8] Ambasht, R.S., Ambasht, P.K., *Environment and Pollution*, Fourth edition, CBS Publishers, **2005**.

[9] Alloway, B.J., Ayres, D.C., *Chemical Principles of Environmental Chemistry*, Blackie Academic & Professional, **1993**.

[10] Sonde C.U., Odoemelam, S.A., *Am. J. Phys. Chem.*, **2012**, 1, 11-21.

[11] Lim, L.B.L., Priyantha, N., Tennakoon, D.T.B., Zehera, T., *J. Ecotechnol. Res.*, **2013**, 17(1), 45-49.

[12] Bandara, C., Priyantha, N. *J. Ecotechnol.Res.*, **2013**, 17(1), 45-49.

[13] Pakshirajan, K., Worku, A.N., Acheampong, M.A., Lubberding, H.J., Lens, P.N.L., *Appl. Biochem. Biotechnol.*, **2013**, 170, 498-513.

[14] Navaratne, A.N., Priyantha, N., Kulasooriya, T.P.K., *Int. J. Earth Sci. Eng.*, **2013**, 6, 807-811.

[15] Priyantha, N. and Bandarnayake, A., *J. Hazard. Mater.*, **2011,** 188, 193-197.

[16] Amer, S. I., *Environmental Technology*, Aquachem INC, **1998.**

[17] Cheremisinoff, N.P., *Handbook of Water and Wastewater Treatment Technologies*, Butterworth Heinemann, **2002**.

[18] Long, F., Gong, J.L., Zeng, G.M., Chen L., Wanga X.Y., Denga, J.H., Niua, Q.Y., Zhang, H.Y., Zhang, X.R., *Chem. Eng. J.*, **2011**, 171, 448– 455.

[19] Huang, X., Liao, X., Shi, B., *J. Hazard. Mater.*, **2006**, 166, 1261-1265.

[20] White, S.A., Taylor, M.D., Albano, J.P., Whitwell, T., Klaine, S.J., *Ecol. Eng.*, **2011**, 37, 1968-1976.

[21] Jellali, S., Wahab, M.A., Anane, M., Riahi, K., Bousselmi, L., *J Hazard. Mater.*, **2010**, 184, 226-233.

[22] The effects of chloride from waste water on the environment, **2013**, *University of Minnesota Morris,* Sharice Fontenot and Sam Lee – Report.

[23] Chloride in Drinking Water, Guidelines for drinking-water quality, Second ed. Vol. 2. *Health Criteria and Other Supporting Information,* World Health Organization, Geneva, **1996**.

[24] Sulphate in Drinking Water, Guidelines for drinking-water quality, 2nd ed. Vol. 2. *Health Criteria and Other Supporting Information*, World Health Organization, Geneva, **2004**.

[25] Carmen, Z., Daniela, S., Textile Organic Dyes –Characteristics, Polluting Effects and Separation/Elimination Procedures from Industrial Effluents – A Critical Overview, *'Gheorghe Asachi' Technical University of Iasi*, Faculty of Chemical Engineering and Environmental Protection, Romania, **2012**.
[26] Reemtsma, T., Jekel, M., (Eds.) Organic Pollutants in the Water Cycle: Properties, Occurrence, Analysis and Environmental Relevance of Polar Compounds, Wiley-VCH, **2006**.
[27] Barakat, M.A., *Arab. J. Chem.*, **2011**, 4, 361-377.
[28] http://nzic.org.nz/ChemProcesses/water/13D.pdf (Accessed 12 December 2015).
[29] Rybicki, S., Advanced Wastewater Treatment: Phosphorus Removal from Wastewater (A Literature Review), Division of Water Resources Engineering, Department of Civil and Environmental Engineering, Royal Institute of Technology, **1997**.
[30] Woodard, F., *Industrial Waste Treatment Handbook*, Butterworth–Heinemann Publishers, **2001**.
[31] Jadhao, R.K., *Int. J. Chem. Sci. Appl.*, **2013**, 4(1), 68-72.
[32] Philippe, C.V., Bianchi, R., Verstraete, W., *J. Chem. Technol. Biotechnol.*, **1998**, 72, 289-302.
[33] Elham, A., Hossein, T., Mahnoosh, H., *J. Appl. Sci. Environ. Manage*. **2010**, 14 (4), 159 – 162.
[34] Amarasinghe, B.M.W.P.K., Williams, R.A., *The Chem. Eng. J.*, **2007**, 132(1-3), 299-309.
[35] Pakshirajan, K., Worku, A.N., Acheampong, M.A., Lubberding, H.J., *Appl. Biochem. Biotechnol.*, **2013**, 170, 498-513.
[36] Saikaew, W., Kaewsam, P., *Songklanakarin J. Sci. Technol.*, **2009,** 31, 547-554.
[37] Priyantha, N., Lim, L.B.L., Wickramasooriya, S., *Desalin. Water Treat. J.*, **2015**, 1–9.
[38] Yadav, A.K., Kaushik, C.P., Haritash, A.K., Kansal, A., Rani, N., *J. Hazard. Mater.*, **2006**, 289–293.
[39] Namasivayam, C., Sureshkumar, M.V., *J. Environ. Eng. Manage*, **2007**, 17(2), 129-135.
[40] Salman, M.S., *Al-Khwarizmi Eng. J.*, **2009**, 5(3), 72 – 76.
[41] Priyantha, N., Perera, S., *Water Resour. Manage.*, **2000**, 14, 417-433.
[42] Gu, D., Zhu, X., Vongsay, T., Huang, M., Song, L., He, Y., *Pol. J. Environ. Stud.*, **2013**, 22(5), 1349-1356.
[43] Malavipathirana, S., Wimalasiri, S., Priyantha, N., Wickramasooriya, S., Welagedara, A., Renman, A.G., *J. Geosci. Env. Protec.*, **2013**. 1(2), 7-12.
[44] Chakraborty, S., Chowdhury, S., Saha, P.D., *Carbohyd. Polym.*, **2011**, 86, 1533-1541.
[45] Saheed, A., Sharif, M., Iqbal, M., *J. Hazard. Mater.*, **2010**, 179, 564-572.
[46] Jain, S., Jayaram, R.V., *Desalination*, **2010**, 250, 921-927.
[47] El-Sayed, G.O., *Desalination,* **2011**, 272, 225-232.
[48] Prasad, A.L., Santhi, T., *Sustain. Environ.Res.*, **2012**, 22(2), 113-122.
[49] Oliveira, L.S., Franca, A.S., Alvis, T.M., Rocha, S.D.F., *J. Hazard. Mater.*, **2008**, 155, 507-512.

[50] Brown, G., The Structures and Chemistry of Soil Clay Minerals. The Chemistry of Soil Constituents. John Wiley & Sons, Inc., NY, **1998**.
[51] Mukherjee, S., Srivastava, S.K., *Energy Fuels,* **2006**, 20(3), 1089-1096.
[52] Ngah, W.S.W., Hanafiah, M.A.K.M., *Bioresource Technol.*, **2008**, 99(10), 3935–3948.
[53] Kumar, A., Mohanta, K., Kumar, D., Parkash, O., *Int. J. Emerg. Technol. Adv. Eng.*, **2012**, 2, 86-90.
[54] Chuah, T.G., Jumasiah, A., Azni, I., Katayon, S., Choong, S.Y.T., *Desalination*, **2005**, 175(3), 305–316.
[55] Kumar U., Bandyopadhyay, M., *Bioresource Technol.*, **2006**, 97(1), 104–109.
[56] Etim, U.J., Umoren, S.A., Eduok U.M., *J. Saudi Chem. Soc.*, **2012**.
[57] Israel, A.U., Ogali, R.E., Akaranta, O., Obot, I.B., *J. Sci. Technol.*, **2011**, 33, 717-724.
[58] Vidhana, L.P., Somasiri, L.L.W., *COCOS*, **1997**, 12, 54-71.
[59] Han, J.S., Rowell, J.S., *Chemical Composition of Agro-based Fibers, Paper and Composites from Agro Based Resource,* CRC Press, **1996**.
[60] Vazquez, A.R.H., Alfaro, R.C.V., Merquez, I.B., *J. Appl. Sci. Environ. Sanit.*, **2011**, 6, 447-462.
[61] Mahmoodi, N.M., Hayati, B., Arami, M., Lan, C., *Desalination*, **2011**, 268, 117.
[62] Karagüzel, C., Can, M.F., Sönmez, E., Çelik, M.S., *J. Colloid Interf. Sci.*, **2005**, 285, 192.
[63] Caramalau, C., Bulgariu, L., Macoveanu, M., *Chem. Bull.*, **2009**, 54, 13-17.
[64] Padmasiri, J.P., Dissanayake, C.B., *Int. J. Env. Health Res.*, **1995**, 5(2), 153-160.
[65] Perera S., Priyantha, N., *Ceylon. J. Sci: Phys. Sci.*, **1999**, 6, 57.
[66] Priyantha, N., Perera, S., *Ceylon J. Sci: Phys. Sci.*, **2002**, 9(2), 01.
[67] Seneviratne, C., Priyantha, N., *Inter. J. Global Env. Issues,* **2009**, 9, 239 -248.
[68] Priyantha, N., Seneviratne, C., Cr(III) Absorption and Concomitant Al(III) Desorption in Aqueous Fired Brick Clay Systems (unpublished results).
[69] Priyantha, N., Bandarnayake, A., *J. Hazard. Mater.*, **2011**, 188, 193-197.
[70] Chieng, H.I., Lim, L.B.L., Priyantha, N., Tennakoon, D.T.B., *Int. J. Earth Sci. Eng.*, **2013**, 6, 791-801.
[71] Karia, G.L., Christian, R.A., *Waste Water Treatment Concepts and Design Approach,* PHI Learning Private Limited, Delhi, **2006**.
[72] Johari, I., Said, S., Jaya, R.P., Bakar, B.H.A., Ahmad, Z.A., *Int. Conference on Env. Sci. Eng.*, **2011**, 8, 171-174.
[73] Omatola, K.M., Onojah, A.D., *Int. J. Phys.Sci.*, **2009**, 4(4), 189-193.
[74] Bandaranayake, A.M.A., Mechanistic investigation of interaction of chromium species and thermally – treated brick clay, M.Phil Thesis, University of Peradeniya, **2012**.
[75] Weththasinghe, W.S.A., Coir dust as a low cost adsorbent to remove Cu^{2+}, Zn^{2+} and Pb^{2+}, M.Sc. Thesis, University of Peradeniya, **2015**.
[76] Appel, C., Ma L.Q., Rhue, R.D., Kennelley, E., *Geoderma*, **2003**, 113, 77– 93.
[77] Cardenas-Peña, A.M., Ibanez, J.G., Vasquez-Medrano, R., *Int. J. Electrochem. Sci.*, **2012**, 7, 6142 – 6153.

[78] Chan, L.S., Cheung, W.H., Allen, S.J., McKay, G., *Chinese J. Chem. Eng.*, **2012**, 20, 535-542.
[79] Foo, K.Y., Hameed, B.H., *Chem. Eng. J.*, **2010**, 156, 2–10.
[80] A new IUPAC classification of adsorption isotherms, Available from: http://www.nigelworks.com/mdd/PDFs/NewClass.pdf (Accessed 12 December, 2015).
[81] Ruthven, D.M., Principles of Adsorption and Adsorption Processes. Newyork: A Wiley-Interscience publications, **1938**.
[82] Ho, Y.S., Porter, J.F., Mckay, G., *Water, Air, Soil Pollut.*, **2002**, 141, 1-33.
[83] Farooq, U., Kozinski, J.A., Khan, M.A., Athar, M., *Bioresource Technol.*, **2010**, 101, 5043–5053.
[84] Israel, A.U., Ogali, R.E., Akaranta, O., Obot, I.B., *Songklanakarin J. Sci. Technol.*, **2011**, 33, 717-724.
[85] Khan, T.A., Dahiya, S., Ali, I., *GU J. Sci.*, **2012**, 25(1), 59-87.
[86] Quintelas, C., Fernandes, B., Castro, J., Figueiredo, H., Tavares, T., *Chem. Eng. J.*, **2008**, 136, 195–203.
[87] YanLiang-HSAB-SSA2011poster.pdf, [Online]. Available: http://img.docstoccdn.com/thumb/orig/111069073.png (Accessed 12 December, 2015).
[88] Bhattacharyya, K.G., Gupta, S.S., *Adv. Colloid Interface. Sci.*, **2008**, 140, 114–131.
[89] Chieng, H.I., Lim, L.B.L., Priyantha, N., Tennakoon, D.T.B., *Int. J. Earth Sci. Eng.*, **2013**, 6(4), 791-801.
[90] Odoemelam, S.A., Iroh, C.U., Igwe, J.C., *Res. J. Appl. Sci.*, **2011**, 6, 44-52.
[91] Igwe, J.C., Abia, A.A., Ibeh, C.A., *Int. J. Sci. Technol.*, **2008**, 5, 83-92.
[92] Mckay and Poots, *J. Chem. Technol. Biotechnol.*, **1980**, 30, 279-292.
[93] Sag, Y., Aktay, Y., *Process Biochem.*, **2000**, 36, 157-173.
[94] Mohammadine, E.H., Mamouni, R., Saffaj, N., Lazar, S., *J.Assoc. Arab Univ. Basic Appl. Sci.*,**2012**, 12, 48–54.
[95] Rathod, M., Mody, K., Basha, S., *J. Cleaner Prod.*, **2014**, 1-10.
[96] Futalan, C.M., Kan, C.C., Dalida, M.L., Pascua, C., Wan, M.W., *Carbohyd. Polym.*, **2011**, 83, 697–704.
[97] Jellali, S., Wahab, M.A., Anane, M., Riahi, K., Bousselmi, L., *J. Hazard. Mater.*, **2010**, 184, 226-233.
[98] Vimala, R., Charumathi, D., Das , N., *Desalination,* **2011**, 275, 291–296.
[99] Alemayehu, D.D., Singh, S.K., Tessema, D.A., *Univ. J. Environ. Res. Technol.*, **2012**, 2(5), 411-420.

3.8 Problems, if Any, Encountered During the Course of the Project: None

3.9 Major Findings:

1. The pH at the points of zero charge (pH_{PZC}) are at 4.6, 4.5, 4.1 and 5.2 for natural rice husk, and rice husk heated at 60 °C, 100 °C and 200 °C, respectively. The pH_{PZC} for feldspar and saw dust are 8.9 and 4.0, respectively.
2. Ca, Mg, K and Na are leached out from aqueous solutions of adsorbents tested. However, Cd, Cr, Pb, Zn, Ni and Cu are not detected.
3. The optimum values for the removal of heavy metals from rice husk are: 10 min shaking time, 10 min settling time, 4.0-5.0 solution pH and 100 °C treatment temperature. The Langmuir isotherm model shows that the adsorption capacity follows order of Pb(II) > Cd(II) > Cu(II) > Ni(II) > Zn(II) > Cr(III) under the optimized conditions. Further, adsorption capacity of brick clay on Cu(II) and Zn(II) are 238 and 1429 mg kg^{-1} for under the optimized conditions.
4. The efficiency of removal of metal ions under dynamic conditions follows the order, brick clay > rice husk-brick clay > brick clay-rice husk > rice husk.
5. Brick clay provides the maximum adsorption capacity of 3333 mg kg^{-1} for removal of phosphate from synthetic effluent solutions, while saw dust shows the highest removal ability of 40% for sulfate. The optimum column height and flow rate for phosphate removal under dynamic conditions are 30 cm and 8.0 cm^3 min^{-1}, respectively. However, adsorbents selected do not remove chloride.
6. Three industrial dyes: Sumifix blue exf (Dye 1), Sumifix rubine exf (Dye 2) and Sumifix yellow exf (Dye 3) show the highest removal ability with brick clay treated at 200 °C. Adsorption capacities of these dyes are 1667 mg kg^{-1}, 5000 mg kg^{-1} and 2500 mg kg^{-1} for Dye 1, Dye 2 and Dye 3, respectively.
7. The extents of removal at wavelengths of 605 nm, 545 nm and 415 nm for the synthetic dye mixture were 95%, 98% and 86%, while the corresponding values for the real dye effluent samples were 87%, 86% and 45%.
8. Two prototype treatment systems with the dimensions given in the table were constructed. The parameters that had been optimized (see above) for treatment of laboratory–prepared metal ion and anion solutions under static and dynamic conditions were further adjusted to identify conditions for satisfactory performance of the above systems. At a flow rate of 100 cm^3 min^{-1}, the above prototype systems achieve 100% Zn(II) removal at the beginning (decreases to about 50% after 225 h). Further rice husk packed system shows much higher removal efficiency throughout the process, as compared to brick clay packed system. These findings demonstrate the remarkable performance of the protype treatment system, which can further be extended for large-scale treatment.

Dimensions of the brick clay component of the reactor: Length	45 cm	16 cm
Width	30 cm	30 cm
Depth	30 cm	30 cm
Dimensions of the rice husk component of the reactor: Length	122 cm	45 cm
Width	30 cm	30 cm
Depth	30 cm	30 cm

SECTION 4

Impact of Research Results

4(a).i Relevance of results achieved to scientific advancement

The main contribution of this project to scientific advancement is to provide technology to remove hazardous pollutants from effluents released from industries, which are harmful to the environment as well as to the human being, and consequently, the removal of such materials from the environment has become a priority. In this context, the study is based on the removal of heavy metal ions [Cd(II), Cr(III), Cu(II), Ni(II), Pb(II) and Zn(II)], anions [Cl^-, NO_3^- and PO_4^{3-}] and textile dyes from industrial effluents using naturally available materials, such as rice husk, brick clay, coir dust, saw dust, dolomite and feldspar, which can be used to develop cost-effective and eco-friendly effluent treatment procedures. The initial activity of this research project was mainly based on the investigation of sorption of industrial pollutants on selected natural substances through parameter optimization, adsorption isotherm studies, kinetics under static conditions; and optimizing bed height and flow rate under dynamic conditions. The next step was to construct a prototype treatment system for the removal of Zn(II) from synthetic effluent at medium scale for treatment of synthetic and eal industrial effluents.

The research focused on the mechanism of interaction of pollutants on different sorbents. It provides useful information for researchers who are interested in environmental management/pollution control. Such studies also have the potential for expansion of more research fields. Additionally, the general public will gather information on the use of naturally available substances and/or industrial byproducts for removal of pollutants.

All the aspects specified above would contribute to scientific advancement.

4(a).ii Dissemination/application of research output

The main application of this project is the successful contruction of the prototype treatment system for treatment of industrial effluents at medium-scale. These findings will be disseminated to the industrial sector through workshops organized by the Postgraduate Institute of Science as the institute is now on its way to strengthen academic-industry partnerships. Further expansion of this system for better performance by modifying the adsorbent surfaces for large scale treatment would be the next next logical step of the project.

Further, knowledge gained by researchers could be disseminated through publications, communications and patents resulted from this project at both national and international levels. This will continue further through more documents to be published. These efforts will also be important for international recognition of scientific achievements in Sri Lanka, in particular in the field of pollution control/management through low-cost and environmentally friendly approaches.

4(b).i Relevance of results achieved to national/socio-economic development

Use of local, readily available adsorbents and industrial byproducts to solve a significant problem of industrial effluent tratement is the main contribution of this project to national/socio-economic development.

This project demonstrates the applicability of many natural adsorbents on the removal of heavy metal ions, anions and textile dyes. In this investigation, mechanistic details, as well as application of eco-friendly treatment systems was attempted. The results obtained lead to better understanding of the treatment of industrial effluents using natural adsorbents.

Small–scale industries are usually reluctant to adopt wastewater treatment systems at the beginning of the industry due its high cost for the implementation and monitoring. The treatment system designed in this project is low-cost in terms of both capital and maintenance expenditure. Therefore, small scale industries as well as large-scale industries, which may not use proper effluent treatment procedures, can adopt the proposed low-cost treatment methodology. Treated effluents released to the environment will thus be of better quality which would contribute to the improvement of well – being of the people.

Use of chemicals, which are currently imported, can be decreased as a result of the proposed project demonstrating the use of natural substances/industrial byproducts for treatment of industrial effluents. As chemicals are replaced by environmentally friendly materials, the project definitely improves environmental sustenance. Further, as pollutants present in industrial effluents are removed, the quality of the environment will be improved.

The proposed treatment system which is in horizontal direction is also useful in the application of the system for the existing treatment plants. This may be an added advantage for industries in order to adopt for the proposed system.

SECTION 5

MISCELLANEOUS

5.1 List of major equipment acquired during the project

Equipment	Value/Rs.	Functionality
Sample storage refrigerator	125,126.40	To store samples at low temperature
Solvent filtration unit	100,800.00	To remove residues after treatment with adsorbents
Thermo-reaction system	138,710.00	To digest samples for various measurements

5.2 List of publications/Communications arising from the project

1. A.N. Navaratne, N. Priyantha and T.P.K. Kulasooriya, Removal of heavy metals using rice husk and brick clay as adsorbents - dynamic conditions, *International Journal of Earth Science and Engineering*, **6**, 807-811 (2013).
2. T.P.K. Kulasooriya, N. Priyantha and A.N. Navaratne, "Adsorption of heavy metal ions on rice husk: Isotherm modeling and error analysis", *International Journal of Earth Science and Engineering*, **8**, 346-352 (2015).
3. A.N. Navaratne, N. Priyantha and T.P.K. Kulasooriya, Removal of heavy metal ions using rice husk: Investigation on adsorption kinetics of heavy metals (submitted).
4. N. Priyantha, A.N. Navaratne and T.P.K. Kulasooriya, Removal of phosphate ions using brick clay: static and dynamic conditions (submitted).
5. N. Priyantha, A.N. Navaratne and T.P.K. Kulasooriya, Treatment of textile industry dye effluent by using naturally available substances (in preparation).
6. N. Priyantha, A.N. Navaratne, T.P.K. Kulasooriya and W.S.A. Weththasinghe, Comparison of the removal of Cu(II) and Zn(II) by using coir dust and brick clay (in preparation).
7. N. Priyantha, A.N. Navaratne and T.P.K. Kulasooriya, Prototype treatment facility for Zn(II) removal from synthetic effluents (Patent in preparation).
8. T.P.K. Kulasooriya, N. Priyantha and A.N. Navaratne, Treatment of industrial effluents using fired brick clay based filter (Patent in preparation).
9. A.N. Navaratne, N. Priyantha and T. P. K. Kulasooriya, Removal of heavy metals using rice husk and brick clay as adsorbents: a study of dynamic conditions, *2nd Int. Symposium on Water Quality and Human Health: Challenges Ahead*, PGIS, University of Peradeniya (2013).
10. N. Priyantha, A.N. Navaratne and T.P.K. Kulasooriya, Adsorption isotherm studies of heavy metal ions on rice husk, *Proc. Pera. Univ. Res. Ses.*, University of Peradeniya (2014).

11. T.P.K. Kulasooriya, A.N. Navaratne and N. Priyantha, Optimization of efficiency of phosphate removal by brick clay, *PGIS Research Congress* (2014).
12. N. Priyantha, A.N. Navaratne and T.P.K. Kulasooriya, Sorption studies of textile dyes using naturally available substances, *4th Int. Symposium of Water Quality and Human Health: Challenges Ahead,* PGIS, University of Peradeniya (2015).

Please see copies of publications/communications attached (Annexure 5).

SECTION 6

Summary Statement of Expenditure

Please see attached.

Annexure 1

Industrial survey on Effluent treatment facilities

1. Name of the industry:

   .....

2. Main products of the industry:

   .....

   .....

   .....

3. Main raw materials used:

   .....

   .....

   .....

   .....

4. Is there a waste water treatment plant available in the industry: Yes ☐ No ☐
5. Treatment method is:

   Biological ☐ Chemical ☐ Other ☐

6. Components used for treatment of waste water:

   1).....

   2).....

   3).....

   4).....

7. Treatment plant contains:

   Industrial effluent ☐

   Other types of Industrial waste water ☐

   Sewage ☐

   Canteen effluents ☐

   Other ☐

   Specify.....

8. Capacity of the collection tank: .....
9. Approximate volume of effluent discharged daily to the treatment system: .....

10. Treated effluents released to:

- Inland water body ☐
- Irrigation purpose ☐
- Reuse for production process ☐
- Other ☐

Specify.....

11. According to your knowledge, comment on the efficiency of the above treatment system:

- Very good ☐
- Good ☐
- Average ☐
- Poor ☐
- Needs improvement ☐

12. Would your industry be willing to adopt a treatment method consisting of environmentally friendly substances:

- Yes ☐
- No ☐
- May be ☐

Annexure 2

Summary of Responses for Questionnaires

All industries categorized in to three types of industries,

- Metal finishing Industry
- Textile Industry
- Dyeing Industry

Different codes indicate in the Questionnaire

Treatment method –

1) Biological
2) Chemical
3) Other

Type of effluent/wastes -

1) Industrial effluent
2) Other types of Industrial waste water
3) Sewage
4) Canteen effluents
5) Other

Way of discharge -

1) Inland water body
2) Irrigation purpose
3) Reuse for production process
4) Other

Efficiency of treatment system (according to their knowledge) -

1) Very good
2) Good
3) Average
4) Poor
5) Needs improvement

Industry is willing to adopt environmentally friendly treatment method -

1) Yes
2) No
3) Maybe

	Type of industry / Main products of industry	Raw materials used	Treatment method	Used components	Treatment plant contained	capacity of plant	Volume of effluent discharged daily	Treated effluents released to	Efficiency of treatment system	willing to adjust to environmentally friendly treatment method
1	Main water treatment plant - All industries in BOI zone	Primary treated waste water	1	Aeration	1, 2, 3, 4, 5	5000 m^3	6000 m^3	1	3	1
2	Apparel Manufacturing Industry	Fabric	2		1, 4	1000 m^3	800 m^3	4	1	1
3	Metal based Jewellery Industry	sterlin silver, brass, tin alloy	2	Alum powder, Sodium hydroxide, Flocculants	1	20000 m^3	5000 m^3	4	2	3
4	Apparel printing industry	Ink, Garments	2	Ferrous sulphate, Coastic soda, Polymer	1	3500 m^3	6000 m^3	4	2	1

5	Kitchen furniture parts manufacturing industry	Stainless steel, mild steel wires	2	lime powder, Sulfuric acid, Sodium metabisulphate	1	1000 m^3	500 m^3	4	2	1
6	Injection mould and mould making industry	Plastis, aluminium, iron	2	flocculator, accelerator, pH adjuster	1	800 m^3	150 m^3	4	1	1
7	Socks and panty hose preparing industry	Cotton, nylon, polyamide	2	Sodium hydroxide, flocculant agent, anti foam	1	250 m^3	150 m^3	4	2	1
8	Garment washing industry	Desizing agent, enzimes, bleach stones, dyes, sizes, acids, coastic soda	2	Sodium hydroxide, flocculant resin, Aluminium sulphate	1	500 m^3	20000 m^3	4	2	1
9	Garment washing industry	Bleaching,	2	Ferrous sulphate, Hydrated lime, Polymer, Sulphuric acid	1	1000 m^3	1250 m^3	4	1	1
10	Garment knitting and dyeing industry	Yarn, Dyes, chemicals	2	Ferrous sulphate, Calcium hydroxide, Poly alumunium chloride, Poly acrylic amide (cation polymer)	1	2000 m^3	2800 m^3	4	2	1
11	Garment washing industry	Dye, Softners, Chlorine	2	Trisodium phosphate, Urea, Sodium hydroxide, Sulphuric acid, Polymer, coagulent	1	600 m^3	960 m^3	4	2	1

12	Garment washing industry	Stain removers, softners, desizing agents	2	Ferrous sulphate, Sodium hydroxide, Sulphuric acid, Lime	1	2000 m^3	1000 m^3	4	1	3
13	Fabric printing industry	Paint, fabrics	2	Aluminium sulphate, ferrous sulphae, Polyelectrolite, Antifoam, Decolorent	1	150 m^3	450 m^3	4	1	1
14	Elastic dyeing industry	Elastic, Nylon, Viscous	2	Polyaluminium chloride, Polymer, Sodium hydroxide, Decolorent	1	800 m^3	300 m^3	4	1	1
15	Apparel dying industry	Dye, Fabrics	2	Ferrous sulphate, Alum, Hydrochloric acid	1	80 m^3	320 m^3	4	2	1
16	Garment dying indusry	Dye, Fabrics	2	Ferrous sulphate, Sodium hydroxide, hydrochloric acid, polymer	1	10000 m^3	1200 m^3	4	2	1
17	Garment dying indusry	Fabric, Dye, elastic	2	Ferrous sulphate, Sodium hydroxide, Sulphuric acid, Lime	1	180 m^3	127 m^3	4	1	3

18	Bicycle assembling industry	Bicycle parts	2	pH adjusters, flocculator, Accelerator	1	40 m^3	7.5 m^3	4	4	1
19	Apparel knitting industry	Sewing	1	Aeration, Settling, Filtering	3,4	10 m^3	2 m^3	4	3	1
20	Apparel knitting industry	Sewing	1	Aeration, Settling, Filtering	3,4	8 m^3	6 m^3	4	2	1

Katunayake, Biyagama and Seethawaka Export Processing Zones were selected to collect data on the current situation of wastewater treatment of industries. According to the information gathered, industries use both biological and chemical treatment methods in order to treat effluents. According to responces for questionnaires distributed to 17 industries in various locations, 85% industries use chemical treatment methods and only 15% industries use biological treatment methods in their treatment process.

Alum powder, sodium hydroxide, ferrous sulphate, lime powder, sulfuric acid and aluminium sulphate are mostly used chemicals for the effluent treatment, while some other chemicals are used as coagulants, anti-foam agents, pH adjusters, accelerators and as decolourants. No industry releases industrial effluents and waste water without treatment.

As shown in Figure Q1, efficiency of the treatment system available in each industry was divided in to four categories. Most treatment systems are in condition according to their knowledge.

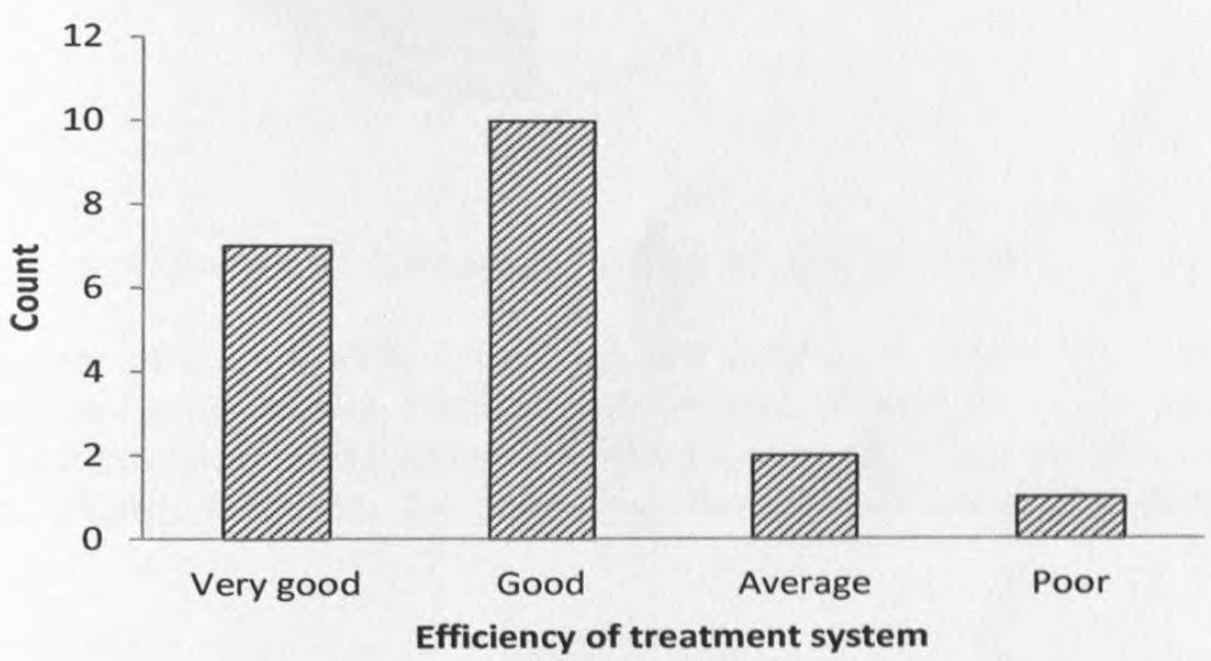

Figure Q1: Counts for the efficiency of treatment systems according to their knowledge

Most industrial treatment systems consist of collection tanks within the capacity range of 500 to 5000 m^3. Only a limited number of industries have collection tanks with capacity less than 100 m^3 and greater than 5000 m^3 (Figure Q2).

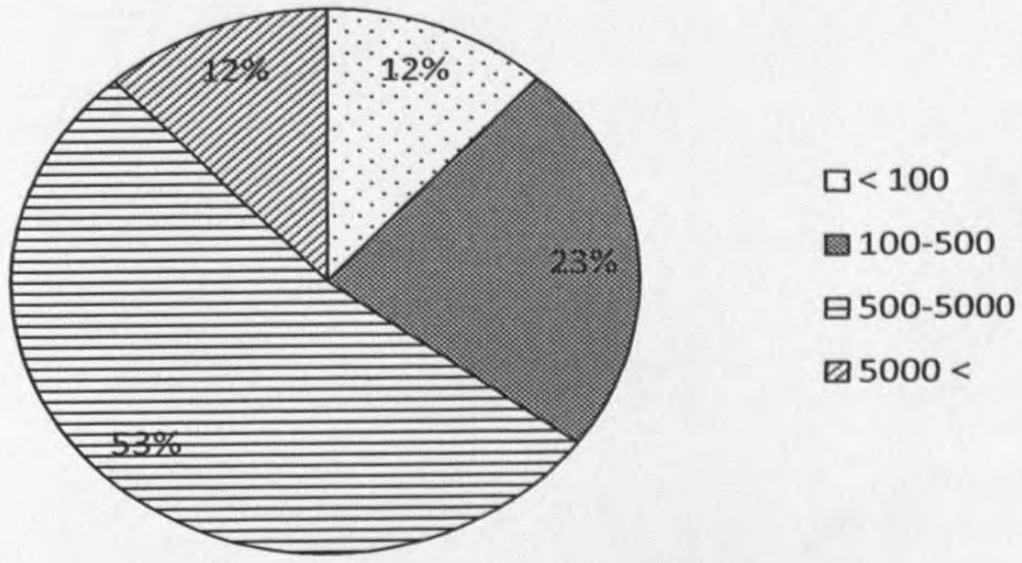

Figure Q2: Capacity of the collection tank

As shown in Figure Q3, most of the treatment systems discharge 100-5000 m^3 of effluents daily. These untreated industrial effluents are treated partially using these techniques, and partially treated effluents were released to the BOI common wastewater treatment system for further treatment. Therefore, at the final stage, the biological treatment methods are applied to complete the waste water purification process.

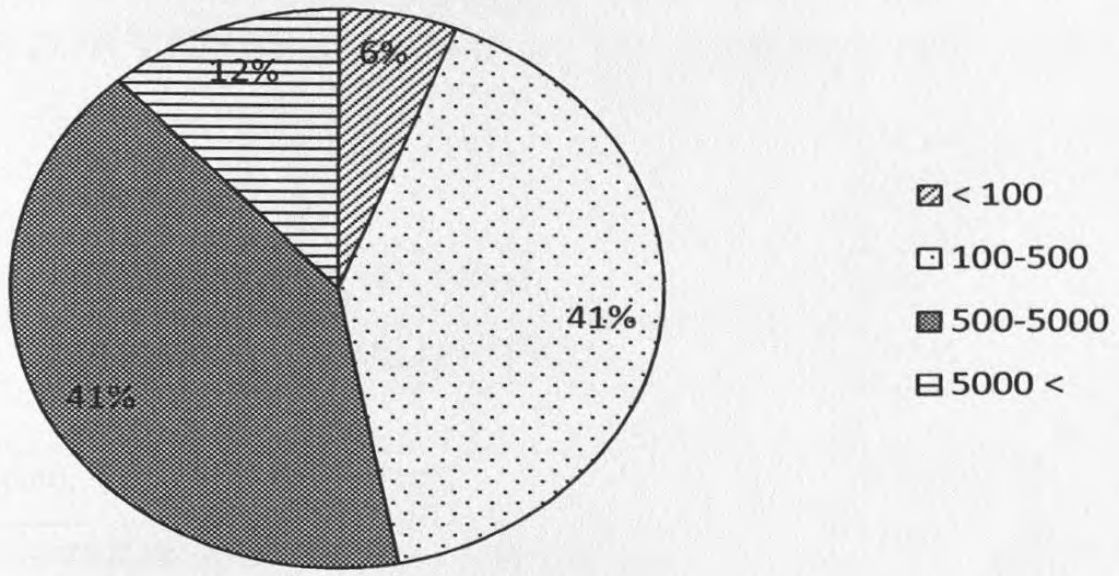

Figure Q3: Volume of effluents discharge daily

From the data obtained, 90% industries are willing to adopt for a treatment system which consists of environmentally friendly substances. However, 10% industries gave an exact answer for the question of whether they like to adopt it. They would use this method if it is low-cost and highly efficient. No industries disliked adopting the proposed treatment system.

ANNEXURE 3

PART I: SEC. (I) - GAZETTE EXTRAORDINARY OF THE DEMOCRATIC SOCIALIST REPUBLIC OF SRI LANKA - 01.02.2008-7A

SCHEDULE I

TOLERANCE LIMITS FOR THE DISCHARGE OF INDUSTRIAL WASTE IN TO INLAND SURFACE WATERS

Parameter	Unit/Type of limit	Tolerance limit values
Total suspended solids	mg/1, max.	50
Particle size of the total suspended solids	µm, less than	850
pH at ambient temperature	-	6.0 - 8.5
Biochemical oxygen demand(BOD5 in five days at 200c or BOD3 in three days at 270c)	mg/1, max	30
Temperature of discharge	^{0}C, max.	Shall no exceed 400 C in any section of the stream within 15 m down stream from the effluent outlet.
Oils and greases	mg/1, max.	10
Phenolic compounds (as C6H5OH)	mg/1, max.	1
Chemical oxygen demand (COD)	mg/1, max.	250
Colour	Wavelength Range 436 nm (Yellow range) 525 nm (Red range) 620 nm (Blue range)	Maximum spectral absorption coefficient $7m^{-1}$ $5m^{-1}$ $3m^{-1}$
Dissolved phosphates (as P)	mg/1, max.	5
Total Kjeldahl nitrogen (as N)	mg/1, max.	150
Ammoniacal nitrogen (as N)	mg/1, max.	50
Cyanide (as CN)	mg/1, max.	0.2
Total residual chlorine	mg/1, max.	1.0
Fluorides (as F)	mg/1, max.	2.0
Sulphides (as S)	mg/1, max.	2.0

Arsenic (as As)	mg/1, max.	0.2
Cadmium (as Cd)	mg/1, max.	0.1
Chromium, total (as Cr)	mg/1, max.	0.5
Chromium, Hexavalent (as Cr6+)	mg/1, max.	0.1
Copper (as Cu)	mg/1, max.	3.0
Iron (as Fe)	mg/1, max.	3.0
Lead (as Pb)	mg/1, max.	0.1
Mercury (as Hg)	mg/1, max.	0.0005
Nickel (as Ni)	mg/1, max.	3.0
Selenium (as Se)	mg/1, max.	0.05
Zinc (as Zn)	mg/1, max.	2.0
Pesticides	mg/1, max.	0.005
Detergents/surfactants	mg/1, max.	5
Faecal Coliform	MPN/100 ml, max	40
Radio Active Material (*a*) Alpha emitters (*b*) Beta emitters	micro curie/ml, max micro curie/ml, max	 10^{-8} 10^{-7}

Note 1 : All efforts should be made to remove unpleasant odour as far as possible.

Note 2 : These values are based on dilution of effluents by at least 8 volumes of clean receiving water. If the dilution is below 8 times, the permissible limits are multiplied by the 1/8 of the actual dilution.

Note 3 : The above mentioned general standards shall cease to apply with regard to a particular industry when industry specific standards are notified for that industry.

Note 4 : Pesticides as per World Health Organization (WHO) and Food and Agriculture Organization (FAO)Requirements.

Annexure 4

Analysis of Industrial Effluents - Data Records

Types of Industries

- Metal Finishing Industry
- Textile Industry
- Dye Industry

Industry codes included in the data sheet

1.	Katunayake Export Procesing Zone	-	Metal Finishing Industry
2.	Katunayake Export Procesing Zone	-	Textile Industry
3.	Katunayake Export Procesing Zone	-	Textile Industry
4.	Biyagama Export Procesing Zone	-	Dye Industry
5.	Biyagama Export Procesing Zone	-	Metal Finishing Industry
6.	Seethawaka Export Procesing Zone	-	Textile Industry
7.	Biyagama Export Procesing Zone	-	Textile Industry
8.	Biyagama Export Procesing Zone	-	Dye Industry
9.	Seethawaka Export Procesing Zone	-	Textile Industry
10.	Seethawaka Export Procesing Zone	-	Dye Industry

Table M1: Industrial effluent analysis data of untreated industrial effluents

Parameter	Industry									
	1	2	3	4	5	6	7	8	9	10
COD	882	399	1218	453	36	249	320	356	53	400
pH	4.7	5.9	6.5	11.2	1.9	11.1	7.2	8.4	10.9	8.3
Conductivity	4.8×10^{-4}	6.7×10^{-4}	5.5×10^{-4}	8.9×10^{-4}	6.0×10^{-3}	2.8×10^{-3}	6.9×10^{-4}	1.5×10^{-3}	5.6×10^{-6}	1.6×10^{-3}
Phosphate	13.696	12.887	11.432	8.133	4.213	1.223	8.535	3.987	2.555	3.108
Sulphate	125	10	697	144	11	454	191	362	2244	400
Cd	<0.26	<0.26	<0.26	<0.26	<0.26	<0.26	<0.26	<0.26	<0.26	<0.26
Cr	<1.0	<1.0	<1.0	<1.0	<1.0	<1.0	<1.0	<1.0	<1.0	<1.0
Cu	67.7	<0.7	<0.7	<0.7	<0.7	<0.7	<0.7	<0.7	<0.7	<0.7
Ni	<1.0	<1.0	<1.0	<1.0	<1.0	<1.0	<1.0	<1.0	<1.0	<1.0
Zn	34.5	<0.2	<0.2	<0.2	2.7	<0.2	<0.2	<0.2	<0.2	<0.2
Pb	<1.5	<1.5	<1.5	<1.5	<1.5	<1.5	<1.5	<1.5	<1.5	<1.5
TSS	1410	124	160	348	4	148	40	120	86	536

Note: All the parameters except pH and conductivity are reported in ppm and conductivity is reported in $\mu S\ cm^{-1}$.

Table M2: Discharge limits for industrial effluents for inland water bodies

Parameter	Tolerance Limit Values
COD	250
pH	6.0-8.5
Conductivity	-
Phosphate	-
Sulphate	-
Cd	0.1
Cr	0.5
Cu	3.0
Ni	-
Zn	2.0
Pb	0.1
TSS	50

Note: All the parameters except pH and conductivity are reported in ppm and conductivity is reported in $\mu S\ cm^{-1}$.

Many visits to industries were made to collect untreated industrial effluents from two metal finishing industrial effluents, three dye industrial effluents and five textile effluent samples. All these samples were analyzed in the laboratory.

Data of different types of industrial effluents, are summarized according to the chemical parameters (Figure 1). Chemical oxygen demand (COD) and sulphate were determined using open reflux method and turbidimetric method respectively, and total suspended solids (TSS) was determined at 105 °C.

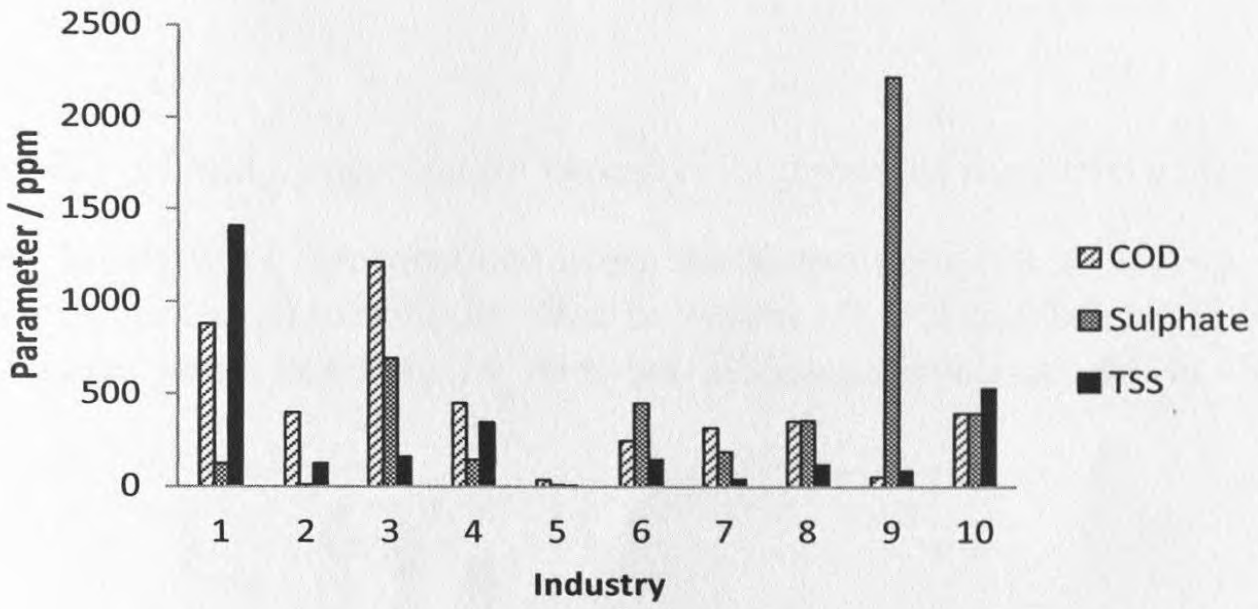

Figure M1: Chemical Oxygen Demand (COD), Sulphate and Total Suspended solids (TSS) data obtained for industrial effluents

As shown in Figure M1, Industry 3 (Textile industry) has the maximum COD value of 1218 ppm and the minimum was 36 ppm. About 80% of effluents exceed the discharge limit of CEA guidelines, requiring effective treatment. Sulphate ion concentrations are higher in Industry 9 and Industry 3 (both are textile industries) with 2250 ppm and 750 ppm. For most samples, TSS is very high, and Industry 1 (Metal finishing industry) and Industry 10 (Dye industry) being the highest. Only two industries show values within the acceptable discharge levels and all other industries obtained values beyond 50 ppm.

pH data of many industrial effluents were not in the neutral pH region [Figure M2(a)]. Acidic pH values were found in 30% industrial effluent samples and 30% of effluent samples were in the basic region. Therefore, pH is a main parameter to be considered in designing a treatment system. Conductivity is also an important on-sight parameter which was tested as measure of the total ions present in the effluent. As shown in Figure M2(b), effluent of Industry 5 had the highest conductivity.

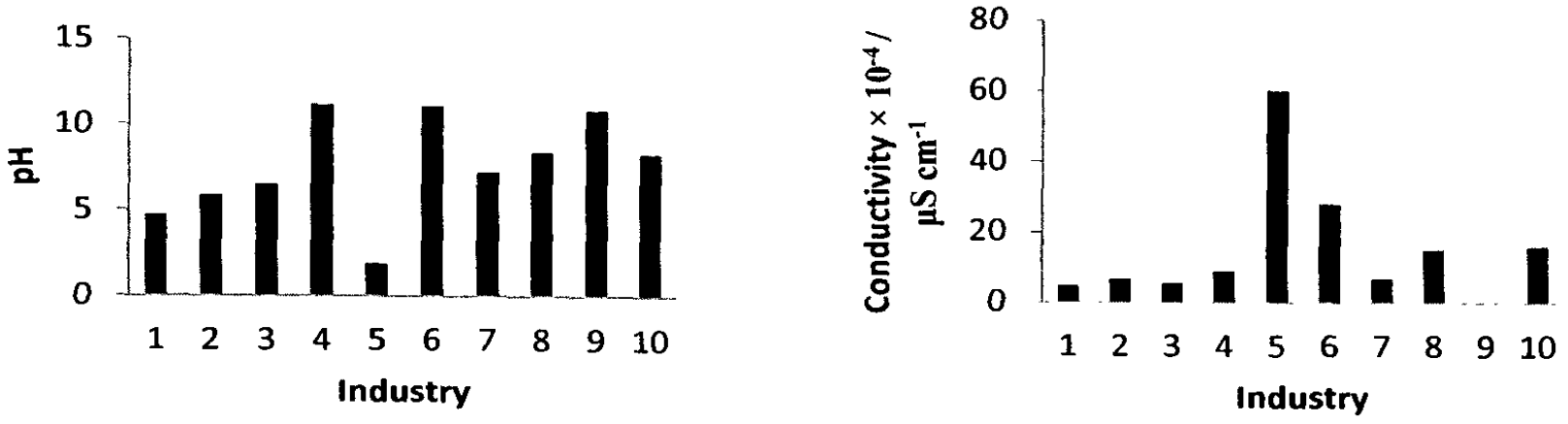

(a) (b)

Figure M2: pH and Concentration variation for untreated industrial effluents

Phospahte levels were then obtained using the Vanadomolybdate method, which were not much high when compared to with the other parameters (COD and Sulphate). As shown in Figure M3, all values were less than 14 ppm but discharge levels are lower than the data obtained.

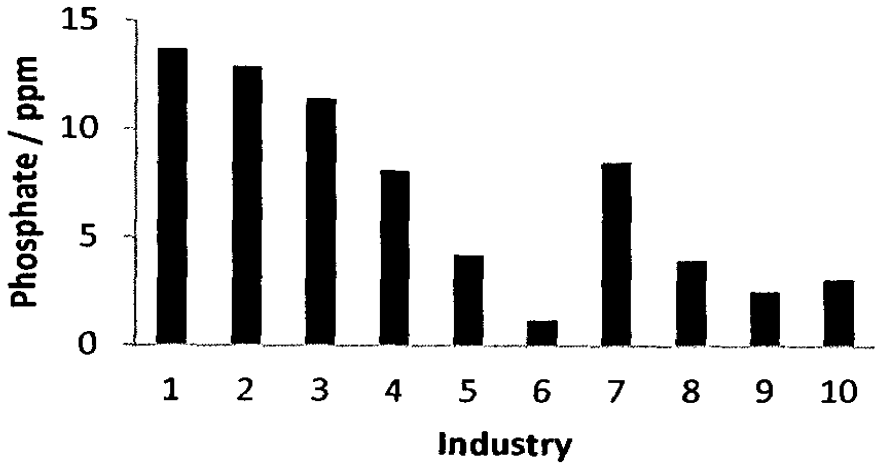

Figure M3: Phosphate data for industrial effluents

The main pollutant considered was heavy metals present in industrial effluents. Effluent samples collected from metal finishing industries contain Cu (MDL=1.0 ppm) and Zn (MDL=0.2 ppm). Other metals such as Cd, Cr, Pb and Ni were not present in any effluent (Figure M4).

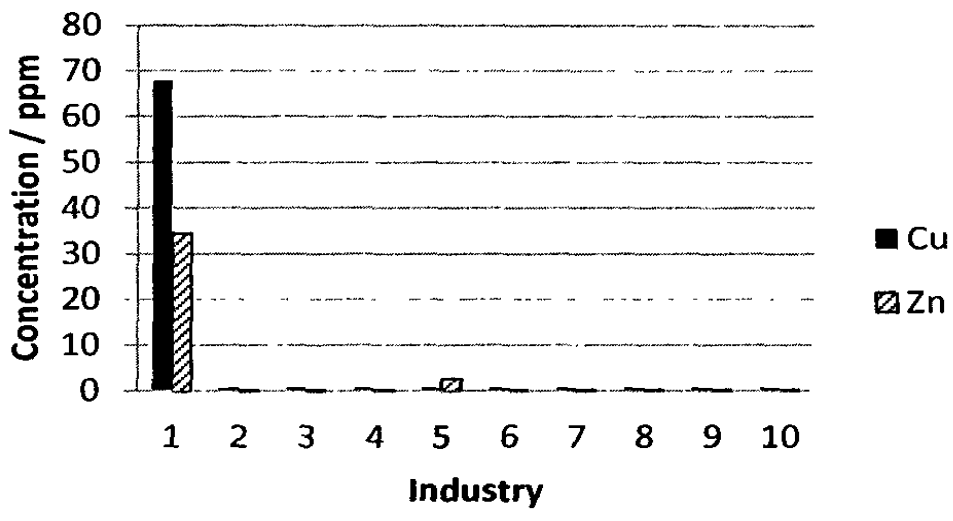

Figure M4: Cu and Zn concentration in industrial effluent samples

Zn and Cu levels of industry 1 are much larger than other samples, and industry 5 contain only about 4 ppm of Zn. All other samples had undetectable levels of heavy metals, which could not be detected using flame atomic absorption spectroscopy.

In order to get a comprehensive idea about the data, all samples analyzed were separated according to the type of industries. Accordingly, two samples were in metal finishing industry, three samples were in dye industry and five samples were in the category of textile industry.

From the data obtained (Table M3) for the category, effluents from metal finishing industries had the mean pH value was 3.31, which is in acidic region, and further, the conductivity of effluent samples lies between 4.8×10^{-4} $\mu S\ cm^{-1}$ and 60.0×10^{-4} $\mu S\ cm^{-1}$.

Table M3: Statistical summary of selected parameters for metal finishing industrial effluents

Variable	Mean	SE Mean	St Dev	Minimum	Median	Maximum
COD	459	423	598	36	459	882
pH	3.31	1.43	2.02	1.88	3.31	4.73
Conductivity $\times 10^{-4}$	32.4	27.6	39.0	4.8	32.4	60.0
Phosphate	8.95	4.74	6.71	4.21	8.95	13.70
Sulphate	68	57	81	11	68	125
Cu	34.2	33.5	47.4	0.7	34.2	67.7
Zn	18.6	15.9	22.5	2.7	18.6	34.5
TSS	707	703	994	4	707	1410

Note: All the parameters except pH and conductivity are reported in ppm and conductivity is reported in $\mu S\ cm^{-1}$.

Textile industries are the most common industries in Export Processing Zones. The results of chemical analysis of textile industries are summarized in Table M4. The COD values vary within 53 ppm to 1218 ppm with a mean value of 448 ppm, while the pH values were mostly in basic region for textile industrial effluents with a mean value of 8.31.

Table M4: Statistical summary of selected parameters for textile industrial effluents

Variable	Mean	SE Mean	St Dev	Minimum	Median	Maximum
COD	448	201	449	53	320	1218
pH	8.31	1.1	2.47	5.86	7.23	11.06
Conductivity $\times 10^{-4}$	9.43	4.81	10.75	0.06	6.7	28
Phosphate	7.33	2.34	5.23	1.22	8.54	12.89
Sulphate	719	399	891	10	454	2244
TSS	111.6	21.9	49	40	124	160

Note: All the parameters except pH and conductivity are reported in ppm and conductivity is reported in $\mu S\ cm^{-1}$.

For dye industrial effluents (Table M5), pH, conductivity and phosphate concentration values are closer to each other as compared to previous results of other industries, and consequently, their standard deviations were much less. The mean pH value was in the high

basic region, and conductivity values of textile and dye industrial effluents are lower as compared those of metal finishing industries.

Table M5: Statistical summary of selected parameters for dye industrial effluents

Variable	Mean	SE Mean	St Dev	Minimum	Median	Maximum
COD	403	28	48.6	356	400	453
pH	9.277	0.937	1.623	8.31	8.37	11.15
Conductivity $\times 10^{-4}$	13.3	2.22	3.84	8.9	15	16
Phosphate	5.08	1.55	2.68	3.11	3.99	8.13
Sulphate	302	79.8	138.1	144	362	400
TSS	335	120	208	120	348	536

Note: All the parameters except pH and conductivity are reported in ppm and conductivity is reported in $\mu S\ cm^{-1}$.

Spearman correlation coefficient was applied to textile and dye industrial effluent samples in order to check the correlation between variables. This was not applied to the metal finishing industry because it has only two samples. According to the Spearman correlation coefficient, used to identify variables which show significant correlation, all chemical variables in textile effluents have significant correlation except for pH and Phosphate which have p values less than 0.01 (Table M6). Similarly for dye effluent samples, there is a significant correlation except for conductivity and sulphate which have a p value less than 0.01 (Table M7).

Table M6: Spearman correlation coefficient applied to textile effluent samples.

	COD	pH	Conductivity $\times 10^{-4}$	Phosphate	Sulphate
pH	**-0.601**				
Conductivity $\times 10^{-4}$	**-0.133**	**0.41**			
Phosphate	**0.621**	-0.991	**-0.458**		
Sulphate	**-0.29**	**0.625**	**-0.414**	**-0.554**	
TSS	**0.553**	**-0.009**	**0.414**	**0.079**	**-0.119**

Note: Bold values represent $p > 0.01$

Table M7: Spearman correlation coefficient applied to dye effluent samples.

	COD	pH	Conductivity $\times 10^{-4}$	Phosphate	Sulphate
pH	**0.883**				
Conductivity $\times 10^{-4}$	**-0.825**	**-0.994**			
Phosphate	**0.805**	**0.989**	**-0.999**		
Sulphate	**-0.821**	**-0.993**	1	**-1**	
TSS	**0.502**	**0.037**	**0.075**	**-0.109**	**0.082**

Note: Bold values represent $p > 0.01$

Annexure 4.1

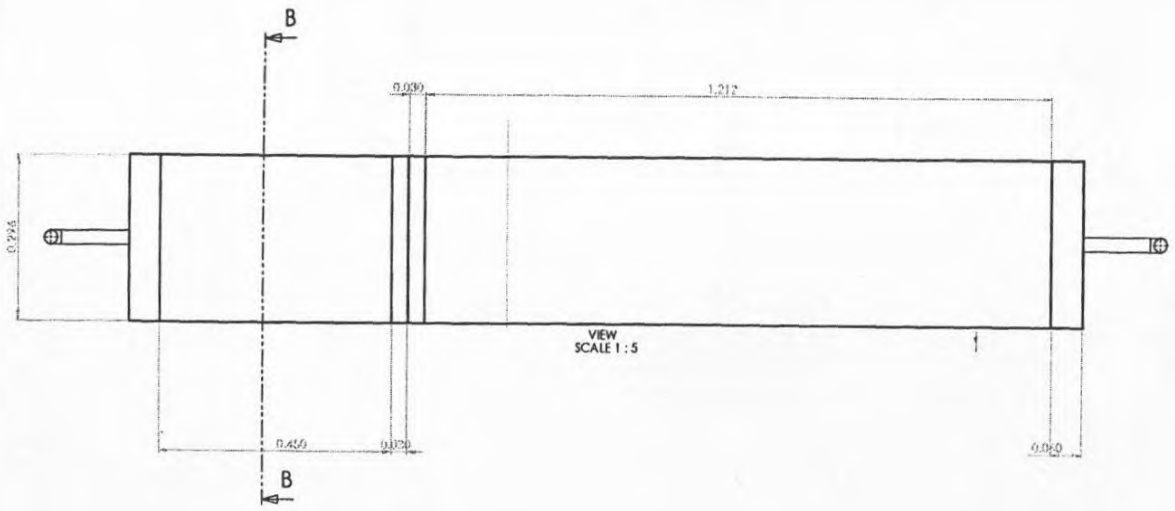

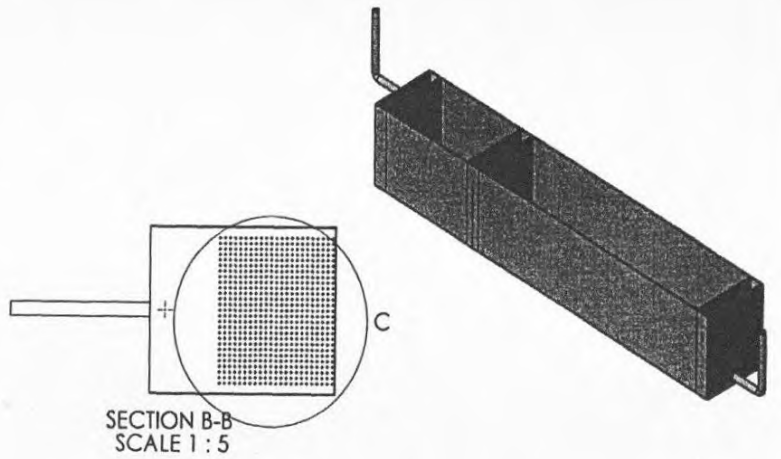

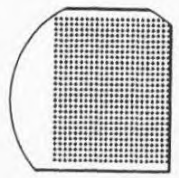

DETAIL C
SCALE 1 : 5

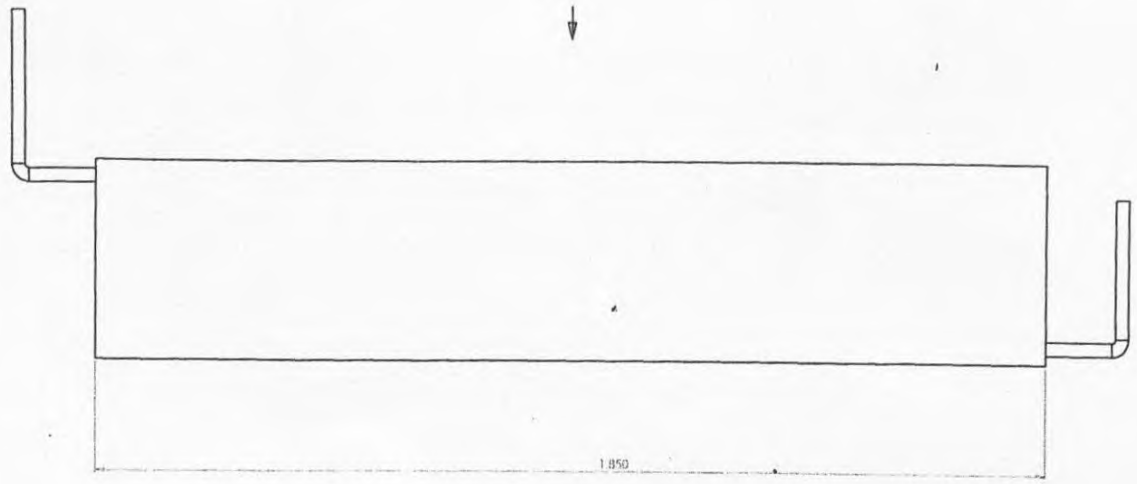

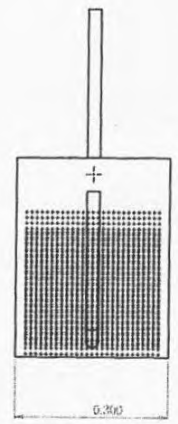

Thanuja Akki drawing new

120

Annexure 4.2

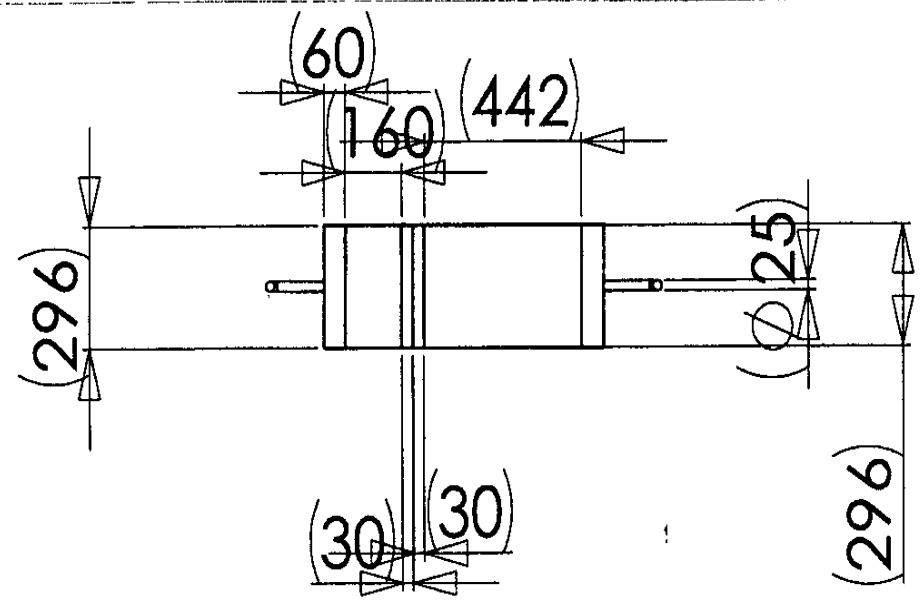

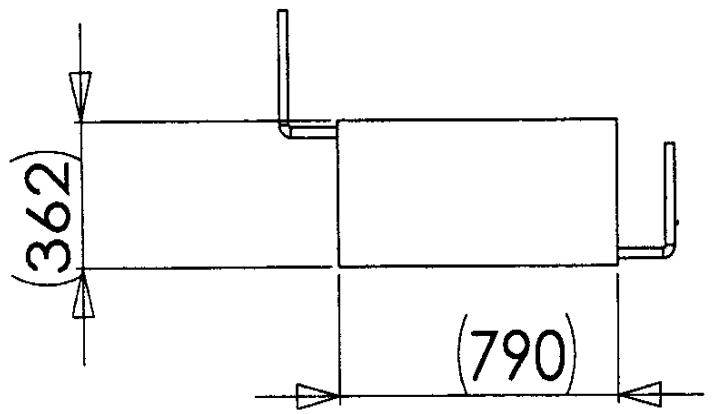

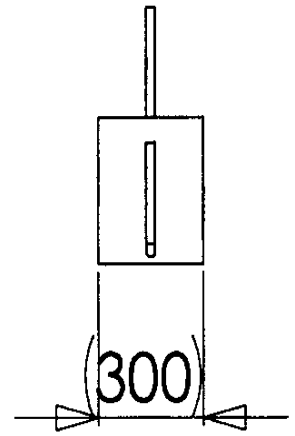

		DIMENSIONS ARE IN MM UNLESS OTHERWISE SPECIFIED		NAME	DATE
		FRACTIONAL ±	DRAWN		
		ANGULAR MACH ± BEND ±	CHECKED		
		TWO PLACE DECIMAL ±	ENG APPR.		
		THREE PLACE DECIMAL ±	MFG APPR.		
		MATERIAL —	Q.A.		
		FINISH —	COMMENTS		
NEXT ASSY	USED ON				
APPLICATION		DO NOT SCALE DRAWING			

PROPRIETARY AND CONFIDENTIAL

THE INFORMATION CONTAINED IN THIS DRAWING IS THE SOLE PROPERTY OF <INSERT COMPANY NAME HERE>. ANY REPRODUCTION IN PART OR AS A WHOLE WITHOUT THE WRITTEN PERMISSION OF <INSERT COMPANY NAME HERE> IS PROHIBITED.

<COMPANY NAME>

SIZE	DWG. NO.	REV
A		

SCALE: 1:5 WEIGHT: SHEET 1 OF 1

121

Zn TREATMENT SYSTEM FOR WIRE NAIL FABRICATION WORKSHOP - KUNDASALE

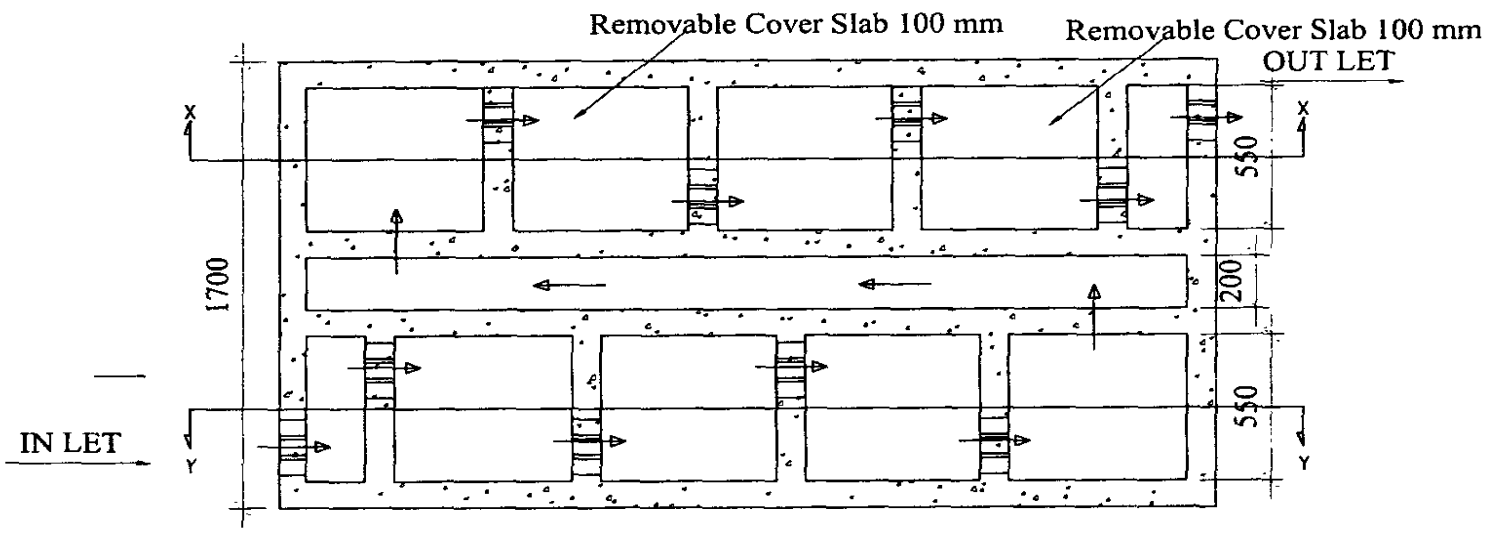

Zn TREATMENT SYSTEM

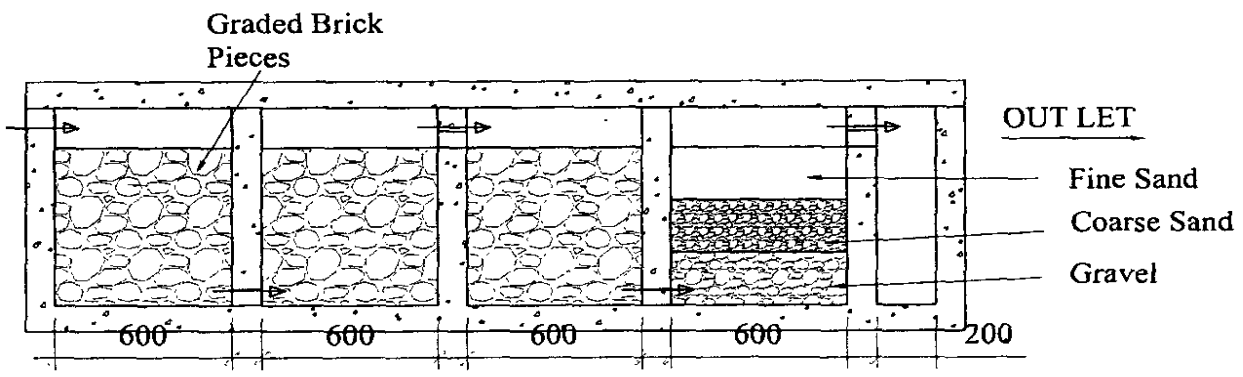

SECTION X-X

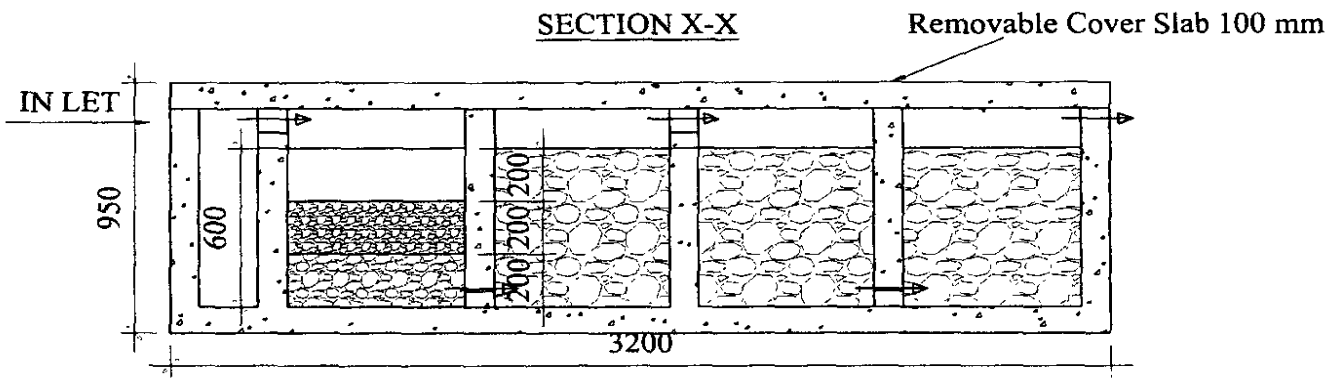

SECTION Y-Y

Annexure 5

Copies of Publications and Communications Arising from the Project

www.cafetinnova.org

Indexed in
Scopus Compendex and Geobase Elsevier, Chemical Abstract Services-USA, Geo-Ref Information Services-USA, List B of Scientific Journals, Poland, Directory of Research Journals

ISSN 0974-5904, Volume 06, No. 04 (01)

International Journal of Earth Sciences and Engineering

August 2013, P.P.807-811

Removal of Heavy Metal Ionsusing Rice Husk and Brick Clay as Adsorbents–Dynamic Conditions

A. NAVARATNE, N. PRIYANTHA AND T. P. K. KULASOORIYA
Department of Chemistry, University of Peradeniya, Peradeniya, Sri Lanka
Postgraduate Institute of Science, University of Peradeniya, Peradeniya, Sri Lanka
Email: *namal.priyantha@yahoo.com*

Abstract: In this study, effectiveness of thermally treated rice husk, brick clay and their combinations was investigated as sorbents for heavy metal ions under dynamic conditions. A mixture of cations consisting of Cd(II), Cr(III), Cu(II), Ni(II), Pb(II) and Zn(II), each at 10 ppm concentration, was tested on these two adsorbents by passing through a column (i.d. = 2.0 cm) packed up to 30 cm with the respective sorbent. The optimum firing temperatures of 100 °C for rice husk and 200 °C for brick clay were used in this investigation for maximum metal ion removal efficiency. After a 5 min interaction period of the cation mixture with the sorbent, effluent fractions were collected at 5 min intervals for the determination of remaining heavy metal ion concentrations. According to atomic absorption spectroscopic analysis of the eluent, the extent and the order of removal of metal ions by each sorbent/sorbent mixture depends on the interaction time. The relative ability of rice husk in removing heavy metals is in the order, Pb(II) > Cu(II) > Ni(II) ≈ Cd(II) > Cr(III) > Zn(II) and that of brick clay and layered types follows the order, Pb(II) ≥ Cr(III) ≥ Cu(II)≥ Cd(II) ≥ Zn(II) ≥ Ni(II), based on the average of ten elutions. Further, the efficiency of removal of metal ions is in the order of brick clay > rice husk-brick clay > brick clay-rice husk > rice husk.

Keywords*: Heavy metals, Rice husk, Brick clay, Adsorption, Dynamic conditions.*

I. Introduction:

Environmental pollution is an uncontrollable problem in the developing world. Increase in population and urbanization, which are important parameters of pollution, results in the expansion of industrialization, which has become the major reason for pollution. Industries usually produce large volumes of effluents, which may contain many environmental pollutants. Among them, heavy metal ions are one category of pollutants which are difficult to be completely removed from water. Heavy metal releasing industries include metal finishing, leather tanning, electroplating, battery and accumulatory, paint, and cement [1], [2].The contamination of heavy metals has adverse effects on soil, water, animal and human health [3].

To overcome these adverse effects, industries use heavy metal ion removal techniques, such as chemical precipitation, oxidation and reduction, ion exchange, reverse osmosis and adsorption [2]. Although most of these techniques are able to successfully remove heavy metal ions from waste water, chemicals are heavily usedin the removal process. Therefore, such methodologies would introduce another pollutants load to the environment [4].

It has been reported that burnt brick clay and saw dust have the ability for the removal of Cr, Mn, Co, Zn, Cd and Pb from industrial effluents and brick clay has shown the most efficient removal for Pb [5]. Ezinachi-okigwe natural clay has shown high adsorption capacitiesfor Cu(II) and Pb(II)under optimized conditions [6]. Further, sodium carbonate treated rice husk has been found to be an efficient medium for the removal of Cd(II) from waste water [7]. Moreover, rice husk and its ash have been successfully used as an adsorbent for the removal of Pb(II) from aqueous solution [8]. The study which was undertaken to investigate the adsorption of Pb, Cd, Cu and Zn on carbonized rice husk and activated rice husk has shown successful removal of these metal ions from the solution [9].

In this research, we report the use of rice husk and brick clay as adsorbents for removal of heavy metals. Both adsorbent materials are naturally available and hence it is a low cost method to remove heavy metals. Dynamic experiments were conducted using columns filled with adsorbents for the removal of heavy metals, namely, Cd(II), Cr(III), Cu(II), Ni(II), Pb(II) and Zn(II) and to characterize adsorption isotherms, order of the adsorption reaction, etc. Systematic studies of the dynamic studies could ultimately lead to the

construction of industrial effluent treatment schemes for industries having heavy metal containing effluents.

II. Materials and Methods:

A. Materials:

Standard solutions of Cr(III), Cd(II), Cu(II), Zn(II), Ni(II) and Pb(II) were prepared using corresponding sulfates or nitrates of analytical grade. All the experiments were conducted under dynamic conditions using mixtures of cations. Raw clay used to make bricks (brick clay) was obtained from a kiln in Gelioya, Sri Lanka and representative samples were fired up to 200 °C for the maximum absorbance of cations according to previous findings [4]. Rice husk samples were obtained from a rice mill in Kandy, Sri Lanka and they were fired up to 100 °C as it was the optimum temperature for the removal of cations. Fired brick clay samples were separated into appropriate sizes and all dynamic experiments were conducted with particles of average diameter (d) ~ 0.5 cm while fired rice husk samples were used in its natural size. Columns used for all experiments were of 2 cm diameter.

B. Instrumentation:

Samples of brick clay and rice husk were fired using Carbolite CTF 12/100/900tube furnace while Spectro-electronic M series atomic absorption spectrophotometer (AAS) was used to measure the total metal ion concentration of solutions.

C. Research design:

As both brick clay and rice husk were natural substances having variable composition, representative samples of rice husk were prepared by mixing large portions of its samples, while samples of brick clay were obtained by crushing many pieces followed by firing at a pre-determined temperature for 4 h and natural cooling down to room temperature.

Columns were packed with rice husk alone and brick clay alone is shown in Fig.1 (a) and Fig.1 (b), respectively. Layered type packings were prepared using rice husk on bottom and brick clay on top as shown in Fig. 1(c), and vice versa. The length of packing in each column was 30 cm, and layered columns had 15 cm of each type of packings. Adsorbate was prepared by mixing all cation solutions such that the concentration of each cation after mixing was 10 ppm. Each solution mixture was passed through the column and allowed a 5 min residence time within the column. Eluent samples were then collected at every 5 min interval.

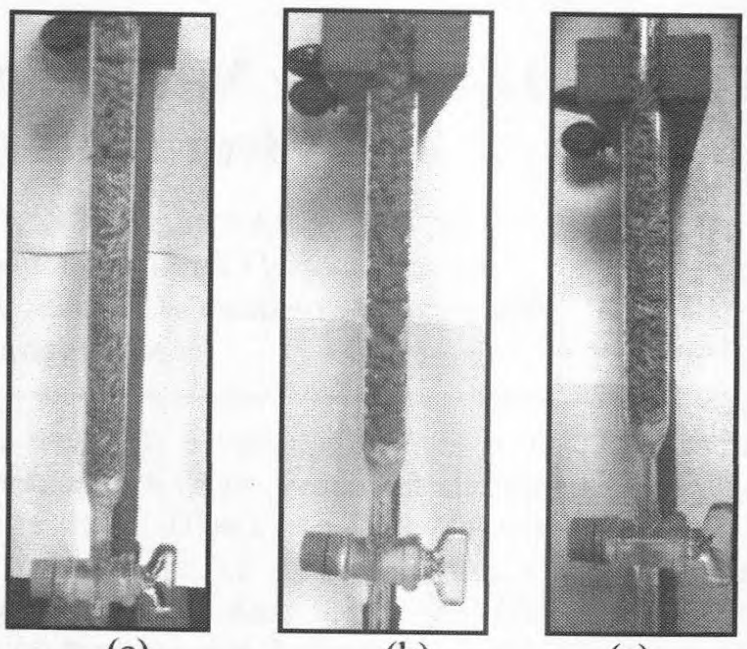

(a) (b) (c)

Fig1: Columns packed with adsorbents (a) Rice husk alone (b) brick clay alone and (c) rice husk on bottom and brick clay on top (layered column)

The extent removal of a metal ion by packed columns in each experiment was determined as the percentage removal using the following relationship,

$$\textbf{Percentage removal} = \frac{C_i - C_f}{C_i} \times 100\%$$

Where C_i is the initial concentration of the metal ion and C_f is the total concentration of the metal ion present in eluents collected from columns.

III. Results and Discussion:

A. Removal of metal ions present in a mixture of solution using brick clay and rice husk:

Experiments conducted by passing solutions of heavy metal ions through columns packed with rice husk, brick clay, and layered type combined adsorbents show that the maximum removal is obtained with columns packed with brick clay alone. In dynamic experiments, 13 representative samples were taken within 5 min apart when metal ion solutions were eluted from the column at a constant flow rate of 50 mL/min. Subsequently, the concentration of each metal ion was determined, and the variation between the concentration and the time of sampling was investigated. Fig 2 illustrates this variation for brick clay packed columns. Although the extent of removal, determined as the percentage removal, did not decrease within 60 min indicating the long-term efficiency of the column, it was clogged due to the wetting of the brick clay fired at a temperature of 200 °C. To overcome this issue, a column packed with rice husk, another adsorbent, was attempted.

Fig.3 shows that the extent of removal of all heavy metal ions investigated by rice husk packed columns is decreased with time in contrast to the constant

efficiency of brick clay packed columns. However, Pb(II) and Cu(II) show much higher removal ability as compared to Cd(II), Cr(III), Zn(II) and Ni(II). Although the removal ability of rice husk packed columns is much lower, the column does not get clogged as with brick clay. The efficiency of brick clay and the non-clogging behavior of rice husk can thus be used complimentary to each other using both adsorbents simultaneously.

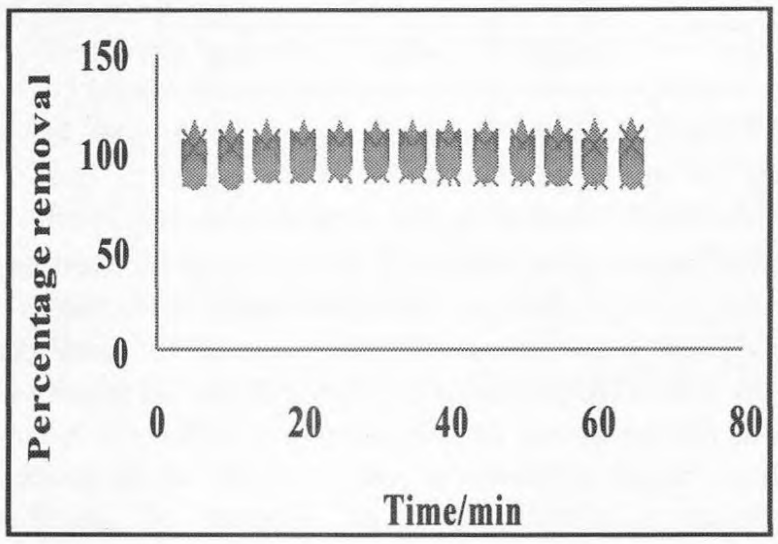

Fig2: *Extent of removal of heavy metal ions by columns packed with brick clay fired at 200 °C: Cu(II) (◆), Cd(II) (■), Cr(III) (▲), Pb(II) (×), Zn(II) (✳) and Ni(II) (●).*

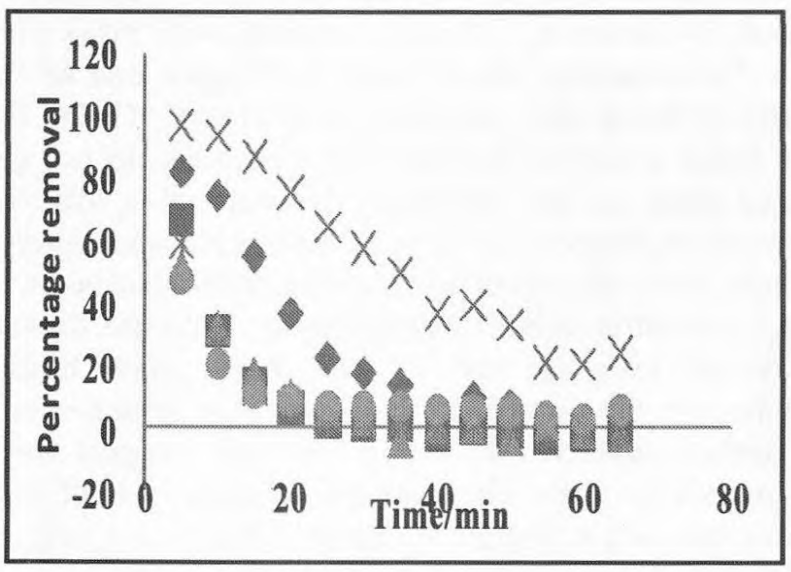

Fig3: *Extent of removal of heavy metal ions by columns packed with rice husk fired at 100 °C:Cu(II) (◆), Cd(II) (■), Cr(III) (▲), Pb(II) (×), Zn(II) (✳) and Ni(II) (●).*

Fig.4 and Fig.5 show the effect of layered type packed columns of brick clay fired at 200 °C and rice husk fired at 100 °C. Brick clay-rice husk column, where rice husk is packed on top of brick clay is better than the columns packed with rice husk alone.

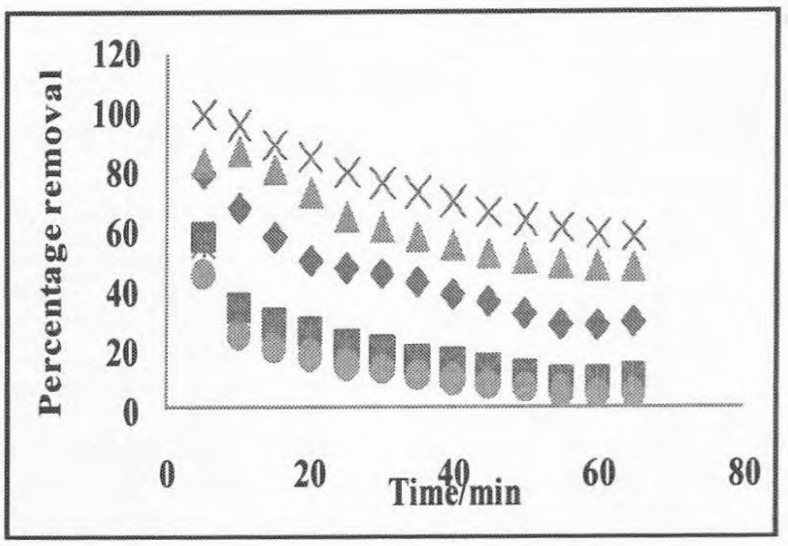

Fig4: *Extent of removal of heavy metal ions by columns packed with brick clay (bottom)-rice husk (top): Cu(II) (◆), Cd(II) (■), Cr(III) (▲), Pb(II) (×), Zn(II) (✳) and Ni(II) (●).*

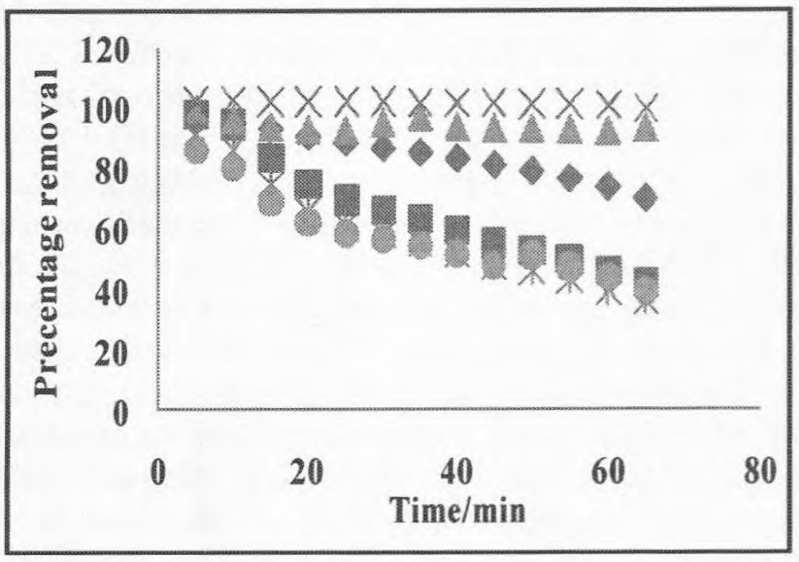

Fig5: *Extent of removal of heavy metal ions by column packed with Rice husk (bottom)-Brick clay (top): Cu(II) (◆), Cd(II) (■), Cr(III) (▲), Pb(II) (×), Zn(II) (✳) and Ni(II) (●).*

The rice husk-brick clay layered column, whose results are shown in Fig. 5, is superior to the brick clay-rice husk column in terms of both efficiency and stability, for all the metal ions investigated. The extent of removal of Pb(II) and Cr(III) by this column is steady at almost 100% even after one hour elution. Further, the clogging behavior encountered for brick clay only packed columns was not observed in any of the layered type columns. Further, from these results, it is clearly shown that, the efficiency of the column strongly depends on the order of packings. It is suggested that the adsorbent of higher efficiency of removal should be packed on top so that the extent of interaction is better.

B. Order of the removal ability of heavy metals:

Percentage removal values of first 10 samples collected from the eluent were averaged to investigate the order of the removal ability of the cations under investigation. Table I shows the results for all cations in every arrangement of adsorbents in columns.

Table I: *Average Percentage Removal Values for each Column Packing*

	Cu(II)	Cd(II)	Cr(III)	Pb(II)	Zn(II)	Ni(II)
Rice husk	32	13	12	64	11	13
Brick clay	≈100	≈100	≈100	≈100	94	94
Rice husk-brick clay	88	72	95	≈100	64	62
Brick clay-rice husk	49	24	66	79	23	17

According to the results shown in Table I, Pb(II) is the most easily removable metal ion from all types of arrangements. Brick clay shows almost 100% removal ability for Cu(II), Cd(II), Cr(III) and Pb(II), while rice husk-brick clay column shows almost 100% removal ability for Pb(II) only. The order of the removal ability by rice husk is determined to be Pb(II) > Cu(II) > Ni(II) ≈ Cd(II) > Cr(III) > Zn(II). Brick clay alone and both types of layered columns show similar order of removal, Pb(II) ≥ Cr(III) ≥ Cu(II) ≥ Cd(II) ≥ Zn(II) ≥ Ni(II). On the other hand, the efficiency of removal of metal ions is in the order of brick clay > rice husk-brick clay > brick clay-rice husk > rice husk. The highest removal ability of Pb(II) for all arrangements can be explained using the relative mobility, charge and hydrated radius of the metal ions. Relative mobility is decreased in the order of Pb(II) > Cu(II) > Cd(II) > Zn(II) > Ni(II) and the hydrated radius varies in the order of Cu(II) > Cd(II) > Pb(II) [10]. Since Pb(II) has lowest hydrated radius among these cations, it easily diffuses into the adsorbent media and its highest relative mobility promotes the fast diffusion in solution.

C. Comparison Of Static And Dynamic Conditions:

Rice husk was used to compare the removal ability of cations present in mixtures of solutions in both static and dynamic conditions.

TableII: *Average Percentage Removal Values for Dynamic and Static Conditions*

Metal ion	Average percentage removal (%)	
	Dynamic	Static
Cd(II)	13	71
Cu(II)	32	80
Zn(II)	11	66
Cr(III)	12	82
Ni(II)	13	53
Pb(II)	64	≈100

According to Table II, static conditions are very successful in removing metal ions as compared to dynamic conditions. This is due to the longer time period of interaction receiving the treatment under static conditions. Nevertheless, there are many advantages of using dynamic conditions for the removal of metal ions, such as cost effectiveness and possibility of expansion towards the treatment of real industrial effluents in large volumes. Small processing time for the whole process, less space required and small amount of adsorbent required are additional advantages. Many of these advantages lead to save energy.

IV. Conclusions:

The maximum removal of metal ions from a mixture of solution is shown by columns packed with brick clay alone. Nevertheless, the column is clogged due to the wetting of brick clay particles fired at 200 °C. On the other hand, columns packed with rice husk do not get clogged although the efficiency of removal is low. To overcome undesirable effects of these columns, layered columns were attempted by packing both adsorbents in the same column in both arrangements. Columns packed with brick clay on top of rice husk show higher percentage removal ability than the other arrangement, and further, layered columns do not get clogged for a long period of time. The removal of heavy metal ions follows the order, Pb(II) > Cu(II) > Ni(II) ≈ Cd(II) > Cr(III) > Zn(II) for columns packed with rice husk alone and Pb(II) ≥ Cr(III) ≥ Cu(II) ≥ Cd(II) ≥ Zn(II) ≥ Ni(II) for columns packed with brick clay alone and layered type columns. The efficiency of removal of metal ions is in the order, brick clay > rice husk-brick clay > brick clay-rice husk > rice husk. Further, static conditions are found to be more effective. Nevertheless, dynamic conditions are associated withmany advantages,and have the potential for expansion for real effluent treatment.

Acknowledgment:

Financial support through research grant by the National Science Foundation (RG/2012/BS/05) is greatly appreciated.

References:

[1] J. O. Nriagu, "A history of globle metal pollution", Science, New series, No. 5259, vol. 272, pp. 223-224, 1996.

[2] W. Saikaew and P. Kaewsarn, "Cadmium ion removal using biosorbents derived from fruit peel wastes", Songklanakarin J. Sci. Technol, vol. 31(5), pp. 547-554, 2009.

[3] G.H. Pino, L.M.S.D. Mesquita, M.L. Torem and G.A.S. Pinto, "Biosorption of cadmium by green coconut shell powder", Miner. Eng., vol.19, pp. 380-387, 2006.

[4] "Control and Treatment Technology for the Metal Finishing Industry– Sulfide Precipitation", US EPA 625/8-80-003, 1980.

[5] N. Priyantha, D. T. B. Tennakoon, S. Keerthiratne and T. Abeysinghe, "Removal of heavy metal ions from polluted water using environmentally-friendly materials", [online]. Available: http://tinyurl.com/pg8sdnf

[6] V.O. Njoku, E. E. Oguaie, C. Obi, O. S. Bello and A. A. Ayuk, "Adsorption of copper(II) and lead(II) from aqueous solutions on to a nigerial natural clay", Aus.J.Basic Appl.Sci., vol 5, pp. 346-353, 2011.

[7] U. Kumar, M. Bandyopadhyay, "Fixed bed column study for Cd(II) removal from wastewater using treated rice husk", J. Hazard. Mater.,vol 129, pp. 253-259, 2005.

[8] A. G. El-said, "Biosorption of Pb(II) ions from aqueous solution on to rice husk and its ash" J. Am. Sci., vol. 6(10), pp. 143-150, 2010.

[9] I. Nhapi, N. Banadda, R. Murenzi, C. B. Sekomo and U. G. Wali, "Removal of heavy metals from industrial wastewater using rice husks" The Open Env. Eng. J., vol. 4, pp. 170-180, 2011.

[10] YanLiang-HSAB-SSA2011poster.pdf, [Online]. Available: http://img.docstoccdn.com/thumb/orig/111069073.png.

www.cafetinnova.org

Indexed in
Scopus Compendex and Geobase Elsevier, Chemical Abstract Services-USA, Geo-Ref Information Services-USA, List B of Scientific Journals, Poland, Directory of Research Journals

ISSN 0974-5904, Volume 08, No. 02

International Journal of Earth Sciences and Engineering

April 2015, P.P.346-352

Adsorption of Heavy Metal Ions on Rice Husk: Isotherm Modeling and Error Analysis

N PRIYANTHA, A N NAVARATNE AND T P K KULASOORIYA
Department of Chemistry, Postgraduate Institute of Science, University of Peradeniya, Peradeniya, Sri Lanka
Email: *namal.priyantha@yahoo.com, namalpriyantha@pdn.ac.lk*

Abstract: Rice husk, a readily available industrial waste, offers strong adsorption characteristics for heavy metal ions, namely, Cd(II), Cr(III), Cu(II), Pb(II), Ni(II) and Zn(II), which are present in effluents of metal finishing industries. Presence of these heavy metals would pose environmental and human threat owing to their highly toxic nature. Adsorption studies conducted using individual metal ion solutions by varying one experimental parameter at a time, while keeping others unchanged, lead to optimum values of 10 min shaking time, 10 min settling time, 4.0-5.0 solution pH and 100 °C firing temperature. Surface titrations carried out suggest variations of the surface charge with solution pH, while thermogravimetric analysis shows the increase in thermal energy after a firing temperature of 100 °C as a result of combustion of organic constituents present in rice husk. Among the six adsorption isotherms investigated; Langmuir, Freundlich, Temkin, Dubnin-Redushkevich, Redlich-Peterson and Sips; the Langmuir isotherm fits the best with a regression coefficient close to unity together with small errors.

Keywords: *Rice husk, Heavy metal ions, Adsorption isotherms, Static conditions.*

1. Introduction

Industrial expansion is a requirement to fulfill the demand of ever increasing population. Many industries, such as metal finishing, leather tanning, synthetic dye production, mining and metallurgy, electroplating, paint and photography, release considerable amounts of heavy metal ions to the surrounding through their effluents. Treatment of industrial effluents has thus become a necessity to safeguard the ecosystem [1, 2].

Biosorption, among many treatment methods in practice, is one of the best methods to remove heavy metals from effluents released from industries. To minimize the risk of using synthetic chemicals to treat waste water, environmentally friendly substances are nowadays introduced. Natural substances, such as agricultural waste, brick clay, fruit peel waste, tea leaf, saw dust and peat have been used to remove heavy metal ions from wastewater [3-7]. Phosphoric acid modified rice husk was also reported as an effective adsorbent to remove Zn(II) from solution [8].

The study reported is on rice husk, a readily available waste material in Sri Lanka. Much of the husk produced from processing of rice is either burnt or dumped as waste. On the other hand, rice husk is used as a raw material for production of organic substances, such as xylitol, furfural, ethanol and acetic acid, and used as a cleaning or polishing agent in metal/machine industry [9]. Use of rice husk as an adsorbent is a main advantage for remediation of environmental pollution problems. For such investigation, the study of adsorption isotherms is much important because it leads to equilibrium concentrations of adsorbate after completion of adsorption. Further, they provide information to determine process parameters which lead to maximum extent of adsorption. The shape of isotherm curves also predicts the type of adsorption. Among many adsorption isotherms available, Langmuir, Freundlich, Temkin, Dubinin-Raduskevich, Redlich-Peterson and Sips are of significance for characterization of adsorbent-adsorbate interactions with regard to environmental pollution.

The main objective of this study is to investigate the removal efficiency of Cd(II), Cr(III), Cu(II), Ni(II), Pb(II) and Zn(II) from aqueous solution using heat-treated rice husk. Effect of firing temperature, shaking time, settling time and solution pH on the extent of metal ion removal was studied to determine the optimum conditions, which were subsequently used for isotherm studies.

2. Materials and Methods

2.1. Materials

Standard solutions of Cd(II), Cr(III), Cu(II), Ni(II), Pb(II) and Zn(II) were prepared using $Cd(NO_3)_2$, $Cr(NO_3)_3$, $CuSO_4$, $NiSO_4$, $Pb(NO_3)_2$ and $ZnSO_4$, respectively. All the experiments were conducted under static conditions using individual metal ion solutions. Rice husk samples were obtained from a rice mill in the

District of Kandy, Sri Lanka. They were thoroughly rinsed with water and used in its natural form.

2.2. Instrumentation

Samples of rice husk were fired using Carbolite CTF 12/100/900 tube furnace, while spectro-electronic M series atomic absorption spectrophotometer (AAS) was used to measure the total metal concentration of all solutions. Mass changes of rice husk and heat flow at different firing temperatures were studied using thermal gravimetric analyzer (TGA) (Model STA-N-650).

2.3. Research Design

2.3.1. Effect of firing temperature

Rice husk is a natural substance having a variable composition. Therefore, representative samples of rice husk were prepared by mixing large portions of its samples, and fired at predetermined temperatures for 4.0 h followed by cooling down to room temperature through natural convection. All experiments were performed under static conditions using metal ion solutions of 10.0 ppm. In each experiment, 50.0 mL of each metal ion solution was shaken with 2.50 g of rice husk, fired at various temperatures, the system was allowed to reach equilibrium and the extent of removal of metal ion by rice husk was determined as a percentage removal using the relationship,

$$\text{Percentage removal} = \frac{C_i - C_f}{C_i} \times 100\% \qquad (1)$$

Where C_i is the initial concentration of metal ion and C_f is the final concentration of metal ion after treatment with rice husk. All experiments were conducted at a rotation speed of 150 rpm.

2.3.2. Effect of contact time

The effect of contact time on adsorption was observed by varying shaking time and settling time, separately by keeping all other variables constant, and determining the percentage removal.

2.3.3. Effect of pH

Heavy metal ion solutions of 10.0 ppm having pH ranging from 2-10 were prepared using HNO_3 and NaOH solutions. Solutions of higher pH were not prepared as precipitation problems were encountered for certain metal ion solutions. Each solution was then treated with rice husk for optimum shaking and settling time periods, and the extent of removal was determined using Equation (1).

2.3.4. Adsorption isotherms

The amount of heavy metal ions adsorbed on rice husk fired at the optimized firing temperature of 100 °C for previously optimized contact time was studied using solutions of concentration varying from 2-1000 ppm. After each solution was filtered, atomic absorption measurements were recorded. These data were fitted to different adsorption isotherm models, namely Langmuir, Freundlich, Temkin, Dubinin-Raduskevich, Redlich-Peterson and Sips [10].

3. Results and Discussion

3.1. Effect of Firing Temperature on Removal of Heavy Metal ions from Aqueous Solutions

Figure 1 shows the percentage removal of heavy metal ions determined using pre-fired rice husk with different metal ion solutions.

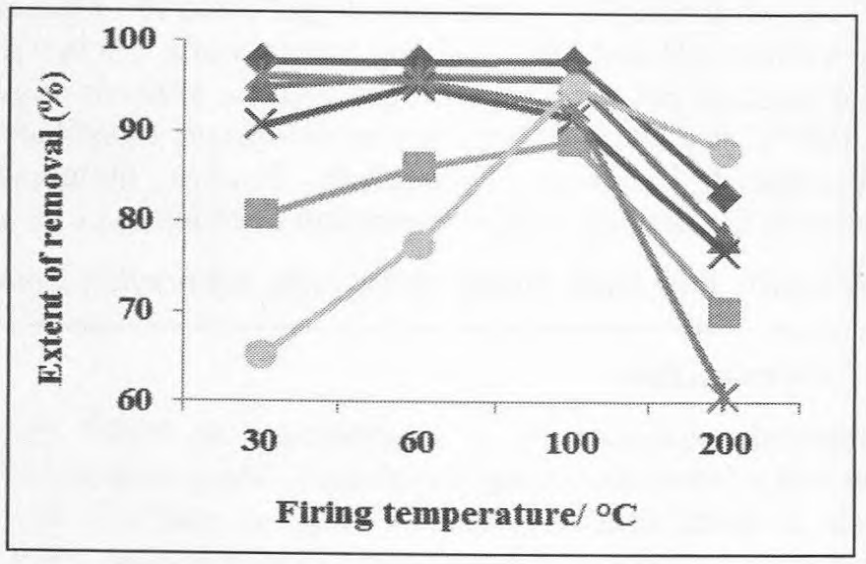

Figure 1*.Extent of removal of heavy metal ions by rice husk fired at different temperatures: Cd(II) (◆), Cu(II) (■), Zn(II) (▲), Cr(III) (×), Ni(II) (✳) and Pb(II) (●). [2.50 g rice husk,50.0 cm³ 10.0 ppm metal ion solution, 60 min shaking, 60 min settling]*

The extent of removal of Cd(II), Zn(II), Cu(II) and Pb(II) is increased with firing temperature up to 100 °C and then decreased up to 200 °C. However the extent of removal of Cr(III) and Ni(II) remains constant up to 100 °C, followed by a decrease by rice husk fired at higher temperatures. Therefore, 100 °C can be taken as the optimum firing temperature of rice husk for the removal of all metal ions investigated.

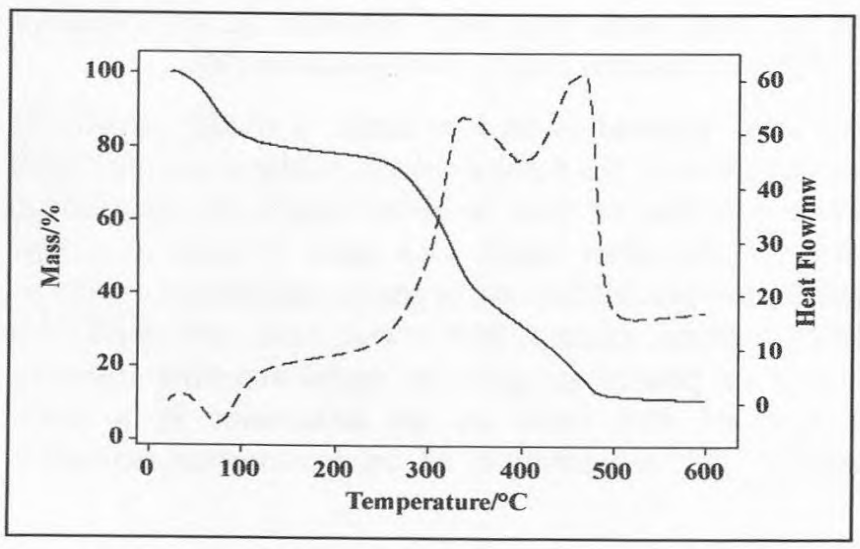

Figure 2.*Variation of mass of rice husk (—) and heat flow (----) when firing at different temperatures*

Variations of mass reduction and heat flow during the firing process are shown in Figure 2, which indicates a significant decrease in mass reduction, beyond the firing temperature of 100 °C, probably due to the combustion of organic matter. The exothermic nature of combustion is evident by observing positive energy release values at firing temperatures beyond 100 °C.

3.2. Surface Titrations

The surface charge of the bio-sorbent was determined to be highly dependent on the pH of the medium as clearly observed from the plots of the surface charge versus pH of the medium for different ionic strengths (Figure 3). $NaNO_3$ is commonly used for surface titrations because its constituent ions do not specifically bind to the bio-sorbent surface. Hence it is assumed that no ion other than protons in the medium binds to the bio-sorbent during surface titrations [11].

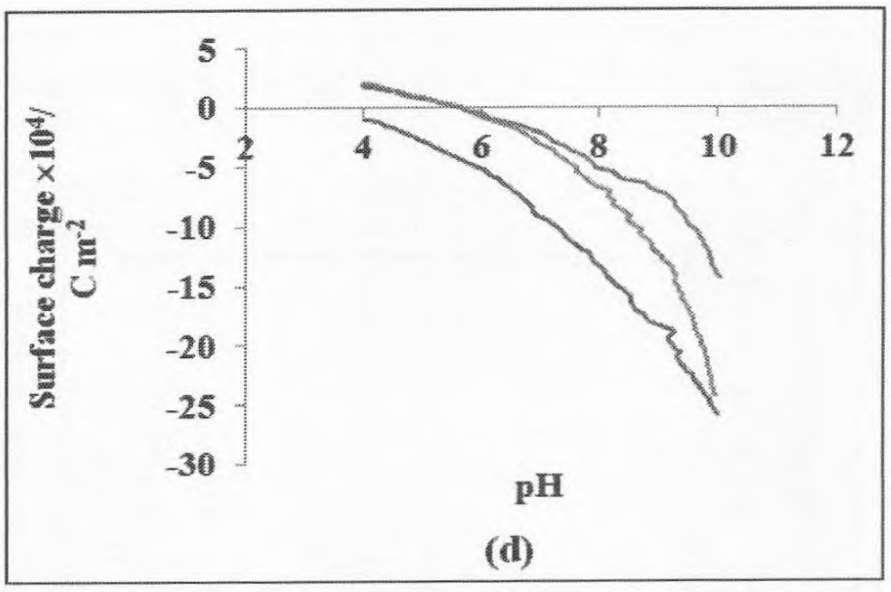

Figure 3.Surface titration curves of rice husk suspensions, plotted as variation of surface charge with pH controlled by different additions of NaOH for rice husk fired at different temperatures. (a) unfired (b) heated in to 60 °C (c) heated in to 100 °C (d) heated in to 200°C. Ionic strengths are 0.1 M (——), 0.01 M (——) and 0.001 M (——)

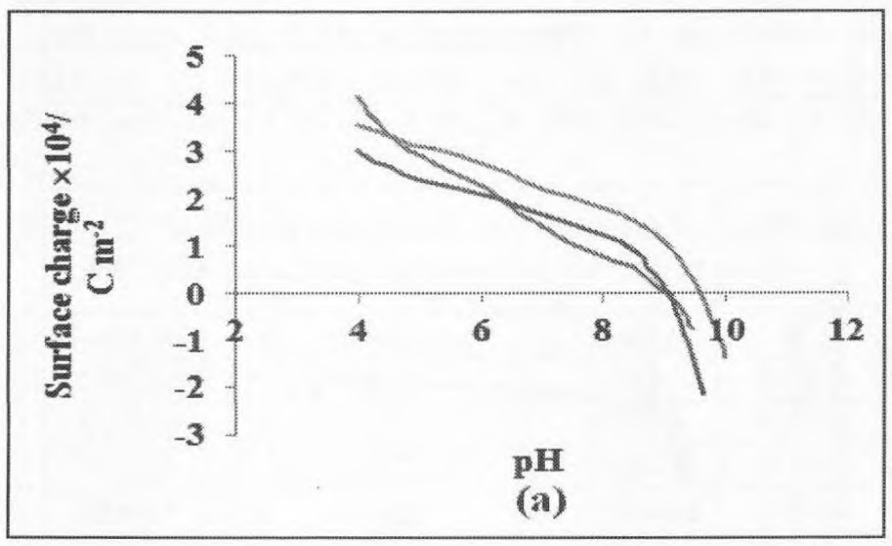

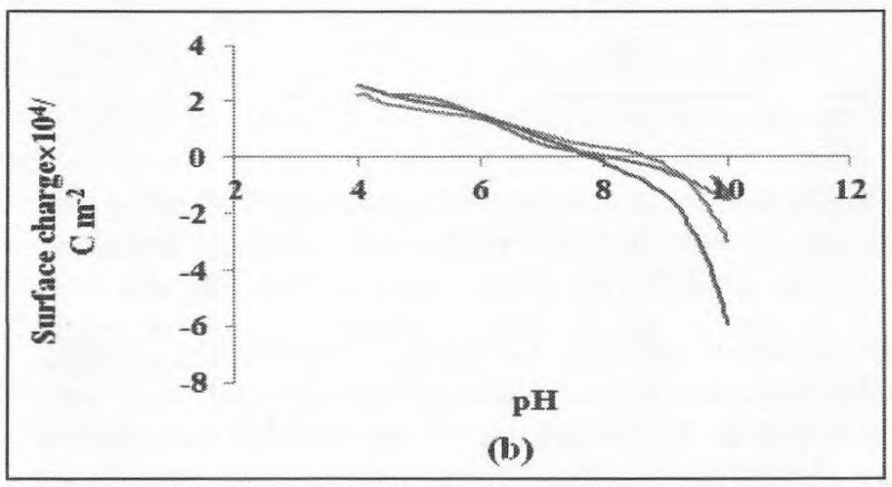

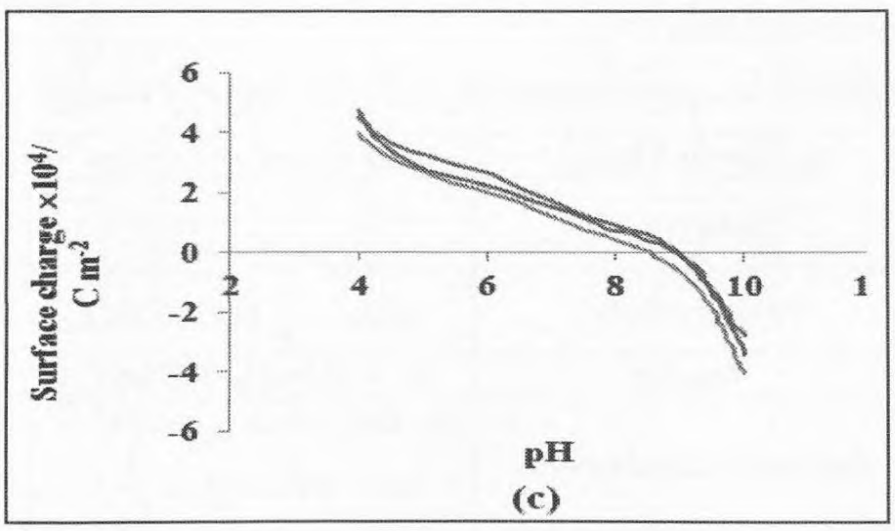

For all rice husk samples, the curves obtained at three ionic strengths do not intersect at a common point, and the curves obtained for 0.1 M and 0.01 M ionic strengths are almost parallel to each other indicating that the pH independent surface charge of rice husk is more predominant compared to the pH dependent charge [12]. The point of zero charge can however be estimated by considering two curves obtained for two lower concentrations at pH of 4.6, 6.0, 4.0 and 5.2 for unfired, 60 °C, 100 °C and 200 °C, respectively.

3.3. Optimization of contact time

The relationship between the extents of removal of heavy metal ions with contact time, as shown in Figure 4, indicates that the rice husk-metal ion solution system reaches equilibrium quickly. For both Cd(II) and Ni(II), percentage removal reaches the maximum and retains at the maximum after 10 min shaking time. Therefore, it is a reasonable assumption that the optimum shaking time for all metal ions used in this study, to be taken as 10 min.

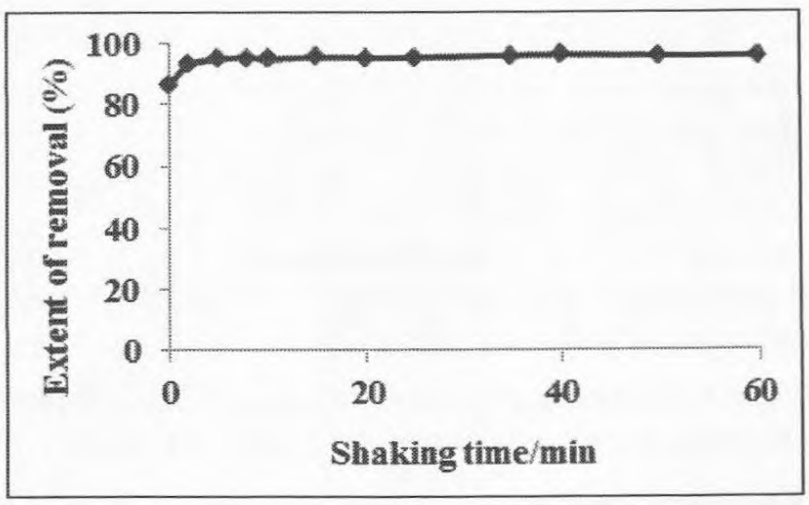

(a)

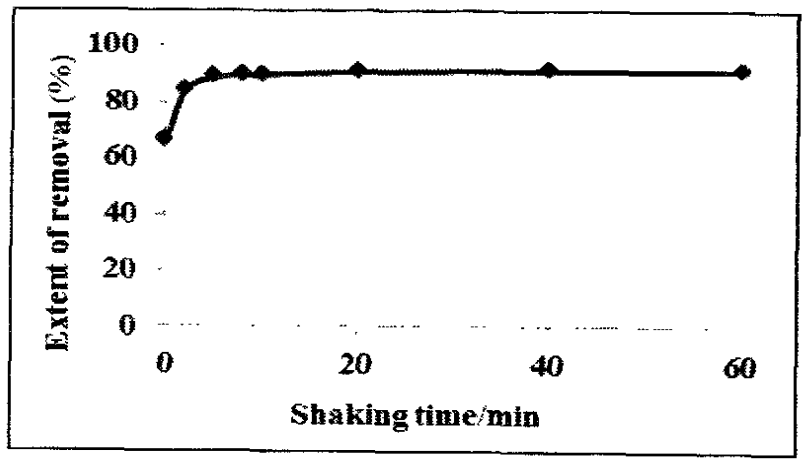

(b)

***Figure 4**. Variation of extent of removal with shaking time for heavy metal ions: (a) Cd(II) (b) Ni(II)*

Further, there is no change in the extent of removal of Cd(II) and Ni(II) with the settling time as observed in Figure 5. However, a time period of 10 min was selected as the optimum settling time to assure that the establishment of equilibrium is complete.

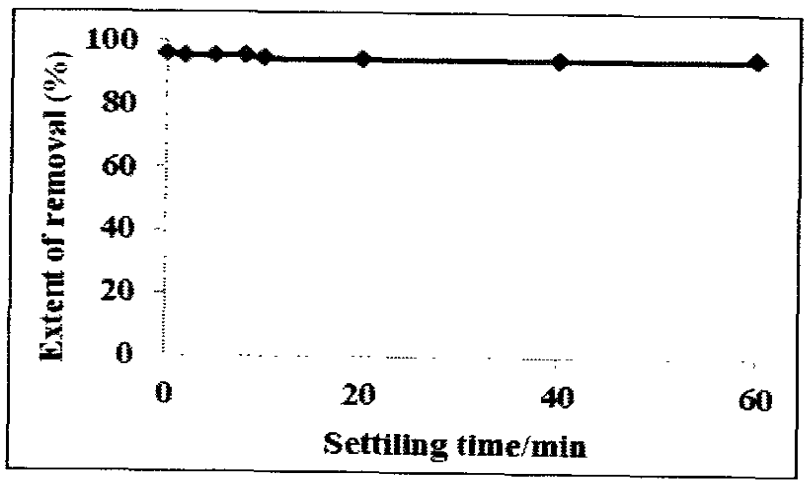

(a)

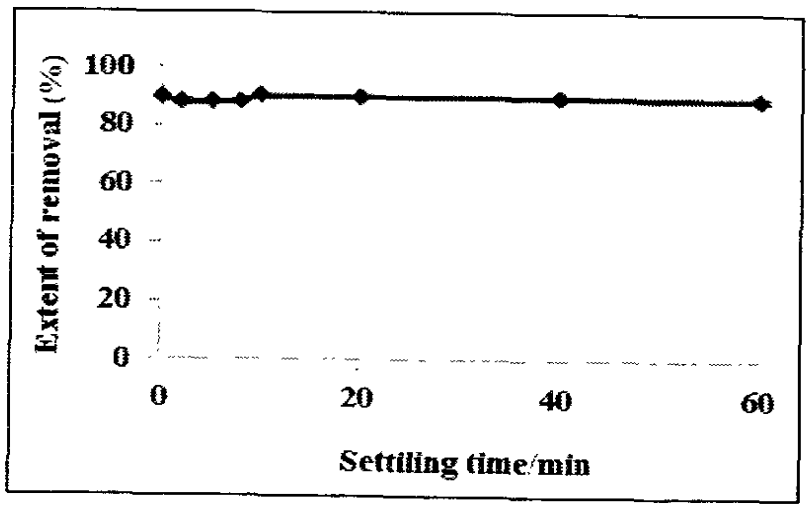

(b)

***Figure 5**. Variation of extent of removal with settling time for heavy metal ions: (a) Cd(II) (b) Ni(II)*

3.4. Isotherm Studies

The amount adsorbed plotted against the initial concentration provides clear indication that the adsorption of all metal ions investigated qualify Type I isotherm according to IUPAC isotherm classification (Figure 6) [13]. This overall behavior suggests that rice husk shows microporous characteristics for adsorption of these metals. However the extent of removal depends on the type of the metal ion [13, 14].

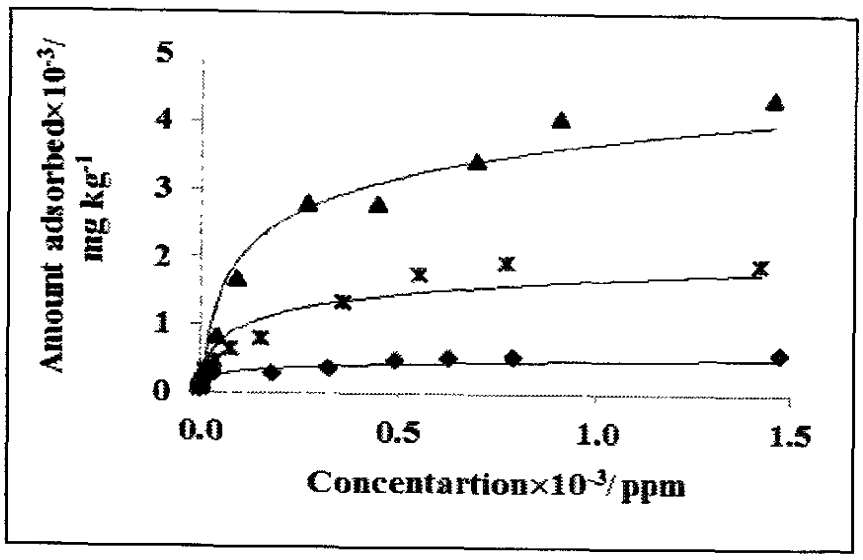

(a)

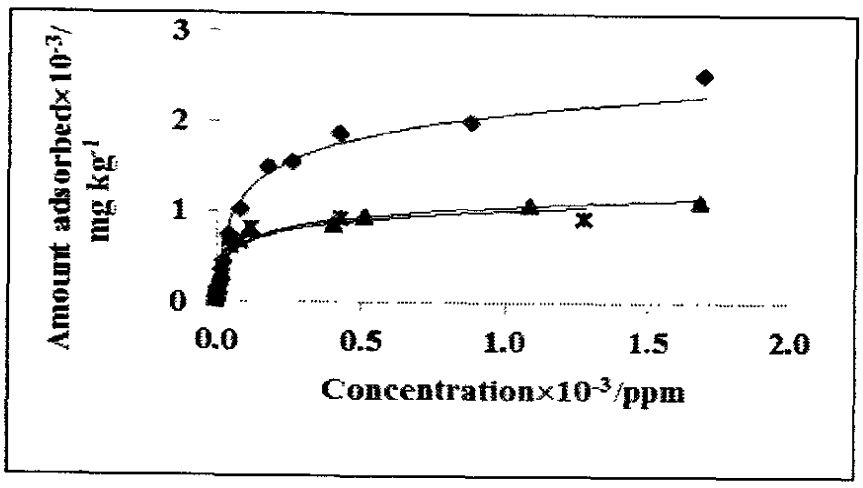

(b)

***Figure 6**. Amount of heavy metal ions adsorbed on rice husk. (a) - Cr(III) (◆), Ni(II) (✳), Pb(II) (▲) and (b) - Cd(II) (◆), Cu(II) (▲), Zn(II) (✳)*

Six isotherm models; Langmuir, Freundlich, Temkin, Dubinin-Raduskevich, Redlich-Peterson and Sips, were attempted to fit for all metal ion adsorption systems. The standard equations of the six isotherm models are given in Table 1.

***Table 1**: Standard equations of the six isotherm models*

Isotherm Model	Standard equations
Langmuir	$\frac{1}{q_e} = \frac{1}{q_m} + \frac{1}{q_m \cdot K_L} \cdot \frac{1}{C_e}$
Freundlich	$\ln q_e = \frac{1}{n} \ln C_e + \ln K_F$
Temkin	$q_e = B \ln K_T + B \ln C_e$
Dubnin-Radushkevich	$\ln q_e = \ln q_s - B\epsilon^2$ $\epsilon = RT \ln [1 + \frac{1}{C_e}]$
Redlich-Peterson	$q_e = \frac{K_R C_e}{1 + a_R C_e^{b_R}}$
Sips (Langmuir - Freundlich Isotherm)	$q_e = \frac{K_s C_e^{1/b_s}}{1 + a_s C_e^{1/b_s}}$

In Table 1, q_m and q_e are maximum adsorption capacity and equilibrium adsorption capacity; C_e is the equilibrium concentration of metal ion; K_L, K_F, K_T, K_R, K_S are Langmuir, Freundlich, Temkin, Redlich-petersom and Sips isotherm constants, respectively; n, B, a_R, b_R, b_S are constants.

Among the six isotherms, constants for Langmuir and Freundlich isotherms, the most widely used models, are given in Table 2 and Table 3, respectively. Langmuir isotherm model assumes monolayer adsorption which occurs on specific sites and is independent on the amount of material adsorbed. On the other hand, Freundlich isotherm model is applied to non-ideal sorption on heterogeneous surfaces as well as multilayer sorption. This is derived by assuming an exponentially decaying sorption site energy distribution [7]. It is clear from values in Tables 2 and Table 3 that the Langmuir adsorption isotherm model, having regression coefficients (R^2) close to unity for all six metal ion systems, is better suited to explain adsorption characteristics of metal ions on rice husk fired at 100 °C.

***Table 2**: Isotherm constants and regression coefficients (R^2) for Langmuir adsorption isotherm model*

Metal ion	$K_L \times 10^2$/L mg^{-1}	q_m/mg kg^{-1}	R^2
Cd(II)	22.2	2500	0.988
Cu(II)	13.9	1000	0.990
Ni(II)	15.3	909	0.985
Pb(II)	3.30	5000	0.986
Zn(II)	37.5	833	0.964
Cr(III)	3.00	769	0.983

According to Table 2, the adsorption capacity varies in the order of Pb(II) > Cd(II) > Cu(II) > Ni(II) > Zn(II) > Cr(III). The highest adsorption capacity towards Pb can be attributed to the lowest hydrated radius of Pb(II), which changes in the order of Cu(II) > Cd(II) > Pb(II), being able to be trapped easily in the pores of the adsorbent [15].

***Table 3**: Isotherm constants and regression coefficients (R^2) for Freundlich adsorption isotherm model*

Metal ion	n	K_F	R^2
Cd(II)	2.73	239	0.895
Cu(II)	2.77	111	0.812
Ni(II)	2.19	97	0.958
Pb(II)	2.12	214	0.915
Zn(II)	2.86	147	0.879
Cr(III)	5.32	130	0.904

Isotherm constants for the adsorption models, Temkin, Sips, Redlich-Peterson (R-P) and Dubnin-Radushkevich (D-R), are given in Table 4.

***Table 4**: Isotherm constants and respective regression coefficient (R^2) for Temkin, D-R, Sips and R-P isotherm model for considered heavy metal ions*

Temkin Isotherm			
Metal ion	B	K_T	R^2
Cd(II)	231	7.74	0.963
Cu(II)	130	3.57	0.968
Ni(II)	228	1.38	0.874
Pb(II)	516	2.03	0.962
Zn(II)	114	9.17	0.990
Cr(III)	58.9	3.21	0.885
Dubnin-Reduskevich (D-R) Isotherm (for higher concentrations)			
Metal ion	$B \times 10^3$	q_S	R^2
Cd(II)	0.10	1894	0.698
Cu(II)	5.6	1106	0.998
Ni(II)	1.9	1798	0.927
Pb(II)	7.1	4298	0.934
Zn(II)	0.20	968.9	0.925
Cr(III)	4.1	518.3	0.940
Sips Isotherm			
Metal ion	K_S	$a_S \times 10^2$	b_S	R^2
Cd(II)	394	9.60	1.69	0.987
Cu(II)	167	16.5	1.20	0.970
Ni(II)	68.9	2.40	1.57	0.975
Pb(II)	451	7.60	2.08	0.967
Zn(II)	264	26.6	1.69	0.987
Cr(III)	76.0	-43.3	2.97	0.947
Redlich-Peterson (R-P) Isotherm				
Metal ion	$K_R \times 10^{-2}$	a_R	b_R	R^2
Cd(II)	12.5	2.3	0.79	0.994
Cu(II)	1.92	0.30	0.93	0.984
Ni(II)	0.195	0.020	0.89	0.966
Pb(II)	4.67	0.40	0.82	0.978
Zn(II)	4.46	0.95	0.88	0.993
Cr(III)	-2.51	-2.9	0.74	0.936

Regression coefficients for all six systems listed in Table 5 shows that the best fitted model for the removal of all six heavy metal ions under investigation using rice husk is the Langmuir isotherm model. Redlich-Peterson isotherm and Sips isotherm also were fitted to a certain extent with high R^2 values. Freundlich, Temkin and D-R isotherms do not explain the adsorption behavior of these metal ions.

***Table 5**: Regression coefficients of adsorption isotherm models for all heavy metal ions under investigation*

Metal ion	Langmuir isotherm	Freundlich isotherm	Temkin isotherm	D-R isotherm Higher concentrations (>100 ppm)	R-P isotherm	Sips isotherm
Cd(II)	0.988	0.895	0.963	0.698	0.994	0.987
Cu(II)	0.990	0.812	0.968	0.998	0.984	0.970
Ni(II)	0.985	0.958	0.874	0.927	0.966	0.975
Pb(II)	0.986	0.915	0.962	0.934	0.978	0.967
Zn(II)	0.964	0.879	0.990	0.925	0.993	0.987
Cr(III)	0.983	0.904	0.885	0.940	0.936	0.947

As the D-R model, tested only for high concentrations, did not show any trend with respect to heavy metal ions investigated, it was not considered for error analysis, which was conducted for further clarification of the validity of adsorption results. The results of error analysis, namely, average relative error (ARE), Sum square error (SSE), Hybrid fractional error function (HYBRID), nonlinear chi-square test and Sum of absolute error (EABS) are shown in Table 6 [3]. The error terms obtained for various isotherm studies vary without any trend. However, the Langmuir isotherm shows smallest error values in general, and hence, the selection of the Langmuir isotherm as the best fitted model is further convinced. The validity of other isotherm models by considering all types of error analyses can be given in the order of Langmuir > R-P > Sips > Temkin > Freundlich for heavy metal ions Cd(II), Cu(II) and Pb(II). However, this order is slightly different for Ni(II), Zn(II) and Cr(III).

***Table 6**: Values of different error analyses for isotherm models*

	Metal ion	ARE	SSE	HYBRID	Non-linear chi-square test	EABS
Langmuir isotherm	Cd(II)	25.82	0.000	0.024	0.002	0.007
	Cu(II)	6.590	0.000	0.001	0.000	0.001
	Ni(II)	50.47	0.000	0.034	0.003	0.005
	Pb(II)	19.20	0.000	0.004	0.000	0.002
	Zn(II)	9.457	0.000	0.004	0.000	0.002
	Cr(III)	2.127	0.000	0.000	0.000	0.000
Freundlich isotherm	Cd(II)	6.217	2.220	4.410	0.485	4.210
	Cu(II)	8.294	2.736	7.431	0.594	4.201
	Ni(II)	3.971	0.852	2.196	0.198	2.116
	Pb(II)	5.818	2.154	3.680	0.331	4.025
	Zn(II)	6.002	1.457	3.819	0.306	3.064
	Cr(III)	1.578	0.196	0.387	0.035	0.995
Temkin isotherm	Cd(II)	High	High	High	High	High
	Cu(II)	198.1	High	High	High	High
	Ni(II)	184.2	High	High	High	High
	Pb(II)	High	High	High	High	High
	Zn(II)	High	High	High	High	High
	Cr(III)	41.76	High	High	High	High
R-P isotherm	Cd(II)	16.17	High	High	94.50	High
	Cu(II)	25.63	High	High	114.1	High
	Ni(II)	38.02	High	High	High	High
	Pb(II)	32.63	High	High	High	High
	Zn(II)	10.91	High	High	43.77	High
	Cr(III)	28.31	High	High	153.3	High
Sips isotherm	Cd(II)	41.33	High	High	High	High
	Cu(II)	28.85	High	High	146.5	High
	Ni(II)	18.14	High	High	196.4	High
	Pb(II)	66.66	High	High	High	High
	Zn(II)	19.06	High	High	69.94	298.7
	Cr(III)	26.87	High	High	143.9	High

4. Conclusions

Rice husk shows microporous characteristics toward adsorption. Among the six isotherms tested for the validity of six heavy meal ions, namely Cd(II), Cr(III), Cu(II), Pb(II), Ni(II) and Zn(II), for adsorption behavior, the best fitted model is the Langmuir isotherm, followed by Redlich-Peterson, Sips, Temkin and Freundlich based on regression analysis. The error analysis based on average relative error (ARE), Sum square error (SSE), Hybrid fractional error function (HYBRID), nonlinear chi-square test and Sum of absolute error (EABS) further supports the validity of the Langmuir isotherm as compared to others, The adsorption capacity of the six metal ions follows order of Pb(II) > Cd(II) >Cu(II) > Ni(II) > Zn(II) > Cr(III) according to the Langmuir isotherm having 5000 mg kg^{-1} for Pb(II) under the optimized conditions employed.

References

[1] J.O. Nriagu, "A History of global metal pollution", *Science*, 272., 223-224., 1996.

[2] W. Saikaew and P. Kaewsam, "Cadmium ion removal using biosorbents derived from fruit peel wastes", *Songklanakarin Journal of Science and Technology*, 31(5)., 547-554., 2009.

[3] R.S.D. Castro, L. Caetano, G. Ferreira, P.M. Padilha, M.J. Saeki, L.F. Zara, M.A.U. Martines and G.R. Castro, "Banana peel applied to the solid phase extraction of copper and lead from river water: Pre concentration of metal ions with a fruit waste", *Industrial Engineering Chemistry Research*, 50., 3446-3451., 2011.

[4] C.V.R Murthy, P. Ramesh and A. Ramesh, "Study of biosorption of Cu(II) from aqueous solutions by coconut shell powder", *Chemical Sciences Journal*, 3., CSJ 17., 2012.

[5] K. Gopalakrishnan, V. Manivannan and T. Jeyadoss, "Comparative study on biosorption of Zn(II), Cu(II) and Cr(VI) from textile dye effluent using sawdust and neem leaves powder", *E-Journal of Chemistry*, 7., S504-S510., 2010.

[6] A. Yoshita, J.L. Lu, J.H. Ye and Y.R. Liang, "Sorption of lead from aqueous solutions by spent tea leaf", *African Journal of Biotechnology*, 8(10)., 2212-2217., 2009.

[7] Y.S. Ho, J.F. Porter and G. Mckay, "Equilibrium isotherm studies for the sorption of divalent metal ions onto peat: Copper, nickel and lead single component system", *Water, Air and Soil Pollution*, 141., 1-33., 2002.

[8] A.O. Dada, A.P. Olalekan, A.M. Olatunya and O. DADA, "Langmuir, Freundlich, Temkin and Dubinin–Radushkevich isotherms studies of equilibrium sorption of Zn^{2+}onto phosphoric acid modified rice husk", *Journal of Applied Chemistry*, 3., 38-45., 2012.

[9] A. Kumar, K. Mohanta, D. Kumar and O. Parkash, "Properties and industrial applications of rice husk: A review", *International Journal of Emerging Technology and Advanced Engineering*, 2., 86-90., 2012.

[10] H.I. Chieng, L.B.L. Lim, N. Priyantha and D.T.B. Tennakoon, "Sorption characteristics of peat of Brunei Darussalam III: Equilibrium and kinetics studies on adsorption of crystal violet (CV)", *International Journal of Earth Science and Engineering*, 6., 791-801., 2013.

[11] L.S. Chan, W.H. Cheung, S.J. Allen and G. McKay, "Error Analysis of adsorption isotherm models for acid dyes onto bamboo derived activated carbon", *Chinese Journal of Chemical Engineering*, 20., 535-542., 2012.

[12] H. Matt, "Synthesis and modification of micro and mesoporous materials as CO_2 adsorbents", *Universiti Technologi Malaysis*, 2006.

[13] S. Lowell and J.E. Shields, "Adsorption isotherms", *Powder Surface Area and Porosity*", 11-13., 1984.

[14] L.T. Arenas, E.C. Lima, A.A.D.Santos. J.C.P. Vaghetti, T.M.H. Costa and E. V. Benvenutti, "Use of statistical design of experiments to evaluate the sorption capacity of 1,4-diazoniabicycle[2.2.2]octane/silica chloride for Cr(VI) adsorption", *Colloids and Surfaces*, 297., 240-248., 2007.

[15] YanLiang-HSAB-SSA2011poster.pdf, [Online]. Available: http://img.docstoccdn.com/thumb/orig/111069073.png.

REMOVAL OF HEAVY METAL IONS USING RICE HUSK: INVESTIGATION ON ADSORPTION KINETICS OF HEAVY METALS

N. Priyantha*, A. N. Navaratne, and T. P. K. Kulasooriya
Department of Chemistry, University of Peradeniya, Peradeniya, Sri Lanka and
Postgraduate Institute of Science, University of Peradeniya, Peradeniya, Sri Lanka
namalpriyantha@pdn.ac.lk, namal.priyantha@yahoo.com

ABSTRACT

Effluents released from industries contain many hazardous materials which are harmful to the environment as well as to the human being, and consequently, the removal of such materials from the environment has become a priority. In this context, the present study is based on the removal of heavy metal ions from synthetic industrial effluents using heat-treated rice husk which can be used to develop cost-effective and eco-friendly effluent treatment procedures. Metal ions commonly present in effluents of metal finishing industries, such as Cd(II), Cr(III), Cu(II), Ni(II), Pb(II) and Zn(II), were specially considered for their removal. The optimum firing temperature of rice husk is determined using 10.0 ppm solutions of each metal ion was 100 °C, and subsequently, the effect of other experimental parameters, such as contact time and pH, were investigated using rice husk fired at the optimized temperature of 100 °C. Kinetics studies conducted for the interaction of these metal ions and rice husk lead to the validity of pseudo second order kinetics with high regression coefficient. The initial rate of adsorption (h_o) of metal ions varies in the order, Zn(II) > Ni(II) > Cr(III) > Cu(II). According to the diffusion models fitted, Weber and Morris intra-particle diffusion model supports the data for rate constant of particle diffusion which varies in the same order as observed in initial adsorption rate measurements (h_o).

Keywords: Rice husk; Heavy metals; Adsorption; Kinetics; Intra-particle diffusion model

N. Priyantha
Department of Chemistry, University of Peradeniya,
Peradeniya, Sri Lanka.
E.Mail: namalpriyantha@pdn.ac.lk

INTRODUCTION

Industrial development is one of the main reasons for environmental pollution. Many industries produce effluents containing hazardous materials, such as oil, dyes, heavy metal ions and their compounds, pesticides, and anions, which are harmful to the environment as well as to the human being (Khan et al.2004;Chieng et al. 2014). Even after treatment of industrial effluents, they would still contain various types of pollutants to some extent, and consequently, these pollutants end up in natural water bodies. Among various hazardous materials, heavy metals are non-biodegradable and affect living tissues via bioaccumulation, causing many diseases and disorders to the human being (Naja and Volesky 2009; Saikaew and Kaewsam 2009).

For the removal of these harmful substances, physical, chemical and biological treatment methods are commonly in practice (Scott and Olli 1995). Many industries use physical and biological treatment methods to treat biodegradable waste, while chemical treatment methods are typically used to treat industrial effluents containing toxic substances, such as heavy metal ions and their compounds. As coagulants, flocculants and pH controlling agents are especially needed for effective chemical treatment processes, the excess of added chemicals would mix up with water bodies deteriorating their quality. Products formed during treatment could also pose another environmental problem (Priyantha et al. 2001).

Many attempts have been made using environmentally friendly substances to remove heavy metal ions from industrial effluents in an attempt to minimize the above stated threats. Natural substances, such as agricultural waste, coconut shell, poplar branches, brick clay, fruit peel waste, tea leaf, coir dust and saw dust, have been used to remove heavy metal ions from wastewater (Zaggout 2005; Al-Masri et al. 2012; Prasad and Santhi 2012; Das et al. 2008; Nikagolla et al. 2013).Since these environmentally-friendly substances successfully remove pollutants from effluents, this approach has become highly attractive, as compared to classical methods involving chemicals.

As rice is the main food in many countries, rice husk, a waste material is excessively produced in rice processing areas, and hence its disposal often creates environmental problems. Use of rice husk in solving an environmental problem is thus be an important approach, and further this treatment process would be cost-effective and eco-friendly. On the other hand, contamination of these metal ions would cause health hazards to human beings as well as for many other living organisms (Stander et al. 1970; Malavipathirana et al. 2013). Renal and liver failures, allergies, vomiting and diarrhea

are some adverse effects of heavy metal contamination, and in certain occasions, introduction of humans to metal fumes may even cause death (Singh et al. 2011). Therefore, it is very important to remove heavy metal ions from industrial wastewater, because it is the main source of heavy metal contamination in natural water bodies.

Although it has been reported that rice husk has the ability to remove heavy metal ions(Nhapi et al. 2011; Navaratne et al. 2013), kinetics studies of the adsorption of heavy metal ions on rice husk have not been reported to the best of our knowledge despite the necessity of rate measurements of adsorption of heavy metal ions in designing efficient treatment plants using such materials. In this context, the main objective of the current research is to investigate adsorption kinetics of heavy metal ions on rice husk under static conditions after optimization of experimental and process parameters. For kinetic studies, individual aqueous metal ion solutions of Cd(II), Cr(III), Cu(II), Ni(II), Pb(II) and Zn(II) were used, and the extent of removal of each metal ion by heat-treated rice husk was determined within a short period of time prior to the establishment of adsorption equilibrium, beyond which reliable results for rate of reaction cannot be obtained. Further, the pseudo order kinetics model was investigated for this heterogeneous system as it is difficult to vary the concentrations of the adsorbent and the adsorbate simultaneously. These results could be used as background information to design industrial wastewater treatment systems.

METHODS AND MATERIALS

Materials

Standard aqueous solutions of Cd(II), Cr(III), Cu(II), Ni(II), Pb(II) and Zn(II), were prepared using analytical grade reagents of their nitrates or sulphates. All the experiments were conducted under static conditions using individual metal ion solutions. Rice husk samples were obtained from a rice mill in Kandy, Sri Lanka, and used in its natural size, after thorough mixing and washing.

Instrumentation

Samples of rice husk were heated up to pre-determined temperatures using Carbolite CTF 12/100/900 tube furnace. Spectro-electronic M series atomic absorption spectrophotometer (AAS) was used to measure the total concentration of each metal in solutions. SEM images were taken using Oxford Instruments – EVO LS 15 (Zeiss) instrument.

Research Design

As rice husk is a natural substance having a variable composition, its representative samples were prepared by mixing large portions of samples, and heated for 4 hat various temperatures and allowed to cool down to room temperature through natural convection. All the experiments were performed under static conditions using individual adsorbate solutions containing each cation at 10.0 ppm concentration level. Aliquots of 50.0 cm^3 of each metal ion solution were shaken for pre-determined time periods with 2.50 g of heat treated rice husk. The extent removal of each metal ion by rice husk in each experiment was determined as a percentage removal using Equation (1),

$$\text{Percentage removal} = \frac{C_i - C_f}{C_i} \times 100\% \quad (1)$$

where C_i is the initial concentration of metal ion and $C_f$is the total concentration of metal ions present in the supernatant of the treated solution.

The effect of contact time on adsorption was observed by varying shaking time and settling time. All other variables were made constant and only the effect of the above two variables was initially checked for the maximum removal. Shaking rate was taken as 150 rpm in all experiments. Then, the pH of solutions was adjusted to check the removal ability of metal ions with various initial pH values. For this purpose, heavy metal ion solutions were prepared at 10.0 ppm concentration and its initial pH was adjusted between 2 and 10 to optimize the pH. High pH values were not employed to avoid precipitation of some metal ions (Ayres et al. 1994; Amer 1998).

To investigate the validity of kinetics models, 500 cm^3 of 10.0 ppm solutions of each metal ion were stirred with 1:20 (w/v) of rice husk heated at 100 °C. Then, in every 1.0 min interval, samples were withdrawn, immediately filtered and the remaining concentration of each metal ion was determined using AAS.

Kinetics modeling

Kinetics modeling was done for better understanding of the rate process. The generalized equation for kinetics, assuming that the activity of the adsorbent is constant, can be written as, (Priyantha and Bandaranayaka 2011)

$$\frac{d(q_t)}{dt} = k'(q_e - q_t)^n \quad (2)$$

Where k' is the apparent rate constant, t is the contact time, q_e and q_t are the masses of metal ions adsorbed by unit mass of the sorbent at equilibrium and at time t, respectively. A linearized integrated form of the above equation leads to the following kinetics models (Priyantha and Bandaranayaka 2011; Odoemelam et al. 2011; Igwe et al. 2008).

Pseudo first order:

$$\log (q_e - q_t) = -\frac{k\prime}{2.303} t + \log q_e \quad (3)$$

Pseudo second order:

$$\frac{t}{q_t} = \frac{1}{q_e} t + \frac{1}{k\prime q_e{}^2} \quad (4)$$

If the initial adsorption rate is h_o,

$$h_0 = k' q_e^2 \quad (5)$$

In order to identify the boundary layer diffusion, the intra-particle diffusion models, as given below (Odoemelam et al. 2011), were considered.

McKay and Poots intra-particle diffusion model:

$$q_t = X_i + k' t^{0.5} \quad (6)$$

Webber and Morris intra-particle diffusion model:

$$\log R = \log k_{id} + n \log(t) \quad (7)$$

where R is the percentage adsorption of a heavy metal, n is the gradient of linear plots and k_{id} is the intra-particle diffusion rate constant.

RESULTS AND DISCUSSION

Effect of Experimental/ Process Parameters on Removal of Heavy Metal Ions from Aqueous Solutions

Determination of the extent of removal of each metal ion by the adsorbent, monitored by changing the parameter of interest within a broad range while keeping the other parameters constant, leads to the optimum values for each parameter for the removal of each heavy metal ion under investigation (Table 1). The percentage removal of heavy metal ions determined using pre-heated rice husk with different metal ion solutions increased with increase in the firing temperature up to 100 °C, and then decreased up to 200 °C. Therefore, 100 °C (percentage removal > 85%) was taken as the optimum firing temperature of rice husk. Rice husk heated at this temperature show 20% more removal as compared to raw rice husk which shows 65% removal for the metal ions investigated (Priyantha et al. 2015).

Since the extent of removal of heavy metal ions using rice husk is increased with heat treatment, SEM analysis was conducted to observe surface features of rice husk samples heated at different temperatures. Fig. 1 clearly indicates surface changes that have occurred during heating.

Effect of pH

The extent of adsorption of metal ions is controlled by the solution pH as both solution properties and the chemistry of the adsorbent depend on pH. The percentage removal vs. pH investigated from an initial pH from 1.0 up to a value at which corresponding hydroxide precipitation starts based on solubility product calculations for 10.0 ppm concentration of each metal ion is shown in Fig. 2.

According to observations in Fig. 2, it is clear that the percentage removal is lower at low pH values, which is due to the competition of metal ions with H_3O^+ ions present in solution for a limited number of binding sites in the adsorbent. The extent of removal of each metal ion then increases with increase in pH up to a certain value, beyond which metal ions tend to precipitate as hydroxides (Table 2).

The lowest pH that leads to the most effective removal of metal ions was determined to be between 4.0 and 5.0, and thus, all the experiments were carried out by adjusting the initial pH within this range.

Physico-chemical characteristics of rice husk

Characterization of rice husk was conducted using XRD, XRF and FTIR analyses. Although XRD provides information on the crystalline nature and minerals present, the composition of individual elements (metals) cannot be obtained. On the other hand, XRF is useful in obtaining the composition of metallic elements, while FTIR provides information on organic functional groups. According to the results, neither XRD patterns nor FTIR spectra provide sufficient information on chemical/physical changes that would occur during heat treatment. XRF spectra obtained for natural and heated rice husk samples provide evidence for the presence of Si, Fe, K and Ca.

Variations of mass reduction and heat flow during the heating process indicates a significant decrease in mass reduction, beyond the temperature of 100 °C, due to the combustion of organic matter. The exothermic nature of combustion is evident by observing positive energy release values at firing temperatures beyond 100 °C (Priyantha et al. 2015). The surface charge of the bio-sorbent was determined to be highly dependent on the pH of the medium for different ionic strengths. The point of zero charge can be estimated by considering curves obtained for different ionic strengths as pH of 4.0 for brick clay heated at 100 °C (Priyantha et al. 2015).

Surface area determinations

Methylene blue (MB) test was performed with rice husk heated at 100 °C to calculate the surface area of rice husk using Equation (8),

$$S_s = m_{MB} A_v A_{MB}/m_s M \quad (8)$$

where S_s is the surface area of rice husk ($m^2 g^{-1}$), m_{MB} is the mass of MB adsorbed at the point of complete cation replacement (g), A_v is the Avogadro constant, A_{MB} is the area covered by a MB molecule (1.30×10^{-18} m^2) (Yukselen and Kaya 2008), m_s is the mass of the brick sample, and M is the molar mass of MB (319.87 g mol^{-1}). Fig. 3 shows the variation of the amount of methylene blue (MB) adsorbed on the rice husk surface with the initial amount of MB added to the solution. According to the Fig. 3, the amount adsorbed is leveled off with the increase in the concentration of MB. The surface area determined based on the saturation point is 110.13 $m^2 g^{-1}$.

The adsorption capacity is greater for materials of higher surface area (larger pore size) due to increased pore volumes. When compared to surface areas of natural substances reported, heated rice husk shows comparable values indicating that it can be used as an effective adsorbent (Table 3).

Surface changes of rice husk after metal ion adsorption

Adsorption patterns of all metal ions investigated qualify Type I isotherm according to IUPAC classification, suggesting that rice husk shows microporous characteristics for adsorption of these metals. According to the data obtained, Langmuir adsorption isotherm model having regression coefficients (R^2) close to unity for all six metal ions, is suited to explain adsorption characteristics of metal ions on rice husk heated at 100 °C. This model assumes monolayer adsorption which occurs on specific sites and is independent on the amount of material adsorbed (Dada et al. 2012).

SEM images of rice husk- pre heated at 100 °C after sorption of heavy metals show the surface coverage by metal ions as compared to untreated samples (Fig. 4).

EDX spectrum of untreated rice husk samples clearly indicates that they mainly contain Si, O, S, Fe and C in its natural form (Fig. 5(a)). Treatment of these samples with heavy metal ions adsorbed (as an example Ni adsorption) given by SEM images (Fig. 4) and the corresponding elemental composition by EDX is shown in Fig 5(b)).

Investigation of Kinetics

Fig. 6 illustrates the variation of the extent of adsorption with contact time for different metal ions when an aqueous solution of each metal ion was individually treated with rice husk, heated at the optimum temperature. The extent of removal of heavy metal ions by rice husk, determined after the system reaches equilibrium, according to the figure follows the order, Ni(II) < Cr(III) < Cd(II) ≈ Zn(II) < Cu(II) < Pb(II). On the other hand, the rate at which rice husk-metal ion solution reaches equilibrium, is different for each ion according to the figure. Adsorption of Pb(II) has reached equilibrium almost instantly, followed by Cd(II), Zn(II) and Ni(II). Adsorption of Cr(III) and Cu(II) takes the longest time to reach equilibrium. Owing to fast adsorption reaction rates, kinetics modeling cannot be applied for the investigation of adsorption of Pb(II) and Cd(II). Further, kinetics modeling for the adsorption of other metal ions should be applied within the time period up to 8 min, beyond which many systems would have reached equilibrium according to the observations of Fig. 6.

Application of adsorption data of metal ions for the linearized pseudo first order model [Equation (3)] is shown in Fig. 7. According to the regression coefficients determined from each linear plot (Table 4), it is concluded that the pseudo first order kinetics is not much in agreement with adsorption of heavy metal ions on rice husk. Therefore, the determination of kinetics parameters based on the pseudo first order model was not attempted. More importantly, application of the pseudo second order kinetics model [Equation (4)] shows much better agreement of experimental data for the heavy metal ions selected, as shown in Fig. 8.

Table 5 shows the parameters determined, such as q_e (adsorption capacity at equilibrium), k' (pseudo second order rate constant), R^2 (correlation coefficient) and h_0 (initial adsorption rate) obtained from the pseudo second order kinetics model. According to the R^2 values obtained, all adsorption processes can be best described by the pseudo second order rate equation. The data reported in the table indicates that the initial rate of adsorption (h_o) of metal ions follows the order, Zn(II) > Ni(II) > Cr(III) > Cu(II), which is a measure of how fast the reaction proceeds. Since ionic radius follows the order Pb(II) > Cd (II) > Zn (II) > Ni(II) ≈ Cr(II) ≈ Cu (II), this may be the reason for the highest rate of adsorption obtained for Zn(II) among other metals. The order determined based on kinetics, which

depends on the path to reach equilibrium, is not in agreement with the order of the extent of removal of metal ions determined when the system has reached equilibrium, due to the fact that kinetics and equilibrium aspects are not inter-dependent.

Many models are available in order to get an idea on the mechanism of metal ion binding for many adsorbents. Intraparticle diffusion, external mass transfer diffusion and chemical binding are some of the methods used to find the rate controlling step. Among these models, chemical binding is assumed to be rapid, and therefore, the rate limiting step is normally either single or combination of other two models. If the boundary layer surrounding particles is much reduced, it reduces the external mass transfer coefficient and hence, intraparticle diffusion is more likely to be the rate controlling step (Sag and Aktay 2000).

External mass transfer diffusion model

This is also called the boundary model which assumes that the surface concentration of a metal ion is negligible at t=0, and consequently, intraparticle diffusion is negligible. The change in the metal concentration with respect to time is related to the liquid-solid mass transfer coefficient (β_L) (Sag and Aktay 2000). With the above assumptions, simplified equation can be written as,

$$\frac{C_t}{C_0} = -\beta_L St \qquad (9)$$

where, C_t, C_0 are metal ion concentration of solution at time t and at t=0, β_L is the liquid-solid mass transfer coefficient and S is the specific surface area for mass transfer.

In order to check whether the process follows the equation, graphs were plotted for C_t/C_0 vs time (t). Table 6 shows the calculated R^2 values in order to check whether the model is applicable for the data set or not.

Since the results obtained for regression coefficient were not much satisfy with the data obtained, intraparticle diffusion models were fitted for the same data set.

Intra-Particle Diffusion Models

The adsorption of metal ions on rice husk would be controlled by either film-diffusion or particle-diffusion (Igwe et al. 2008). The adsorbate may diffuse from the bulk of the so-

lution to the film surrounding the adsorbent and then into the micropores and macropores of the adsorbent in the film diffusion model (Odoemelam et al. 2011; Sonde and Odoemelam2012). In the particle diffusion model, the bulk of the solution diffuses through the pores present in the sorbent and the adsorbate goes along the pore walls to the sorbent (Sonde and Odoemelam 2012).

Variation of the amount of metal ions adsorbed with $t^{1/2}$ plotted to check the validity of the McKay and Poots intra-particle diffusion model did not result in desirable regression coefficients (Table 7), and hence, the validity of the Weber and Morris model was fitted (Fig.9).

Since this model provides information on the rate determining step of the adsorption process, resulting graphs obtained does not go through the origin, suggesting that the rate limiting step has another contribution in addition to the McKay and Poots intraparticle diffusion model. Therefore in order to get an idea on the intraparticle diffusion rate constant, Weber and Morris intraparticle diffusion model was applied.

Weber and Morris intra-particle diffusion model

The plots of the Weber and morris intra-particle diffusion for the four heavy metals tested are shown in Fig. 10 results in satisfactory regression coefficients (Table 8). According to the values of regression coefficients (Table 7), it is concluded that the Weber and Morris intra-particle diffusion model is in good agreement for adsorption of heavy metal ions on rice husk. The gradient of plots (n) and intra-particle diffusion rate constant (k_{id}) determined from the slope and the intercept of the linear plots, respectively, are given in Table 8.

The value k_{id} is taken as a rate factor, which increases in the order of Zn(II) > Ni(II) > Cr(III) > Cu(II), where higher values of k_{id} show an improvement in the rate of adsorption. The increasing order of the intra-particle diffusion rate constant (k_{id}), determined from the Weber and Morris model, and that of the pseudo second order rate constant(k') follow the same trend, demonstrating the validity of the two models for adsorption of heavy metal ions investigated on rice husk. Further, larger n values show strong adsorption indicating strong bonding between the metal ion and the adsorbent (Odoemelam et al. 2011).

CONCLUSION

The extent of removal of heavy metal ions by rice husk is determined by comparing the concentrations before and after the treatments. Among all metal ions investigated, kinetics modeling was not applied for the metals Pb(II) and Cd(II) due to fast adsorption reaction rates. Furthermore, kinetics modeling for the adsorption of Cu(II), Ni(II), Zn(II) and Cr(III) on rice husk were applied only within the time period up to 8 min, at this point adsorption systems under study would have reached the equilibrium. The interaction between selected heavy metal ions and rice husk heated at 100 °C follows pseudo second order kinetics. The best fit ($R^2 > 0.980$) with high correlation obtained according to the linearized kinetics equations. The initial adsorption rate (h_o) of the selected heavy metals are 56, 385, 1111, 159 mg $kg^{-1}min^{-1}$ for Cu(II), Ni(II), Zn(II) and Cr(III), respectively, and these values varies in the order of Zn(II) > Ni(II) > Cr(III) > Cu(II). Between two models namely external mass transfer diffusion model and intraparticle diffusion model, latter model is in good agreement for the removal process according to the regression coefficient values. Application of the Weber and Morris intra-particle diffusion model for adsorption of the metal ions investigated yielded high regression coefficients (> 0.900). Further, the rate constant of particle diffusion according to the Weber and Morris intra-particle diffusion model are 20.40 min, 63.59 min, 74.87 min, 47.08 min for Cu(II), Ni(II), Zn(II) and Cr(III), respectively, and it increases in the same order as observed in initial adsorption rate measurements (h_o).

ACKNOWLEDGMENT

Financial support through research grant by the National Science Foundation (RG/2012/BS/05) is greatly appreciated.

REFERENCES

Al-Masri MS, Amin Y, Al-Akel B, Al-Naama T (2012) Biosorption of cadmium, lead and uranium by powder of popler leaves and branches.ApplBiochemBiotechnol 160:976-987.

Amer, S.I. Treating metal finishing waste water.Environ technol, 1998

Ayres DM, Davis AP, Gietka PM(1994) Removing heavy metals from waste water, Engineering Research Center Report, University of Maryland.

Chieng HI,Zehra T, Lim LBL,Priyantha N,Tennakoon DTB (2014) Sorption characteristics of peat of Brunei Darussalam IV: equilibrium, thermodynamics and kinetics of adsorption of methylene blue and malachite green dyes from aqueous solution. J Environ Earth Sci 72:2263-2277.

Dada AO, Olalekan AP, Olatunya AM, Dada O (2012) Langmuir, Freundlich, Temkin and Dubinin–Radushkevich Isotherms Studies of Equilibrium Sorption of Zn^{2+} Unto Phosphoric Acid Modified Rice Husk. IOSR J. ApplChem 3: 38-45.

DasN,Karthika P,Vimala R,VonodhinV,(2008) Use of natural products as biosorbent of heavy metals – An overview. Natural Product Radiance 7:133-138.

Igwe JC,Abia AA,Ibeh CA (2008) Adsorption kinetics and intra-particle diffusivities of Hg, As and Pb ions on unmodified and thiolated coconut fiber. IntJ Sci Techno 5:83-92.

KhanNA, Ibrahim S,Subramanium P (2004) Elimination of heavy metals from waste water using agricultural wastes as adsorbents. Malays J Sci 23:43-51.

Malavipathirana S, Mubarak MNA,Perera KMPAH (2013) An assessment of heavy metal contamination in marine sediments, Precautionary measures for environmental impact management at harbor development: Galle harbor Sri Lanka. J Ecotechno Res 171:29-33.

Naja GM and Volesky B (2009) Toxicity and Sources of Pb, Cd,Hg, Cr, As, and Radionuclidesin the Environment, in Heavy Metals in the Environment 14-21.

Navaratne A,Priyantha N,Kulasooriya TPK (2013) Removal of heavy metal ions using rice husk and brick clay as adsorbents – dynamic conditions. Int J Earth SciEng 6:807-811.

Nhapi I,Banadda N,Murenzi R,Sekomo CB,Wali UG (2011) Removal of heavy metals from industrial wastewater using rice husks. Open Environ Eng J 4:170-180.

Nikagolla C,Chandrajith R,Weerasooriya R,Dissanayake CB (2013) Adsorption kinetics of chromium(III) removal from aqueous solutions using natural red earth. J Environ Earth Sci 68:641-645.

Odoemelam SA,Iroh CU,Igwe JC (2011) Copper (II), Cadmium (II) and Lead (II) adsorption kinetics from aqueous metal solutions using chemically modified and unmodified cocoa pod husk (theoproma cacao) waste biomass. Res J ApplSci6:44-52.

Prasad AL,Santhi T (2012) Adsorption of hazardous cationic dyes from aqueous solution on to Acacia nilotica leaves as an ecofriendly adsorbent. Sustainable Environ Res 22:113-122.

Priyantha N,Bandaranayaka A (2011) Investigation of kinetics of Cr(VI)-fired brick clay interaction. J Hazard Mater 188:193-197.

Priyantha N,Keerthirathne S,Lokuge I,Gajanayake H (2001) Removal of blue colouration from industrial effluents by burnt brick particles. JNatlSci Found Sri Lanka. 28: 287-299.

Priyantha N, Navaratne AN, Kulasooriya TPK (2015) Adsorption of Heavy Metal Ions on Rice Husk: Isotherm Modeling and Error Analysis.Int J Earth SciEng 8: 346-352.

Sag Y, Aktay Y (2000) Mass transfer and equilibrium studies for the sorption ofchromium ions onto chitin. Process Biochemistry 36: 157-173.

Saikaew W,Kaewsam P (2009) Cadmium ion removal using biosorbents derived from fruit peel wastes. Songklanakarin J SciTechnol 31:547-554.

Scott JP,Ollis DF (1995) Interaction of chemical and biological oxidation processes for water treatment: Review and recommendation. Environmental progress. 14:88-103.

Shaima N (2013) Removal of heavy metals using saw dust as an adsorbent.B.Sc. project report. University of Peradeniya, Peradeniya, Sri Lanka.

Singh R,Gautam N, Mishra A, Gupta R (2011) Heavy metals and living systems: An over-view. Indian J Pharmacol 43:246–253.

Sonde CU,Odoemelam SA (2012) Sorption studies on the use of African breadfruit (treculia Africana) seed hull as adsorbent for the removal of Cu^{2+}, Cd^{2+} and Pb^{2+} from aqueous solutions. Am J PhysChem 1:11-21.

Stander GJ,Henzen MR,Funke JW (1970) The disposal of polluted effluents from Mining, Metallurgical and Metal Finishing Industries, their effects on receiving water and re-medial measures. J South AfrInst Min Metall 71: 5-103.

Weththasinghe WSA (2014) Coir dust as a low cost adsorbent to remove Cu^{2+}, Zn^{2+} and Pb^{2+}. M.Sc. project report.Postgraduate Institute of Science, University of Peradeniya, Peradeniya, Sri Lanka.

Yukselen Y, Kaya A (2008) Suitability of the methylene blue test for surface area, cationexchange capacity andswell potential determination of clayey soils. Eng Geolo-gy 102: 38-45.

Zaggout FR (2005) Kinetic removal of lead from water by decaying tamrix leaves. J Envi-ron EngSci 4:299-305.

REMOVAL OF PHOSPHATE IONS USING BRICK CLAY: STATIC AND DYNAMIC CONDITIONS

N. Priyantha, A. Navaratne and T. P. K. Kulasooriya,

Department of Chemistry, University of Peradeniya, Peradeniya, Sri Lanka

Postgraduate Institute of Science, University of Peradeniya, Peradeniya, Sri Lanka

Introduction

Inland water resources, such as streams, lakes, rivers and ponds are associated with all forms of living beings. Daily activities of living beings cause input of excessive amounts of nitrates and phosphates leading to nutrient pollution of water resources. This problem is further intensified by the use of naturally occurring phosphate minerals, in raw and processed form, in agriculture and industries. Although the natural occurrence of phosphorous is minimal, it is an element of concern because minute amounts of phosphorous would result in significant growth of algal and other biological organisms [1]. Since phosphate is a nonrenewable source, it would be advantageous to reuse it if possible. Main uses of phosphates are the production of water based paints and coatings (polyphosphates); processing of various ceramics; preparation of chemical polish (brighten) for aluminum and aluminum alloys; as flame-retardants for textiles, plastics, coatings, paper and sealants; and treatment of potable (drinking) water. Farmers also apply phosphate included fertilizers to the fields several times throughout the year although it is not much needed, which could be the main phosphate pollution source in rural areas. On the other hand pollution occur in urban areas due to phosphate owing to limitless use of detergents. The phosphate species, a main aquatic pollutant, contributes to eutrophication, which results in lower light penetration, decreased dissolved oxygen levels of reservoirs, causing harmful effects to the aquatic life and human health.

Potential for algal growth in water is possible when dissolved phosphate level becomes higher than 0.02 mg l^{-1} (USEPA, 1995). This can be overcome, without further damaging the

environment, by removal of phosphate before phosphate contaminated wastewater reaches reservoirs.

The removal of phosphate can be achieved by physicochemical and biological processes. Chemical precipitation with alum, lime and iron salts is often used for the removal of phosphate from wastewater. These methods are associated with sludge handling problems, and further chemical precipitation is less effective when the concentration of phosphate is in trace level [2]. Biological methods can also be used to treat phosphate although it is effective to remove only about 10-30% of phosphate from the sample [3]. Biological treatment can hardly reduce the concentration to the discharge limit of 0.5 mg l^{-1} due to the fact that phosphate is one of the necessary elements for metabolism, and for some microorganisms which cannot live in the absence of phosphate. As adsorption techniques are found to be superior to existing chemical methods in many respects, they have become attractive. Adsorption methods prove that it is much effective due to their low cost, effective treatment in dilute solutions, high uptake capacity, faster regeneration kinetics and greater selectivity [4].

Recent reports in this regard include the removal of phosphate from aqueous solutions using mine waste [4], metal-loaded skin split waste [1] and iron-coated natural and engineered sorbents [5]. Further, phosphate-bound brick clay has been shown high strength [6], although the mechanism of interaction of phosphate with brick clay (used for the production of brick) and the determination of the efficiency of its removal have not paid much attention. The objective of this study is therefore to investigate the type of adsorption of phosphate on burnt brick clay particles and kinetics of adsorption, and to determine optimum conditions for phosphate-burnt brick clay interaction under both static and dynamic conditions. Experimental results were plotter for different adsorption isotherm models namely Langmiur, Freundlich Temkin and D-R isotherms in order to get an idea on the adsorption behavior of the system.

Materials and methods

Materials

Standard phosphate solutions were prepared using analytical grade $KH_2(PO_4)$, and experiments were conducted under both static and dynamic conditions. In each measurement,

charcoal was used to remove colored substances and the effect of charcoal was corrected against a blank run and all experiments were conducted in triplicates.. Brick clay, feldspar and dolomite were obtained from the Central Province, Sri Lanka.

Instrumentation

Representative samples of brick clay were fired using "Carbolite CTF 12/100/900" tube furnace, while UV-Vis spectrophotometer (Shimadzu-1800UV) was used to measure the total phosphate concentration of all solutions.

Research design

Selection of an adsorbent

Phosphate removal was tested using three adsorbents: brick clay, feldspar and dolomite. All three adsorbents were used for the selection test without any heat treatment. For all static experiments, 10.0 ppm phosphate solution was used and 5.00 g if each sorbent was shaken with solution at 150 rpm. After completion of 1 h shaking time and 1 h settling time, solutions were filtered using a filtration system using Whatman 0.45 μm filter paper. Next, clear solutions were prepared for phosphate determination using the Vanadomolybdophosphate colorimetric method. Then, samples were tested with standard phosphate solutions covering the range 2 ppm – 10 ppm at the wavelength of 420 nm. The percentage removal was calculated using the relationship,

$$\text{Percentage removal} = \frac{C_i - C_f}{C_i} \times 100\% \quad (1)$$

where, C_i is the initial phosphate concentration of solution and C_f is the final phosphate concentration after treatment with the adsorbent.

Effect of firing temperature

Since brick clay was selected as the best adsorbent for the removal of phosphate from synthetic effluents, it was fired in to different temperatures for 4 h and placed it for natural cooling down to room temperature. Effect of firing temperature was determined using the same procedure, and the optimum firing temperature was determined by considering the extent of removal.

Static conditions

Effect of contact time

The effect of contact time on adsorption was observed by varying shaking time and settling time, separately by keeping all other variables constant, and the extent of removal was determined using Equation (1).

Adsorption isotherms

In order to examine the relationship between removal of phosphate and equilibrium concentration, various isotherm models were tested. Initial phosphate concentrations were varied from 2 - 1000 ppm and all other parameters were at optimized conditions. After each solution was filtered, UV/Vis spectrophotometric measurements were recorded followed by the colour removal process. The Langmuir model gives an idea about the maximum phosphate uptake which could not be reached in the experiments, and the Freundlich isotherm gives the idea on liquid phase sorption [2]. The constant n in the model can quantify the favorability of sorption and the degree of heterogeneity of the surface. The validity of the Temkin adsorption isotherm also was tested for further clarification.

Kinetics

Kinetics studies were conducted for brick clay fired at 200 °C by withdrawing 35 cm^3 volumes of samples from different sample containers prepared under identical conditions. Samples were withdrawn at every 1 min interval for 20 min before the system reached equilibrium. Validity of the pseudo first order and pseudo second order kinetics models were then tested.

Dynamic conditions

All dynamic experiments for phosphate removal were conducted using columns of internal diameter 2.0 packed with brick clay of particle size 0.5 cm 1.0 cm. Column height and

flow rate were optimized by determining the extent of removal after five minutes interaction time when phosphate solution of 10.0 ppm was passed through the column.

Effect of packing height on adsorption

Different packing heights (15.0 cm, 22.5 cm, 30.0 cm, 37.5 cm) at a constant flow rate of 8 cm^3 min^{-1} were used for optimization of column height while different flow rates (8 cm^3 min^{-1}, 12 cm^3 min^{-1}, 20 cm^3 min^{-1}) at the optimum packing height of 30.0 cm were used for optimization of flow rate.

Isotherm studies

In order to do isotherm experiments on dynamic conditions, column studies were conducted for different initial concentrations at the optimized column height (30.0 cm) and the optimized flow rate (8.0 ml min^{-1}). For each concentration, 20 eluent samples were collected at 5.0 min intervals. The colour of samples were developed for the Vanadomolybdate method, and the absorbance values at the wavelength of 420 nm were recorded.

Results and discussion

Batch adsorption study

The exent of removal of phosphate from synthetic solutions prepared in the laboratory by common naturally available adsorbents is shown in Figure 1. Among them, unfired brick clay is found to be the most efficient adsorbent with more than 80 % removal under experimental conditions. As feldspar and dolomite shows much less removal ability for phosphate, further experiments were conducted using brick clay.

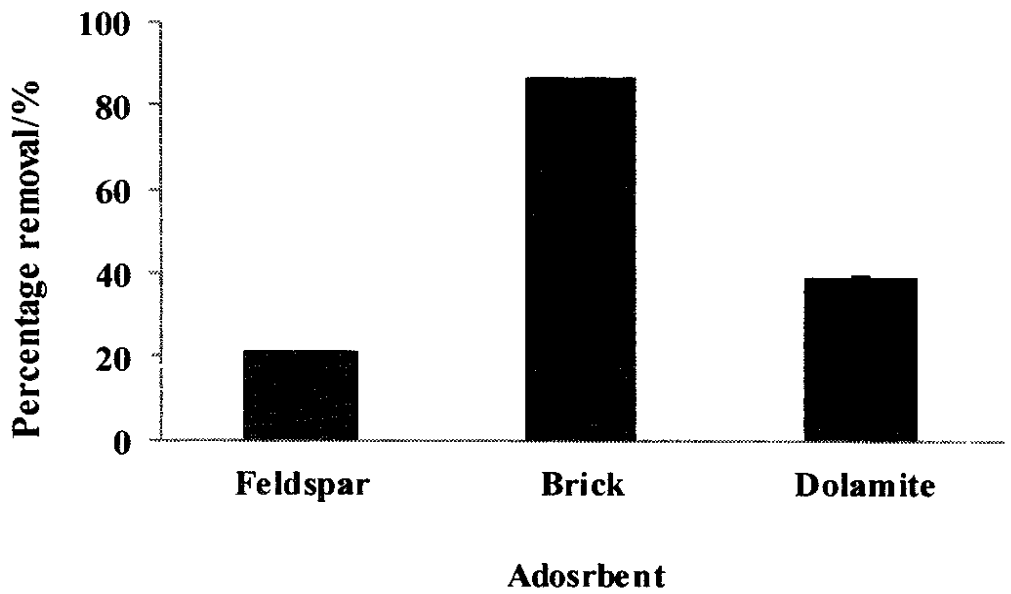

Figure 1: Extent of removal of phosphate using various adsorbents (50.0 cm^3 of 10.0 ppm PO_4^{3-} solution, 5.0 g of each adsorbent).

Optimization of firing temperature of adsorbent

The extent of removal of phosphate by brick clay treated at three temperatures, compared to untreated adsorbent is shown in Figure 2. As shown in figure, the percentage removal is not significantly changed at the temperatures employed for treatment.

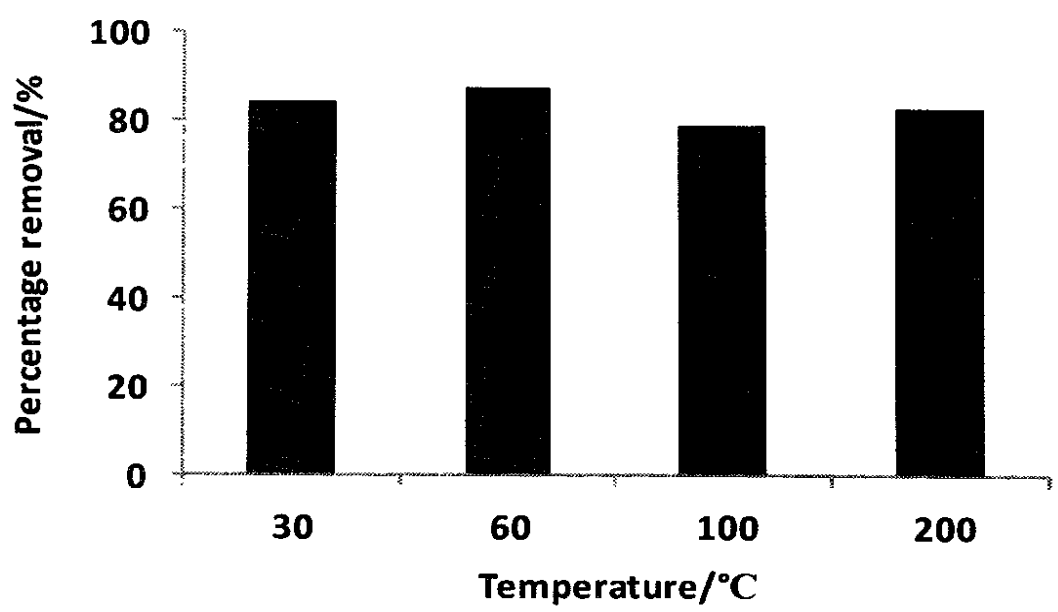

Figure 2: Extent of removal of phosphate for different adsorbent firing temperatures: (50.0 cm^3 of 10.0 ppm PO_4^{3-} solution, 5.0 g of brick clay fired at 200 °C).

However, brick clay treated at low temperatures results in turbid solutions, and hence, it is not possible to control particles of sufficient sites. Further, brick clay treated at 200 °C or higher

temperatures has been shown to have strong ability for the removal of heavy metal ions and dyes (ref). Therefore, brick clay fired at 200 °C was selected for phosphate removal experiments as well so that a common temperature of treatment would be used for the removal of many pollutants including phosphate.

Contact time optimization

Shaking time and settling time are important experimental parameters in the investigation of adsorption equilibrium aspects and hence their optimization is usually the first step in adsorption research. The variation of the extent of removal of phosphate determined within a range of shaking times and sis shown in figure 3. The extent of removal becomes leveled off after certain period shaking and settling. Therefore, the optimum time periods for both shaking and settling were selected as 30 min each for future adsorption experiments.

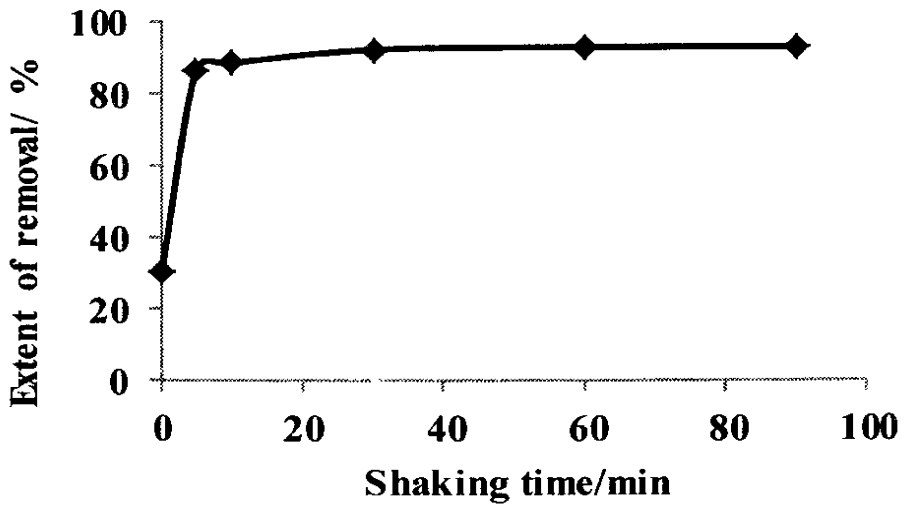

(a)

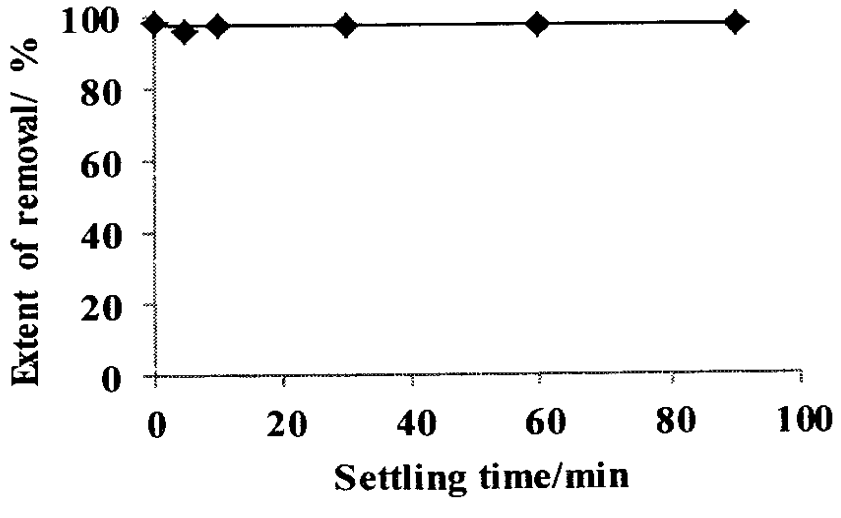

(b)

Figure 3: Optimization of (a) shaking time with 1 h settling time (b) settling time at optimized shaking time for the removal of phosphate ions (50.0 cm^3, 10.0 ppm PO_4^{3-}, 5.0 g brick clay fired at 200 °C).

Adsorption Isotherms

Variation of the amount of phosphate removal with the initial concentration of phosphate indicates that the brick clay surface fired at 200 °C does not reach saturation even at concentrations as high as 1000 ppm (Figure 4). The extent of removal is continuously on the increase, indicating that the adsorption of phosphate on burnt brick clay particles is not limited to monolayer coverage.

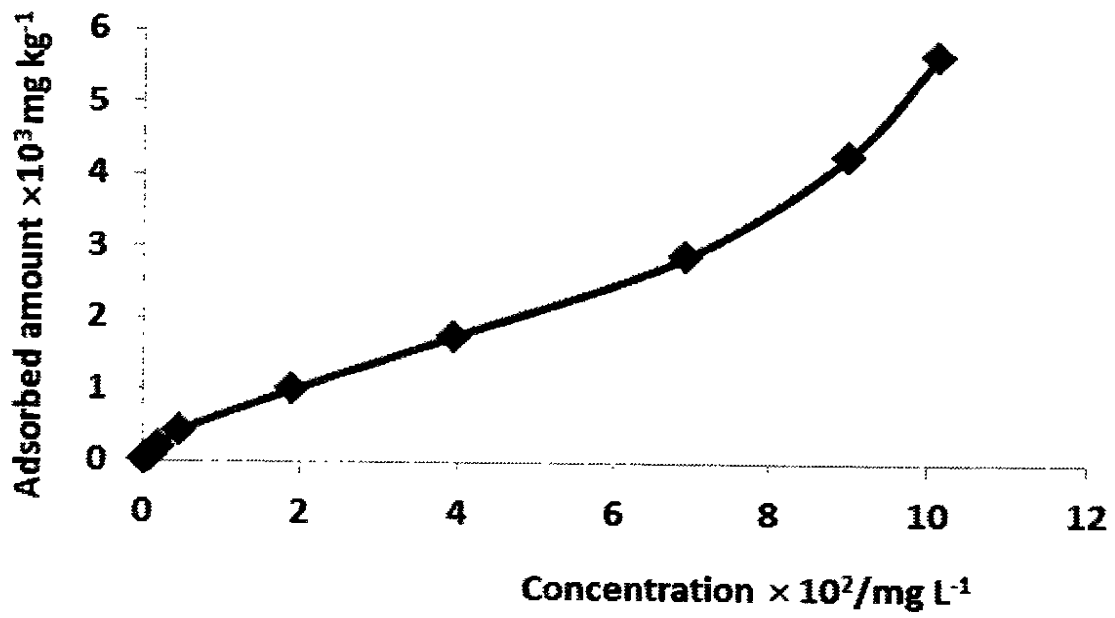

Figure 4: Amount of phosphate adsorbed on burnt brick clay (50.0 cm^3 solutions of different concentrations of phosphate shaken with 5.0 g of brick clay fired at 200 °C).

The Langmuir adsorption isotherm is mainly used for chemisorption processes leading to monolayer coverage. This isotherm is based on the main assumption [7, 8], that monolayer adsorption occurs at localized adsorption and the heat of adsorption is independent of the amount of material adsorbed.

A linear form of this isotherm is presented by,

$$\frac{C_e}{q_e} = \frac{C_e}{q_{max}} + \frac{1}{K_L q_{max}} \quad (2)$$

where q_{max} and q_e are the maximum adsorption capacity and equilibrium adsorption capacity, respectively; C_e is the equilibrium solution concentration; K_L is the Langmuir isotherm constant related to the free energy of adsorption

The Freundlich isotherm, which is based on multilayer adsorption, can be derived theoretically with the assumption that the heat of adsorption varies exponentially with the extent of surface coverage.

The linearized form of this isotherm is presented by the equation,

$$\ln q = \frac{1}{n} \ln C_e + \ln k \quad (3)$$

where q is the adsorption capacity; and n and k are constants.

The Temkin isotherm assumes that the heat of adsorption decreases linearly with the coverage. This isotherm mainly takes in account of adsorbate - adsorbent interactions [98].

The isotherm is presented by the equation,

$$q_e = B \ln K_T + B \ln C_e \quad (4)$$

where K_T is the Temkin isotherm equilibrium binding constant, T is absolute Temparature in kelvin (298 K), B is a constant related to heat of sorption and C_e is the solution concentration.

Among three adsorption isotherm models described above, Freundlich model fits better than other models for phosphate adsorption on brick clay. Figure 5 illustrates the Langmuir and Freundlich adsorption isotherm models with regression coefficients of 0.8104 and 0.9929, respectively. Isotherm constants for both models are shown in Table 1.

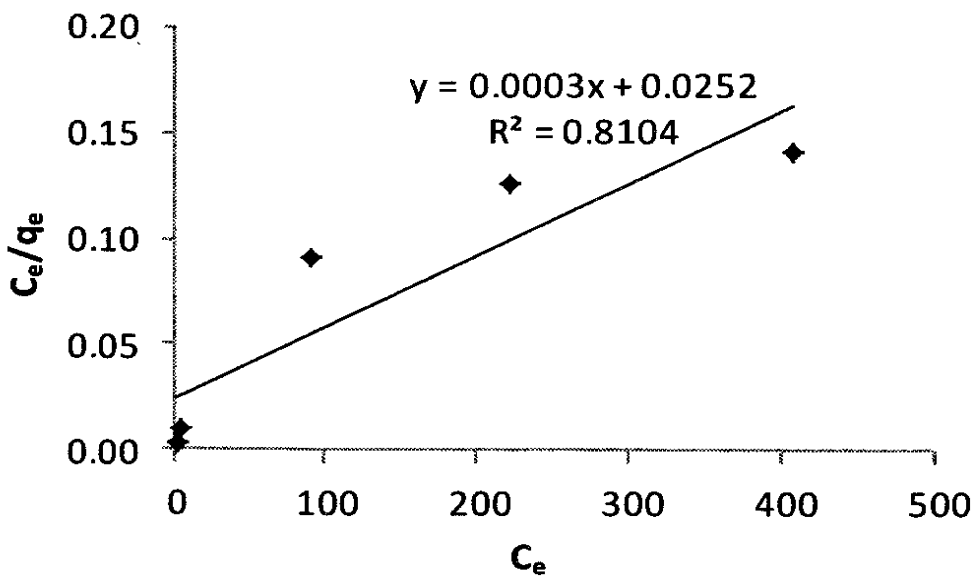

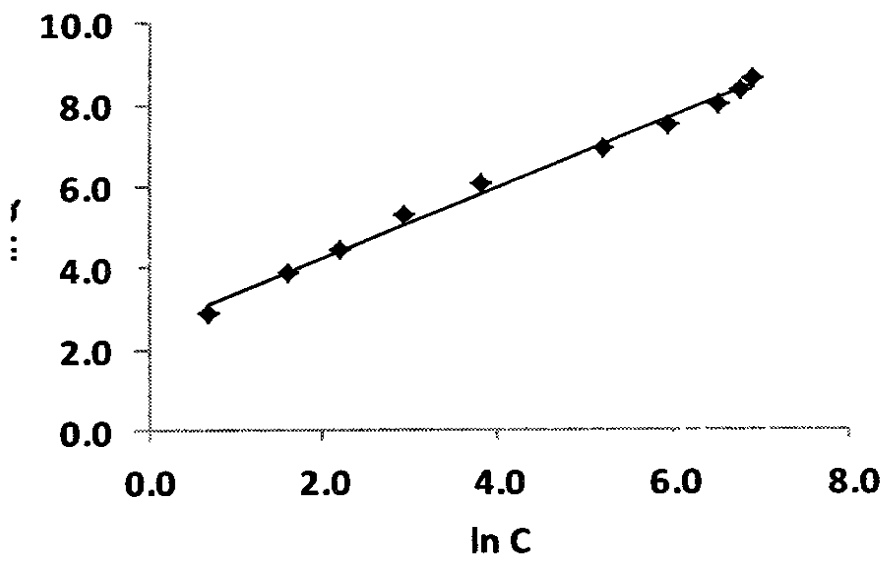

Figure 5: Isotherm models for removal of phosphate from brick clay: (a) Langmuir isotherm (b) Freundlich isotherm (50.0 cm^3 PO_4^{3-}, 5.0 g brick clay fired at 200 °C).

Table 1: Adsorption isotherm constants for both models

Langmuir Isotherm		Freundlich Isotherm	
k_L (L mg^{-1})	q_m (mg kg^{-1})	n	k
0.011	3333	1.16	12.36

According to the data obtained, the maximum adsorption capacity (q_m) for the adsorption of phosphate on brick clay is 3333 mg g^{-1}. The value of n > 1 indicates more favorable physisorption [5].

Kinetics

Equilibrium of sorption and sorption kinetics are two important physicochemical aspects for evaluation of a sorption process, and the latter is important to determine sorption rates [6]. Kinetics modeling was mainly done for better understanding of the rate process. The generalized equation for kinetics, assuming that the activity of the adsorbent is constant, can be written as (13),

$$\frac{d(q_t)}{dt} = k'(q_e - q_t)^n \qquad (2)$$

where k' is the apparent rate constant, t is the contact time, q_e and q_t are the masses of adsorbate adsorbed by unit mass of the sorbent at equilibrium and at time t, respectively. A linearized integrated form of the above equation leads to the following kinetics models models (13 - 15).

Pseudo first order:

$$\log (q_e - q_t) = -\frac{k'}{2.303} t + \log q_e \qquad (3)$$

Pseudo second order:

$$\frac{t}{q_t} = \frac{1}{q_e} t + \frac{1}{k' q_e^2} \qquad (4)$$

If the initial adsorption rate is h_o,

$$h_0 = k' q_s^2 \qquad (5)$$

Pseudo first order model shows that the sorption process comprised of extracellular transfer (include attraction by the active sites on the surface) and intracellular transfer (biotransformation and intracellular accumulation). Pseudo second order model was used to describe chemisorption involving forces such as covalent forces and ion exchange.

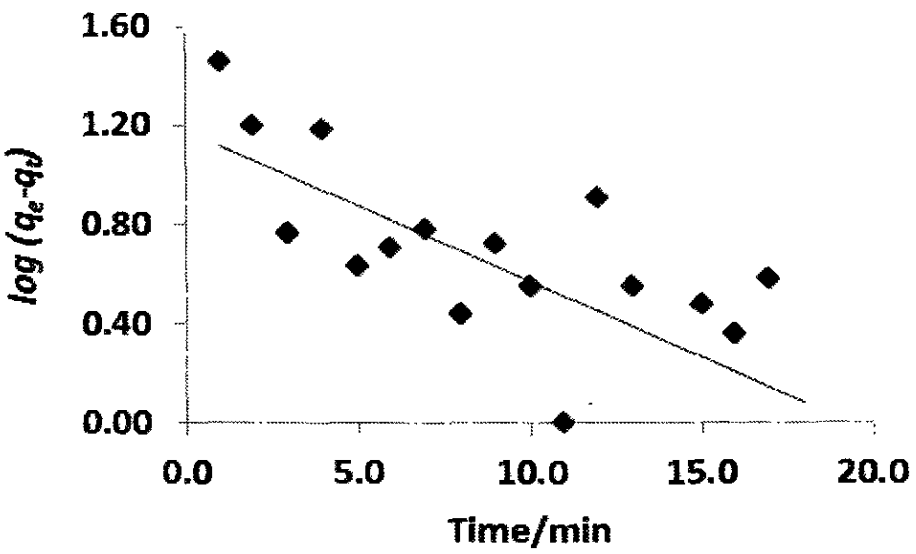

(a)

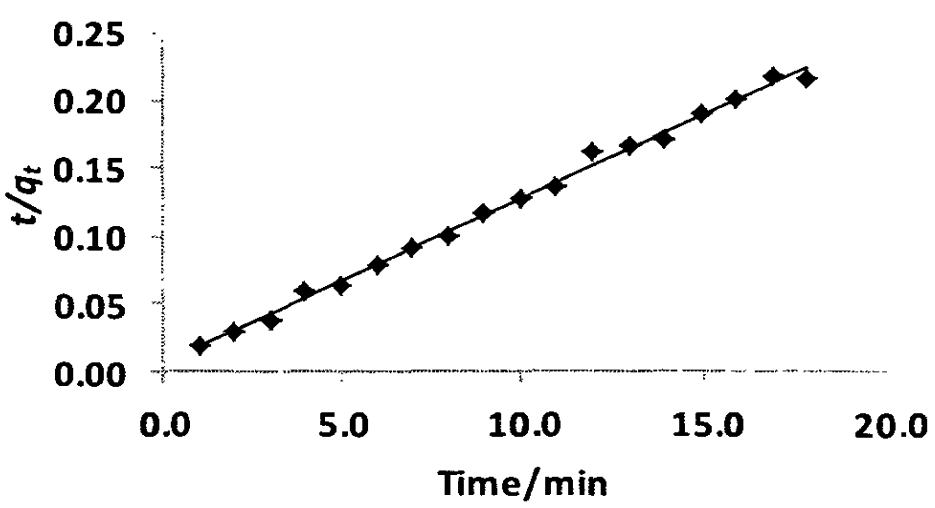

(b)

Figure 6: Adsorption kinetics studies for removal of phosphate from brick clay: (a) Pseudo first order kinetics (b) Pseudo second order kinetics (1000 cm^3 of 10 ppm PO_4^{3-}, 100.0 g brick clay fired at 200 °C).

Linear regression analysis of kinetics data leads to a higher regression coefficient, R^2 of 0.996 for pseudo second order kinetics as compared to a much smaller R^2 value of 0.429 for the pseudo first order model. Further calculations proceeded for the pseudo second order model result in the pseudo second order rate constant (k') of 22.5 g mg^{-1} min^{-1} and adsorption capacity of 83.33 mg kg^{-1}.

Intraparticle diffusion model

In order to identify the boundary layer diffusion, the intra-particle diffusion models, as given below (14), were considered.

McKay and Poots intra-particle diffusion model:

$$q_t = X_i + k' t^{0.5} \quad (6)$$

Webber and Morris Intra-particle diffusion model:

$$\log R = \log k_{id} + n \log(t) \quad (7)$$

In the above equation, R is the percentage adsorption of a heavy metal, n is the gradient of linear plots and k_{id} is the intra-particle diffusion rate constant.

Figure 7 shows the plots of intra-particle diffusion models according to Equations (6) and (7). The regression coefficient of none of the models is in agreement with the linearity of the models. However, it is reasonable to assume that the Webber and Morris model, having a higher regression coefficient, R^2 of 0.725 contributes more to the phosphate removal process. The intra-particle diffusion rate constant (k_{id}) determined from this model is 62.3 min.

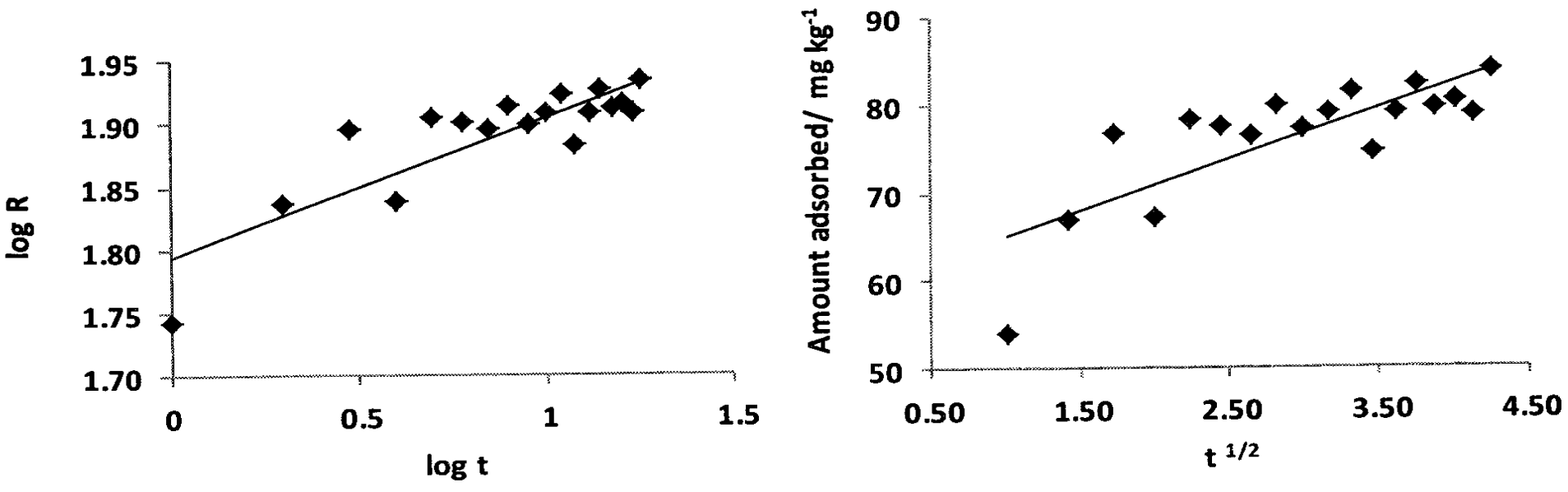

(a) (b)

Figure 7: Adsorption kinetics studies for removal of phosphate from brick clay: (a) Weber and Morris intra-particle diffusion model (b) Mckay and Poots intra-particle diffusion model

Column studies

Effect of flow rate

Breakthrough characteristics for the removal of phosphate is monitored by investigating the relative concentration of phosphate in the eluent as a function of time with continuous supply of phosphate solution through the adsorbent packing at a constant flow rate are shown in Figure 8.

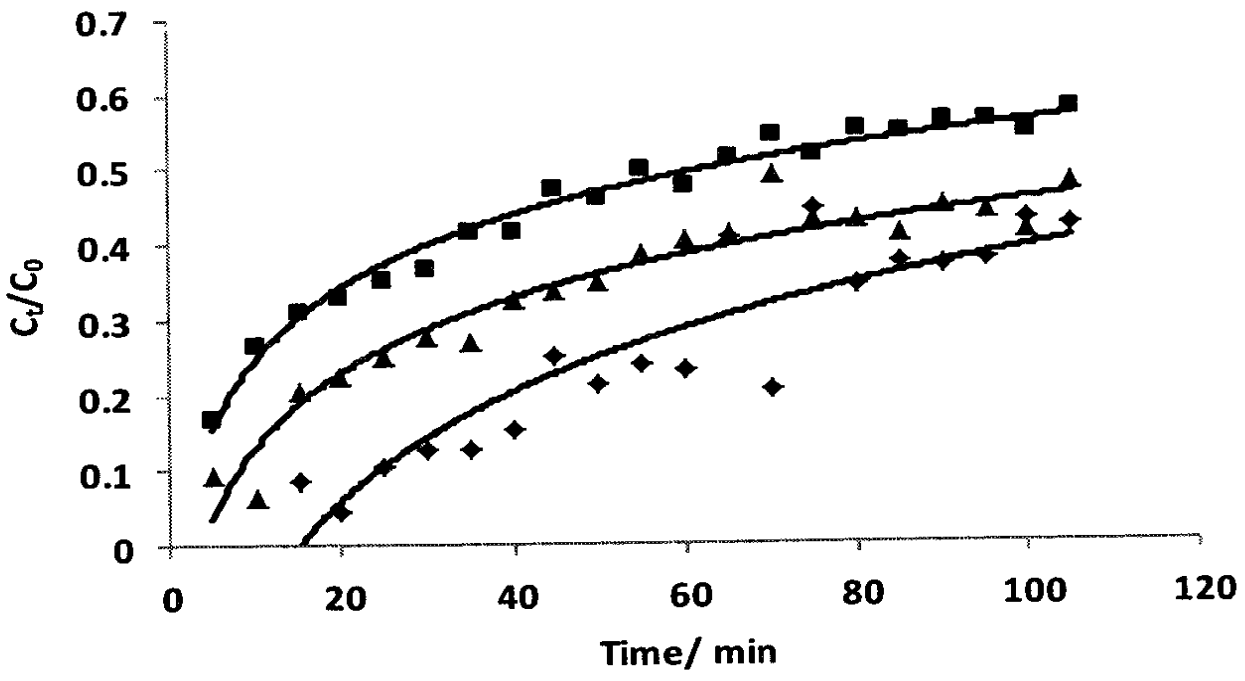

Figure 8: Flow rate optimization for the removal of phosphate by using brick clay, at rate of 8.0 $cm^3\ min^{-1}$ (◆), 12.0 $cm^3\ min^{-1}$ (▲) and 20.0 $cm^3\ min^{-1}$ (■). (Bed height of 30 cm and initial concentration of 10 ppm)

The adsorption process increased rapidly at the initial stage, due to the availability of readily accessible surface sites. As expected, the column performed better at lower feed flow rates, resulted in a longer breakthrough and exhaustive time. With the increase in feed flow rate from 8 to 20 $cm^3\ min^{-1}$, an earlier breakthrough and exhaustion time were observed. Increasing hydraulic loading rate illustrates a steady increase in adsorption zone speed resulting in decrease in breakthrough time, saturation time and column capacity. According to mass transfer fundamentals, this behavior is mainly due to the diffution limitation and insuffitient residence time for the solution within the bed at higher feed flow rate [1]. Higher turbulence at higher feed flow rate may lead to weaker interaction and intraparticle mass transfer within the system. By considering the above facts, the flow rate of 8 ml min^{-1} was taken as the optimized flow rate among other two flow rates for further experiments.

Effect of bed height

Figure 9 illustrates the breakthrough curves obtained at different bed heights with a constant influent concentration of 10.0 ppm and a feed flow rate of 8 ml min^{-1}. As the bed height increases, both breakthrough and exhaustive time increases for the removal of phosphate from brick clay. The increase in adsorbent mass availability at higher bed heights provide a greater service area and more binding sites for the adsorbate species to be interacted. The slope of the breakthrough curve decreases with increase in the bed height, which resulted in a broadened mass transfer zone. At lower bed heights, the solute molecules have insufficient time to diffuse into the pores of brick clay resulting in shorter breakthrough time.

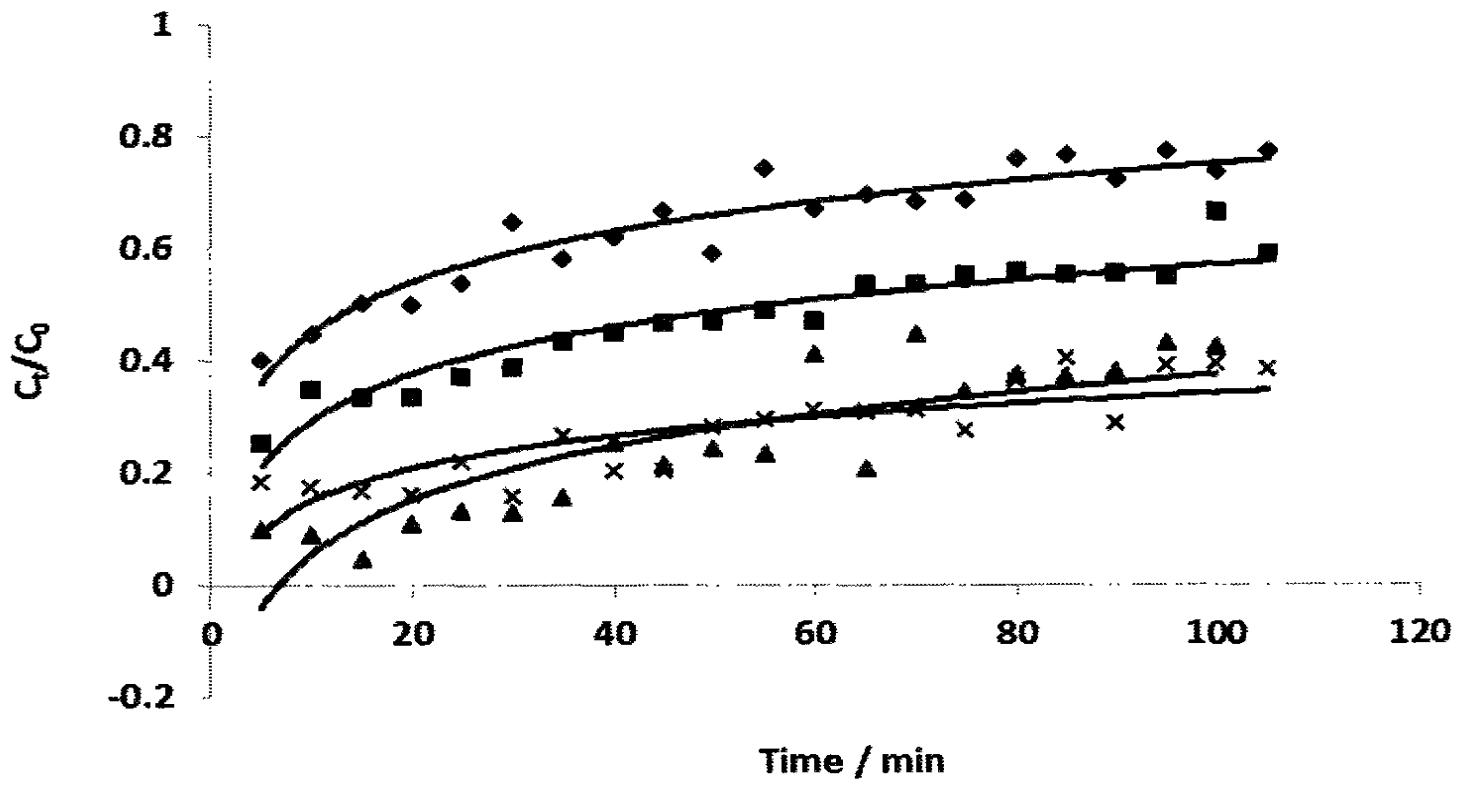

Figure 9: Optimization of column height for removal of phosphate using brick clay fired at 200 °C. Column height: 15.0 cm (◆), 22.5 cm (■), 30.0 cm (▲), 37.5 cm (×) (Flow rate of 8 ml min^{-1} cm and initial concentration of 10 ppm).

Since there is no much difference in exhaustion time for column heights of 30.0 cm and 37.5 cm, and by considering the amount of the adsorbent, a bed height of 30.0 cm was taken as the optimized column height for the removal of phosphate using brick clay fired at 200 °C.

Effect of initial influent concentration

The effect of initial influent concentration on the extent of phosphate removal by brick clay packed column determined for previously optimized conditions as shown in figure 10. Increase in influent concentration results in a sharper breakthrough curve as well as a shorter bed service time indicating that brick clay fixed bed system is saturated more quickly at high concentrations, and hence the time to reach both the breakthrough and exhaustion time is much less [97]. Increase in the influent concentration affects to the volume of effluent treated and finally the removal of total phosphate may decrease. Low influent concentration causes the slow transport of phosphate ions from the film layer to the surface of brick clay adsorbent due to the lower concentration gradient, which implies a decreased diffusion coefficient and decreased mass transfer driving force. [96]

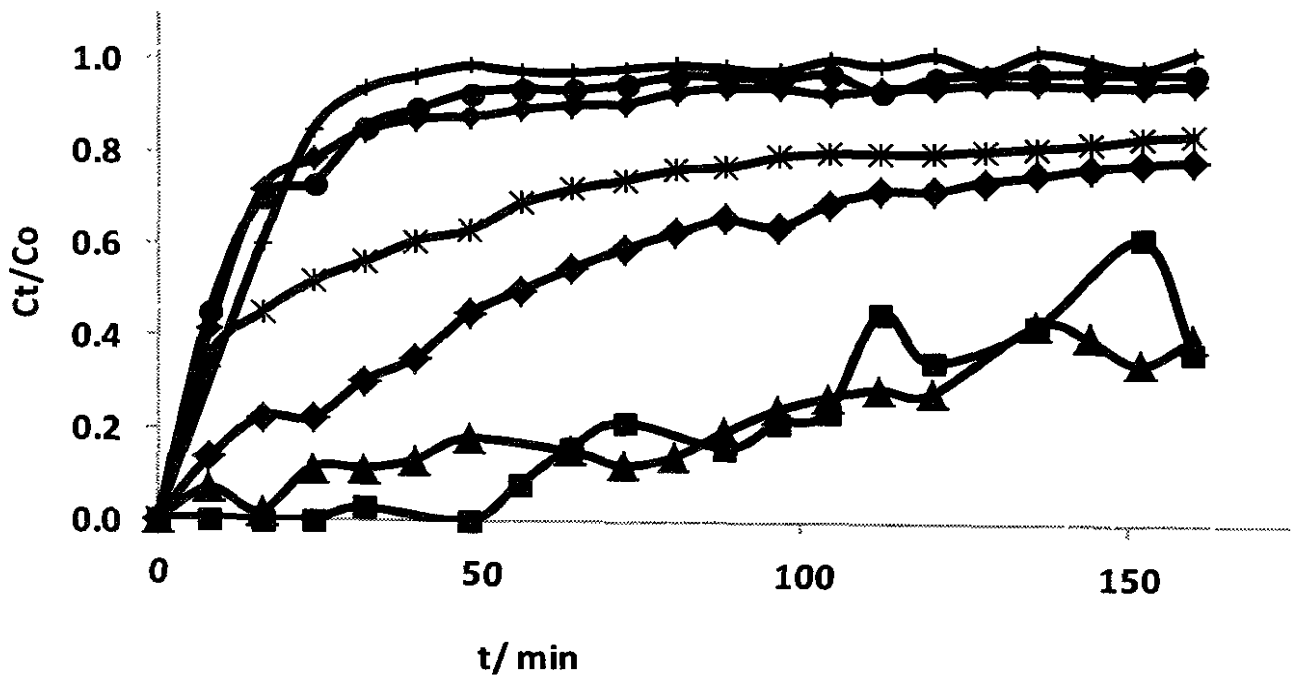

Figure 10: Optimization of column height for removal of phosphate using brick clay fired at 200°C. Column height: 3.08 ppm (-■-), 8.83 ppm (-▲-), 21.46 ppm(-◆-), 110.83 ppm (-✳-), 425.95 ppm (-●-), 748.65 ppm (-●-), 1027.03 ppm (-+-) (bed height of 30.0 cm and flow rate of 8 ml min^{-1}).

Dynamic adsorption models

Among dynamic adsorption models, Adam – Bohart model, BDST model, Thomas model and Yoon – Nelson model are more common, whose significant concentrations are given below (8).

Adams-Bohart model [97]

Adam bohart sorption model was applied in order to describe the initial part of the breakthrough curve.

$$\ln\left(\frac{C_t}{C_0}\right) = k_{AB}C_0 t - k_{AB}N_0\left(\frac{z}{U_0}\right) \qquad (8)$$

Where, z – bed height (cm)

k_{AB} – mass transfer coefficient (L/mg min)

N_0 – saturation concentration (mg/L)

U_0 – superficial velocity (cm/min) = flow rate / cross sectional area of column

C_0, C_t - inlet and outlet concentration

From this equation, values describing the characteristic operational parameters of the column can be determined using the plot of $ln\frac{C_t}{C_0}$ against t at a given bed height and flow rate. This approach mainly focused on the estimation of characteristic parameters such as maximum adsorption capacity (N_0) and mass transfer coefficient (k_{AB}). Linear plots of Adam-Bohart model for different bed heights, flow rates and initial concentrations were plotted and the constnts were calculated from the slope and intercept of the linear curves (Table 2).

Although the model gives a simple and comprehensive approach for evaluating column dynamics, its validity is limited to the range of condition used. According to the results, both mass transfer coefficient (k_{AB}) and the sorption capacity (N_0) decreased with increase in flow rate and concentration but increased with increasing column bed height.

The Bed Depth Service Time (BDST) model [98]

BDST model is one of the simplified fixed bed analysis method model described by Bohart-Adams, but it was modified by Hutchins [96]. This assumed that rate of adsorption is governed by the surface reaction between the adsorbate and the unused capacity of the adsorbent. Equation 9 shows a linear relationship between service time (t) and $\ln\left(\frac{C_t}{C_0}-1\right)$.

$$\ln\left(\frac{C_t}{C_0}-1\right) = \left(\frac{N_0 z k}{U_0}\right) - C_0 k t \qquad (9)$$

N_0 = adsorption capacity of bed

z = adsorbent bed height (cm)

U_0 = superficial velocity (cm/min)

k = rate constant (L mg^{-1} mn^{-1})

The rate constant (k) describes the mass transfer from the liquid phase to the solid phase. According to the results shown in Table 2, rate constant (k) and the adsorption capacity (N_0) increased with increase in flow rate, column height and initial solution concentration. Thomas model (ref 2,7)

Thomas model is one of the most widely used in describing the column performance and prediction of breakthrough curve. The model follows the Langmuir kinetics of adsorption – desorption. The linearized form of the Thomas model is as follows.

$$ln\left[\left(\frac{C_0}{C_t}\right)-1\right]=\left(\frac{k_{TH}q_0m}{Q}\right)-\left(\frac{k_{TH}C_0V_{eff}}{Q}\right) \quad (10)$$

Where, Q = Flow rate

q_0 =Sorption capacity of the adsorbent per unit mass of the adsorbent

m = Mass of adsorbent

k_{TH} =Thomas rate constant

V_{eff} = Volume of effluent treated

t = Service time

The correlation coefficient values (Table 2) indicates a good agreement to Thomas model. According to the constants obtained from the Thomas model, the values of q_0 increases while k_{TH} decreased with increasing initial concentration. The opposite trend is observed for the column data obtained in varying flow rate. The similar trend has been observed for sorption of Mn(II) ions on *mangostana garcinia* peel based granular activated carbon [2].

Yoon nelson model (ref 2)

Yoon – Nelson model derived based on the assumption that the rate of decrease in the probability of adsorption for each adsorbate molecule is proportional to the probability of adsorbate adsorption and the probability of adsorbate breakthrough on the adsorbent [2].

$$ln\left[\frac{C_t}{C_0-C_t}\right]=k_{YN}t-\tau k_{YN} \quad (11)$$

Where, k_{YN} =Yoon nelson rate constant

τ = time required for 50% adsorbate breakthrough

The values of Yoon–Nelson rate constant (k_{YN}) and the time required for 50% adsorbate breakthrough were estimated from the slope and intercept of the graphs of different flow rates, bed heights and different initial concentrations. According to the results shown in Table 2, k_{YN} decreases with increasing flow rate and column height and τ value shows same trend for flow rate and with increasing the column height the τ values also increases.

Table 2: Kinetics model parameters for four kinetic model- Dynamic conditions

Adams-Boharat model	**$k_{AB} \times 10^{-3}$ (L min^{-1} mg^{-1})**	**N_0 (mg L^{-1})**	**R^2**
Flow rate (ml min^{-1})			
8.0	1.711	122.02	0.657
12.0	1.357	181.61	0.657
20.0	0.743	377.30	0.774
Column height (cm)			
15.0	0.564	230.22	0.807
22.5	0.729	183.14	0.878
30.0	1.708	122.02	0.657
37.5	0.951	132.84	0.818
Concentration (mg L^{-1})			
3.1	10.130	29.04	0.790
8.8	2.492	98.01	0.746
21.5	0.718	174.99	0.790
110.8	0.063	984.17	0.753
425.9	0.010	3134.58	0.420
748.6	0.006	4975.38	0.455
1027.0	0.003	5880.58	0.304
BDST model	**$k \times 10^{-3}$ (L min^{-1} mg^{-1})**	**N_0 (mg L^{-1})**	**R^2**
Flow rate (ml min^{-1})			
8.0	2.198	93.24	0.684
12.0	1.858	122.48	0.720
20.0	1.249	176.04	0.846
Column height (cm)			
15.0	1.475	21.88	0.852
22.5	1.348	72.20	0.910
30.0	2.198	93.24	0.684
37.5	1.298	90.07	0.825
Concentration (mg L^{-1})			
3.1	13.149	23.76	0.818
8.8	3.069	79.76	0.796
21.5	1.449	80.11	0.911
110.8	0.192	66.31	0.886
425.9	0.062	1269.83	0.772
748.6	0.048	1694.44	0.793
1027.0	0.043	3619.61	0.598

Yoon – Nelson model	**$k_{YN} \times 10^{-2}$ (min^{-1})**	**τ (min)**	**R^2**
Flow rate (ml min^{-1})			
8.0	2.15	112.36	0.684
12.0	1.89	94.63	0.720
20.0	1.48	70.03	0.846
Column height (cm)			
15.0	1.44	13.21	0.852
22.5	1.33	64.67	0.910
30.0	2.15	112.36	0.684
37.5	1.27	135.68	0.825
Concentration (mg L^{-1})			
3.1	4.05	90.91	0.818
8.8	2.71	106.46	0.796
21.5	3.11	44.00	0.912
110.8	2.13	7.05	0.886
425.9	2.66	35.14	0.772
748.6	3.60	26.68	0.793
1027.0	4.47	41.54	0.598
Thomas model	**$K_{TH} \times 10^{-3}$ (L min^{-1} mg^{-1})**	**q_0 (mg g^{-1})**	**R^2**
Flow rate (ml min^{-1})			
8.0	2.21	145.84	0.684
12.0	2.83	126.31	0.720
20.0	3.04	113.73	0.846
Column height (cm)			
15.0	1.48	34.38	0.852
22.5	1.38	110.96	0.910
30.0	2.21	145.84	0.684
37.5	1.31	140.43	0.825
Concentration (mg L^{-1})			
3.1	13.25	37.06	0.818
8.8	3.08	124.88	0.796
21.5	1.45	125.48	0.912
110.8	0.19	102.76	0.886
425.9	0.06	2010.57	0.772
748.6	0.05	2662.70	0.793
1027.0	0.04	5675.26	0.598

References

[1] Bandaranayake, A.M.A., Mechanistic investigation of interaction of chromium species and thermally – treated brick clay, M.Phil Thesis, University of Peradeniya, **2012**.

[2] Mohammadine, E.H., Mamouni, R., Saffaj, N., Lazar, S., *J of the Association of Arab Universities for Basic and Applied Sciences,*2012, 12, 48–54.

[3] Rathod M, Mody K, Basha S, *J cleaner production*, **2014**, 1-10.

[4] Futalan,C.M., Kan, C.C., Dalida, M.L., Pascua, C., Wan, M.W., *Carbohyd Polym,* **2011**, 83, 697–704.

[5] Jellali, S., Wahab, M.A., Anane, M., Riahi, K., Bousselmi, L., *J Hazard Mater*, **2010**, 184, pp 226-233.

[6] Vimala, R., Charumathi, D., Das , N., *Desalination,* **2011**, 275, 291–296.

[7] A new IUPAC classification of adsorption isotherms, Available from: http://www.nigelworks.com/mdd/PDFs/NewClass.pdf (Accessed 12 December, 2015).

[8] Khan, T. A., Dahiya, S., Ali, I., *GU J Sci*, **2012**, 25(1), 59-87.

Ileperuma, O.A., Priyantha, N., Chandrajith, R., Navaratne, A., Perera, A., Yatigammana, S.K., Wijesundara, C. and Rathnayake, S. (editors) (2013): Symposium Proceedings, Second International Symposium on Water Quality and Human Health: Challenges Ahead, 15-16 March, PGIS, Peradeniya, Sri Lanka

REMOVAL OF HEAVY METALS USING RICE HUSK AND BRICK CLAY AS ADSORBENTS: A STUDY OF DYNAMIC CONDITIONS

N. Priyantha[1,2*], A. Navaratne[1,2] and T.P.K. Kulasooriya[1,2]

[1]*Department of Chemistry, University of Peradeniya, Peradeniya, Sri Lanka.*
[2]*Postgraduate Institute of Science, University of Peradeniya, Peradeniya. Sri Lanka.*

Treatment of industrial waste water has become a necessity to remediate environmental pollution problems which occur mainly due to urbanization and industrialization. Most of the treatment methods available at present are neither economical nor environmentally friendly. Therefore, low-cost and environmentally friendly effluent and waste water treatment methods based on sorption onto natural substances have become attractive alternatives.

In this research, effectiveness of thermally treated rice husk and brick clay were investigated as sorbents for heavy metal ions under dynamic conditions. A mixture of cations consisting of Cd(II), Cr(III), Cu(II), Ni(II), Pb(II) and Zn(II), each at 10 ppm concentration, was tested on these two adsorbents by passing through a column (i.d. = 2.0 cm) packed up to 30 cm with the respective sorbent. The optimum firing temperatures of 100 °C for rice husk and 200 °C for brick clay were used in this investigation for maximum metal ion removal efficiency. Subsequently, two sandwich types of packing: rice husk at the bottom (15 cm) and brick clay on the top (15 cm) [rice husk – brick clay packing], and the reverse order were also employed. After a 5 minute interaction period of the cation mixture with the sorbent, effluent fractions were collected at 5 min intervals for the determination of remaining heavy metal ion concentrations.

According to atomic absorption spectroscopic analysis of the effluent, the extent and the order of removal of metal ions by each sorbent/sorbent mixture depend on the interaction time. The relative ability of rice husk in removing heavy metals is in the order, Pb > Cu > Ni ≈ Cd > Cr > Zn and that of brick clay in the order, Pb ≈ Cr ≈ Cu ≈ Cd > Zn ≈ Ni, based on the average of ten elutions. On the other hand, sandwich columns follow the order, Pb > Cr > Cu > Cd > Zn > Ni for both brick clay- rice husk and rice husk-brick clay packings.

The solutions collected from the column packed with a combination of the sorbents, rice husk-brick clay column results in a higher removal than the brick clay-rice husk column. Further, it is the general observation that Pb(II) shows the highest removal while Ni(II) gives the lowest removal among the cations investigated. It can also be concluded that brick clay is superior to rice husk for the removal of heavy metal ions from solution. This methodology can be extended for treatment of industrial effluents containing heavy metal ions.

*namal.priyantha@yahoo.com

Abstract No: 541 ***Climate and Environment***

ADSORPTION ISOTHERM STUDIES OF HEAVY METAL IONS ON RICE HUSK

N. Priyantha[1, 2]*, A.N. Navaratne[1] and T.P.K. Kulasooriya[1, 2]

Department of Chemistry, Faculty of Science, University of Peradeniya, Sri Lanka
Postgraduate Institute of Science, University of Peradeniya, Sri Lanka
**namal.priyantha@yahoo.com*

Heavy metals cause a severe problem to the ecosystem due to their highly toxic nature. Consequently, their removal from the environment, mainly from wastewater systems, is of essential to maintain the health of the environment. Use of naturally occurring, environmentally friendly substances has been attractive in this regard. Ability of rice husk, in its natural size, to remove heavy metal ions from simulated industrial effluents and is reported in this research. Different shaking and settling times at 150 rpm speed indicates that the optimum time period for the removal of all heavy metal ions investigated [Cd(II), Cr(III), Cu(II), Pb(II), Ni(II) and Zn(II)] is 10 minutes. Further, variation of solution pH and firing temperature of rice husk with the extent of heavy metal ion removal leads to the optimum firing temperature and the solution pH of 100 °C and 4.0-5.0, respectively. Adsorption isotherm experiments conducted with metal ion solutions of initial concentrations varying from 2-1000 ppm under optimized conditions demonstrate that all six heavy metal ions follow the Langmuir adsorption isotherm model with a high regression coefficient of about 0.99. According to linearized Langmuir isotherm plots, the highest adsorption capacity of 5000 mg g^{-1} is observed for Pb(II), and the capacity of other metals varies in the order of Pb > Cd > Cu > Ni > Zn > Cr.

Financial assistance given by the National Science Foundation of Sri Lanka (RG/2012/BS/05) is acknowledged.

Abstract No: 106 Earth and Environmental Sciences

OPTIMIZATION OF EFFICIENCY OF PHOSPHATE REMOVAL BY BRICK CLAY

N. Priyantha[1,2]*, A. Navaratne[1,2] and T.P.K. Kulasooriya[2]

[1]Department of Chemistry, Faculty of Science, University of Peradeniya, Sri Lanka
[2]Postgraduate Institute of Science, University of Peradeniya, Sri Lanka
**namalpriyantha@pdn.ac.lk*

The phosphate species, a main aquatic pollutant, contributes to eutrophication, which results in decreased dissolved oxygen levels of reservoirs, causing harmful effects to the aquatic life. This can be overcome, without further damaging the environment, by removal of phosphate using adsorption techniques before phosphate contaminated wastewater reaches reservoirs. As adsorption techniques are found to be superior to existing chemical methods in many respects, such as environmentally friendliness, low-cost and selectivity. Although adsorption techniques may not be as efficient as chemical methods, they have become attractive owing to the above advantages. Among many adsorbents, burnt brick clay, feldspar and dolomite investigated for the removal of phosphate from synthetic solutions prepared using NaH_2PO_4, burnt brick clay shows the highest efficiency of adsorption. Under the optimized conditions, brick clay burnt at 200 °C shows 87% removal from 10.0 ppm phosphate solution at 1:10 adsorbent/solution ratio. The Langmuir adsorption isotherm, in its linear form, shows the validity for the burnt brick clay-phosphate adsorption system at equilibrium with a high adsorption capacity of 11.11×10^3 mg kg^{-1} with respect to phosphate. The Freundlich adsorption isotherm is also determined to be valid indicating that adsorbate species equivalent to more than a monolayer have been transferred to the adsorbent phase. Regression analysis of linearized kinetics models indicates the validity of pseudo second order kinetics with an apparent rate constant of 0.375 g mg^{-1} s^{-1}. Further, removal of phosphate by brunt brick clay packed in columns is found to be efficient at low flow rates below 0.17 cm^3 s^{-1}. Results of dynamic experiments would be much useful in the development of real-type effluent treatment systems.

Financial assistance provided by the National Science Foundation, Sri Lanka (NSF Grant RG/2012/BS/05), is greatly acknowledged.

Keywords: Phosphate, Parameter optimization, Adsorption isotherms, Kinetics

Ileperuma, O.A., Priyantha, N., Yatigammana, S.K., Wijesundara, C. and Madawala, H.M.S.P. (editors) (2015): Symposium Proceedings, Fourth International Symposium on Water Quality and Human Health: Challenges Ahead, 01 & 02 August, PGIS, Peradeniya, Sri Lanka

SORPTION STUDIES OF TEXTILE DYES USING NATURALLY AVAILABLE SUBSTANCES

N. Priyantha[1, 2*], A.N. Navaratne[1, 2] and T.P.K. Kulasooriya[1, 2]

[1]*Department of Chemistry, University of Peradeniya, Peradeniya, Sri Lanka.*
[2]*Postgraduate Institute of Science, University of Peradeniya, Peradeniya, Sri Lanka.*

Textile industry releases several types of dyes to the environment. The contamination from these substances may adversely affect any ecosystem. Over the past few decades, many treatment techniques were introduced to remove dyes from industrial effluents. The current study is mainly based on the removal of dyes present in effluent samples using naturally available substances. Textile dyes, namely Sumifix Blue Exf (Dye 1), Sumifix Rubine Exf (Dye 2) and Sumifix Yellow Exf (Dye 3), obtained from a textile industry show their λ_{max} values at 605 nm, 545 nm and 415 nm, respectively. Among different adsorbents (e.g. brick clay, rice husk, coir dust, saw dust, feldspar and dolomite), investigated for the removal of dyes from aqueous solutions, using 50 mg L^{-1} individual dye solutions under batch mode, brick clay shows the highest efficiency. The optimum values of various parameters, such as adsorbent firing temperature, adsorbent dosage, shaking time, settling time, solution initial pH, for brick clay were 200 °C, 4.0 g, 15.0 min, 15.0 min and pH < 10, respectively. Adsorption data obtained at ambient temperature modeled using Langmuir, Freundlich, Temkin, Dubinin-Reduskevich isotherm relationships, results in the validity of the Langmuir adsorption isotherm with high regression coefficients close to 1.0. The kinetics of dye adsorption on brick clay can be best described by the pseudo second order model having a high regression coefficient of 0.999 for all three types of dyes. These results indicate that fired brick clay could be used as an effective option for removal of dye present in industrial effluents.

Financial assistance given by the National Science Foundation (NSF Grant No RG/2012/BS/05) is acknowledged.

Keywords: Textile industry, dye effluents, burnt brick clay, isotherm studies, kinetics

*namal.priyantha@yahoo.com

SECTION 7

7.1 Signature of Investigators:

Prof. Namal Priyantha

7.2 Comments of the Head of the Department/Signature:

Recommended.

Head
Department of Chemistry
University of Peradeniya

7.3 Head of the Institution's signature:

Prof. H M D Namal Priyantha
Director
Postgraduate Institute of Science
University of Peradeniya
Sri Lanka.

National Digitization Project

National Science Foundation

Institute : National Science Foundation

1. Place of Scanning : Sanje (Private) Ltd. Hokandara

2. Date Scanned : ....2017../..04../..05.....

3. Name of Digitizing Company : Sanje (Private) Ltd, No 435/16, Kottawa Rd, Hokandara North, Arangala, Hokandara

4. Scanning Officer

Name : .....Angelo Melvin.....

Signature : .....A. M. Lud.....

Certification of Scanning

I hereby certify that the scanning of this document was carried out under my supervision, according to the norms and standards of digital scanning accurately, also keeping with the originality of the original document to be accepted in a court of law.

Certifying Officer

Designation : Information Officer

Name : Renuka Sugathadasa

Signature : R. P. Sugathadasa

Date : .....

"This document/publication was digitized under National Digitization Project of the National Science Foundation, Sri Lanka"